



THE UNIVERSITY OF  
**SYDNEY**

## **COPYRIGHT AND USE OF THIS THESIS**

This thesis must be used in accordance with the provisions of the Copyright Act 1968.

Reproduction of material protected by copyright may be an infringement of copyright and copyright owners may be entitled to take legal action against persons who infringe their copyright.

Section 51 (2) of the Copyright Act permits an authorized officer of a university library or archives to provide a copy (by communication or otherwise) of an unpublished thesis kept in the library or archives, to a person who satisfies the authorized officer that he or she requires the reproduction for the purposes of research or study.

The Copyright Act grants the creator of a work a number of moral rights, specifically the right of attribution, the right against false attribution and the right of integrity.

You may infringe the author's moral rights if you:

- fail to acknowledge the author of this thesis if you quote sections from the work
- attribute this thesis to another author
- subject this thesis to derogatory treatment which may prejudice the author's reputation

For further information contact the University's Director of Copyright Services

**[sydney.edu.au/copyright](http://sydney.edu.au/copyright)**

# Precipitating Change

Holocene climate change in the Asian monsoon  
based on sediment archives from tropical lakes

Roshni R. Sharma

A thesis submitted in fulfilment of the degree of:

Masters of Applied Science (Geosciences)

School of Geosciences, Faculty of Science  
The University of Sydney, NSW 2008, Australia



2014

*Front cover image: An aragonite crystal from Yeak Kara lake sediment archive, viewed under a scanning electron microscope at 3,540 times magnification. Taken by the author on 27 June 2013.*

## **Statement of Originality**

This thesis is submitted to the University of Sydney in fulfilment of the requirements of the degree of Masters of Applied Science (Geosciences). The work embodied in this thesis is the result of original research and has not been previously submitted for a degree to this or any other institution for the award of a degree. This thesis has been written under the supervision of Dr Dan Penny, who assisted with some minor editing.

A handwritten signature in black ink, appearing to read 'Roshni R. Sharma', is written on a light-colored rectangular background.

Roshni R. Sharma

30 April 2014

## **Abstract**

The Asian monsoon is a complex and dynamic system and a significant driver of hydrological change in the global climate system. A number of monsoon subsystems, distributed over various geographical areas, make up the larger Asian monsoon system. The dynamics of climate change in the Asian monsoon over the Holocene in these subsystems is of key interest, given that the instrumental record is short and geographically biased and there is a low density of palaeoclimate records of sufficient length and resolution to capture long-term broader scale change and variability.

The response of the Asian monsoon over mainland Southeast Asia is an important yet little studied aspect of the monsoon system. This region is of interest due to its location on the cusp of the Indian monsoon and East Asian monsoon subsystems. Gaining a better understanding of broad scale events in the Holocene as experienced by this region can assist in clarifying whether climatic responses in the various geographical provinces of the Asian monsoon occur asynchronously or in concert. This deepens the understanding of the geographical behaviour of the monsoon in relation to teleconnections and forcing mechanisms.

This study provides a high resolution independently dated record of climate variability from the early Holocene, from stable isotopes from authigenic carbonates held in lake sediment archives. It presents new insights into the timing of the onset of dryer conditions in this region following the Holocene Optimum, which will herald valuable insight into the climate dynamics and teleconnections in the tropics in the recent past.



## Acknowledgements

First and foremost, I would like to thank my supervisor, Dr Dan Penny, for his guidance, encouragement, wisdom and positivity through this project in helping keep me focused, giving me direction and making me laugh. Alongside this, I would like to humbly thank my parents for the immeasurable support they have given me, in many forms, in this journey.

My sincere and earnest thanks to the staff and students of the School of Geosciences at University of Sydney. Foremost, I have great appreciation for the assistance and guidance from Tom Savage in all lab-related tasks. I am very grateful to have had the chance to work with Andy Maxwell, and am especially thankful for his wisdom on all things Yeak Kara and his patience and humour during fieldwork. I would also like to thank my colleagues in the Cambodian Crater Lakes Project, Rebecca and Georgia. I sincerely thank Troy Mutton at USYD library, as well as Nikki Montenegro, Ramana Karanama and Sue Taylor. I am also endlessly grateful to all of my colleagues who partook meals with me, shared the highs and the lows of the research process, gave me advice and inspiration, helped me to keep taking one step after another – Tiffany-Anne Carroll-McDonald, Ashish Aggarwal, Michael Rubey, Logan Yeo among others.

Enormous thanks to the collaborators in this project from the Cambodian Ministry of Environment, especially those who partook in fieldwork - Chap Yuthy, Khem Rongden, Seang Channa.

Dr Evan Pickett, thank you for your kind assistance in helping me to grasp R, and to all of my friends in Australia and around the world – thank you for the continuous support, for pushing me to keep finding inspiration and putting in the hard work when I couldn't see much light at the end of the tunnel, and for putting up with my ridiculous

levels of excitement when I had (even the tiniest) breakthroughs – especially Stacey, Sharon and Gregg. My very deepest gratitude to Dr Manjula Sharma and Dr Neeraj Sharma, for their love and support through the journey, and helping me to get started, and to Mukesh Chand for his patience and kindness.

This journey has been an inner one almost as much as an outer one for me, and I have come out the other side a wiser person on many fronts. For helping me to keep my head above water when times got tough, I am deeply grateful to Dr Blake Hamilton, Dr Wendy Rees and Dr Meredith Gray.

To all of my forefathers – the proverbial giants upon whose shoulders I stand upon, I am deeply grateful. Without the steady advancements in scientific knowledge through time and the pursuit of excellence by the men and women who have dedicated their time and effort to science, technology and philosophy, this world would be a very different place and I would most certainly not have been able to write this thesis. Especially, to my first teacher of earth system sciences and global change, Dr Russell Drysdale - thanks for sparking my interest in this most intriguing and thought provoking of areas.

# Contents

Statement of Originality		
Abstract .....		i
Acknowledgements .....		ii
<b>Chapter 1</b>	<b>Purpose.....</b>	<b>1</b>
<b>Chapter 2</b>	<b>Literature Review .....</b>	<b>5</b>
2.1.	The Asian monsoon climatic system .....	5
2.2.	Changes in Holocene precipitation dynamics of the Indian and East Asian summer monsoons from direct climate proxy records .....	13
2.3.	Lake sediments as proxies for past climate .....	18
2.3.1.	Deep tropical lakes and climate .....	18
2.3.2.	Stable isotopes and the amount effect in tropical areas .....	20
<b>Chapter 3</b>	<b>Materials &amp; Methods .....</b>	<b>22</b>
3.1.	Study sites .....	23
3.2.	Limnology and geochemistry of tropical crater Lakes .....	26
3.2.1	Data acquisition .....	26
3.2.1.1.	Field Methods .....	26
3.2.1.1.a.	Bathymetric survey .....	26
3.2.1.1.b.	Water quality profiling .....	27
3.2.1.1.c.	Major ions analysis .....	28
3.2.1.2.	Laboratory methods .....	28
3.2.1.2.a.	ICP-AES elemental analysis for major ions .....	28
3.2.2	Data analysis.....	30
3.2.2.a	Bathymetric survey .....	30
3.2.2.b	Water quality profiling .....	31
3.2.2.c	ICP-AES elemental analysis for major ions .....	31
3.3.	Stable isotopes in meteoric and lake waters .....	32
3.3.1.	Data acquisition .....	32
3.3.1.1.	Field Methods .....	32
3.3.1.1.a	Lake water sampling .....	32
3.3.1.1.b	Rain water sampling .....	33
3.3.1.2.	Laboratory methods .....	34
3.3.1.2.a	Stable isotope analysis of water samples .....	34
3.3.2	Data analysis .....	34
3.3.2.a	Temporal variation in stable isotopes in rainfall and lake surface waters over the study region from the summer and winter monsoon periods ..	34
3.4.	Sediment archives of palaeoclimate .....	35
3.4.1.	Data acquisition .....	35
3.4.1.1	Field Methods .....	35
3.4.1.1.a.	Sediment core retrieval .....	35
3.4.2.	Data analysis .....	36
3.4.2.1.	Laboratory methods .....	36
3.4.2.1.a	Physical analysis of sediments .....	36

<b>Chapter 3</b>	<b>Materials &amp; Methods (continued)</b> .....	37
3.4.2.1.b	Magnetic susceptibility analysis .....	37
3.4.2.1.c	Particle size analysis .....	39
3.4.2.1.d	Loss on ignition analysis .....	40
3.4.2.1.e	Geochemical analysis .....	41
3.4.2.1.f	Characterisation of carbonate species using electron microscopy .....	43
3.4.2.1.g	Stable isotope analysis of carbonates in sediments .....	44
3.4.2.1.h	<sup>14</sup> C dating of charcoal in sediments .....	
<b>Chapter 4</b>	<b>Results</b> .....	46
4.1.	Bathymetry and basin morphology of crater lakes .....	46
4.2.	Stable isotope dynamics of lake waters, rain waters and regional climate .....	52
4.3.	Limnology of the Cambodian Crater Lakes .....	56
4.3.1.	Temperature and stratification .....	56
4.3.2.	Specific conductivity .....	57
4.3.3.	Dissolved oxygen saturation .....	58
4.3.4.	pH .....	59
4.4.	Stable isotope dynamics in lake waters with depth over time .....	61
4.5.	Biogeochemistry of lake waters .....	70
4.5.1.	Sodium, magnesium and potassium .....	70
4.5.2.	Calcium, barium and aluminium .....	76
4.5.3.	Silica and strontium .....	81
4.5.4.	Iron and sulfur .....	84
4.6.	YK0712B sediment core .....	87
4.6.1.	Sediment characteristics .....	87
4.6.2.	Loss on ignition analysis .....	90
4.6.3.	Particle size analysis .....	93
4.6.4.	Magnetic susceptibility .....	96
4.6.5.	Sediment geochemistry .....	99
4.6.6.	Characterisation of carbonate species .....	102
4.6.7.	Stable isotopes of oxygen in sediment .....	116
4.6.8.	<sup>14</sup> C Dating of the YK0712B sediment core .....	118
<b>Chapter 5</b>	<b>Discussion</b> .....	121
5.1.	Scientific value of the Cambodian crater lakes .....	121
5.2.	Physical and chemical processes in lake waters .....	122
5.2.1.	Limnology .....	122
5.2.2.	Geochemistry .....	125
5.3.	Stable isotope ratios in lake waters and meteoric waters .....	127
5.3.1.	Relationship between meteoric waters and regional climate .....	127
5.3.2.	Relationship between lake waters and regional climate .....	130
5.4.	Lake sediments and regional climate .....	131
5.4.1.	Palaeoclimatic interpretation of lake sediment archives .....	132
5.4.2.	Response of the Asian monsoon over mainland Southeast Asia to forcing mechanisms .....	139

<b>Chapter 6</b>	<b>Conclusions .....</b>	<b>142</b>
	Reference List .....	145
	Appendix I .....	iv

## List of figures

Figure 2.1	Region affected by the Asian monsoon (from Black, 2002, p. 28).....	6
Figure 2.2	Schematic representation of (a) summer (August) and (b) winter (January) low level monsoon winds over Asia and associate areas of intense precipitation. Grey shaded areas indicate rainfall in excess of 300mm/month. Precipitation data NOAA NCEP CPC CAMS_OPI, wind data NOAA NCEP-NCAR CDAS-1 mc6190 Intrinsic Pressure Level x 925mb. Data source: National Weather Service Climate Prediction Centre (data are not subject to copyright protection). Image and caption sourced from Penny, 2012, p. 209.....	7
Figure 3.1	Location of study region in a global context .....	23
Figure 3.2	The location of the Cambodian crater lakes in the Ratanakiri province .....	24
Figure 4.1	Bathymetric basin map and satellite image of Yeak Loam .....	47
Figure 4.2	Bathymetric basin map and satellite image of Yeak Oam .....	48
Figure 4.3	Bathymetric basin map and satellite image of Yeak Kara .....	49
Figure 4.4	Bathymetric basin map and satellite image of Boeng Lumkut .....	50
Figure 4.5	Regional meteoric water line, lake surface water line and global meteoric water line .....	52
Figure 4.6	Relationship between rainfall amount (Ban Lung rain gauge), $\delta^{18}\text{O}$ in rain waters and $\delta^{18}\text{O}$ in lake surface waters (Yeak Loam) .....	54
Figure 4.7	Relationship between $\delta^{18}\text{O}$ of rainwater and lake surface waters and peak rainfall intensity .....	55
Figure 4.8	Temperature variation with depth over time in Cambodian crater lakes. Depths are in metres and temperature in $^{\circ}\text{C}$ .....	57
Figure 4.9	Specific Conductivity with depth over time in the Cambodian crater lakes. Depths are in metres and specific conductivity levels are in $\mu\text{S}/\text{cm}$ .....	58
Figure 4.10	ODO variation with depth over time in the Cambodian crater lakes. Depths are in metres and dissolved oxygen (ODO saturation) levels are displayed as percentages .....	59
Figure 4.11	pH variation with depth over time in the Cambodian crater lakes. Depths are given in metres .....	60
Figure 4.12	$\delta^{18}\text{O}$ Isotopic composition of Yeak Loam waters with depth over time..	64
Figure 4.13	$\delta^2\text{H}$ isotopic composition of Yeak Loam waters with depth over time....	65
Figure 4.14	$\delta^{18}\text{O}$ isotopic composition of Yeak Oam waters with depth over time....	66
Figure 4.15	$\delta^2\text{H}$ isotopic composition of Yeak Oam waters with depth over time....	67
Figure 4.16	$\delta^{18}\text{O}$ isotopic composition of Boeng Lumkut waters with depth over time .....	68
Figure 4.17	$\delta^2\text{H}$ isotopic composition of Boeng Lumkut waters with depth over time.....	69
Figure 4.18	$\delta^{18}\text{O}$ composition of Yeak Kara waters with depth over time .....	70
Figure 4.19	$\delta^2\text{H}$ composition of Yeak Kara waters with depth over time .....	70

Figure 4.20	Sodium ion content in lake waters over time (note that the axis for Yeak Kara is expanded by a factor of 10 because of significantly higher iron content). Charts on the right show difference from average values for that lake .....	73
Figure 4.21	Magnesium ion content in lake waters over time (note that the axis for Yeak Kara is expanded by a factor of 10 because of significantly higher iron content). Charts on the right show difference from average values for that lake.....	74
Figure 4.22	Potassium ion content in lake waters over time (note that the axis for Yeak Kara is expanded by a factor of 5 because of significantly higher iron content). Charts on the right show difference from average values for that lake .....	75
Figure 4.23	Calcium ion content in lake waters over time (note that the axis for Yeak Kara is expanded by a factor of 5 because of significantly higher iron content). Charts on the right show difference from average values for that lake .....	78
Figure 4.24	Barium ion content in lake waters over time (note that the axis for Yeak Kara is expanded by a factor of 250 because of significantly higher iron content). Charts on the right show difference from average values for that lake .....	79
Figure 4.25	Aluminium ion content in lake waters over time (note that the axis for Yeak Kara is expanded by a factor of 1000 because of significantly higher iron content). Charts on the right show difference from average values for that lake .....	80
Figure 4.26	Silica ion content in lake waters over time (note that the axis for Yeak Kara is expanded by a factor of 6 because of significantly higher iron content). Charts on the right show difference from average values for that lake .....	82
Figure 4.27	Strontium ion content in lake waters over time. Charts on the right show difference from average values for that lake .....	83
Figure 4.28	Iron ion content in lake waters over time (note that the axis for Yeak Kara is expanded by a factor of 5 because of significantly higher iron content). Charts on the right show difference from average values for that lake .....	85
Figure 4.29	Sulfur ion content in lake waters over time. Charts on the right show difference from average values for that lake .....	86
Figure 4.30	Breakdown of Loss on ignition data through YK0712B .....	92
Figure 4.31	Particle size analysis data and summary statistics plotted by depth.....	95
Figure 4.32	Magnetic susceptibility for 0-13m of YK0712B .....	98
Figure 4.33	Calcium and strontium XRF counts (top) and rubidium XRF counts (bottom) from ITRAX geochemical analysis. Rubidium plot showing a 20-sample average in black to display trends in the dataset more clearly .....	101
Figure 4.34	SEM micrograph from the laminated section showing calcite and aragonite .....	103
Figure 4.35	SEM micrograph of the laminated section of the core.....	103
Figure 4.36	SEM micrograph of sample from non-laminated section.....	104

Figure 4.37	SEM micrographs of acicular aragonite crystals .....	105
Figure 4.38	SEM micrographs of the orthorhombic dipyramidal structure of an aragonite crystal .....	106
Figure 4.39	EDS spectra of aragonite in the laminated section.....	108
Figure 4.40	EDS spectra of calcite in the laminated section.....	109
Figure 4.41	EDS spectra of aragonite in the non-laminated section .....	110
Figure 4.42	EDS spectra of calcite in the non-laminated section .....	111
Figure 4.43	EBSD phase map for sample A (sample from non-laminated section still containing calcium carbonate, of average chemistry) showing micrograph (top), phase map (mid) and legend (bottom) .....	112
Figure 4.44	EBSD phase map for sample B (sample from laminated section of average chemistry) showing micrograph (top), phase map (mid) and legend (bottom) .....	113
Figure 4.45	EBSD phase map for sample C (sample from laminated section high in iron) showing micrograph (top), phase map (mid) and legend (bottom) .....	114
Figure 4.46	EBSD phase map for sample D (sample from laminated section high in strontium) showing micrograph (top), phase map (mid) and legend (bottom) .....	115
Figure 4.47	$\delta^{18}\text{O}$ (‰PDB) record from YK0712B core .....	117
Figure 4.48	$^{14}\text{C}$ dates with error for YK0712B .....	119
Figure 4.49	Cal yr BP age model for YK0712B .....	120
Figure 5.1	Paleoclimate proxies held in YK0712B core plotted by age .....	134
Figure 5.2	Comparison of broad trends in Donnge cave record (Wang et al., 2005) and Yeak Kara record of changes in the Holocene Asian monsoon. Both series are displayed with a three year moving average tend line .....	137
Figure 5.3	Comparison of stable isotope data from YK0712B with total solar irradiance, GISP2 volcanic sulphates, Vostok atmospheric $\text{CO}_2$ and GISP2 atmospheric methane .....	141



## List of Tables

Table 2.1	Chronology of inferred precipitation changes of the summer monsoon strength in different regions and sub-monsoons of the Asian monsoon system through the late to early Holocene. Upper boundary of ‘gradual weakening’ of monsoon flow due in some cases to the termination of available records .....	15
Table 3.1	Qualitative summary of meteorological conditions in Ratanakiri province during monitoring expeditions .....	25
Table 3.2	Sampling locations .....	27
Table 3.3	Details of standards prepared for ICP-AES analysis of lake water samples .	29
Table 4.1	Depth values generated from sonar data. Surface area estimate underestimates true surface area, and true volumes are likely to be slightly higher.....	55
Table 4.2	Recovered sediment for each drive for core YK0712B .....	88
Table 4.3	EBSD of aragonite in laminated section .....	108
Table 4.4	EBSD of calcite in laminated section .....	109
Table 4.5	EBSD analysis of aragonite in non-laminated section .....	110
Table 4.6	EBSD analysis of calcite in non-laminated section .....	111
Table 4.7	<sup>14</sup> C dating and calibration for YK0712B. Samples in bold used for age model; samples in italics not used, thought to show anomalously old dates as a result of old carbon from the hardwater effect. Relative area under probability distribution after Reimer et al 2013 .....	119
Table 5.1	Position of the thermocline (metres below the lake surface) in studied lakes over the sampling period.....	122
Table 5.2	Inferred timing of the end of the Holocene Optimum and transition to a weaker monsoon from Yeak Kara sediment δ <sup>18</sup> O records in the context of these changes in other geographical areas of the Asian monsoon .....	138

# CHAPTER 1: Purpose

The behavior of the Earth's hydrological system determines the type and distribution of ecosystems and human societies geographically and temporally (Bowen, 2011). In the Earth's tropics, human societies are directly reliant on the regularity and consistency in the timing and duration of rainfall through the year to support fisheries (Zahn, 2003; Badjeck et al., 2010; Allison et al., 2009; Stanford et al., 2013; Payne, 2013), agriculture (Overpeck and Cole, 2007; McPhaden et al., 2006; Sinha et al., 2011; Selvaraju et al., 2011; Wassmann et al., 2009; Zahn, 2003) and other natural resources (de Lopez, 2002). In the Asian tropics, changes in the amplitude and frequency of 'extreme' weather events can have particularly negative impacts on societies, displacing tens of thousands of people and costing millions of dollars to recover from (An et al., 2000, Kouadio et al., 2012; Guhathakurta et al., 2012; Wind et al., 2013). These issues are not only significant for modern societies, however – stability and variability in the Asian monsoon system have been instrumental factors in the rise, growth and fall of ancient civilisations (Buckley et al., 2010, Hodell et al., 2011; Wang et al., 2013). For example, during the 14<sup>th</sup>-15<sup>th</sup> centuries and again from the 17<sup>th</sup>-19<sup>th</sup> centuries, a series of multidecadal megadroughts were felt across monsoonal Asia, resulting in famine and political reorganisation in India and significant social upheaval in China, Sri Lanka and Cambodia's Khmer civilisations (Lieberman & Buckley, 2012; Sinha et al., 2011; Buckley et al., 2010; Wathen, 2011; Overpeck & Cole, 2006).

The Earth's climate is dynamic, with changes occurring over a range of timescales as a result of both internal and external climate forcing mechanisms (Bridgeman & Oliver, 2006; Wanner et al., 2008). The complexity of the Earth System is not fully represented in the instrumental record, which is spatially fragmentary and

rarely more than a century in length (Berkelhammer, 2010; Gadgil et al., 2007; Wang, 2002; Yuan et al., 2008; Rajeevan et al., 2008; Kucharski et al., 2008). It is necessary to look further back, however, to understand climatic processes and their forcing mechanisms which operate over long temporal and large geographic scales (Lunt et al., 2013). Climate-sensitive proxies preserved in natural archives such as sediment records, ice cores, tree-rings and speleothems are an effective tool to achieve this understanding (Cronin, 1999; Bradley, 1999). This knowledge can be used, then, in modelling future climate, aiding in the mitigation of the impacts of future extreme weather and climate events (Jung et al., 2004; Goswami & Krishnan, 2013; Kumaresan, 2011; Lunt et al., 2013; Lenton et al., 2008; Nutall, 2012)

### **The Asian monsoon over mainland Southeast Asia**

The Asian monsoon is the largest atmospheric circulation of its kind on Earth (Clift & Plumb, 2008). The rainfall regimes of the Asian monsoon system support, directly and indirectly, more than half of the Earth's population (Alley, 2003; Boyd, 2008). There are two sub-monsoons that form the Asian monsoon system, the Indian and East Asian monsoon systems. The geographical position of mainland Southeast Asia falls within the boundary zones of these two distinct sub-monsoon systems, making it an interesting area to observe the interactions of these sub-monsoons within the broader Asian monsoon system (Kumar et al., 2010; Yihui & Chan, 2005; Yan et al., 2011; Wang et al., 2003).

Forcing mechanisms, such as variation in insolation (Renssen et al., 2012; Berger & Loutre, 1991), are known to have a large influence on the strength and variability of the monsoon over long periods of time (Haug, 2001). Changes in the strength and timing of monsoonal rainfall are also mediated over small and large timescales by teleconnections with other parts of the global climate such as the El Niño Southern

Oscillation (ENSO) (Charles et al., 1997; Sarachik & Cane 2010; Bridgman & Oliver 2006), and the North Atlantic Oscillation and North Atlantic sea-surface temperatures (SST) (Hurrell, 1995; Black et al., 1999; Zuo et al., 2013; Nagashima & Tada, 2012).

The boundary conditions of the Earth's climate system have remained relatively stable since the last deglaciation, and current concerns about climate change in the near future require reference to this time period (the Holocene) and the light it can shed on the climate processes that are occurring today (Wanner et al., 2008; Buckley et al., 2010; Bridgman & Oliver, 2006). There is an increasingly well-resolved understanding of the response of the monsoon in various geographical provinces that it covers. However, within this, there has not thus far been a high-resolution direct climate proxy record of Holocene climate from mainland Southeast Asia (Clift & Plumb, 2008; Negendank, 2004, Cronin, 1999, Chiang, 2009). Located between two monsoon subsystems, this particular region has the potential to reveal a greater understanding of the coupling between the Indian and East Asian sub-monsoons, revealing the complex dynamics that exist within the Asian monsoon system (Jung et al., 2004; Black, 2002).

This research project aims to present a high-resolution, independently dated Holocene-aged record of climate variability from mainland Southeast Asia. A record of precipitation/evaporation based on stable isotopes preserved in the sediment of closed volcanic crater lakes will be used as a proxy for past monsoon behaviour. An earth systems science framework will be used to analyse the teleconnections between the tropical Asian monsoon as revealed in this new palaeoclimate record and other parts of the global climate system in the Holocene (Cronin, 1999; Lenton, 2012; Kageyama, 2012).

To understand the climate sensitivity of these Cambodian crater lakes, the limnology, geochemistry and stable isotope ( $\delta^{18}\text{O}$ ,  $\delta^2\text{H}$ ) dynamics in lake waters will be investigated with references to the impact of basin morphology of these crater lakes.

The stable isotope dynamics in lake waters will be compared to meteoric waters to investigate how these lakes are related to regional climate. Understanding these processes will give an insight into the palaeoclimate information archive held in sediment records, with the primary outcome of this study a  $\delta^{18}\text{O}$  stable isotope record from carbonates in the sediment.

## CHAPTER 2: Literature Review

This chapter will begin by describing the Asian monsoon circulation and its key sub-monsoon systems (the Indian monsoon and the East Asian monsoon). The forcing mechanisms and teleconnections that are major influences on these systems are then discussed, in order to understand the ways in which climatic change is mediated spatially and temporally in this region. To tie this together, the change in the geographical provinces of the monsoon system over the Holocene as recorded in direct climate proxies are then described and discussed, focusing on the mid-Holocene.

In order to better understand lake sediment archives and the proxy records they contain, the ways in which deep tropical lakes record climate and the associated stable isotope dynamics of precipitation in the tropics will then be considered.

### **2.1. The Asian monsoon climatic system**

The Asian monsoon is among the most important components of the global climate system. It is an important link in global-scale atmospheric circulation and the primary manifestation of the hydrological cycle in the tropics (Clift & Plumb, 2008). Geographically, the Asian monsoon covers the region from the western Arabian Sea, over the Indian subcontinent and East Asia, across the South China Sea and over parts of China and the Tibetan Plateau, as well as reaching over the equatorial and sub-equatorial Indian Ocean and over the Indonesian Islands and northernmost parts of Australia (Wang et al., 2005; Clift & Plumb, 2008).



*Figure 2.1: Region affected by the Asian monsoon (from Black, 2002, p. 528)*

The Asian monsoon is a complex set of subsystems, each with slightly different characteristics manifesting uniquely over different provinces depending on geographical scales and regions of interest. The two key monsoon provinces relevant to the mainland Southeast Asia region are the Indian monsoon and the East Asian monsoon. These systems are controlled by the same physical mechanisms; however, their underlying geography is different, resulting in sometimes quite distinct and different processes (Penny 2012).

The Asian summer monsoon is driven by trans-equatorial pressure differences that are sensitive to changes in insolation over time in tropical and subtropical areas (Leushner & Sirocko, 2003; Maher et al. 2008). Heating and cooling of terrestrial land masses and adjacent ocean areas occur out of phase as a result of their differing thermal properties. Thermal energy stored in the landmass is transferred to the air mass above much faster than oceans, and the resulting pressure gradient force causes low-level monsoonal winds (Penny, 2012; Riehl, 1979; Hastenrath, 1991). These are reversed during Northern-Hemisphere summer and winter in response to changes in the heating dynamics of the landmasses involved (Figure 2.1) and these processes are drivers for

larger-scale circulation and transfer of moisture through the Earth system (Liu et al., 2010; Leuschner et al., 2003; Hastenrath, 1991).

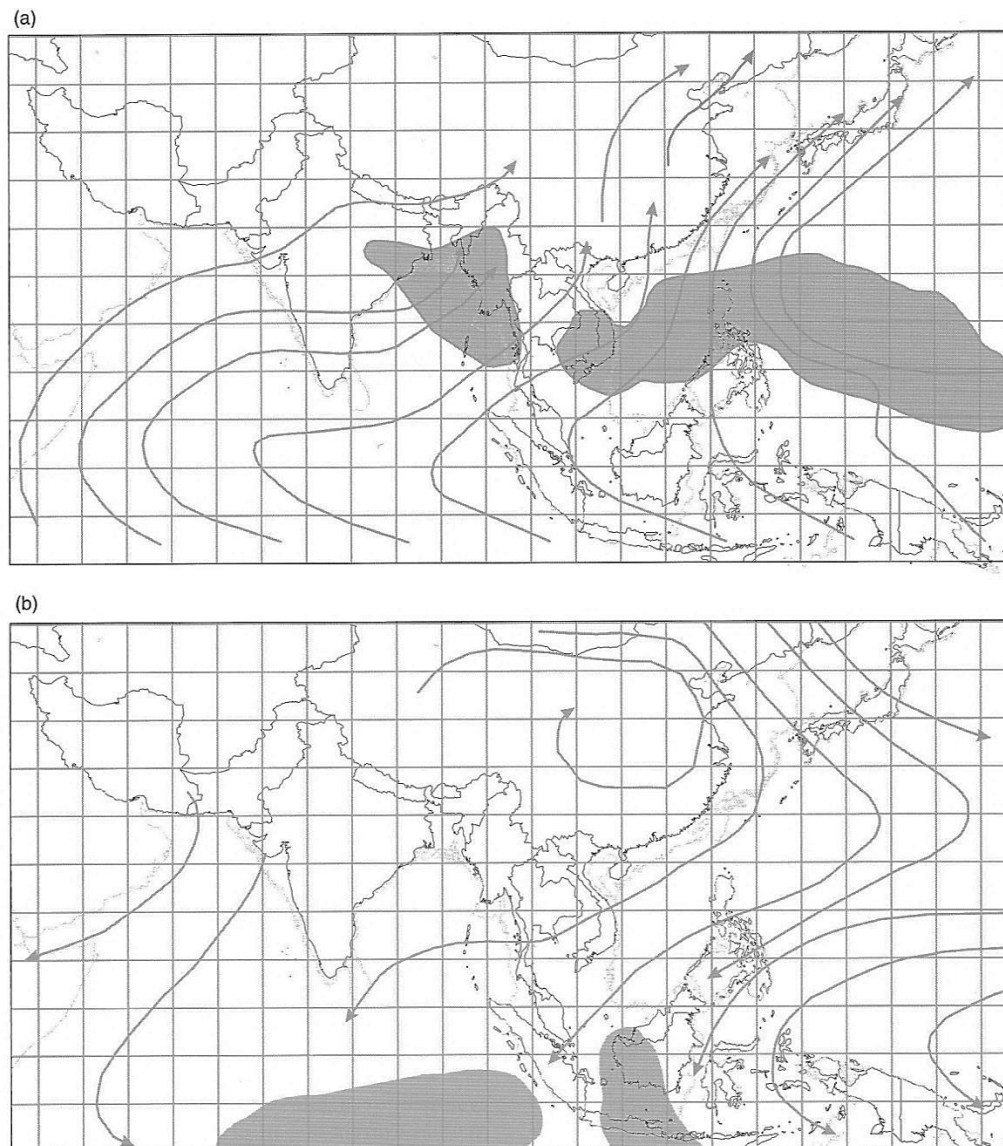


*Figure 2.2. Schematic representation of (a) summer (August) and (b) winter (January) low level monsoon winds over Asia and associated areas of intense precipitation. Grey shaded areas indicate rainfall in excess of 300mm/month. Precipitation data NOAA NCEP CPC CAMS\_OPI, wind data NOAA NCEP-NCAR CDAS-1 mc6190 Intrinsic Pressure Level x 925mb. Data source: National Weather Service Climate Prediction Centre (data are not subject to copyright protection). Image and caption sourced from Penny, 2012, p. 209.*

Terrestrial and oceanic regions affected by the Asian monsoon experience a biannual change in meteorological conditions – a wet summer monsoon, which brings precipitation onto continental areas, and a dry winter monsoon during which there are low amounts of precipitation in these areas (Clift & Plumb, 2008). The summer and



winter monsoons are loosely coupled systems which respond to a range of internal and external forcing mechanisms over a range of timescales (Clift & Plumb, 2008). Mainland Southeast Asia lies on the boundary of the Indian summer monsoon (ISM) and the East Asian summer monsoon (EASM), making it an important location to understand the relationship between these two subsystems and teleconnections that exist between the monsoon and other components of the Earth's climate system. This knowledge can aid in the development of robust climate models for the projection of future climate change (Masson-Delmotte et al., 2013; Collins & Long, 2012; Clement, 2012; Dearing, 2013).

Forcing mechanisms directly and indirectly impact the Asian summer and winter monsoons, causing variations in strength of each subsystem and in seasonality over time (Bradley, 1999, 2005; Maher et al. 2008). This manifests as leads and lags in the onset and duration of climatic changes in different parts of the Asian monsoon system (Leng & Marshall, 2004; Shakun et al., 2007). Climatic trends overlay and control weather, and study of the Asian monsoon system through proxy records stored in terrestrial and marine archives indicate that, through the Holocene the Asian monsoon has changed strength. In both the Indian monsoon and the East Asian monsoon systems there was a strong and rapid intensification of the summer monsoon at the Pleistocene-Holocene transition which peaked in response to insolation forcing during a period known as the Holocene Optimum, followed by a weakening of summer monsoon flow through the late Holocene to drier conditions that in some cases are comparable to the present-day monsoon systems. There are debates in the literature regarding the rate and timing of these phase changes of the Asian monsoon system (discussed further below).

Changes in insolation through the Holocene have been instrumental in the evolution of monsoonal strength (Hoyt & Schatten, 1997). Through the late to early Holocene, the pole-to-equator insolation gradient decreased as summer insolation in the Northern-Hemisphere decreased (Berger & Loutre, 1991). This resulted in an

increase of the relative temperature gradient in the Northern-Hemisphere, which impacted the position of the ITCZ (Cai et al., 2012; Dong et al., 2010; Haug et al., 2001; Fleitmann et al., 2007; Gergana et al., 2007). The precession-driven shift in timing of Northern-Hemisphere peak insolation through the early and mid-Holocene amplified contrasts between the Asian summer and winter monsoon, which increased seasonality compared to the early Holocene (Maher, 2008; Cosford et al., 2008).

The strength of the Asian monsoon subsystems (Indian and East Asian) have been linked to changes in atmospheric and oceanic circulation regimes in the North Atlantic (North Atlantic Oscillation and sea-surface temperatures respectively). Strong summer monsoonal rainfall has a tendency to correlate with anomalous high sea-surface temperature anomalies in the northwest Atlantic and low temperatures in the tropical and subpolar ocean (North Atlantic sea-surface temperature tripole) over decadal timescales (Gu et al., 2009; Black et al., 1999; Berkelhammer et al., 2010). The North Atlantic is teleconnected to the Asian summer monsoon through atmospheric processes via diabatic heating of the North Atlantic-Eurasia region which impacts energy dispersion through Rossby waves (Zou et al., 2013). In addition, changes in the oceanic thermohaline circulation that originate in the North Atlantic due to changes in solar activity could result in a cooling of (and decrease in warmth delivered to) the Indian Ocean, which would then act to enhance the heat differential between the ocean and landmass, impacting the strength of summer monsoon flow (Hong et al., 2003; Cai et al., 2012; Charles et al., 1997). Similar teleconnections have been made between sea-surface temperatures in the western tropical Pacific, the primary moisture source for the East Asian monsoon, to changes in rainfall over continental areas of East and South China (Jiang et al. 2012).

The Asian summer monsoon has been linked to the palaeo-ENSO through ocean thermohaline circulations, which facilitated a connection between the North Atlantic

ice-raft debris events and sea-surface temperatures and the tropical Pacific during the deglaciation (Hong et al., 2003, 2005; Selvaraj et al., 2007). The Hongyuan peat bog in the Tibetan Plateau and Kusai Lake, northwest China, shows evidence of the teleconnections between the North Atlantic and the Asian monsoon continuing into the Holocene (Hong et al., 2003, 2005; Liu et al., 2009b, Bond et al., 1997, 2001). The mechanism behind this teleconnection is believed to be abrupt reorganisation of the ocean thermohaline circulation, causing redistribution of energy in the oceans and changing temperature and moisture gradients in the subtropical Indian Ocean, hence affecting the land-sea thermal contrast which drives Indian monsoonal circulation (Sung et al., 2006; Huang & Sun, 1992; Zhou et al., 2012; Rogers, 1984). Tree-ring records in Java, Indonesia, have suggested a link between Pacific and Indian Oceans impacting upon monsoonal precipitation through ENSO (D'Arrigo et al., 2008). Terrestrial records of Indian Monsoon precipitation in India from the late Holocene (Charles et al., 1997; Yadava & Ramesh, 2005, 2007; Sinha et al., 2007) report teleconnections between the Asian monsoon and solar activity and ENSO in the late Holocene period, while some marine records show linkages between the Indo-Pacific Warm Pool and ENSO impacting monsoonal circulation in the Holocene (Gagan et al., 2004; Wanner & Bronniman, 2012). There is evidence of megadroughts in India in the 14<sup>th</sup> and 15<sup>th</sup> centuries (Sinha et al., 2007), and broad-scale abrupt climate change events, for example the Little Ice Age (ca. 1400-1850 A.D.) (Mann, 2002a) and Medieval Warm Period (ca. 900-1300 A.D.) (Mann, 2002b), have been recorded in the Indian speleothems. Links have also been made in historic records showing lower summer monsoonal rainfall when the Pacific Decadal Oscillation and ENSO are in phase and vice versa (Chan & Zhou, 2005).

There is a large body of work focused particularly on the Quaternary history of the Asian monsoon, representing the last 2.6 million years, including the most recent glacial maximum and the subsequent deglaciation (Shakun et al., 2007, Alley et al., 1993,

Anderson et al., 1993; Burns et al., 2003; Chiang et al., 2003; Chiang & Bitz, 2005; Dykoski et al., 2005; Hughen et al., 1996; Hughen et al., 2000; Lea et al., 2000; Lea et al., 2003; Overpeck et al., 1996; Sinha et al., 2005; Sirocko et al., 1996; Wang et al., 2005; Yadava & Ramesh 2007). There are, however, fewer higher-resolution records of Holocene climate, particularly in regions on the boundary between Indian and East Asian monsoon provinces. It is important to extend the body of knowledge regarding the dynamics and mechanisms of the Asian monsoon system as a whole, as well as the interactions and couplings between subsystems, in the context of the global climate system (Jouzel et al., 2000; Thompson et al., 2006).

The majority of terrestrial archives of Holocene Asian monsoon climate capture changes in precipitation in the summer monsoon over time. There are a number of studies that consider the Indian summer monsoon in Oman using speleothem archives and the Arabian Sea using sediment archives that extend through the early to late Holocene (Anderson et al., 2010; Clemens et al., 1991; Tiwari et al., 2006; Doose-Rolinski et al., 2001; Sirocko et al., 1993; Gupta et al., 2003, 2005), however speleothem studies in India do not extend back beyond the early to mid Holocene (Sinha et al., 2007). The Tibetan plateau has a number of lake sediment studies that extend through the Holocene, and in Southwest China there are some key speleothem studies which capture changes in the Asian monsoon at the boundary between the Indian and East Asian provinces, as will be further discussed. In South China and Central China, there are also a host of key studies in Holocene climate dynamics of the East Asian summer monsoon utilising speleothem archives. Over all of these studies, there is debate surrounding the timing and rate of change of the transition from the Holocene Optimum in both the Indian and East Asian subsystems, where a strong summer monsoon from the early Holocene weakened (Nakamura et al., 2012). The timing and extent of this transition through the entire Asian monsoon system is not clearly resolved, as there is a

low density of studies into the response of the Asian monsoon provinces in the mid Holocene provinces through the South and Southeast Asia region (Charles et al., 1997; Yadava & Ramesh, 2005, 2007; Sinha et al., 2007; Berkelhammer et al., 2010; Sinha et al., 2007). Mainland Southeast Asia is an ideal location to explore this further, due to its key location on the boundary between the Indian summer monsoon province and the East Asian summer monsoon province.

The exploration of changes in the strength of the summer monsoon alongside the winter monsoon, expressed as increases or decreases in seasonality, are not common in high-resolution terrestrial records. Marine sediment records are more often used to consider changes in strength and stability of the Indian winter monsoon (such as studies in the Arabian Sea by Gupta et al., 2005; Thamban et al., 2007; Anderson et al., 2002) and East Asian winter monsoon (such as studies in the South China Sea by Steinke et al., 2011; Liu et al., 2010; Wang et al., 1999). Although the primary focus of this study is the changing precipitation dynamics over the mainland Southeast Asian region through the Holocene, mention will be made of changes in seasonality linked to the winter monsoon.

A number of abrupt climatic changes have been recorded in palaeoclimatic studies of the Asian monsoon. These abrupt changes have been very rapid reorganisations in the ocean-atmosphere system passing through teleconnections to manifest in changes in monsoon circulations (and other parts of the Earth system) (Trenberth et al., 2000; Street-Perrot & Perrot, 1990; Wanner et al., 2011). North Atlantic Cold Events (Bond et al., 1997) are of key interest to the Asian monsoon as they have been recorded in records from a number of sites (Thamban et al., 2007; Morrill et al., 2003; Overpeck & Cole, 2006; Wang et al., 2005; Mayewksi et al., 2004; Stager & Mayewski, 1997).

## **2.2. Changes in Holocene precipitation dynamics of the Indian and East Asian summer monsoons from direct climate proxy records**

The Holocene Optimum was a period of peak postglacial warmth related to orbitally-forced insolation changes in the precession band, amplified by feedback mechanisms internal to the Earth System (Renssen et al., 2012). Precipitation records from various areas around the Earth correlate with this temperature optimum, indicating a generally warm, humid period between 9-5ka BP that occurred asynchronously across the globe with anomalies of  $>5^{\circ}\text{C}$  in high latitudes and as small as  $<0.5^{\circ}\text{C}$  over tropical oceans compared to the preindustrial climate (Renssen et al., 2012). In the body of literature exploring the behavior of the Asian monsoon through the Holocene, there are spatial variations in the reported time of weakening of the summer monsoon circulation in the early-mid Holocene, after the wet Holocene optimum period. Table 2.1. shows broad trends in the difference geographical regions of the Asian monsoon relevant to this study.

Fleitmann et al., (2006), Fleitmann et al., (2003) and Neff et al., (2001) concluded that changes in the mean latitudinal position of the intertropical convergence zone (ITCZ) are related strongly to changes in the hydrological cycle in the tropics. They interpret the continuous southward migration of the ITCZ during the mid to late Holocene, a result of solar forcing as a result of changes in insolation, being instrumental in the gradual decrease in the strength of the Indian summer monsoon over the Oman region. Speleothem records from Hoti cave in Northern Oman, Qunf and Defore Cave in Southern Oman, and Dimarshim Cave in Socotra, Yemen suggest that in this region, monsoon precipitation was generally high from 9.6-5.5 yrBP, with a long-term gradual decrease in monsoonal precipitation starting at  $\sim 8\text{ka BP}$ . There is a hiatus in the record from 2.7-1.4ka BP, and when the stalagmite record resumed at 0.4ka BP,  $\delta^{18}\text{O}$  values are

Table 2.1: Chronology of inferred precipitation changes of the summer monsoon strength in different regions and sub-monsoons of the Asian monsoon system through the late to early Holocene. Upper boundary of 'gradual weakening' of monsoon flow due in some cases to the termination of available records.

Region	<sup>14</sup> C yr	1000	2000	3000	4000	5000	6000	7000	8000	9000
	Cal yr BP	930	1940	3200	4400	5700	6800	7800	8800	10000
Oman	Indian Summer Monsoon				Gradual weakening				Strong summer monsoon	
Tibetan Plateau	Indian Summer Monsoon / East Asian Summer monsoon	Gradual weakening					Asynchronous start of weakening	Strong summer monsoon		
Southwest China	Indian summer monsoon / East Asian Summer monsoon		Gradual weakening				Strong summer monsoon			
South China	East Asian Summer monsoon	Gradual weakening						Strong summer monsoon		
Central China	East Asian Summer monsoon	Gradual weakening					Strong summer monsoon			

comparable to the present day. Although providing a valuable insight into the dynamics and mechanisms of the Indian summer monsoon in this region of the monsoon province, these records are not definitive, with fragmentary time series spanning a very narrow latitudinal transect and thus not able to capture broad scale temporal or latitudinal responses to changes in the position of the ITCZ comprehensively. However, their contribution to understanding the dynamics and mechanisms of the Indian summer monsoon is, nonetheless, valuable.

In India, speleothem records tend to cover the early or late Holocene. The amount effect, a distinctive feature of stable isotopes in precipitation in tropical areas defined by Dansgaard (1964) & Rozanski et al., (1993) which will be described in detail later in this chapter, strongly influences the oxygen stable isotope records in this region (Yadava & Ramesh, 2005, 2007). Studies from Akalgavi cave in the UK district of India link seasonal, decadal and century-scale variability in the Indian summer monsoon to solar activity, with a number of large-scale droughts in the past 2ka BP linked to low solar activity and (Yadava & Ramesh, 2007; Bhattacharya & Narasimha, 2005). Late Holocene records from Dandak cave in Chhattisgarh, southern central India, link multidecadal sea-surface temperature variability in the North Atlantic (North Atlantic Oscillation, NAO) with variability in Indian summer monsoon rainfall amount (Sinha et al., 2007; Berkelhammer et al., 2009). The Indian summer monsoon maintains a strong teleconnections with the NAO and the El Nino southern oscillation (ENSO) over multidecadal timescales which may have weakened through the late Holocene (Berkelhammer et al., 2009; Krishna Kumar et al., 1999). Changes in the North Atlantic cause a displacement of the ITCZ and intensification of the low-level monsoon jet, and impact the meridional temperature gradient across the south Asian landmass (Li et al 2008, 2013; Goswami et al., 2006; Berkelhammer et al., 2009; Srivastava et al., 2002). ENSO influences on ISM are thought to be dependent upon prevailing regional boundary



conditions and so are non-stationary, varying with changes to other boundary conditions such as the Indian Ocean Dipole (IOD) (Goswami & Xavier, 2005; Kumar et al., 2006; Ashok et al., 2004; Chang et al., 2001). Although these records are relatively short in timescale, the insight they offer on the mechanisms involved in change in the broader Asian monsoon highlight the importance of understanding the full spectrum of monsoon behavior on all timescales (Berkelhammer et al., 2009; Meehl et al., 2009).

Over long time scales, the Qinghai-Tibet Plateau has impacted the evolution of the Asian monsoon, and continues to strongly impact upon global circulation dynamics (Cai et al., 2012). Clear responses to orbitally-forced insolation changes in the Holocene and teleconnections to high Northern latitude temperature changes and NOA on a variety of timescales have been made in studies on the Indian summer monsoon in this region (Liu et al., 2009a; Bard & Frank, 2006; Shen et al., 2005; Rind, 2002; An et al., 2001; Ruddiman & Kutzbach, 1991; Overpeck et al., 1996; Haigh, 1996; Gasse et al., 1991; Thompson et al., 1989). Records from the Tibetan Plateau indicate strong early-mid Holocene Indian summer and East Asian summer monsoons which persisted as far into the mid-Holocene as 5500 yr BP before a gradual decline through the mid to late Holocene (Cai et al., 2012; Zhang et al., 2011; Hong et al 2003). Other studies suggest abrupt declines in summer monsoon strength at 7500-7000 yr BP, and again at 4700 yr BP in this region (Morrill et al., 2006). Recent speleothem aragonite records from Siddha Baba Cave, central Nepal, suggest a recent shift towards more humid conditions in the region since ~1.5kaBP (Denniston et al, 2000).

The  $\delta^{18}\text{O}$  record from Shigao cave in Southwest China clearly shows evidence for strong summer monsoonal circulation from the early Holocene until 6.6 kaBP, after which there is a gradual decline in precipitation until 1.6ka BP and relatively low precipitation from 1.6 kaBP until the present (Jiang et al., 2011). This cave is located in an area that receives rainfall from both the Indian summer and East Asian summer

monsoons, thus receiving moisture sourced from both the Indian Ocean and the western tropical Pacific. It is suggested that this combination of moisture sources contributed to the spatially asynchronous end of Holocene Optimum conditions in this region (Jiang et al., 2011; Liu et al., 2008).

Dongge cave in Southern China (Wang et al., 2005; Dykoski et al., 2005; Hu et al., 2008) shows a strong East Asian summer monsoon circulation from 9-7ka BY, followed by a gradual weakening until 0.2 kaBP. Sanbao cave in Central China shows evidence for a strong East Asian summer monsoon circulation through the early Holocene to 9.5ka BP followed by a relatively stable period from 9.5-6.5ka BP, after which there is a gradual decrease in intensity of monsoonal flow until 0.2 kaBP (Dong et al., 2010). This is a key record of East Asian monsoon summer variability through the Holocene, however Maher (2008) argues that these records could be reinterpreted to represent rainfall source rather than rainfall amount. Zhang et al (2011) suggest that rainfall dynamics in the Indian summer monsoon provinces and the East Asian summer monsoon provinces are different, as are their moisture sources. This reinforces the need to further clarify the dynamics of the interactions of the Indian summer monsoon and East Asian summer monsoon.

The Cambodian crater lakes, which will be considered in this study, are relatively unstudied and their value as archives for Holocene climate change and variability is almost untapped. Maxwell (1999) conducted the first study exploring the use of lake sediment archives from these lakes, undertaking sedimentological and palynological study on the sediments of Yeak Kara. Based upon his analyses, he constructed a high-resolution record of the major transitions in monsoon behavior from an abrupt transition to a warmer, more humid system at the Pleistocene-Holocene transition ca. 8400 <sup>14</sup>C BP, a Holocene Maximum where the summer monsoon was at its strongest through the Holocene from 8400-5300 <sup>14</sup>C BP, a sharp transition to a dryer monsoon

from 5300 <sup>14</sup>C BP. Maxwell's core was not absolute dated and generated a vegetation record to indicate these climatic shifts and transitions. Vegetation filters the climate signal, and Maxwell's work serves to highlight the potential of these lakes for palaeoclimate studies, begging the possibilities for the possibility of a high-resolution absolute-dated record using a direct climate proxy for clarifying the behavior of the monsoon over mainland Southeast Asia over these time periods.

## **2.3. Lake sediments as proxies for past climate**

### **2.3.1. Deep tropical lakes and climate**

Lakes in tropical regions differ in a number of ways from lakes in mid and high latitudes (Lewis Jr., 1996). Primarily, lakes in the tropics receive higher annual irradiance with little variation through the year as compared to lakes of higher latitudes (Lewis, 1987). This has key implications for the temperature and density dynamics in tropical lakes, where mixing is not as strongly related to changes in temperature as a result of seasonality as in higher latitudes (Lewis, 2010). Water bodies can be much more stable in tropical areas and biological yields can be quite high because of higher temperatures through the year (Lewis, 2010). Mixing in tropical lakes is linked to changes to the meteorological and climatic parameters of wind stress and heat content due to low Coriolis effect, low maximum stability and high response of stability to changes in heat content, unlike temperate and polar lakes which are more sensitive to seasonal temperature (Lewis, 1987; Williams, 2013; Cohen et al., 2003). Deep stratified tropical lakes can produce high-resolution archives of past climate, as they can have high sedimentation rates as a result of high primary productivity, accompanied by low levels of sediment disturbance due to anoxic conditions near the lake bottom as a result of stratification (Zolitschka, 2005).

Stable isotopes in lake sediment archives are commonly used as a proxy for past climate (Leng & Marshall, 2004). When considering past climate, it is of vital importance to consider how the proxy links to past climatic conditions, which is often quite complex, in order to ensure that the interpretation is valid (Darling, 2003; Li & Ku, 1997; Gat & Lister, 1995). A number of closed-basin stratified lakes have been studied for present day limnological characteristics (e.g. Katsev et al., 2010; Reid et al., 2012; Kebede et al., 2006; Holm-Hansen et al., 1976; Crowe et al., 2008) and palaeoclimate in China (Johnson & Ingram, 2004; Peng et al., 2005; Wang et al., 2008; Hodell et al., 1999), Siberia (Kalugin et al., 2013), Tibet (Cai et al., 2012; Liu et al., 2009), South America (Vazquez et al., 2004; Schwalb et al., 1999; Lewis & Welbezahn, 1981), North America (Schelske & Hodell, 1995, 1991; Treese et al., 1981; Brenner et al., 1999; Kirby et al., 2004; Cohen et al., 2000), Africa (Lamb et al., 2005; Blaauw et al., 2011; Shanahan et al., 2008, 2007; Giresse et al., 1991), Greenland (Anderson & Leng, 2004), Europe (Leng et al., 1999; Mingram, 1998), Switzerland (Teranes & McKenzie, 2001; Schaller et al., 1997), Indoneisa (Crausbay et al., 2006) and Australia (Walker, 2007; Walker et al., 2000; Last & de Deckker, 1990; Chivas et al., 1993).

In closed-basin stratified lakes, vertical mixing can be a vehicle for the resupply of nutrients from nutrient-rich hypolimnion waters to epilimnion waters (Lewis Jr, 2010; Hodell et al., 1998; Walter, 2002; Chu et al. 2000; Nelson et al., 2009). Such conditions do not occur annually in tropical lakes but are triggered by changes in meteorological conditions, which are mediated by climate forcing mechanisms on longer timescales (Leng & Marshall, 2004; Boehrer & Schultze, 2008; Williams, 2013; Brauer et al., 2004). Biogenic carbonates form when calcium ions, normally in solution in the surface waters of the lake, precipitate out due to super-saturation in response to increasing alkalinity (Rickaby & Schrag, 2005; Nelson et al., 2009; Leng & Marshall, 2004). This increase in alkalinity occurs as a result of a surge of biological activity, for example algal blooms, in

response to lake turnover whereby nutrient-rich hypolimnion waters mix with epilimnion waters, resulting in increased nutrient availability in surface waters. These carbonates may form as euhedral crystals in the water column or as early-diagenetic features within the sediment column (Rickaby & Schrag, 2005; Nelson et al., 2009). The distinction between these pathways of precipitation is critical from a climate science perspective, because carbonates that form in the sediment column record the isotope chemistry of interstitial pore waters rather than lake surface waters, while lake surface waters are exposed to climate variations (Eugster et al., 1978; Leng & Marshall, 2004).

### **2.3.2. Stable isotopes and the amount effect in tropical areas**

Stable isotopes in precipitation are a key tool in understanding the dynamics of monsoon processes and driving mechanisms over time. The complexities of isotopic fractionation during processes such as precipitation, condensation and mixing within air masses during transportation can highlight regional-scale processes and patterns in stable isotope distribution (Rozanski, 2005; Gat, 2005; Liu et al., 2009; Wei & Gasse, 1999; He et al., 2006; Jouzel et al., 2000; Aggarwal et al., 2004; Rozanski et al., 1992; Singh, 2013; Gourcy et al., 2005). These features also occur on regional scales, but can be blurred in broad-scale global analyses (Kurita et al., 2009). In addition to spatial variations in isotope distribution, there are temporal variations that occur on a range of time scales from minutes to decades and longer, and these can be linked to broader-scale regional and global processes (Jouzel et al., 2005).

In low-latitude areas, there is a strong negative correlation between the amount of precipitation and stable isotope ratios in precipitation and weak correlation with temperature on regional scales, known as the amount effect (Dansgaard, 1964; Rozanski et al., 1993). The amount effect is potentially of particular interest in this study, which

focuses on the Asian tropics, as it is the principal factor controlling spatial and temporal distribution of stable isotope in precipitation in tropical areas. At 30°N/S, there is a sharp transition in the dominating factor affecting the isotopic content of precipitation from the amount effect to the temperature effect (Bowen, 2008). Rainfall in the Asian monsoon region tends to display the amount effect in summer (monsoonal) precipitation. Analyses of stable isotope values of precipitation in the Asian monsoon region reveal rhythmic cycles over the course of a year, with depletion in measured values evident during monsoonal (summer) months and enrichment in dryer months in a range of studies that have been carried out on the isotopic composition of meteoric waters of mainland southeast Asia (Yang et al., 2011, Aggarwal et al., 2004; Kumar et al., 2010a, 2010b; Warriar & Babu, 2011; Araguas-Araguas & Froehlich, 1998; Bhattacharya et al., 2003; He et al., 2006; Conroy & Overpeck, 2011). Sites across this area vary in specific timing of monsoonal rainfall. However, the same trend in the isotopic content of precipitation during wet and dry months appears across the region. Although the amount effect is a dominating factor influencing the isotopic content of precipitation throughout the year, temperature, distance from the coast (continentality) and altitude coexist alongside it although having significantly weaker influence on the isotopic content of precipitation (van der Veer et al., 2009).

## CHAPTER 3: Materials & Methods

This chapter has three key themes –the geochemistry of lake waters, links between stable isotope dynamics in meteoric and lake waters, and the details of sediment archives of palaeoclimate. The field, laboratory and data analysis methods used in each of these will now be described after the study sites and sampling periods are introduced.

### 3.1. Study sites

This study is focused on Ratanakiri province, northeastern Cambodia (Figure 3.1).



Figure 3.1: Location of study region in a global context

Within this province there are a number of maar lakes – Yeak Loam, Yeak Oam, Yeak Kara and Boeng Lumkut near the small town of Ban Lung (Figure 3.2).



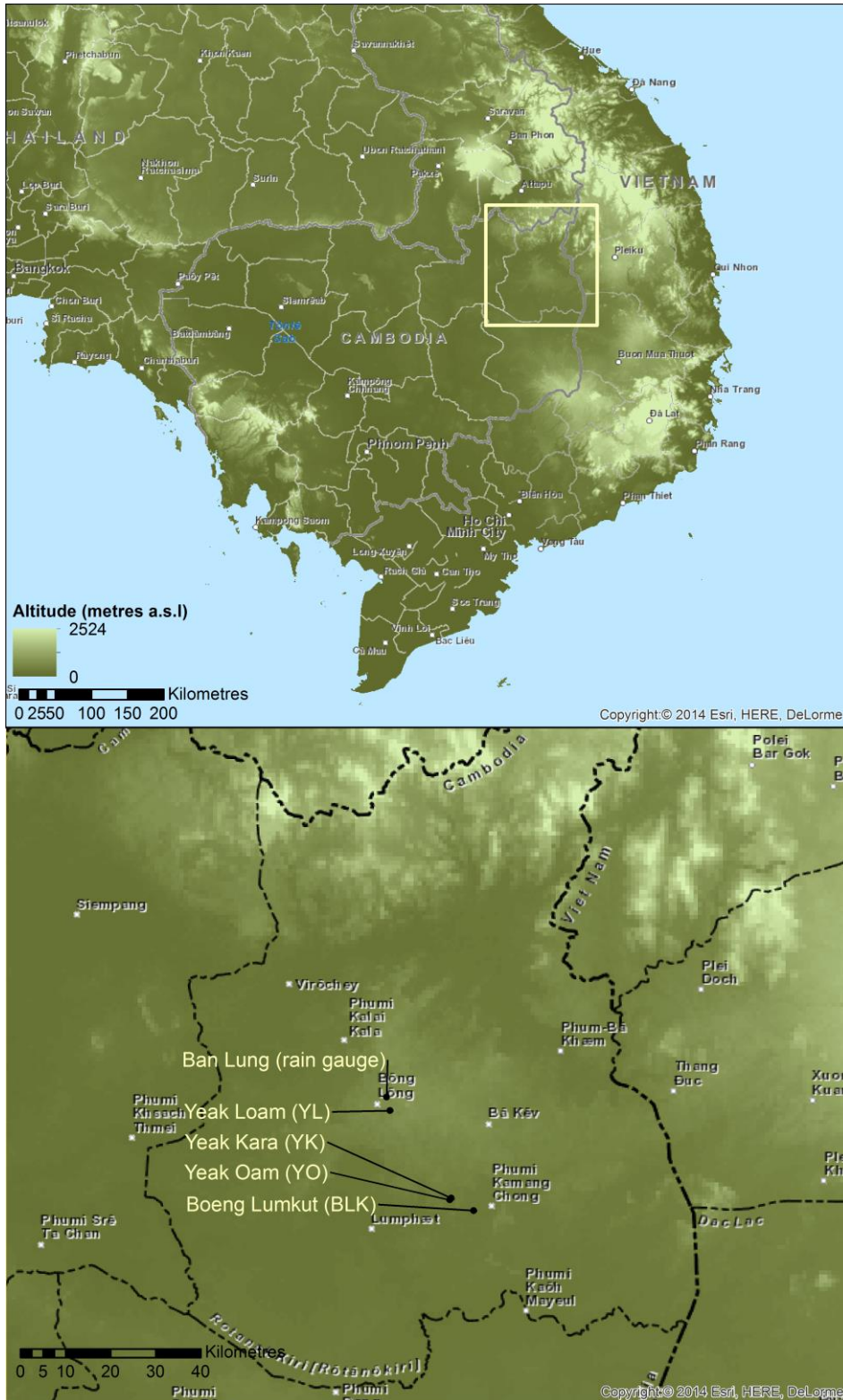


Figure 3.2: The location of the Cambodian crater lakes in the Ratanakiri province

The Cambodian crater lakes are maars located in north-eastern Cambodia. A large, diffuse basalt province produced in the Cenozoic extends over large parts of

northeast Cambodia, central Vietnam and southern Laos (Hoang & Flower 1988). A series of phreatic explosions have occurred in this basalt, resulting in the formation of a number of hollows that have since filled with water and formed lakes. Over time, aeolian-derived, eroded and authigenically produced material fill the crater basins, settling as sediment at the bottoms of these lakes (Wetzel, 1957).

Lake waters have been sampled with depth over time to investigate patterns of change in water quality, chemistry and stable isotopes, and sediments have been cored and analysed for geochemistry and stable isotopes.

*Table 3.1: Qualitative summary of meteorological conditions in Ratanakiri province during monitoring expeditions*

<b>Time period</b>	<b>Nov/Dec 2011</b>	<b>February 2012</b>	<b>July 2012</b>	<b>November 2012</b>	<b>April 2013</b>
<b>Active monsoon period</b>	Dry (start of NE Winter monsoon)	Dry (mid/end of NE Winter monsoon)	Wet (start of SW Summer monsoon)	Dry (start of NE Winter monsoon)	Wet (start of SW Summer monsoon)
<b>Temperature</b>	Low, decreasing	High, increasing	High, decreasing	Low, decreasing	Peak hot
<b>Precipitation</b>	Low	Low	High	Low	High

Water samples taken in Nov/Dec 2011, February 2012 and November 2012 are taken to be representative of stages of the dry winter (northwest) monsoon (Table 3.1). Within these samples, Nov/Dec 2011 and Nov 2012 samples are noted to be closer the beginning of the dry season, while Feb 2012 samples are more towards the end of the dry season, and limnological, biogeochemical and isotopic processes for these time periods are interpreted within this context. Samples taken in July 2012 and April 2013 are taken to give an indication of how these processes respond to the beginning of the wet season brought on by rainfall from the southeast. Within these two samples, in April

2013 annual temperatures were at their peak, while in July 2012 temperatures were declining.

## **3.2. Limnology and geochemistry of tropical crater lakes**

### **3.2.1. Data acquisition**

#### **3.2.1.1. Field Methods**

##### **3.2.1.1. a. Bathymetric survey**

In a lake system, basin morphology can control to a large degree the types of physical, chemical and biological processes that occur and the timing and rates at which they change (Wetzel, 1957). In late November-early December 2011, sonar and GPS measurements were used to conduct bathymetric surveys for all lakes, and these data were used to estimate water depth and basin morphology.

Sonar depth measurements were taken using a single-beam CEESTAR sonar with a high-frequency transducer affixed to an inflatable boat. The sonar procured depth measurements (in metres) every second along a series of parallel and perpendicular swaths across the lakes. A Trimble Nomad GPS running ArcPAD 10 provided coordinates (WGS-84 UTM zone 48N) for each measurement, and the data were streamed to a laptop using HyperTerminal. Bathymetric maps were subsequently made, and these data were used to assist in selecting suitable sites for sediment coring, specifically to avoid slopes and areas adjacent to slopes where slides and debris flow could potentially compromise the sediment sequence, and to assist in understanding the limnological and biogeochemical processes within these lakes. The locations selected for sediment coring were used as reference points for all subsequent water sampling, relocated at the time of sampling using GPS coordinates.

### 3.2.1.1. b. Water quality profiling

In order to understand the limnological characteristics through the water columns of these lakes over time, water quality profiling was conducted on all lakes (Yeak Loam, Boeng Lumkut, Yeak Kara, Yeak Oam) at roughly four month intervals over the course of the fifteen-month period spanning December 2012 to April 2013 (November/December 2011, February 2012, July 2012, November 2012 and April 2013) in order to monitor changes in water chemistry over time. Bathymetry data were used to select the deepest point in the lake basin to deploy the sonde, enabling a comprehensive snapshot of the water column to be captured (Table 3.2).

*Table 3.2: Sampling locations*

<i>Location</i>	<i>Latitude (decimal degrees)</i>	<i>Longitude (decimal degrees)</i>
Yeak Loam	13.726640 N	107.018480 E
Yeak Lumkut	13.526621 N	107.184905 E
Yeak Oam	13.547023N	107.137071 E
Yeak Kara	13.549304 N	107.139844 E

A YSI L6920V2-M water quality sonde was used to measure depth (m), temperature (°C), electrical conductivity (uS/cm), pH and optical dissolved oxygen (saturation %). The sonde was fitted with a number of probes (YSI 6560 conductivity/temperature probe, YSI 6160+ ROX optical dissolved oxygen sensor and YSI 6561 pH sensor) and calibrated using EcoWatch Lite 1.0.0.3. Conductivity and temperature were calibrated in the lab, while pH and dissolved oxygen were calibrated in the field prior to deployment (for pH calibration, an acidic standard at pH 4.0 was used alongside a neutral standard).

Using a laptop, the EcoWatch software package was used to program the sonde to record measurements at one-second intervals in unattended mode. Measurements of

water quality parameters were captured as the sonde was deployed at a slow, steady rate vertically through the water column.

### **3.2.1.1. c. Major ions analysis**

The analysis of major ions in lake waters with depth over time gives insights into the chemical processes occurring within the lakes as well as biological and geochemical processes and their triggers (Eugster & Hardy, 1978).

The collection of lake water samples for major ion analysis using ICP-AES occurred alongside and in the same locations as sonde measurements of in-situ water column water quality measurements. A Ruttner water sampler attached to a rope that had been pre-marked at one metre increments was used to collect discrete water samples at ten-metre depth intervals. For each sample, a 500 mL plastic beaker was triple rinsed with collected water before being filled with sample water. A 12 mL volumetric syringe fitted with a 0.45 µm filter was used to fill two 7mL plastic centrifuge tubes, to which a few drops of nitric acid were added. The acid was used to reduce the pH of the sample to prevent elements in solution precipitating in transit. In order to check for precision during ICP-AES, duplicate samples were taken at each sampling depth.

### **3.2.1.2. Laboratory methods**

#### **3.2.1.2. a. ICP-AES elemental analysis for major ions**

To understand the changes in distribution and concentration of nutrients in the water columns of the studied lakes, a selection of major ions were measured from water

samples using an Inductively Coupled Plasma Atomic Emissions Spectroscopy unit (ICP-AES) concurrently at specific wavelengths - calcium (measurement  $\lambda = 317.933$ ), potassium (measurement  $\lambda = 766.491$ ), magnesium (measurement  $\lambda = 279.800$ ), sodium (measurement  $\lambda = 589.592$ ), sulfur (measurement  $\lambda = 181.972$ ), iron (measurement  $\lambda = 238.204$ ), aluminium (measurement =  $\lambda 396.152$ ), barium (measurement  $\lambda = 455.403$ ), silica (measurement  $\lambda = 181.972$ ) and strontium (measurement  $\lambda = 407.771$ ). Wavelengths against which each element was measured were chosen to provide the best balance between sensitivity and minimal interferences from other elements.

Four standards for each element of interest were made over the range of expected concentrations, with concentrations doubling for each successive standard (Table 3.3). Standards were prepared by serial dilution from a commercially prepared standard solution containing all elements to be determined used alongside blanks of distilled water for calibration.

*Table 3.3: Details of standards prepared for ICP-AES analysis of lake water samples*

Element:	Al	Ba	Ca	Fe	K	Mg	Na	S	Si	Sr
Blank (distilled water)	0	0	0	0	0	0	0	0	0	0
Standard 1	2.5	0.625	2.5	2.5	2.5	2.5	2.5			0.625
Standard 2	5	1.25	5	5	5	5	5			1.25
Standard 3	10	2.5	10	10	10	10	10			2.5
Standard 4	20	5	20	20	20	20	20			5
Standard 5								3.02679	2.5	
Standard 6								6.05357	5	
Standard 7								12.1071	10	

One to ten dilutions of each sample were injected into the instrument three times so that there were three replicate values for each sample, enabling determination of measurement precision.

### **3.2.2. Data analysis**

#### **3.2.2. a. Bathymetric survey**

Interpolated models of the lake basin bathymetry were generated as triangulated irregular network (TIN) models in ArcMap 10.1 using the 3D analyst extension. Delaunay triangulation was used to determine topology between points, and this method was more effective than generating DEMs given that data points were not evenly distributed (Burrough & McDonnell, 1998). Contours were then extrapolated from TINs using linear interpolation.

The sonar signal returned falsely shallow depths in some cases, due to the presence of macrophytes in shallower regions of the lake basins such as the southwestern edge of Boeng Lumkut and throughout Yeak Kara . The generated bathymetry data for Yeak Kara are particularly low quality since the lake is shallow and macrophytes are prolific throughout the basin. There were too few datum points to generate a credible bathymetric map of Yeak Mai, which also supported extensive macrophytes communities.

The use of sonar to determine the bathymetry of a lake makes it inherently difficult to gain an accurate view of the lake edge and hence accurately determine the surface area of the lake. Sonar data may give a smaller than actual surface area for these lakes, given that the boat did not navigate around the water edges, instead staying a few metres in where water was deep enough to not get falsely shallow signals from macrophytes and underlying logs. As the focus of use for bathymetric data is on the centre of these lakes, where sonar measurements should be more accurate, uncertainty regarding the shape of the basin around the lake edges should have minimal impact on the study. The bathymetric maps used in this study utilise the WGS1984 UTM zone 48N

projected coordinate system, meaning that the calculated surface area and volume of these lakes are in m<sup>2</sup> and m<sup>3</sup> respectively which were later converted into km<sup>2</sup> and megalitres.

### **3.2.2. b. Water quality profiling**

In order to understand stratification in these lakes and the degree of change with depth of limnological characteristics over time, water quality profiling of these lakes was conducted through the water column during a number of sampling periods.

Water quality parameters (depth, temperature, pH, dissolved oxygen and specific conductivity) were plotted in R 3.0.3 using the 'ggplot' package for display. The script used to generate these plots is given in Appendix 1.

The thermocline for each lake in each time period was quantified as the rate of change of temperature using the following equation:

$$\frac{\Delta T}{\Delta z} = \frac{(T_n - T_m)}{(n - m)}$$

where for each 1 m segment of water,  $n$  is the temperature at the top of the metre-high segment of water, and  $m$  is the temperature at the bottom. Results of these analyses were tabulated and are available in subsequent chapters.

### **3.2.2. c. ICP-AES elemental analysis for major ions**

In the analysis of these data, multiple measurements were taken for each sample. An average value with standard deviation was generated, making it possible to estimate the precision associate with each sample.



### **3.3. Stable isotopes in meteoric and lake waters**

When considering the stable isotope composition of precipitation, it is important to investigate how representative these ratios at a particular sampling location are of their vapour source (Liu et al., 2009; Wei & Gasse, 1999; He et al., 2006; Jouzel et al., 2000; Aggarwal et al., 2004; Rozanski et al., 1992; Singh, 2013; Gourcy et al., 2005). In order to understand the  $\delta^{18}\text{O}$  and  $\delta^2\text{H}$  stable isotope dynamics that occur within the Cambodian crater lake systems and whether these relate to regional climate (the Asian monsoon system), lake surface waters and meteoric waters were sampled and isotopic dynamics compared over time. In addition to this, the isotopic composition of lake waters with depth was monitored to explore the extent to which the input of meteoric waters to the lake modified isotopic composition of waters.

#### **3.3.1. Data acquisition**

##### **3.3.1.1. Field Methods**

###### **3.3.1.1. a. Lake water sampling**

To explore  $\delta^{18}\text{O}$  and  $\delta^2\text{H}$  stable isotope dynamics through the water column, a series of samples of lake water were taken with depth in each lake over the sampling periods. The collection of lake water samples for stable isotope analysis was conducted at the same locations and times as the collection of lake water for major ions analysis. For each depth, the water collected using a Ruttner water sampler (as outlined in Section 3.1.1.3) and transferred into two 3mL glass MacArthur bottles using a 12mL volumetric syringe fitted with a 0.45 $\mu\text{m}$  filter, filling each bottle completely to avoid air bubbles that could permit further isotopic fractionation within the sample bottle. These

were labelled and bagged, with duplicate samples taken to allow the precision to be verified.

#### **3.3.1.1. b. Rain water sampling**

Rainwater was collected and analysed for  $\delta^{18}\text{O}$  and  $\delta^2\text{H}$  stable isotope ratios over a two year period from 14 July 2012 to 15 July 2014 to assess changes over time and relationship to the global meteoric water line, hence regional climate (Gat, 2005). These samples were collected from a rain gauge on the rooftop of the Ministry of Environment offices in Ban Lung, Ratanakiri province [13.746804 N, 107.004519 E decimal degrees, 331m a.s.l.]. This location was chosen for convenience for monitoring personnel, and the short distance between the rainwater monitoring station and the lake meant that it was likely that precipitation over these two sites would be sourced from the same or nearby rainfall cells. Collection of these water samples followed the technical procedures suggested for stable isotope analysis by the Global Network of Isotopes in Precipitation technical procedures (IAEA-WMO 2012).

Rainfall volume and timing was monitored using an ICT tipping bucket rain gauge connected to an ML1 Mini Log data logger. The data logger recorded each 0.2 mL of water that entered a plastic funnel and fell through the rain gauge into the bottom of a collection spigot by a pipe. Evaporative fractionation within the sample bottle was prevented by a 2 cm thick layer of paraffin oil, following the Global Network of Precipitation technical procedures (IAEA-WMO 2012). A Ministry of Environment staff member transferred collected water into 3mL Macarthur tubes on a regular basis, using a 12 mL volumetric syringe to deposit samples into labelled bottles before storage. A sample of lake surface water was also taken at regular intervals during the monitoring

period, following the same protocols. This enables direct comparison of the isotopic composition of meteoric water with surface waters.

### **3.3.1.2. Laboratory methods**

#### **3.3.1.2. a. Stable isotope analysis of water samples**

The  $\delta^{18}\text{O}$  and  $\delta^2\text{H}$  ratios of collected lake and rain waters were directly measured using a Picarro L1102-i liquid and vapour isotopic water analyser using wavelength-scanned cavity ringdown spectroscopy in high-precision liquid mode. Each sample was injected into the instrument five times and the results of the final two injections were used in data analysis.

### **3.3.2. Data analysis**

#### **3.3.2. a. Temporal variation in stable isotopes in rainfall and lake surface waters over the study region from the summer and winter monsoon periods**

A plot of the global meteoric water line (Craig, 1960) alongside the local meteoric water line and the water line for lake surface waters from collated data was created. This was done in order to explore whether a link exists between the rain waters and regional climate via the isotopic chemistry of meteoric waters and regional moisture sources, and between local meteoric water and lake surface waters. These data, therefore, provide a means of identifying any systemic offset caused by the 'amount effect' (Craig, 1961; Rozanski et al., 1993).

## **3.4. Sediment archives of palaeoclimate**

### **3.4.1. Data acquisition**

#### **3.4.1.1. Field Methods**

##### **3.4.1.1. a. Sediment core retrieval**

A modified Livingstone-type corer using PVC pipes of 35mm inner diameter was used to retrieve a 13 m core from Yeak Kara on 16-17 July, 2012 at 13.552080°N, 107.1382933°E. This site was close to the centre of the lake and an approximation of the location of the core taken by Maxwell (1999). A coring platform, consisting of two inflatable boats joined by a deck made of aluminium planks, was anchored at this location.

Coring was undertaken as a series of 1 m long drives, commencing with drive 1 for 0-1 m (beginning at the sediment-water interface) and ending with drive 13 at 12-13 m sediment depth. The sampling tube was attached to a 1 m long shaft, and a piston was attached on a steel shaft that 'unlocked' when the corer reached the desired drive depth. The shaft, with the piston secured in place at the base, was lowered through the sampling hole on deck, through the water column and driven into the sediment, and then retrieved back to deck.

Upon retrieval of the corer to deck, sediment in the shaft was extruded from the corer sampling tube onto pre-split PVC pipes (inner diameter 60mm) lined with cling film. The total length of extruded material for each section and significant visual features were noted and core sections were photographed. Samples were then wrapped in cling film and the remaining half of the pipe was used to cap the samples. Cased cores were taped together, placed in core sheathing and labelled for transportation.

Drives 1-13 proceeded successfully and an attempt was made at drive 14 (13-14 m depth below sediment-water interface), however pushing the corer shaft through the sediment at this point was not possible, presumably due to cumulative friction or a more resistant horizon at that depth. At this point it was estimated that the desired sequence through the mid-Holocene was likely to have been reached according to sedimentation rates for Yeak Kara from Maxwell (1999), and the decision was made to cease coring.

### **3.4.2. Data analysis**

The YK0712B core was corrected for depth under the assumption that the contents of the core had been compressed. For each metre-section, the actual core length was plotted against a one-metre length model and a regression line generated to correlate recovered sediment amount out to one metre.

#### **3.4.2.1. Laboratory methods**

##### **3.4.2.1. a. Physical analysis of sediments**

###### *Splitting and logging of cores*

Core sections were photographed before being logged for sedimentary and lithological structures according to visual analysis. Features logged included section boundaries, sediment type, colour, structure, texture, and features such as pores and mottling. Sediment colour descriptions were based on the Munsell Colour Guide (1994).

After logging, the split surface was covered with cling film, labelled and wrapped inside core sheathing with ends taped to minimise oxidation and drying of samples (Simpson et al., 2005). Samples were then placed in cold storage at 2°C.

#### **3.4.2.1. b. Magnetic susceptibility analysis**

Sediment core sections of the YK0712B core were analysed for magnetic susceptibility using the Barrington MS3 magnetic susceptibility meter with the MS2E sensor (Dearing 1994). The degree of magnetisation of materials can be an indicator for rates of weathering and other indirect climatic changes which bring varying amounts of magnetized materials into the lake basin (Nowaczyk, 2001; Thompson et al., 1980; Rummery et al., 1983).

Core sections were sampled at room temperature in one-metre sections. Samples were measured at 3 mm depth intervals in order to generate a high-resolution log of magnetic susceptibility of each core. Three measurements were taken at each depth over a two-second measurement period. Multiple measurements from each depth in the core allowed an assessment of instrument precision in the context of an episodically 'noisy' magnetic environment. The mean and standard deviation of the three replicate values for each depth was calculated, and these values plotted over depth.

#### **3.4.2.1. c. Particle-size analysis**

The range and distribution of particle-sizes within a sample of sediment material can give insight into the amount of energy present in the lake system at the time (Kakanson & Jansson, 1983). Thus, observing the variation in particle-size distributions over samples in a sediment core can allow an indirect interpretation of climatic processes over time.

*Sample preparation:*

Samples for particle-size analysis were taken every 10 corrected centimetres and, as a result of this depth correction, sampling resolution was higher in core sections which contained more sediment compared to those with less sediment.

From each 1 cm section at 10 corrected-centimetre intervals, a representative sample of the core weighing approximately 0.6 g was placed into a 50 mL centrifuge tube, wet with deionised water and mixed with 10 mL of 10%w.v hydrogen peroxide to oxidise out organic materials which would otherwise be measured as mineral clasts by the laser diffraction technique. Samples were left for 24-48 hours at room temperature or until the reaction ceased. 40 mL of distilled water was added to each centrifuge tube and centrifuged at 3000 rpm for 3 minutes. The supernatant was decanted and the rinsing process repeated. 30 mL of 5% w/v sodium hexametaphosphate (trade name Calgon T) was then added to the oxidized sample to ensure consistent dispersion of mineral clasts within the sample, and particularly to break the bonds between clay plates that would otherwise be measured as a single larger clast. The centrifuge tubes were then placed on a 'spinning wheel' agitator for a minimum of four hours before particle-size analysis was conducted.

*Particle-size analysis of sample:*

A Malvern MasterSizer-2000 with Hydro 2000G wet dispersion bath was used to conduct particle-size analysis of samples. The samples were added to the dispersion bath which pumped the dispersed samples through the MasterSizer-2000 for laser particle-size analysis. Particle-size values were calculated using Mie theory based on the

degree of scattering of a laser beam (blue light) directed at the sample, held between two high-quality quartz lenses.

#### *Analysis of results*

Particle size analysis results were plotted with depth in MS Excel. Summary statistics were also calculated and used alongside results in analyses – skewness (the degree of symmetry to one side of the average), kurtosis (the degree of concentration of grains relative to the average), variance and standard deviation. Examination of the particle size summary statistics allow for interpretation of varying amounts of energy within the lake system over time through estimating the level of sorting of grain sizes and changes in trends of average grain sizes over points in time (Blott & Pye, 2001).

#### **3.4.2.1. d. Loss on ignition analysis**

Loss on ignition analysis on the sediment core was undertaken in order to gain a snapshot of the proportions of organic matter, inorganic carbon and siliciclastic material in the YK0712B core. The inorganic carbon that is used for stable isotope analysis, which will be described later, form part of the inorganic carbon fraction of loss on ignition data, and understanding these sedimentological features will allow for a deeper understanding of the climatic conditions impacting the lake basin over time (Hakanson & Jansson 1983).

Samples for loss on ignition analysis were taken at the same depths as those taken for particle-size analysis. Mean sample size was 0.3 g and a total of 130 samples were taken. Samples were generally small, however were large enough to give a



snapshot of the sample organic carbon, inorganic carbon and siliciclastic material compositions (Dean Jr, 1974; Heiri et al., 2001).

The wet mass of samples was measured before they were dried in an oven at 40°C for 24 hours and ground using a ceramic mortar and pestle. Ceramic crucibles were cleaned and pre-fired in a muffle furnace at 550°C for 2 hours to remove moisture and any residual organic material from previous uses. After cooling to room temperature in a dessicator, the mass of each labelled empty crucible was recorded. Each ground sediment sample was then placed into a crucible, which were then reweighed to ascertain the dry mass of each sample. Samples were then placed in a muffle furnace to burn off organic carbon at 550°C for 4 hours and re-weighed after cooling to ~40°C. They were placed back into the furnace at 950°C for 2 hours to burn off carbonates before being weighed after cooling again.

#### **3.4.2.1. e. Geochemical analysis**

The ITRAX core scanner is an automated energy-dispersive x-ray fluorescence (XRF) instrument which takes nondestructive optical and radiographic images and scans elemental variation along the length of the longitudinal axis of the sediment core split (Croudace et al., 2006). Analysis of lacustrine cores using this instrument can provide a vast amount of accurate high-resolution data for a large number of environmental proxies (Kylander et al., 2011; Francus et al., 2009).

This study utilized the ITRAX core scanner located in the Environmental Radioactivity Measurement Centre at the Australian Nuclear Science and Technology Organisation (ANSTO) to undertake sub-millimetre scale measurements of the inorganic geochemistry of the YK0712B core. Major elemental characteristics and molecular

composition was analysed for a number of elements, with all possible elements scanned for while the core was being analysed, should this data be required for future studies. Of key interest were counts of Ca, Sr and Rb as climate proxies, but counts of Al, Si, P, S, Cl, Ar, K, Ti, V, Cr, Mn, Fe, Ni, Cu, Zn, Ga, As, Zr, Pd, Sn, Y, Zr, Pd, Sn, Ba, La, Ce, Ta and W were also recorded. Calcium counts through the core as it can be allocthenically (through erosion) and authigenically (produced within the lake system) produced as a result of changes in erosion (within the catchment) and lake water biogeochemistry (within the lake) that occur as a result of changes in climate over time (Kylander et al., 2011; Cohen, 2003). Strontium ions are of interest as a proxy for changes in lake level and productivity associated with changes in climate (Cohen, 2003; Kylander et al., 2011). Rubidium has low mobility in the environment because it is a component in many common minerals and adsorbs to clays well, and is used as a proxy for moist climatic conditions with relation to erosion and rates of weathering (Kylander et al, 2011; Dypvik & Harris, 2001). This data was analysed using ReDiCore and plotted in MS Excel. The results of these scans revealed high-resolution trends for a range of proxies that reveal trends in hydrological and climate for this lake.

#### **3.4.2.1. f. Characterisation of carbonate species using electron microscopy**

Physical analysis and ITRAX geochemical analysis of the core indicate the presence of carbonate in the sediment, supporting prior work by Maxwell (1999). In order to understand whether this carbonate had formed in surface waters, in which case they would display euhedral shape, or sediment pore waters, in which case they would display anhedral shape, it was necessary to observe the morphology of the crystals (Leng & Marshall, 2004; Lamb et al., 2005). This distinction is an important one to make if these crystals are to be used as palaeoclimatic proxies.

### *Sample preparation*

Four samples were extracted from both laminated (12.26-12.28 m, 12.28-12.30 m) and non-laminated sections (10.20-10.24 m, 12.32-12.34 m) of the core. These were placed into 50 mL centrifuge tubes to which 25 mL of 8% w/v sodium hypochlorite solution (adjusted to pH of 9.0-9.5 following Ito, 2001) in order to remove organic components. The samples were left for 24-48 hours or until reactions had ceased in the tubes before being sieved at 125  $\mu\text{m}$  with the <125  $\mu\text{m}$  fraction retained for analysis. The samples were then triple-rinsed with ultra-pure water and centrifuged at (3000 rpm for 3 minutes each rinse). After rinsing, the solutions were dried in an oven prior to mounting.

### *Sample analysis*

A scanning electron microscope (SEM) with energy dispersive spectroscopy (EDS) and electron backscatter diffraction (EBSD) capabilities was used to characterize the species of calcium carbonate present in the YK0712B core through visual observation of the crystal shape and chemical composition analysis using electron dispersive spectroscopy (EDS) and electron backscatter diffraction (EBSD). Visual observation was also used to determine the nature of their growth form - euhedral crystals indicate planktonic detrital formation in surface waters of the lake, which are of value for palaeo-climate reconstruction, while anhedral crystals, which can form as carbonate 'cements' in interstitial pore spaces in sediment profiles are not in equilibrium with surface waters and not, therefore, of value for palaeoclimate reconstruction (Allison & Pye, 1994).

A Zeiss EVO SEM was used to examine clean carbonate samples using energy dispersive spectroscopy (EDS) for geochemistry. A Zeiss Ultra Plus SEM was used for both EDS and electron backscatter diffraction (EBSD) to characterise chemical composition of the carbonate crystals observed in SEM micrographs in order to identify the specific species of carbonate present in the sample and estimate their relative abundance. EBSD was utilised to generate phase maps quantifying the distribution of carbonate species.

For the Zeiss EVO, an EHT of 20.00kV and beam current of 5nA was used. SEM stubs were prepared using carbon tape, upon which a very small amount of sample was scattered and patted down gently before being coated with 20nm of carbon. SEM stubs for Zeiss Ultra Plus analysis were prepared in the same manner, but a carbon coating of 10nm was used. In this case, an EHT of 20.00kV and beam current of 5nA were used.

#### **3.4.2.1. g. Stable isotope analysis of carbonates in sediments**

ITRAX XRF scanning of the YK0712B core showed elevated levels of calcium in the 4-13m section of the core (discussed further in Chapters 4 & 5). In order to explore the variability in this data through  $\delta^{18}\text{O}$  analysis, a range of samples of various resolutions (1 cm, 4 cm and 10 cm) were extracted from the core for analysis. Two hundred and seventy four samples of sediment were extracted, freeze-dried and pre-treated following the protocol described in Section 3.4.2.1. f. above (as per Ito, 2001). A preliminary chronological model derived from Maxwell (2001), who worked on a core from Yeak Kara taken at a similar location to Yeak Kara, was used as independent dates had not yet been received for the current core. The core was divided into sections of

varying resolutions in an attempt to capture, in high-resolution, the 4.1 ka event, 5.9 ka event and 8.2ka event as recorded

2 mg of each sample were placed into 1 mL Weaton V-vials, sealed with a Kel-F and silicone septa for analysis. A Micromass PRISM III stable isotope mass spectrometer was used to analyse stable isotope ratios in samples using the Micromass Multiprep device (using internal standards NBS18 and NBS19 for calibration). Vials were placed in a heated block at 90°C and a double-bore needle used to push through the septa to evacuate the vial and inject 103% phosphoric acid onto the sample. Evolved CO<sub>2</sub> was then passed through a water trap to remove moisture and cryogenically collected in an external cold finger. The sample gas was then released into the sample side of the dual inlet and analysed against the working gas (on the other side of the dual inlet). Detected isotopic ratios were compared to a measured standard in order to determine the isotopic makeup of the original sample. For this research, the V-SMOW (Vienna Standard Mean Ocean Water) was used.

#### **3.4.2.1. h. <sup>14</sup>C dating of charcoal in sediments**

A series of depths were selected from the Yeak Kara YK0712B core based on periods of distinct transitions in the δ<sup>18</sup>O stable isotope data. Bulk sediment samples from the chosen depths were extracted and sent to Beta Analytic for analysis of sediment for AMS charcoal dating. These samples were sent as wet samples in small labelled zip-lock bags, which underwent pre-treatment by Beat Analytic prior to analysis to ensure organic and carbonate residues are removed. This ensures that the AMS dating is conducted only on charcoal pieces, making it unlikely that there will be an age bias because of organic or carbonate contamination. This pre-treatment involved

washing the sample in hot hydrochloric acid to remove carbonates, followed by washing with sodium hydroxide to remove residual organic acids, and a final acid wash to neutralise alkali prior to drying.

Results were calibrated using intcal04 in Calib 7.0 to express radiocarbon dates as calibrated years B.P. (Stuiver et al., 1986; Stuiver et al., 1993).

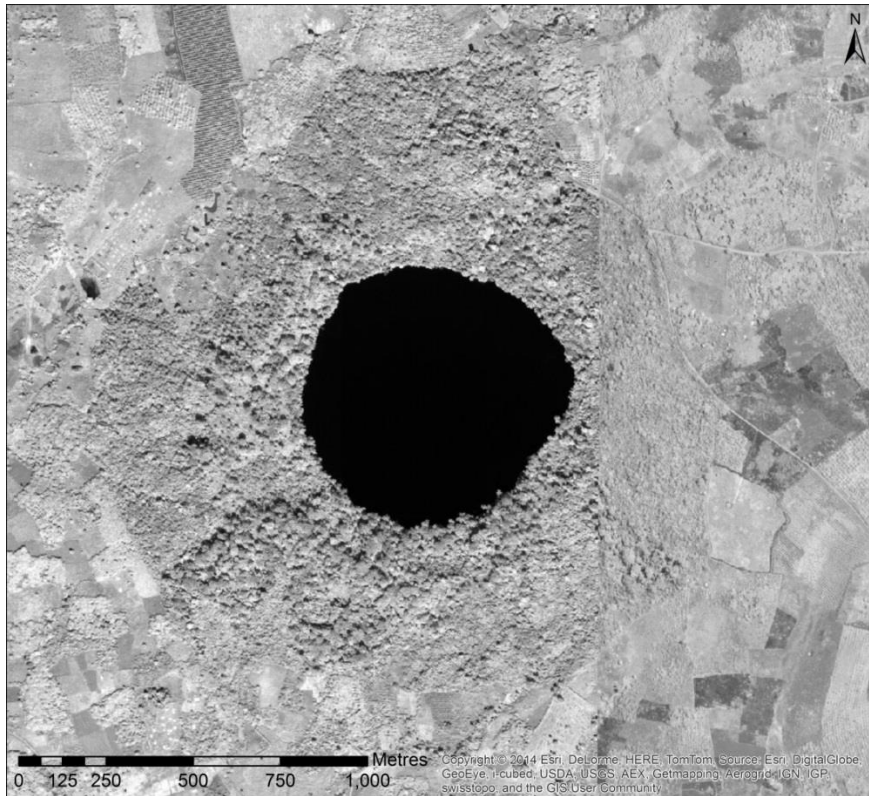
## CHAPTER 4: Results

The results of the analyses of water and sediment samples following the methods described in Chapter 3 will now be described.

### 4.1. Bathymetry and basin morphology of crater lakes

A number of crater lakes exist in mainland Southeast Asia, including north-eastern Cambodia, central Vietnam and Southern Laos. The north-east Cambodian crater lakes will be used in this study to explore stable isotope dynamics of rainfall in the region. These lakes exhibit parabolic-shaped basins that have steep sides and flat, slightly sloping bottoms, fitting the profile for maar-type volcanic lakes described by Hutchinson (1957). Some of these lakes, such as Yeak Loam, are distinctively round in shape (Figure 4.1) while some are more irregular, such as Boeng Lumkut which has a basaltic outcrop on the eastern side of the lake basin that may have resulted from more than one phreatic eruption (Figure 4.4). Yeak Oam and Yeak Kara may also have resulted from multiple phreatic explosions, sharing a common larger crater rim. The two lakes are now separated by a low basalt sill (Figures 4.2 and 4.3). Yeak Loam, Yeak Oam and Boeng Lumkut display very steep sides and flat to slightly sloping bottoms (Figures 4.1-4.4). Yeak Kara is the most terrestrialised of these lakes; it is shallow and biologically productive, with a distinctly lenticular cross-sectional form (Figure 4.3).

Satellite imagery and bathymetry models for Yeak Loam, Yeak Oam, Yeak Kara and Boeng Lumkut are shown below (Figures 4.1-4.4). Track logs for sonar/GPS are depicted on bathymetry maps as a series of small black dots to indicate the source data for the interpolation of bathymetry, so as to give an indication of the density of source data points used to generate bathymetry maps.



Yeak Loam)

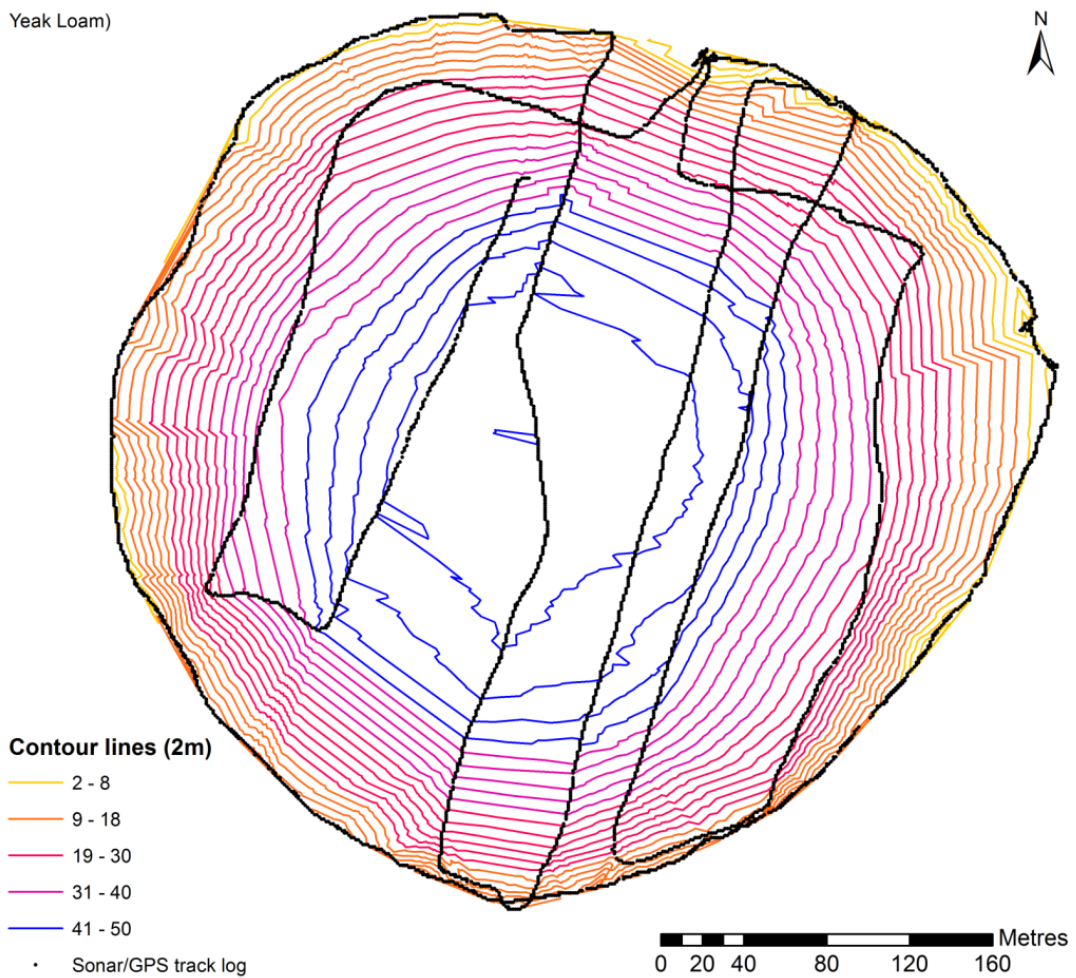


Figure 4.1: Bathymetric basin map and satellite image of Yeak Loam





Yeak Oam)

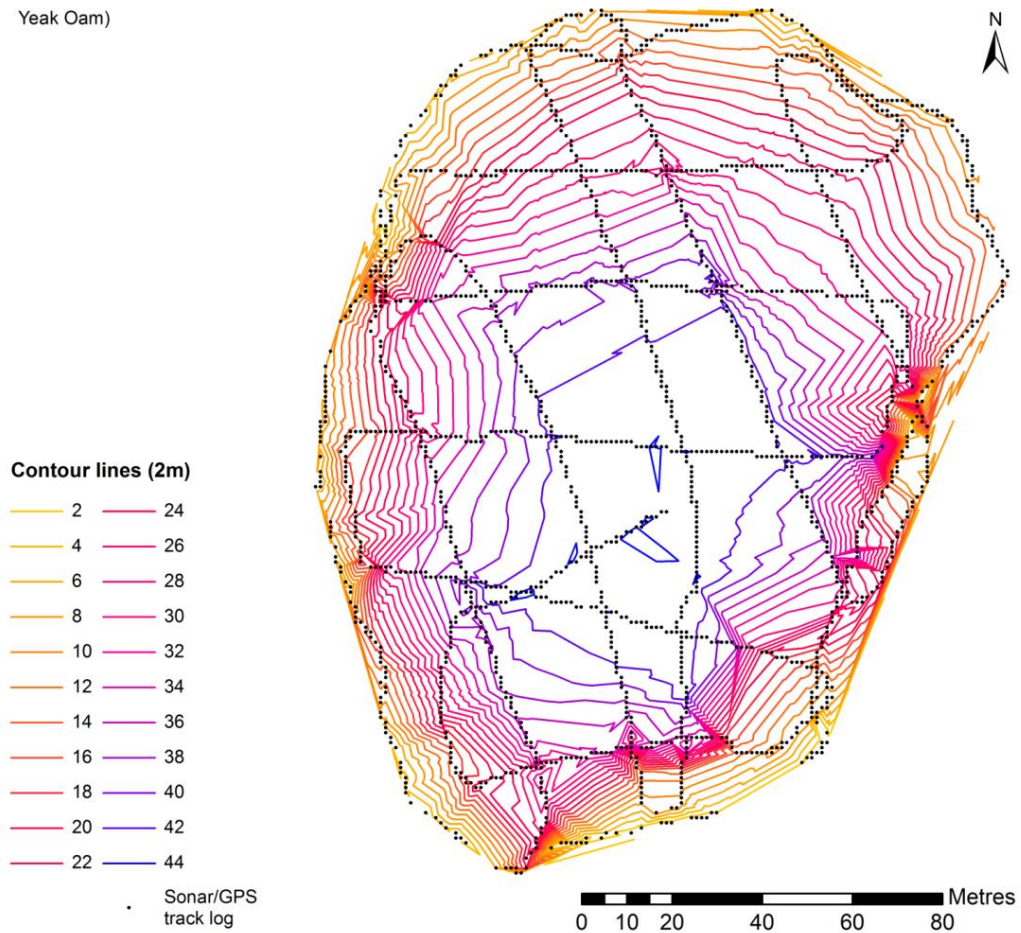


Figure 4.2: Bathymetric basin map and satellite image of Yeak Oam



Yeak Kara)

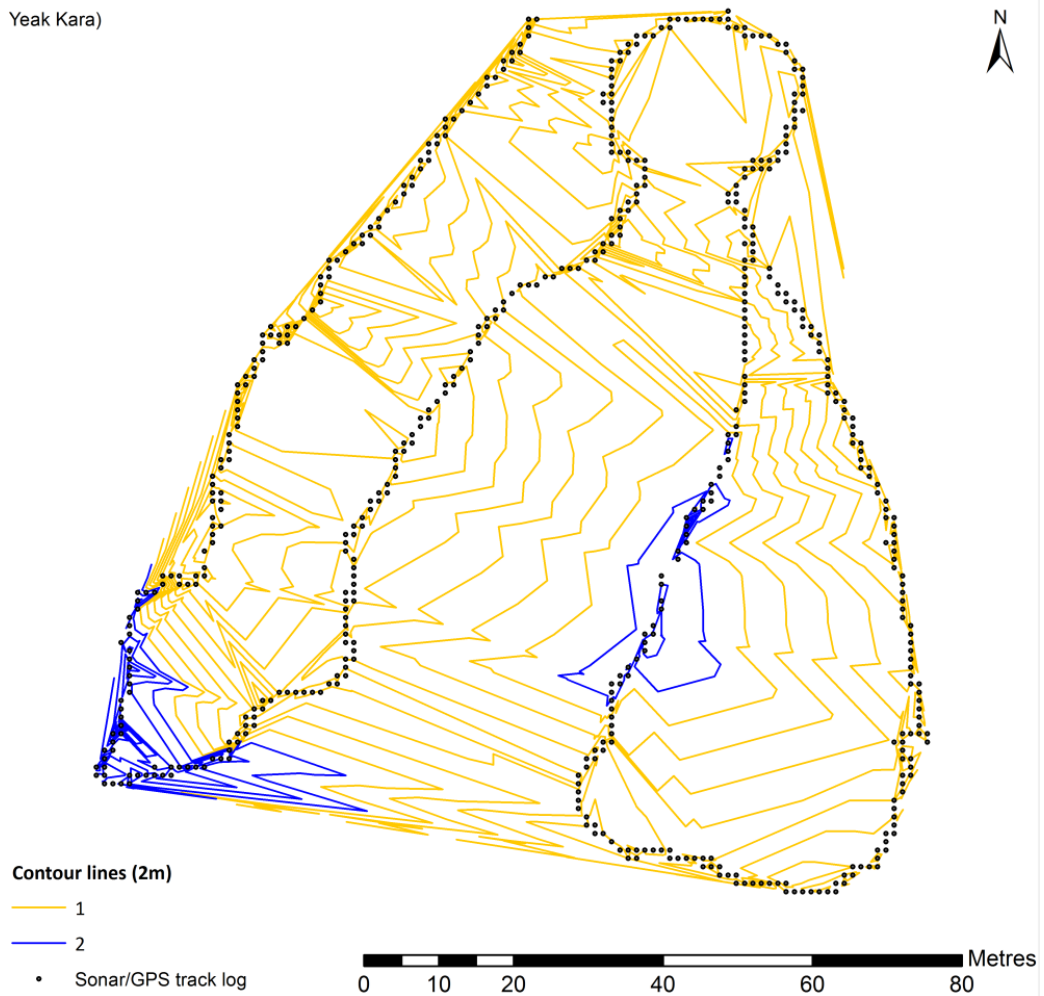
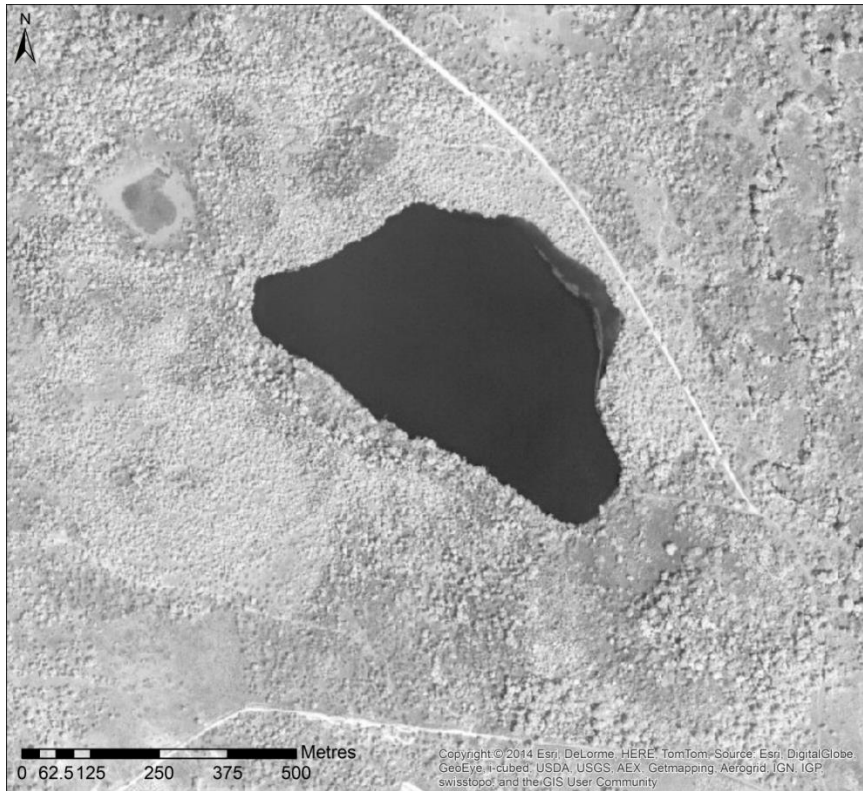


Figure 4.3: Bathymetric basin map and satellite image of Yeak Kara





Boeng Lumkut)

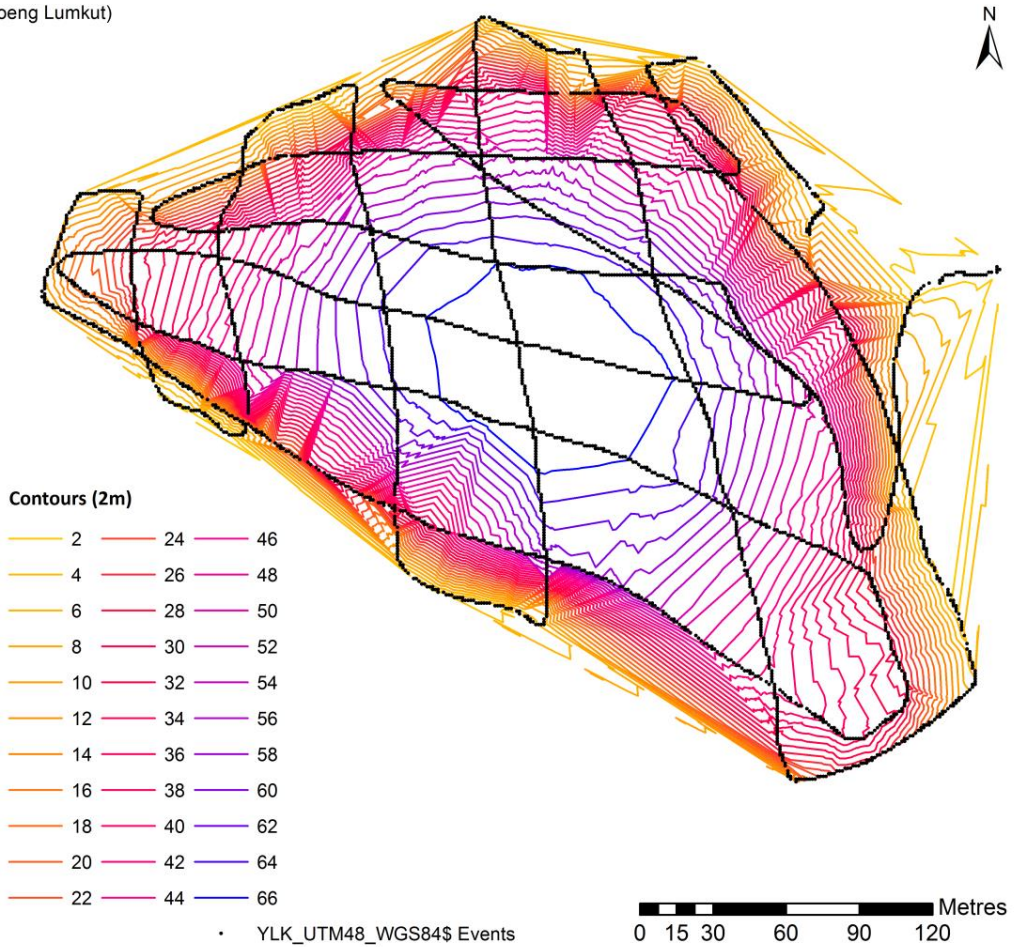


Figure 4.4: Bathymetric basin map and satellite image of Boeng Lumkut

*Table 4.1: Lake depth values generated from sonar data (NB: surface area estimate underestimates true surface area, and true volumes are likely to be slightly higher).*

Lake	Plane height (m)	Surface area (m <sup>2</sup> )	Surface area (km <sup>2</sup> )	Volume (m <sup>3</sup> )	Volume (ML)	SA:V
YL	50.62	148464.1	0.148464	2749282	2.749282	0.054
BLK	67.99	75315.63	0.075316	2265791	2.265791	0.033
YO	45.07	22244.51	0.022245	386655	0.386655	0.057
YK	2.04	9397.835	0.009398	8680.687	0.008681	1.082

The surface-area-to-volume ratio for these lakes has implications for the degree to which evaporative fractionation impacts the stable isotope ratios of surface waters, as well as giving insights into physical, chemical and biological dynamics that may be occurring. Yeak Loam and Yeak Oam have similar morphology, with similar basin shape and basin depth, have a surface-area-to-volume ratio of ~0.05 (Table 4.1). Boeng Lumkut has a lower surface-area-to-volume ratio of ~0.03, which is not surprising given its maximum depth of almost 70 m. Yeak Kara has the highest surface area to volume ratio, at 1.08. This is not surprising, given that Yeak Kara is very shallow with a maximum depth of 3 m in the wet season, which halves during the dry season to 1.5 m. From these data, we can see that Yeak Kara is significantly more sensitive to evaporation/precipitation than the other lakes, making it a better study site for the analysis of hydrological changes associated with the wet summer and dry winter monsoons.

## 4.2. Stable isotope dynamics of lake waters, rain waters and regional climate

In order to understand how representative the isotopic characteristics of meteoric water is of its vapour source, and how representative lake surface waters are of meteoric waters, the stable isotope ratios of precipitation and the surface waters of the Yeak Loam lake were monitored over a one-year period. Yeak Loam was chosen due to its geographic proximity to the town of Ban Lung, allowing sampling to occur frequently.

Correlation of stable isotope ratios of oxygen and hydrogen reveal that stable isotopes of rainwaters received at Yeak Loam align closely with the global meteoric water line (GMWL) (Figure 4.5).

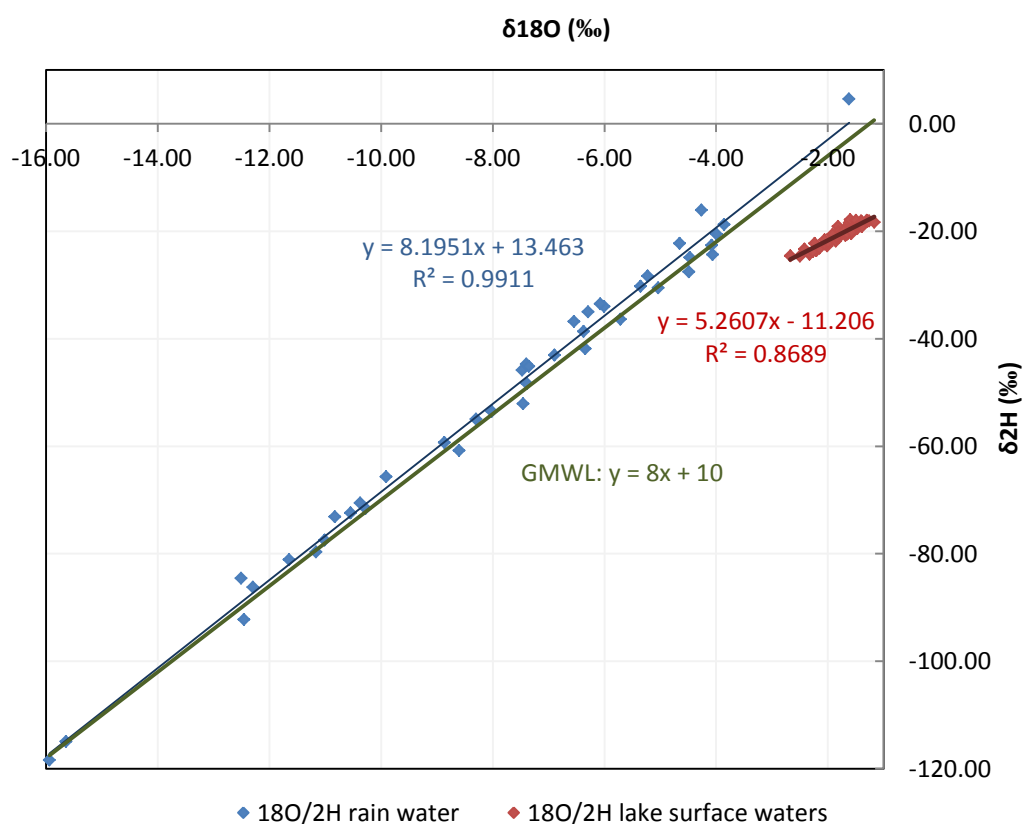


Figure 4.5: Regional meteoric water line, lake surface water line and global meteoric water line

This is a very significant finding, because the similarity of the gradient of the local meteoric waterline (blue) with the global meteoric water line (green) indicates that the stable isotope ratios of meteoric waters are closely representative of regional climate. It is also clear that evaporative fractionation has a substantial factor in determining the stable isotope ratios of lake surface water, with the water line for lake waters offset from the LMWL and GMWL but of a similar gradient (Craig, 1951; Gat, 2005; Leng & Marshall, 2004; Jouzel et al., 2013). These results have significant implications - that meteoric (rainfall) waters can be used as a proxy for the isotopic content of regional climate, and that lake surface waters capture evaporation-precipitation dynamics.

The beginning of the sampling period (15 July 2012) falls in the middle of the wet summer monsoon season. Precipitation from the southwest summer monsoon increases over July and August (Figure 4.6). Rainfall ceases abruptly in early October with a few rainfall events thereafter with low precipitation amount continuing into early November. After this, there are no recorded rainfall events while the dry northwest winter monsoon dominates until the wet summer monsoon resumes in early April the following year. Isotope ratios for oxygen and hydrogen in both meteoric waters and lake surface waters respond to rainfall by becoming more negative as the wet season progresses, more positive over the dry season, and more negative again with the advent and progression of the subsequent wet season (Figure 4.7).

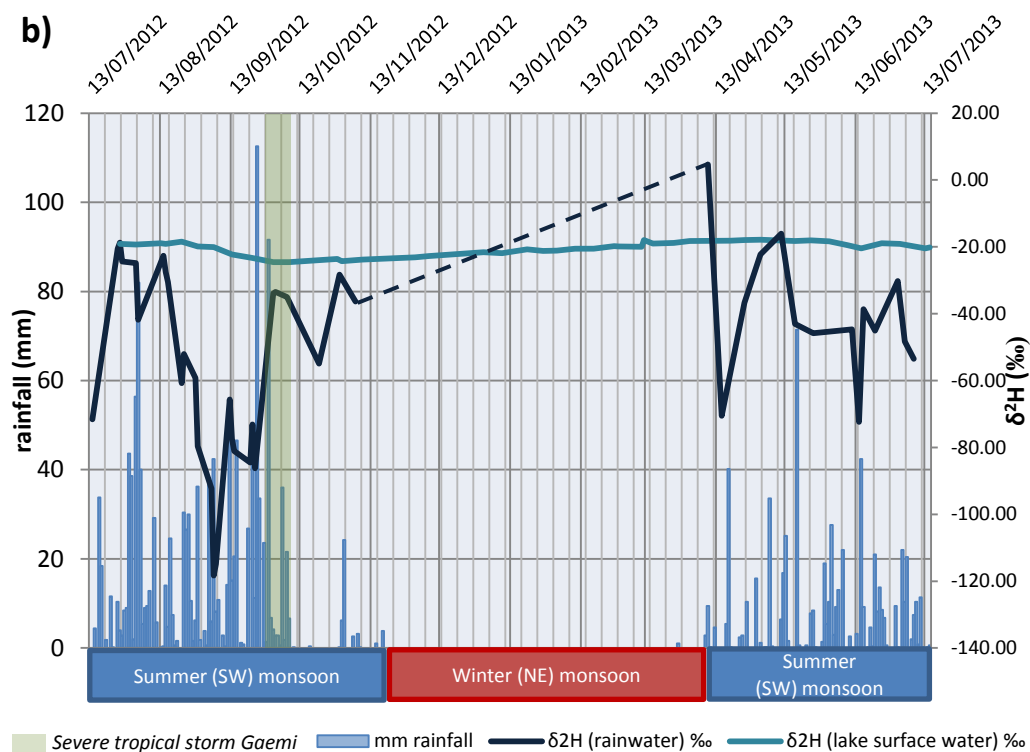
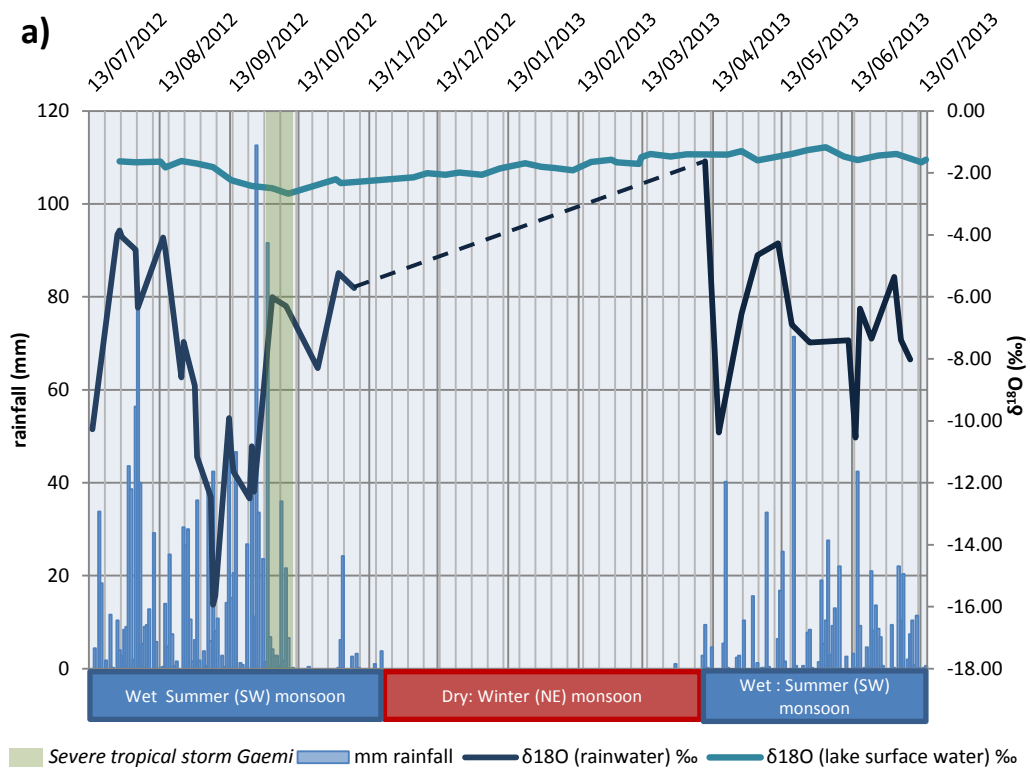
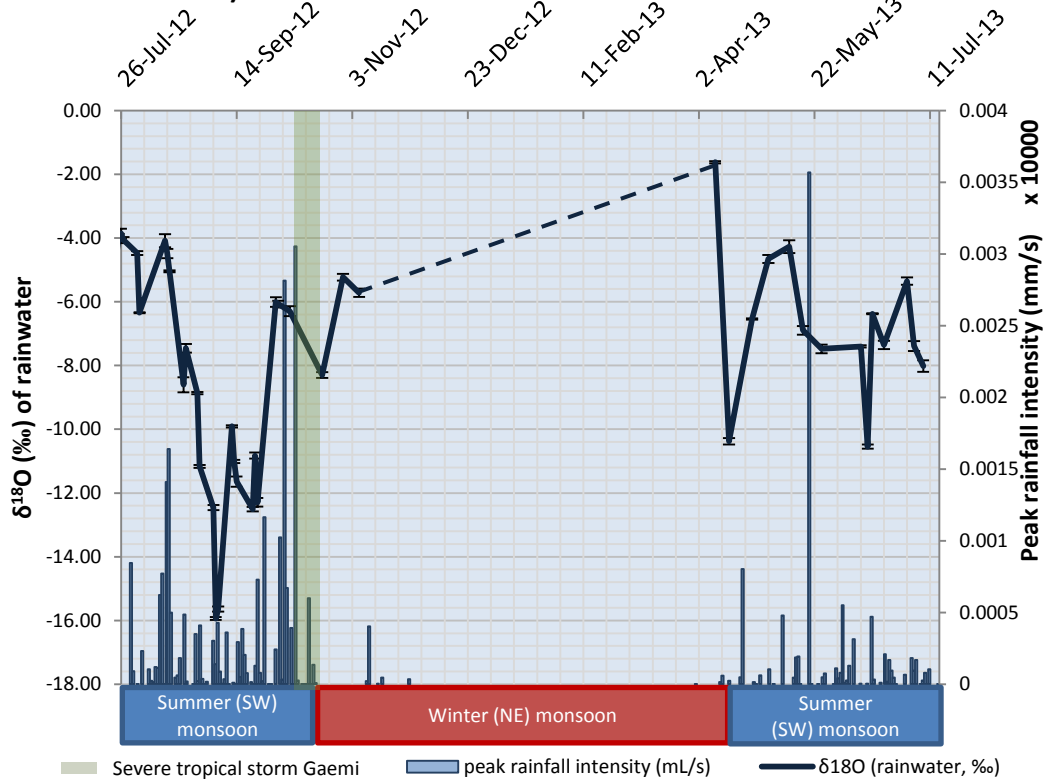


Figure 4.6: Relationship between rainfall amount (Ban Lung rain gauge),  $\delta^{18}\text{O}$  in rain waters and  $\delta^{18}\text{O}$  in lake surface waters (Yeak Loam)

**$\delta^{18}\text{O}$  in rainwater)**



**$\delta^{18}\text{O}$  in lake surface waters)**

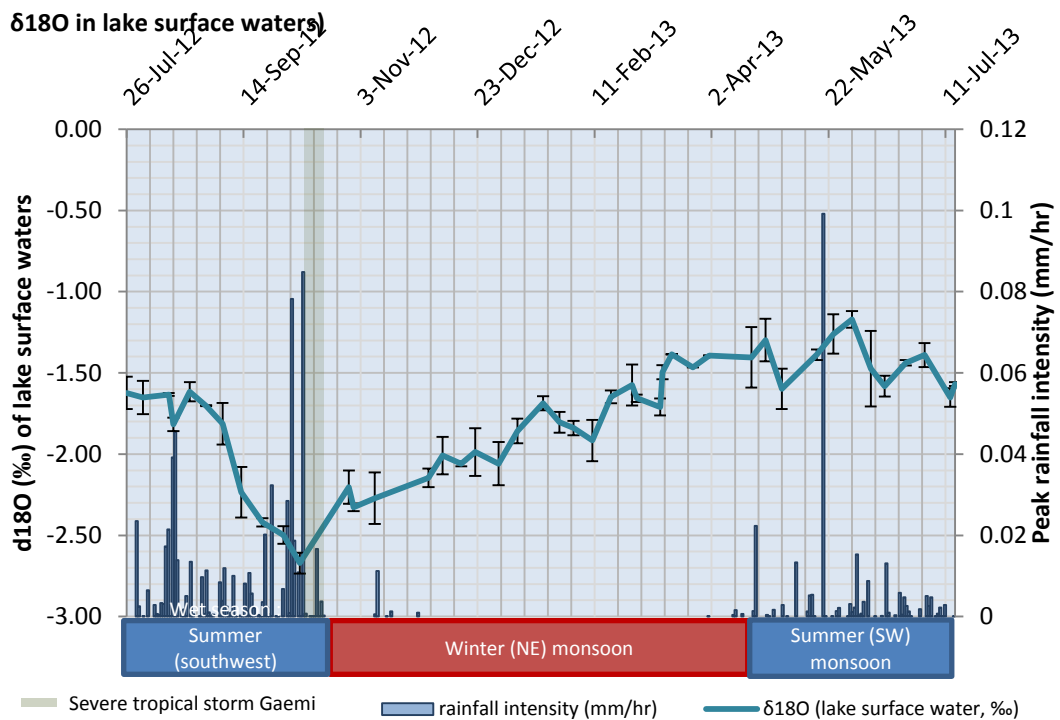


Figure 4.7: Relationship between  $\delta^{18}\text{O}$  of rainwater and lake surface waters and peak rainfall intensity



### **4.3. Limnology of the Cambodian Crater Lakes**

Basin shape and morphology strongly influence the physical, biological and chemical processes that occur within a lake basin (Wetzel, 1957). An understanding of the limnological characteristics of a lake is instrumental in being able to conceptualise the biochemistry of and the relationship between lake waters and meteoric waters.

#### **4.3.1. Temperature and stratification**

Temperature is an important feature of lake waters, effecting water density and hence stratification dynamics (Imboden & Wüest, 1995). Yeak Kara is a shallow, polymictic lake, quite unlike Yeak Loam, Yeak Oam and Boeng Lumkut, all of which are deep meromictic lakes with temperature/density profiles typical of stratified lakes (Figure 4.8). Stratification in these stratified lakes was maintained throughout the monitoring period with the exception of a slight breakdown in February 2012, suggestive of a mixing event (Williams, 2013). From these data, it is clear that the majority of these water bodies retain a reasonably constant temperature profile over time once thermal stratification is established.

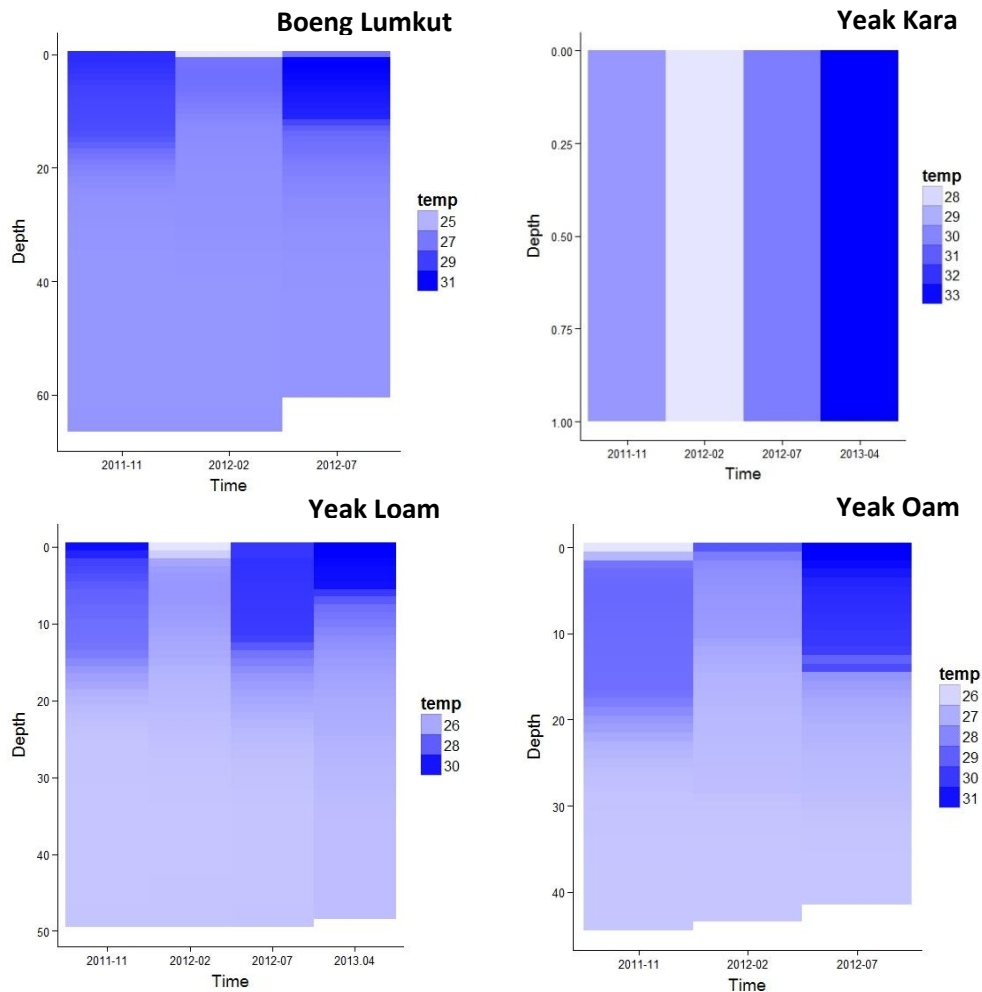


Figure 4.8: Temperature variation with depth over time in Cambodian crater lakes. Depths are in metres and temperature in °C.

### 4.3.2. Specific conductivity

An understanding of the dynamics associated with specific conductivity in lake waters assists in understanding the biochemical and biological aspects of a lake system (Lewis Jr, 2010). Yeak Loam and Yeak Oam show comparable levels of specific conductivity over the sampling periods, although Yeak Loam has slightly higher levels of materials in solution (Figure 4.9). The hypolimnions of both of these lakes show higher conductivity as compared to the epilimnions, a trend which also occurs in Boeng Lumkut but is overshadowed in graphical representation by the high specific conductivity of the epilimnion and metalimnion in December 2011. Yeak Loam and Yeak Oam show a

significant increase in conductivity in July 2012 throughout the entire water depth, while Boeng Lumkut shows a significant drop in conductivity through the entire water column at this time. Yeak Kara shows similar high levels of specific conductivity in November 2011 and February 2012, compared to July 2012 and April 2013 when values are lower.

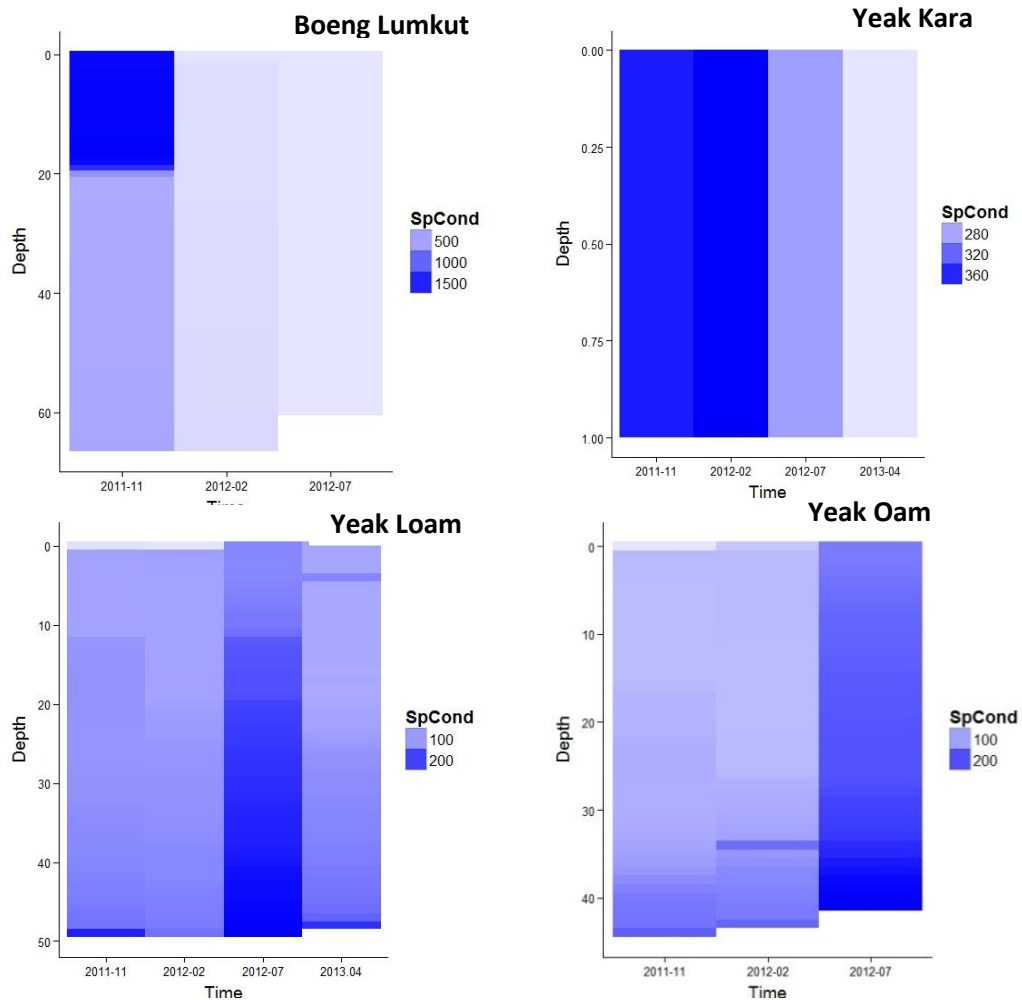


Figure 4.9: Specific Conductivity with depth over time in the Cambodian crater lakes. Depths are in metres and specific conductivity levels are in  $\mu\text{S}/\text{cm}$ .

### 4.3.3. Dissolved oxygen saturation

Dissolved oxygen is an important feature of lake waters, determining to a large degree of biological activity and redox processes (Harnung & Johnson, 2012; UNEP/WHO, 1996; Jantzen, 1978). Dissolved oxygen levels with depth in these lakes show similar trends to those of temperature. Across all deep stratified lakes and

regardless of the time period, there is a distinct pattern of having high dissolved oxygen levels in the epilimnion and anoxia in the hypolimnion (Figure 4.10). Yeak Kara shows a decrease in dissolved oxygen levels in July 2012, coinciding with the start of the wet season, but high values through the water column at all other times when sampling occurred.

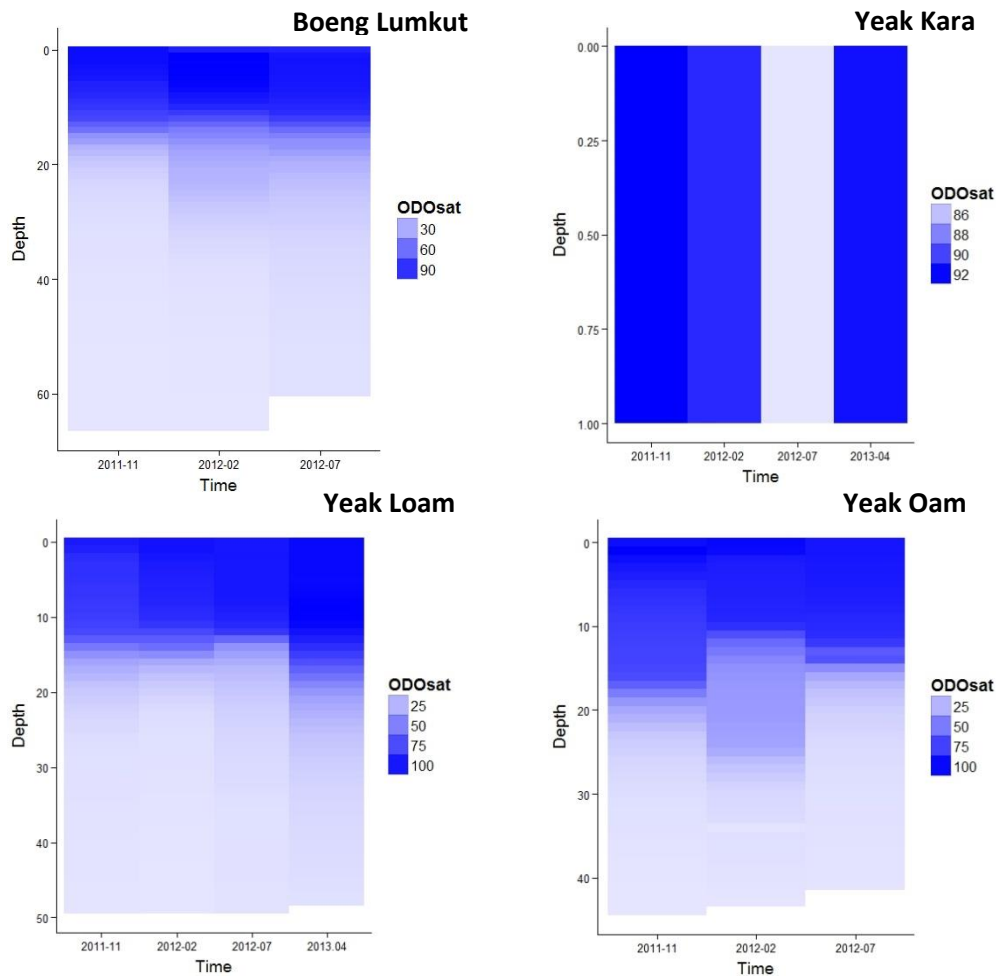


Figure 4.10: Optical Dissolved Oxygen (ODO) variation with depth over time in the Cambodian crater lakes. Depths are in metres and dissolved oxygen (ODO saturation) levels are displayed as percentages.

#### 4.3.4. pH

It is important, when looking at a lake system, to consider pH dynamics as these are closely linked to chemical and biological activity (Stumm & Schnoor, 1995). There is small variation in pH with depth over time in these lakes. In Yeak Loam, pH levels remain

stable and tend towards 8, which is similar to pH levels in Boeng Lumkut (Figure 4.11). There are, however, some instances where there is greater acidity with depth in Boeng Lumkut, as observed in July 2012. Yeak Oam shows an anomalously alkaline reading for surface waters in February 2012, although other than this the lake waters tend to be neutral or slightly alkaline.

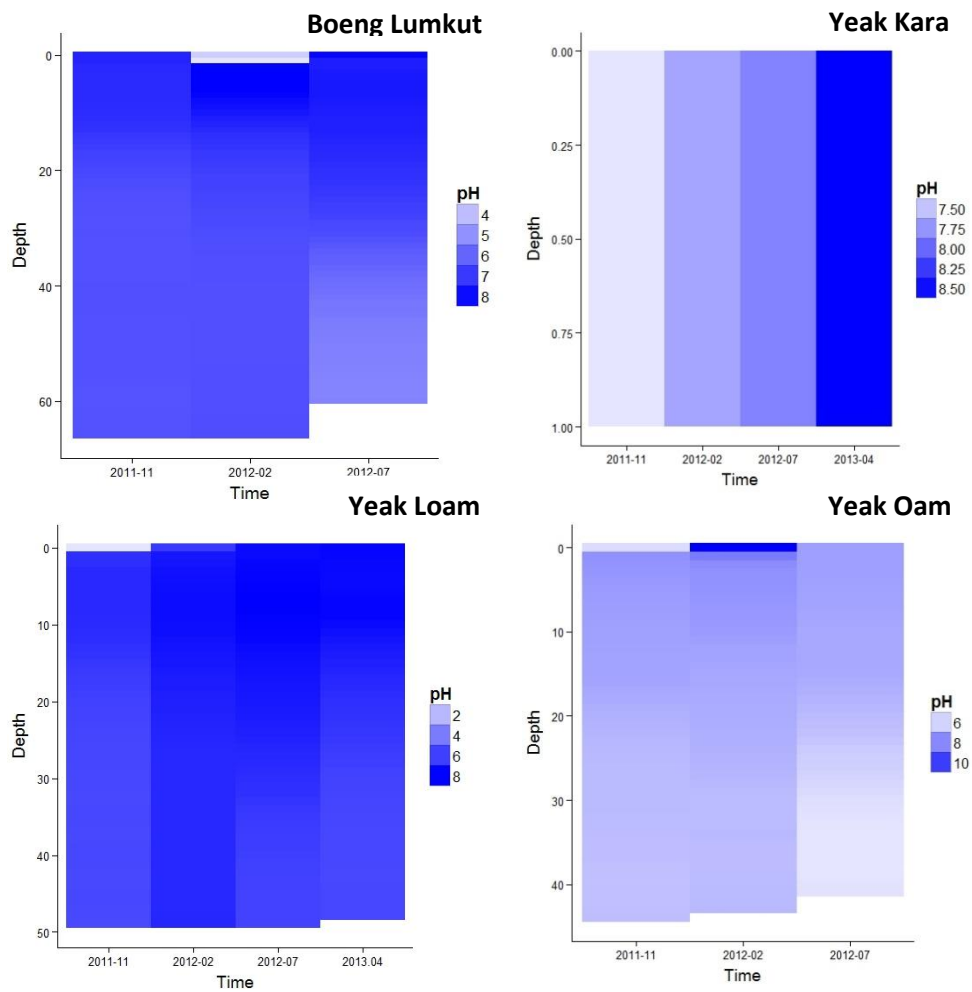


Figure 4.11: pH variation with depth over time in the Cambodian crater lakes. Depths are given in metres.

#### 4.4. Stable isotope dynamics in lake waters with depth over time

The isotopic characteristics of the surface waters of these lakes vary over time, but with a clear seasonal trend. There are similarities between the isotopic characteristics of surface water samples across all lakes taken during the summer monsoon period (wet season, July 2012 and April 2013) and samples taken in the winter monsoon period (dry season, November 2011, February and November 2012), shown in Figures 4.12-4.17. Yeak Oam and Boeng Lumkut show strong stratification, with uniform distribution of stable isotope values through the hypolimnion and little variation in  $\delta^{18}\text{O}$  or  $\delta^2\text{H}$  over time, despite clear variation in the epilimnion. These lakes also experience less variation in stable isotope ratios in their epilimnions compared to Yeak Loam. The largest change between wet and dry seasons in lake surface waters are roughly the same across all stratified lakes, at 1.32‰ (Yeak Loam), 1.17‰ (Boeng Lumkut) and 1.09‰ (Yeak Oam). Yeak Kara stands out with a difference of 5.52‰ between the most positive and most negative values. Yeak Kara has the largest surface area to volume ratio of the studied lakes (Table 4.1) and Boeng Lumkut the least, hence it can be seen that a relationship exists between evaporation and relative surface area with regard to controlling the stable isotope ratios of the epilimnions of these tropical crater lakes.

Stratification keeps the isotopic values distinct, with a clear and persistent differentiation between the isotopic characteristics of the epilimnion and hypolimnion across all stratified lakes over the sampling period (Figures 4.12-4.19). The seasonal isotopic changes in meteoric water are clear in the epilimnion during the sampling period, but are muted in the hypolimnion.

*Yeak Loam (refer to Figures 4.12 and 4.13)*

At the start of the summer monsoon rainfall period, the  $\delta^{18}\text{O}$  ratio of the surface waters of Yeak Loam increase in value by more than 0.5‰, and  $\delta^2\text{H}$  values by 4‰. These values continue to increase as monsoonal rainfall continues, with the surface waters becoming enriched with  $^{18}\text{O}$  and  $^2\text{H}$ , causing  $\delta^{18}\text{O}$  values to continue to increase. During the dry season as the cool, moisture-barren winds of the northwest monsoon predominate, isotope ratios in lake surface waters decrease to an average of about -2.4‰  $\delta^{18}\text{O}$  and -24 to -25‰  $\delta^2\text{H}$  (as observed in both 2011 and 2012). On average, the deeper waters of Yeak Loam tend to be characterised by slightly lower  $\delta^{18}\text{O}$  and  $\delta^2\text{H}$  values during drier periods (winter monsoon) than in wetter periods (summer monsoon). Water samples taken during the winter monsoon period show sharp increase in  $\delta^{18}\text{O}$  and  $\delta^2\text{H}$  over the thermocline depth, and a slow trend of increasing  $\delta^{18}\text{O}$  with depth in the hypolimnion. In contrast, water samples taken during the summer monsoon period show slower rates of  $\delta^{18}\text{O}$  and  $\delta^2\text{H}$  decrease over the thermocline but a slightly more rapid increase of  $\delta^{18}\text{O}$  and  $\delta^2\text{H}$  with depth in the hypolimnion due to thermal stratification.

*Yeak Oam (refer to Figures 4.14 and 4.15)*

The  $\delta^{18}\text{O}$  and  $\delta^2\text{H}$  trends in Yeak Oam follow a similar trend to those that occur in Yeak Loam. The  $\delta^{18}\text{O}$  and  $\delta^2\text{H}$  of Yeak Oam are generally more positive than those of Yeak Loam by ~1‰  $\delta^{18}\text{O}$  and 5‰  $\delta^2\text{H}$ . There are more pronounced differences in  $\delta^{18}\text{O}$  and  $\delta^2\text{H}$  variations between 2012 and 2013 samples in both the summer and winter monsoon periods for Yeak Oam; however, there are still clear patterns of increasing  $\delta^{18}\text{O}$  and  $\delta^2\text{H}$  from the epilimnion to hypolimnion in the winter monsoon period. In the summer monsoon period there tends to be decreasing  $\delta^{18}\text{O}$  and  $\delta^2\text{H}$  with depth in the

epilimnion, a rapid decrease in  $\delta^{18}\text{O}$  and  $\delta^2\text{H}$  over the thermocline, followed by a small increase with depth of  $\delta^{18}\text{O}$  and  $\delta^2\text{H}$  in the hypolimnion.

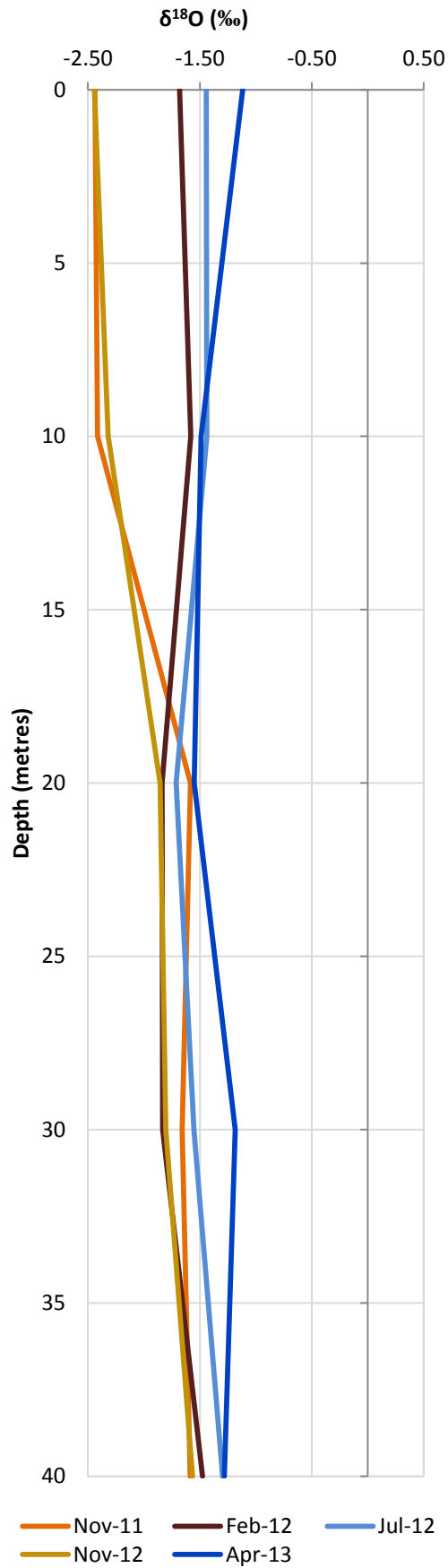
*Boeng Lumkut (refer to Figures 4.16 and 4.17)*

It is clear that in Boeng Lumkut too, stratification controls variation in isotopic composition through the water column over time. This lake, being deeper than the others, shows much stronger stratification, with isotopic composition of the hypolimnion fairly similar across all sampling periods regardless of the dominance of summer or winter monsoon.

*Yeak Kara (refer to Figures 4.18 and 4.19)*

Yeak Kara is presently a relatively saline (see Section 4.4), shallow and unstratified lake, with a maximum observed water depth of ~5m during the wet season of 2012. Because of this lack of stratification, there are no significant changes in stable isotopes with depth (hence depth is not shown using multiple plots), but the lake waters clearly reflect seasonal changes in isotope dynamics (Figure 4.18 – 4.19). There is a marked decrease in stable isotope ratios of oxygen and hydrogen in response to the wet southwesterly summer monsoon and a notable increase in response to the cessation of this rainfall and the onset of drier conditions associated with the northeastern winter monsoon.





Isotopic variation at depths with time

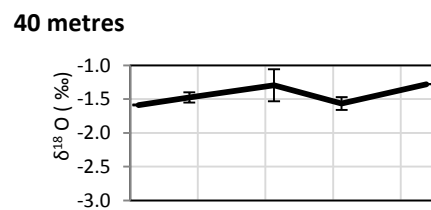
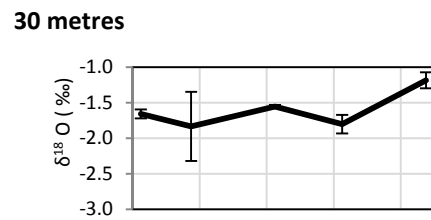
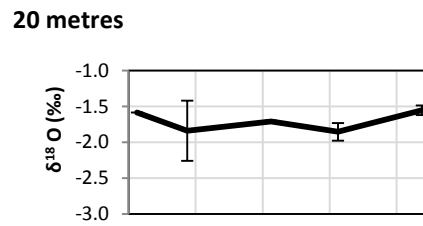
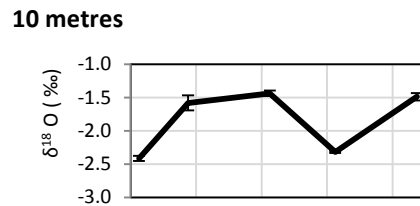
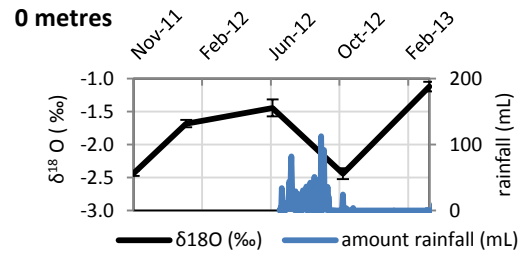


Figure 4.12:  $\delta^{18}\text{O}$  Isotopic composition of Yeak Loam waters with depth over time

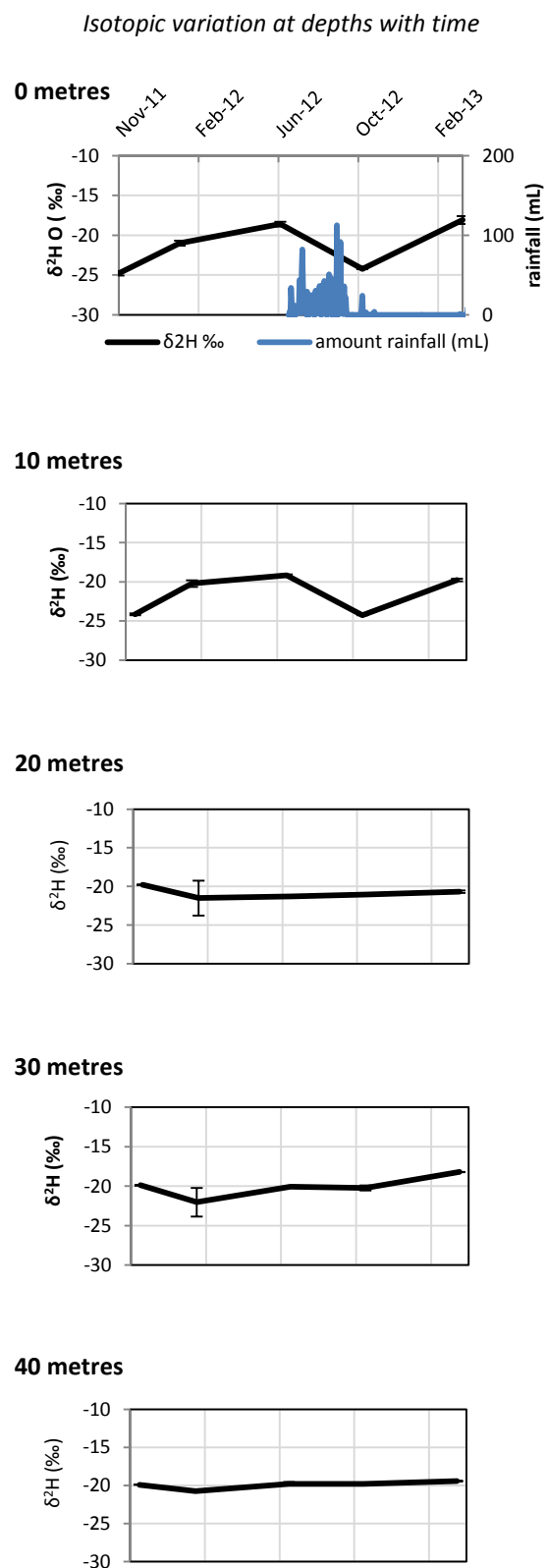
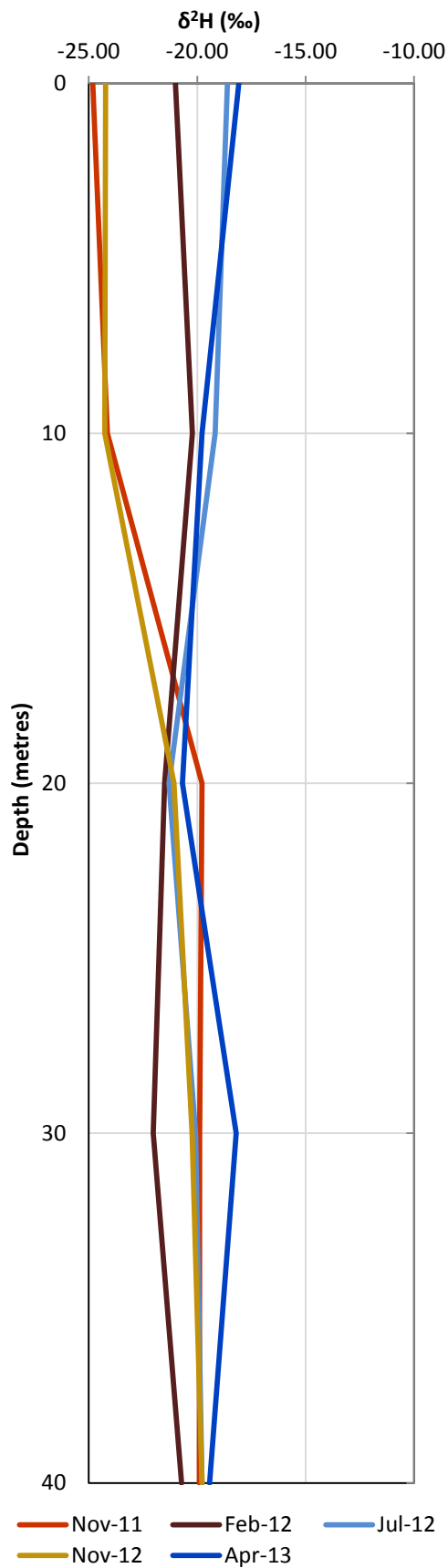


Figure 4.13:  $\delta^2\text{H}$  isotopic composition of Yeak Loam waters with depth over time

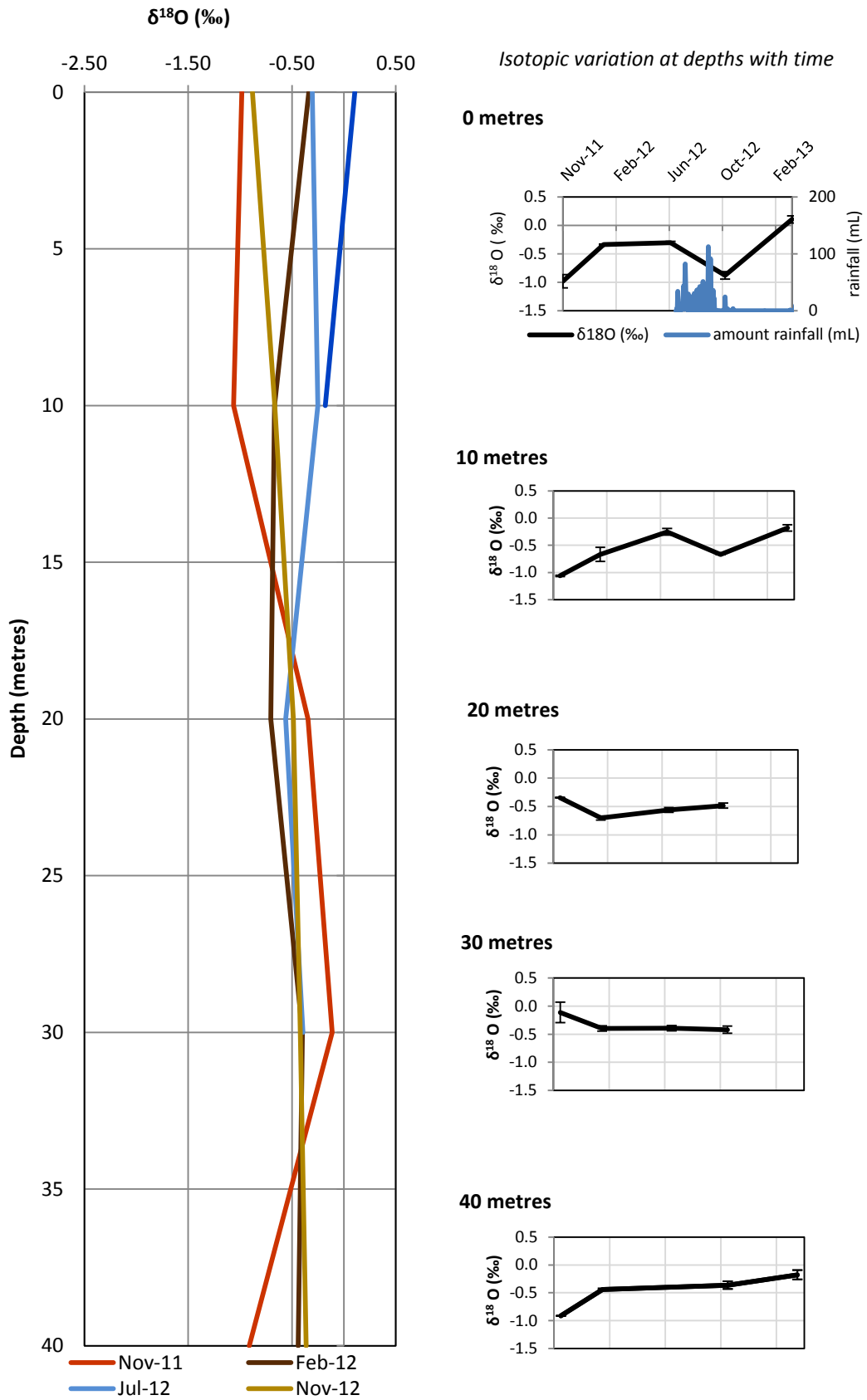
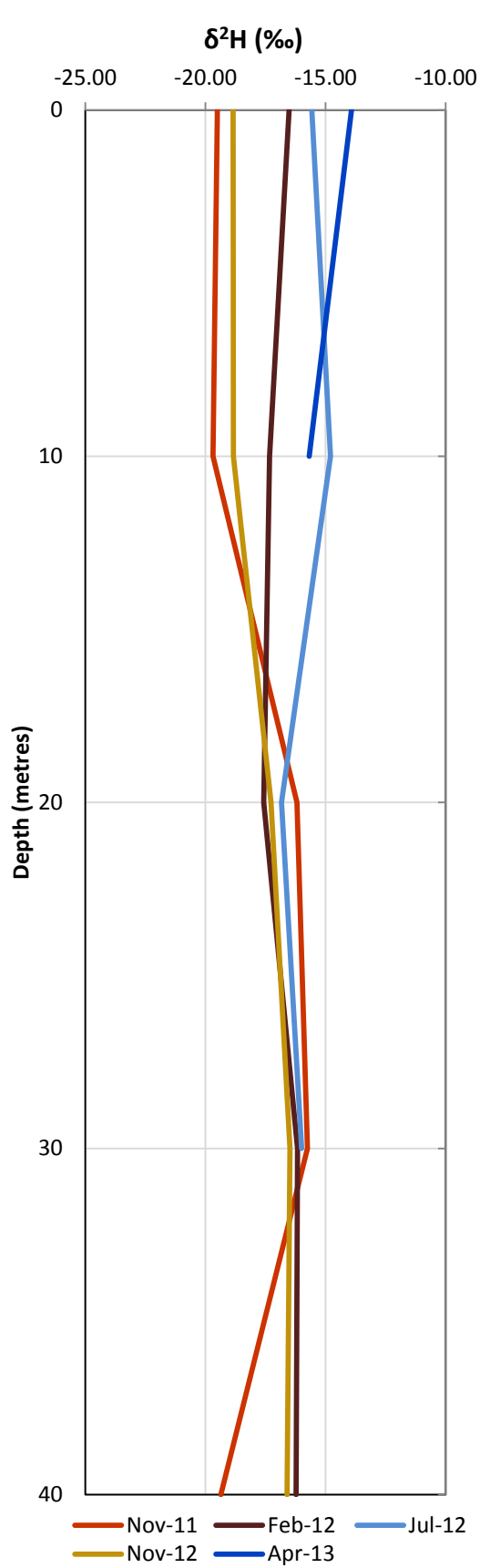
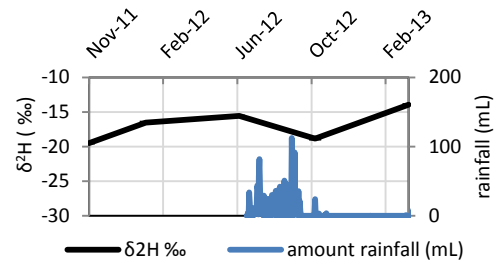


Figure 4.14:  $\delta^{18}\text{O}$  isotopic composition of Yeak Oam waters with depth over time



Isotopic variation at depths with time

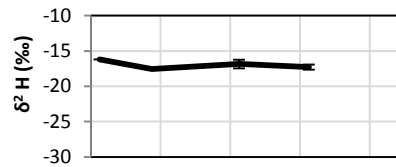
0 metres



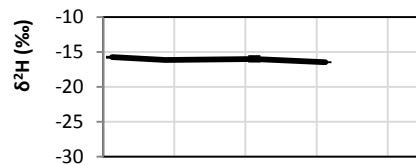
10 metres



20 metres



30 metres



40 metres

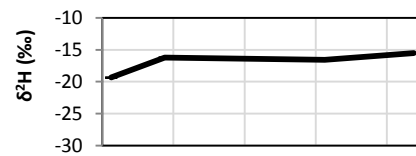


Figure 4.15:  $\delta^2\text{H}$  isotopic composition of Yeak Oam waters with depth over time

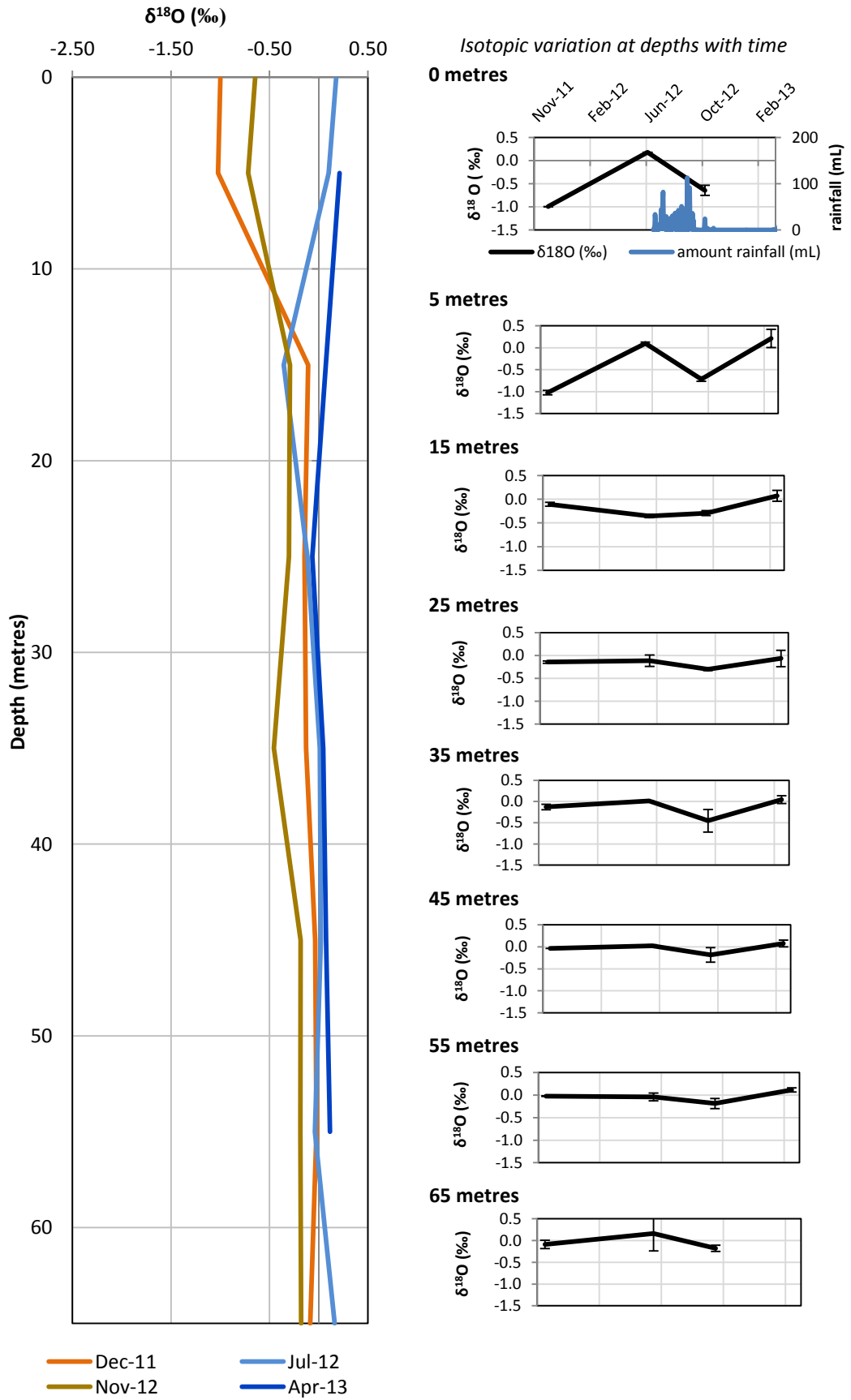


Figure 4.16:  $\delta^{18}\text{O}$  isotopic composition of Boeng Lumkut waters with depth over time

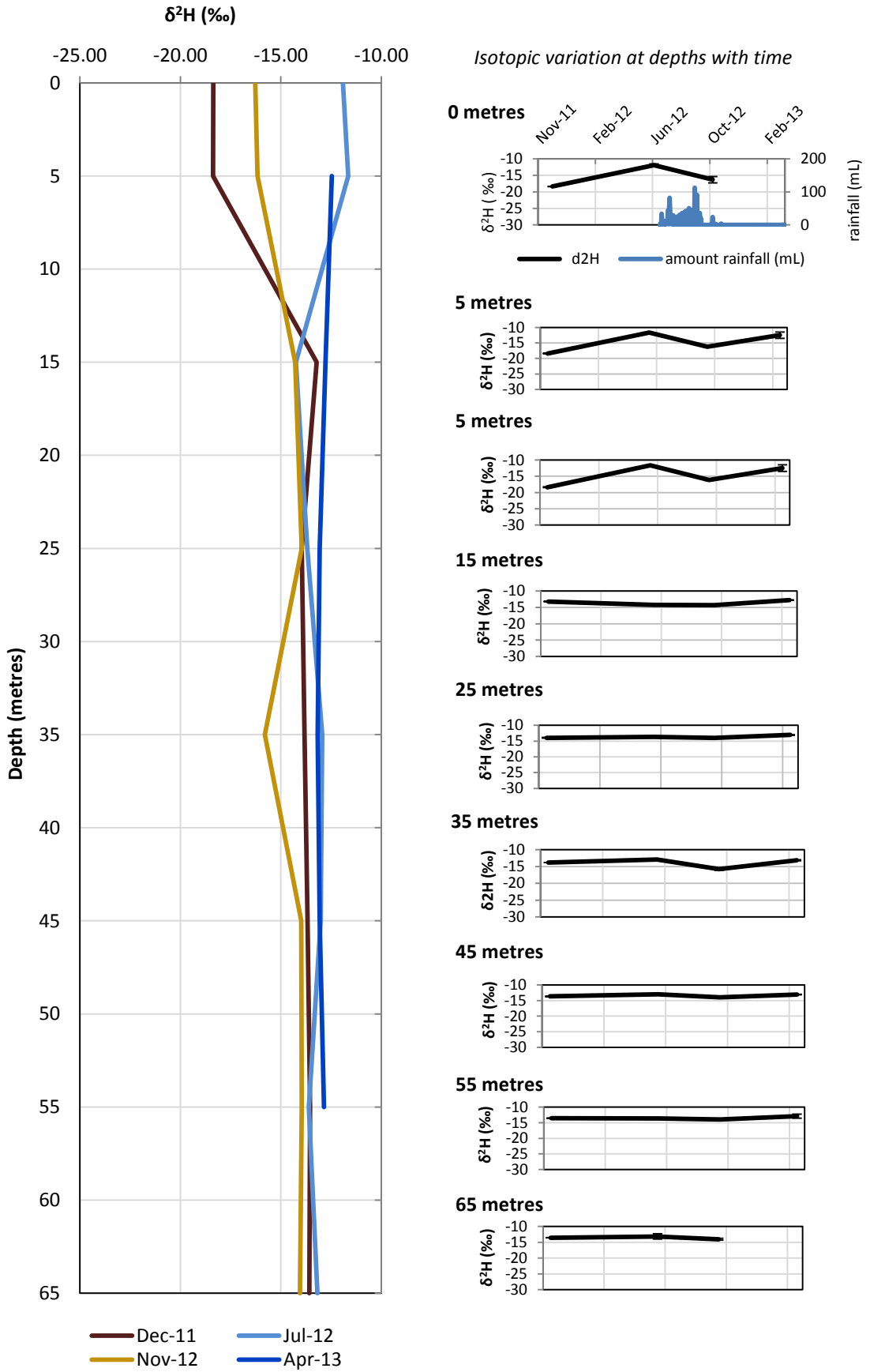


Figure 4.17:  $\delta^2\text{H}$  isotopic composition of Boeng Lumkut waters with depth over time

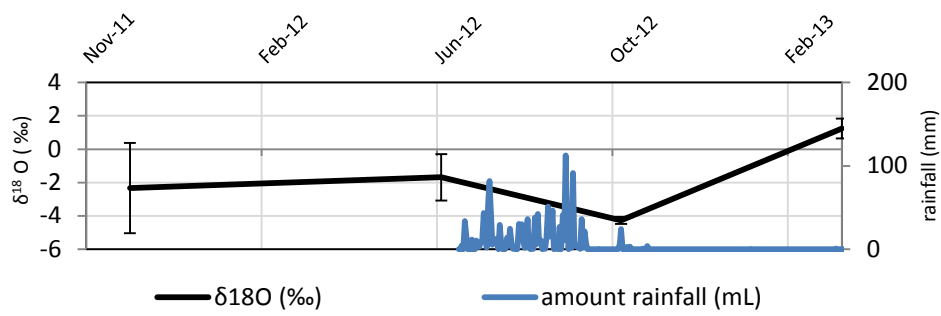


Figure 4.18:  $\delta^{18}O$  composition of Yeak Kara waters over time

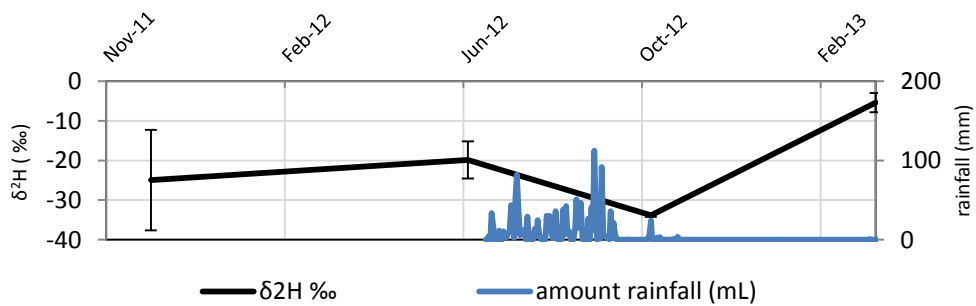


Figure 4.19:  $\delta^2H$  composition of Yeak Kara waters over time

## 4.5. Biogeochemistry of lake waters

Biogeochemical and chemical mediation of dissolved ions are an important indicator of lake primary productivity, and their flux over time is linked to the changing hydrological cycle of a lake and its catchment (Hamilton-Taylor & Davison, 1995). The changes over depth and time observed in these lakes are described below. Results are graphed to show concentrations (left column) and differences from lake average for all time periods (right column) in order to highlight trends in dissolved ion concentrations between ions and across all lakes. As some lakes were not sampled in some time periods, there may be time periods missing from some graphs.

### 4.5.1. Sodium, magnesium and potassium

Concentrations of sodium, magnesium and potassium in the deep stratified lakes as well as in shallow Yeak Kara are comparable. In stratified lakes, these ions show

stable concentrations throughout the water column over time. In Yeak Kara, there are comparatively higher concentrations throughout the year, but with relatively low values in November 2011 that increase progressively over subsequent sampling periods.

Sodium concentrations throughout the water columns of the three deep, stratified lakes (Boeng Lumkut, Yeak Loam and Yeak Oam) are fairly consistent and with low standard deviation over time (Figure 20). Where a higher sodium concentration is shown at 15 m depth in February 2012 for Boeng Lumkut, error bars suggest that it is actually in line with other recorded values with depth in that lake. There are, however, different concentrations of sodium present across lakes. Generally, Yeak Loam shows the lowest sodium concentrations, ranging between 0.77-1.11 g/mL, but these are only slightly less than sodium concentrations in Boeng Lumkut, which range between 0.69-2.23 g/mL. Yeak Oam shows the lowest concentrations of sodium, ranging from 0.773-1.118 g/mL. Yeak Kara has higher sodium concentrations in general and shows an increasing trend with subsequent sampling periods (8.9 g/ml in July 2012; 12.7 g/ml at November 2012, and 19.1 g/ml at April 2013).

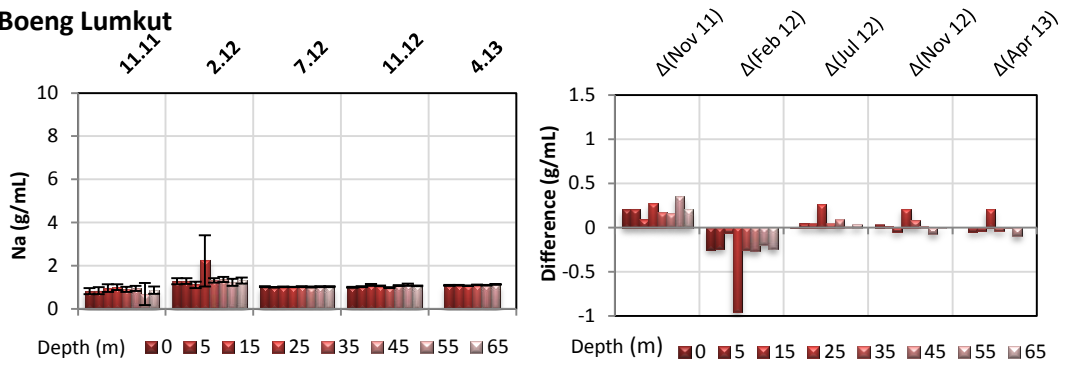
Concentrations of magnesium in these lakes display a similar trend to those of calcium ions with depth over time, and across all sampling periods, for Boeng Lumkut, Yeak Loam and Yeak Oam, magnesium ion concentrations remain fairly consistent with depth over time (Figure 21). In Boeng Lumkut, magnesium concentrations remain reasonably consistent at ~3 g/mL for all sampling periods. It is notable that the two lower values (55 m in November 2011 and 15 m in July 2012) have significantly larger standard deviations than other samples. Yeak Loam shows a similar trend of consistency in magnesium concentrations through the water column (~3 g/mL for all sampling periods), but samples show a slight decrease in epilimnion waters in the July 2012 and November (~0.3 g/mL lower than hypolimnion waters). Yeak Oam too shows fairly consistent magnesium concentrations with depth across time, with values ranging from



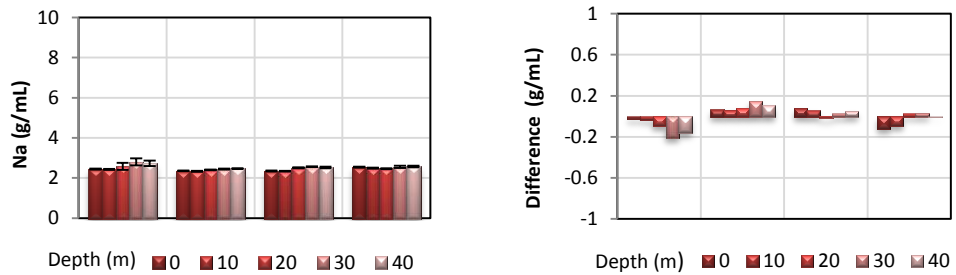
~2.4–2.6 g/mL, which are lower than Boeng Lumkut and Yeak Oam. Yeak Kara displays different trends in magnesium concentrations over time, with magnesium concentrations lower in July 2012 (13.96 g/mL) compared to November 2012 (19.5 g/mL). In April 2013, there is an increase to 27.7 g/mL. Across all lakes and sampling periods, standard error is low for magnesium concentrations.

In stratified lakes, potassium concentrations are generally stable with depth over time (Figure 22). In Boeng Lumkut, potassium concentrations are fairly consistent for all sampling periods, ranging between 1.45-2.59 g/mL. There are occasional elevated concentrations in the hypolimnion, though these show high standard deviations suggesting that true concentrations may not be as elevated as these values suggest. Yeak Loam displays relatively stable concentrations through the water column over time, however these range from 1.26-2.35 g/mL and are generally lower than Boeng Lumkut. Potassium concentrations in Yeak Oam for all sampling periods are also quite consistent through the water column, and are slightly higher than concentrations found in Boeng Lumkut and Yeak Loam (within the range of 1.9-3.36 g/mL). Samples in November 2012 show larger variability than those for other sampling periods, but are accompanied by larger errors which suggest that a stable trend with depth is possible. Yeak Kara shows very low concentrations of potassium in November 2011 (0.11 g/mL) and February 2012 (0.033 g/mL), but much higher concentrations in subsequent sampling periods (5.71-12.55 g/mL).

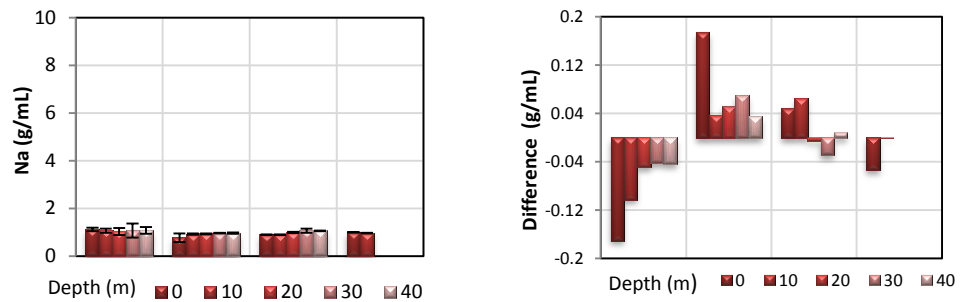
### Boeng Lumkut



### Yeak Loam



### Yeak Oam



### Yeak Kara

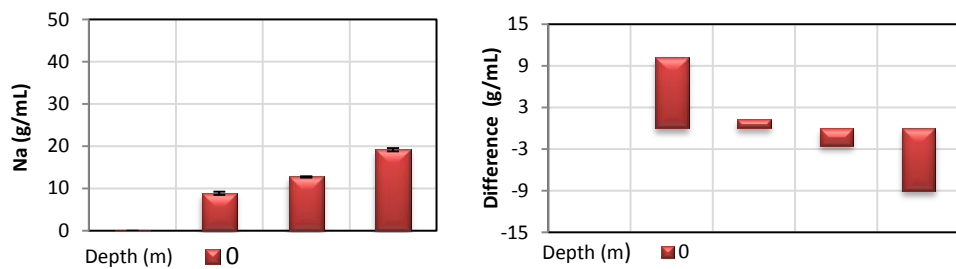
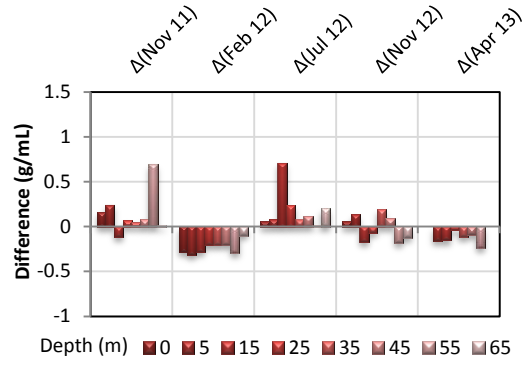
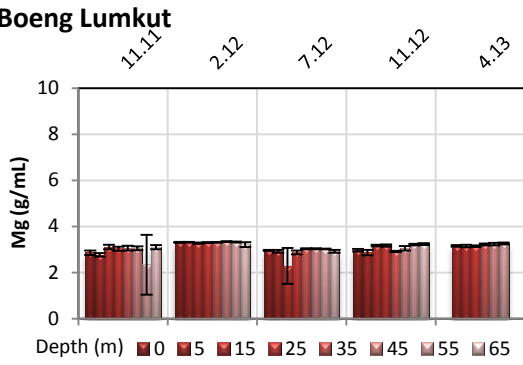
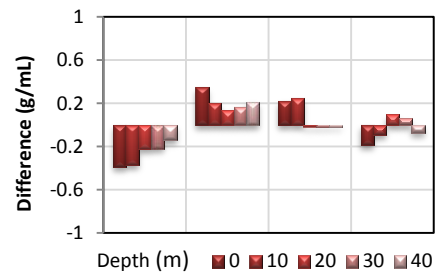
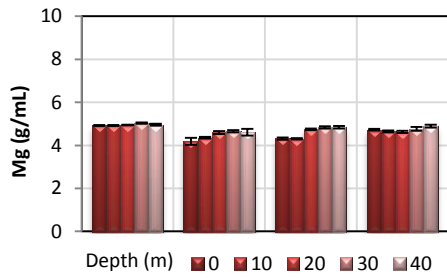


Figure 4.20: Sodium ion content in lake waters over time (note that the axis for Yeak Kara is expanded by a factor of 10 because of significantly higher iron content). Charts on the right show difference from average values for that lake.

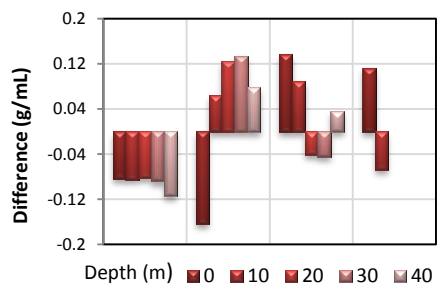
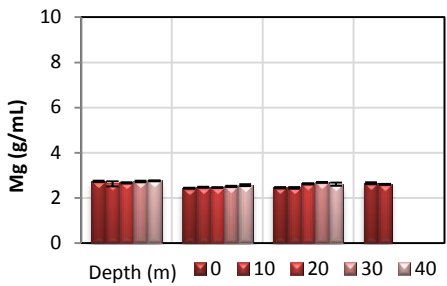
### Boeng Lumkut



### Yeak Loam



### Yeak Oam



### Yeak Kara

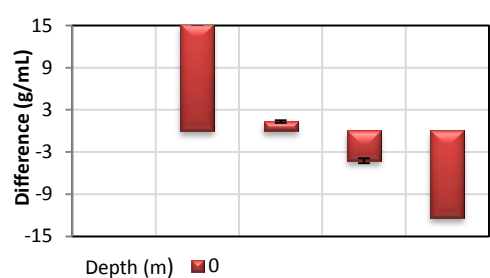
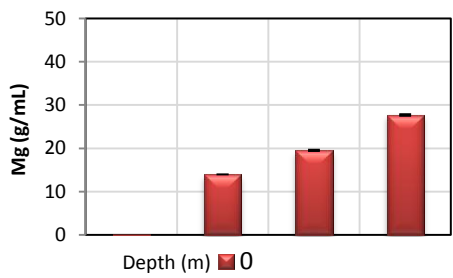
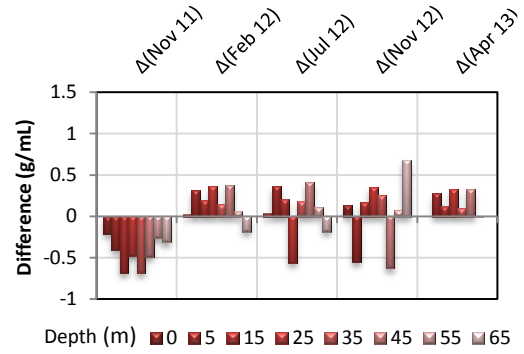
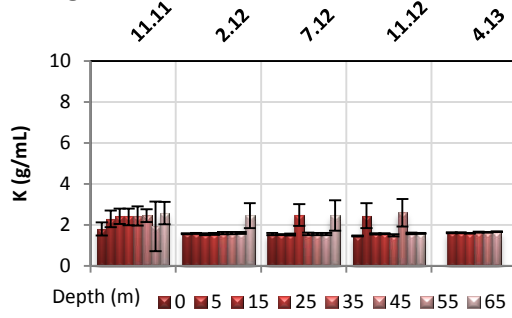
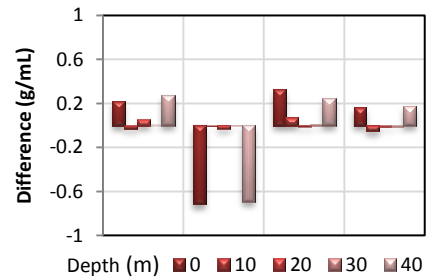
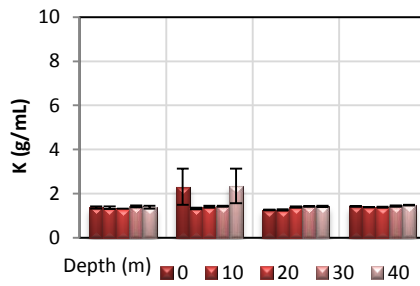


Figure 4.21: Magnesium ion content in lake waters over time (note that the axis for Yeak Kara is expanded by a factor of 10 because of significantly higher iron content). Charts on the right show difference from average values for that lake.

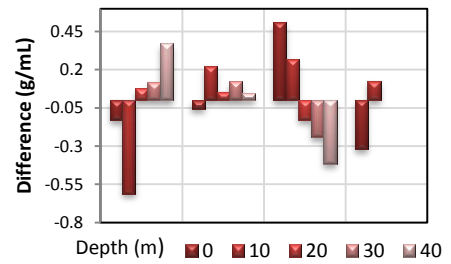
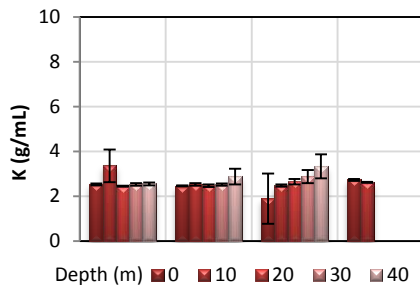
### Boeng Lumkut



### Yeak Loam



### Yeak Oam



### Yeak Kara

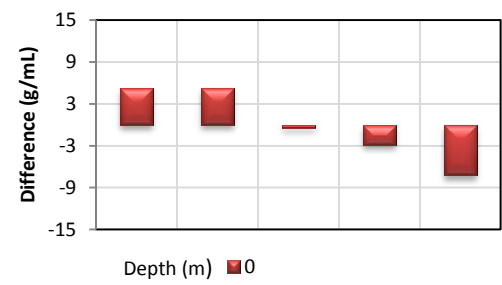
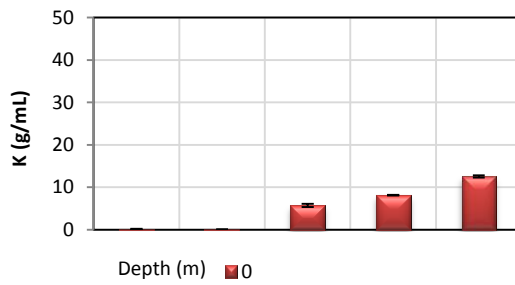


Figure 4.22: Potassium ion content in lake waters over time (note that the axis for Yeak Kara is expanded by a factor of 5 because of significantly higher iron content). Charts on the right show difference from average values for that lake.

#### 4.5.2. Calcium, barium and aluminium

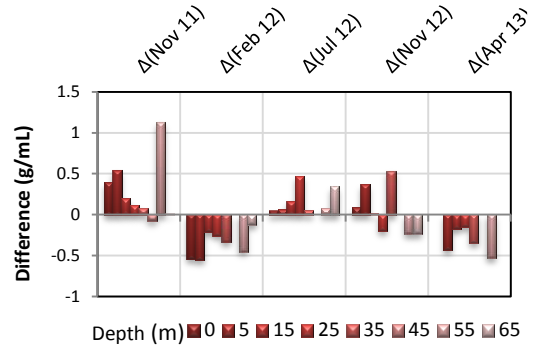
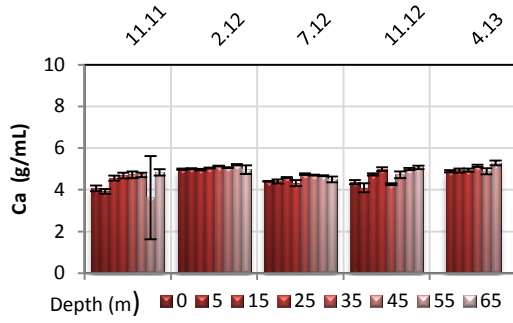
There are similarities in concentrations of calcium and barium in the deep stratified lakes, as well as in shallow Yeak Kara. In stratified lakes, concentrations of these ions are higher in the hypolimnion compared to the epilimnion, however concentrations of aluminium are very low and have high standard deviations, making it difficult to discern whether this trend occurs as well. In shallow Yeak Kara, calcium, barium and aluminium show significantly higher concentrations in November 2011 and February 2012, with comparatively low values in subsequent sampling periods.

Boeng Lumkut, Yeak Loam and Yeak Oam display fairly steady levels of calcium concentration with a slight increasing trend with depth during all sampling periods (Figure 23). Concentrations of calcium are quite comparable, between ~5-6.3 g/mL in Yeak Loam and from ~5-6.3 g/mL in Yeak Oam and slightly lower in Boeng Lumkut, ranging from ~4-5.2 g/mL. Yeak Kara displays much higher overall values. The November 2011 sampling period, at the end of wet monsoonal season, displays a lower calcium concentration (20.21 g/ml) than at the end of the dry winter monsoon period in December 2012 (26.27 g/ml). Concentrations of calcium are lower in July 2012 (17.4 g/ml), increasing in November 2012 (28.9 g/ml) and further increasing during April 2013 (34.1 g/ml).

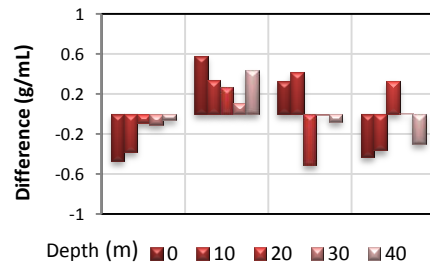
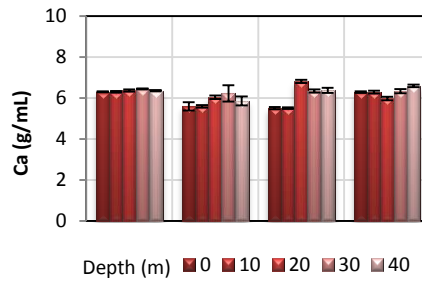
In all of the deep stratified lakes, barium concentrations increase in the hypolimnion although are present and stable in the epilimnion (Figure 24). There are higher concentrations of barium ions in Yeak Oam (within the range of 0.11-0.19 g/mL), with slightly lower concentrations of barium in Yeak Loam (within the range of 0.04-0.08 mg/L) and Boeng Lumkut (within the range of 0.02-0.05 mg/L). Yeak Kara shows comparatively very high barium concentrations in November 2011 (8.83 mg/L) and February (9.29 mg/L) and low barium concentrations in the other sampling periods (0.091-0.131 mg/L). Standard deviations are low overall.

In general, measured concentrations of aluminium ions do not show particularly strong trends with depth or time and show large errors in all lakes, in part because concentrations are very low (Figure 25). In Boeng Lumkut, there is little observed consistency in aluminium concentrations across the sampling periods, and several instances of very large standard deviations. There are much higher concentrations in February 2012, especially at 0 m depth (0.03 g/mL) and at 56 m depth (0.41 g/mL). There are much lower values in July 2012, but the lowest values are observed in November 2012 (0.002 -0.008 g/mL). In April 2013, values for 5 m depth (0.12 g/mL) and 35m (0.01 g/mL) are higher than but not as high as for 0 m and 5 m depths in February 2012. In Yeak Loam, concentrations of aluminium are quite low through the water column in February 2012. Concentrations could potentially have remained similar to February 2012 levels with depth over time through the other sampling periods in this lake, given that standard deviations for elevated values are extremely high. In Yeak Oam, aluminium ion concentrations are generally low in February 2012 (0.003 g/mL), with an anomalously high value for 30 m depth that has a large standard deviation and is likely to actually be in line with the other concentrations observed through the water column. In July 2012, concentrations of aluminium are two or more times as high as those in February 2012, especially in metalimnion waters. November 2012 and April 2012 both show very low concentrations of aluminium. In Yeak Kara, aluminium concentrations are highest in November 2011 and February 2012, peaking at 32.8 g/mL, but are very low in subsequent sampling periods (lowest concentration 0.003 g/mL).

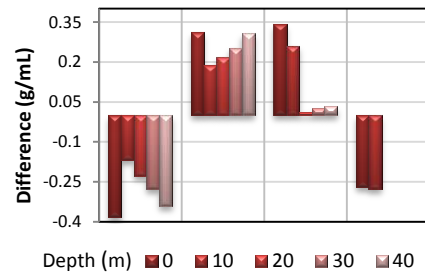
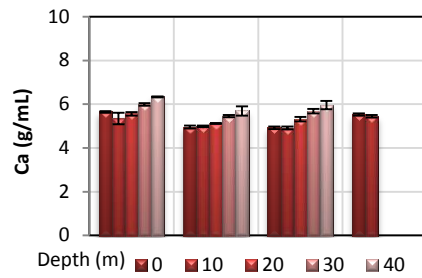
### Boeng Lumkut



### Yeak Loam



### Yeak Oam



### Yeak Kara

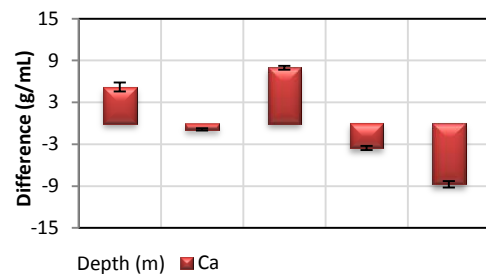
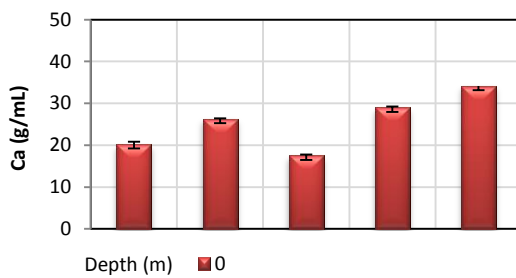
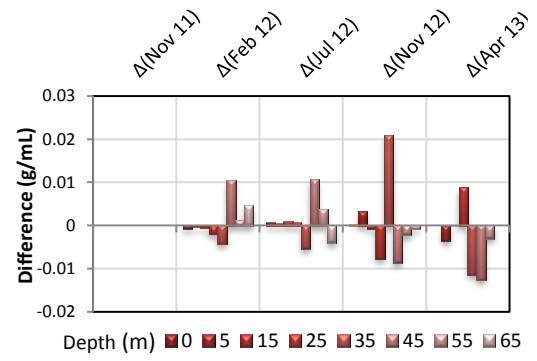
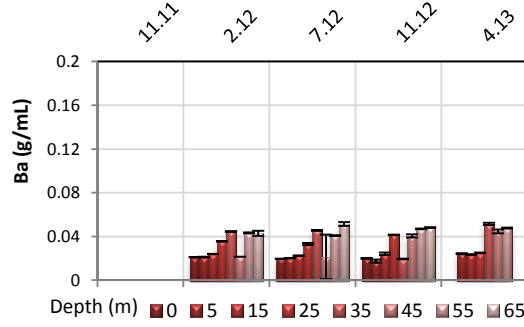
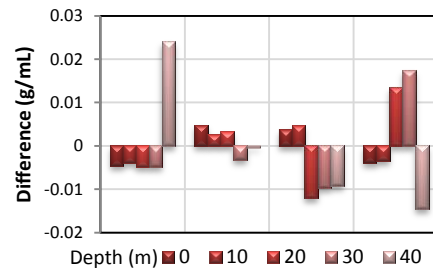
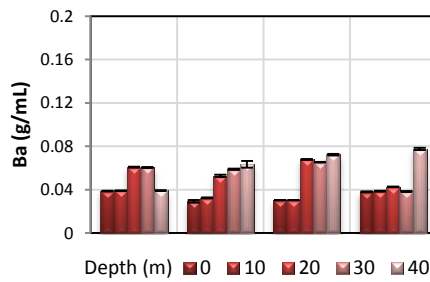


Figure 4.23: Calcium ion content in lake waters over time (note that the axis for Yeak Kara is expanded by a factor of 5 because of significantly higher iron content). Charts on the right show difference from average values for that lake.

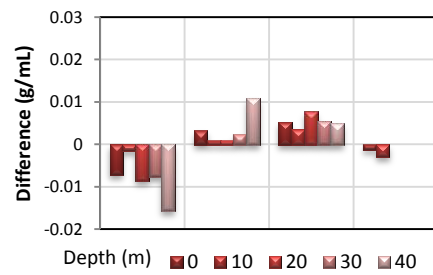
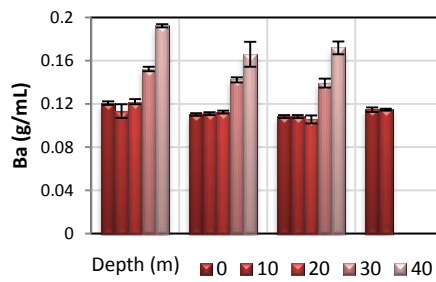
### Boeng Lumkut



### Yeak Loam



### Yeak Oam



### Yeak Kara

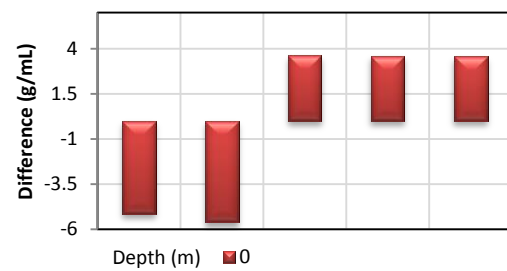
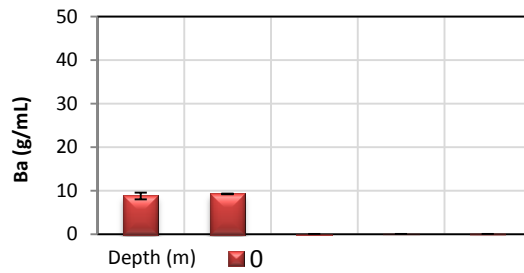
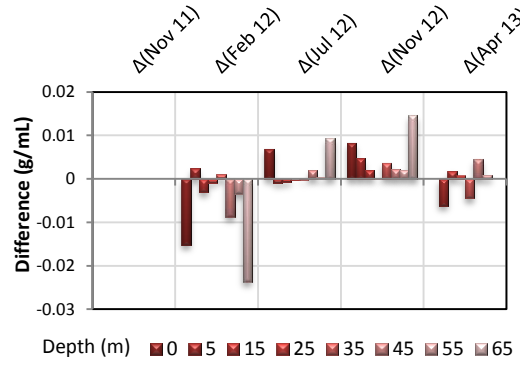
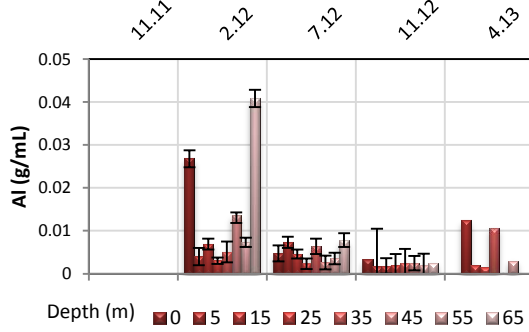


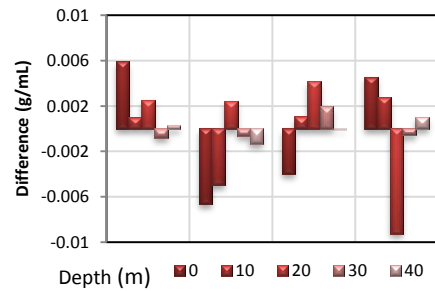
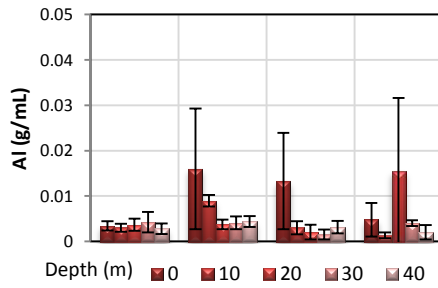
Figure 4.24: Barium ion content in lake waters over time (note that the axis for Yeak Kara is expanded by a factor of 250 because of significantly higher iron content). Charts on the right show difference from average values for that lake.



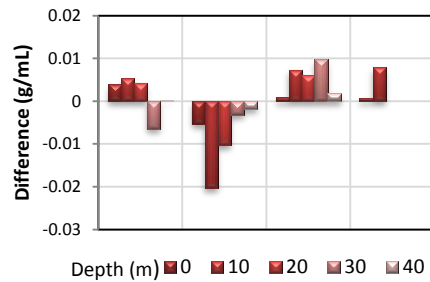
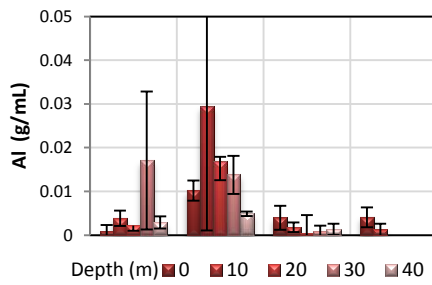
### Boeng Lumkut



### Yeak Loam



### Yeak Oam



### Yeak Kara

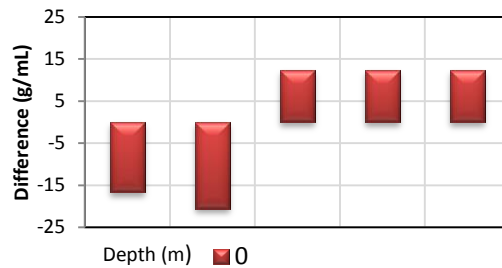
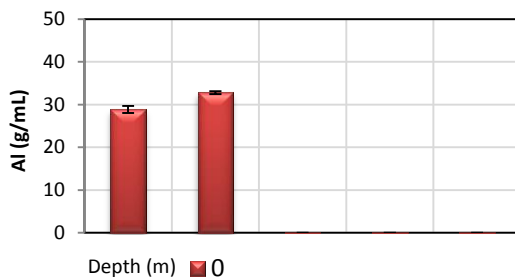


Figure 4.25: Aluminium ion content in lake waters over time (note that the Axis for Yeak Kara is expanded by a factor of 1000 because of significantly higher iron content). Charts on the right show difference from average values for that lake.

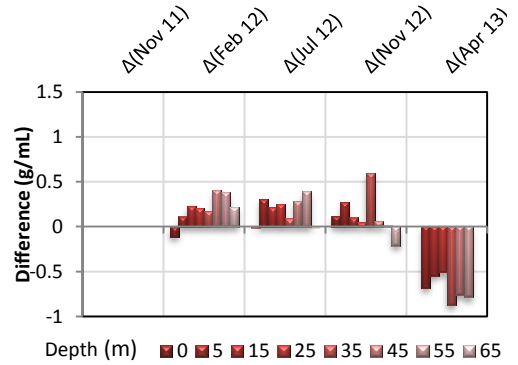
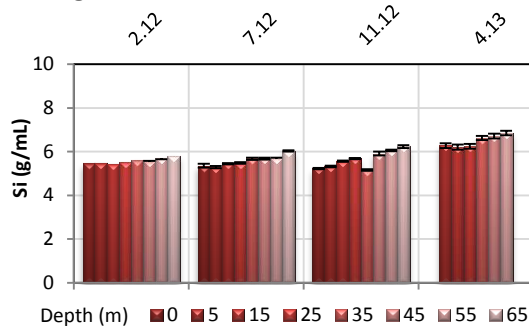
#### 4.5.3. Silica and strontium

There are similarities in concentrations of silica and strontium in the deep stratified lakes, as well as in shallow Yeak Kara. These ions increase in concentration with depth in stratified lakes, and in shallow Yeak Kara are lowest in February 2012, higher in November 2011 and 2012, and highest in April 2013.

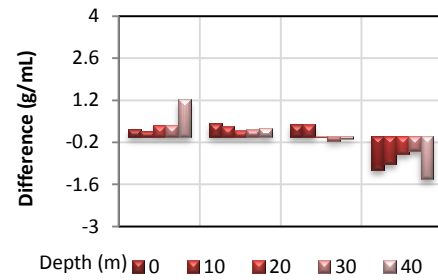
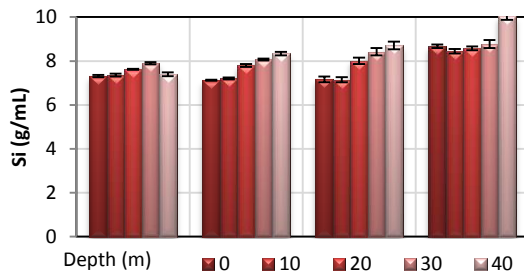
In the stratified deep tropical lakes, concentrations of silica increase slightly with depth across all sampling periods (Figure 26). Silica concentrations are highest in Yeak Loam (7.12-10.02 g/mL) and Boeng Lumkut (5.26-6.68 g/mL), but lower in Yeak Oam (2.25-4.47 g/mL). In Yeak Oam, there is a steeper rate of increase in the concentration of silica with depth compared to Boeng Lumkut. Yeak Kara shows lowest concentrations of silica in July 2012 (10.09 g/mL), higher concentrations in November 2012 (33.85 g/mL) which are comparable to concentrations in November 2011 (37.11 g/mL), and highest concentrations in April 2013 (47.26 g/mL). Standard deviations in measurement of silica concentration are very low across all depths and sampling periods for all lakes.

Strontium concentrations in deep stratified lakes are very stable with depth and time, with a consistent trend of slightly increased levels in hypolimnion waters (Figure 27). Concentrations in Boeng Lumkut are the lowest in these lakes, and range from 0.041-0.54 g/mL. In Yeak Loam, strontium concentrations are slightly higher, ranging between 0.06-0.08 g/mL over depth and time, and Yeak Oam has the highest strontium concentrations of these lakes, ranging between 0.16-1.89 g/mL over depth and time. Yeak Kara shows different trends in strontium concentration, with a low of 0.077 g/mL in July 2012, a slightly higher concentration of 0.248 g/mL in November 2012 which is comparable to the November 2011 strontium concentration of 0.302 g/mL, and a higher concentration of 0.377 g/mL in April 2013. This trend is similar to concentrations of silica in Yeak Kara over time. Errors across all values with depth and time in these lakes are quite low.

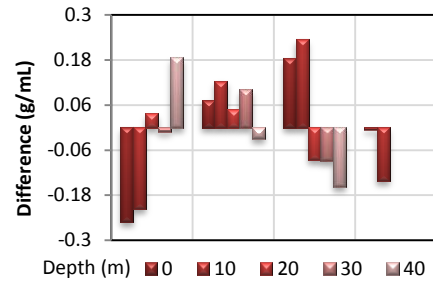
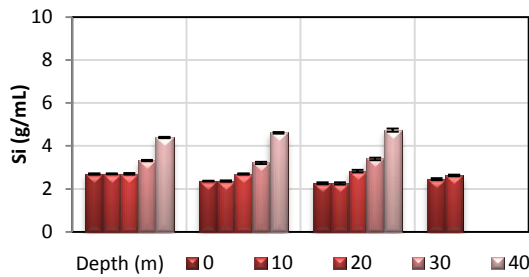
### Boeng Lumkut



### Yeak Loam



### Yeak Oam



### Yeak Kara

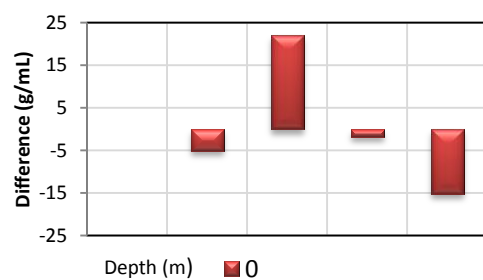
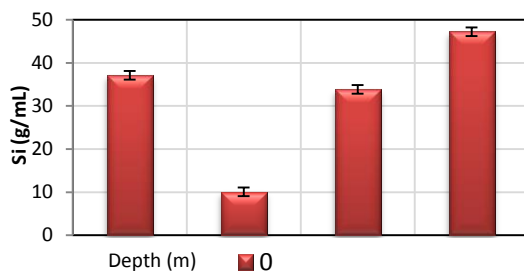
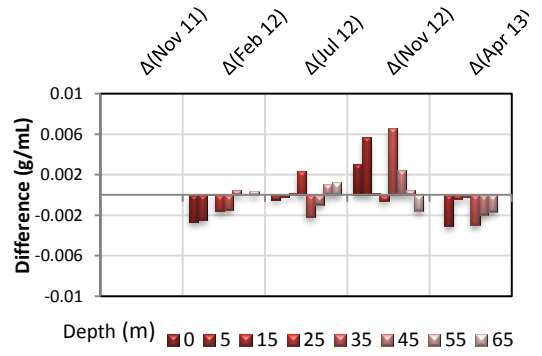
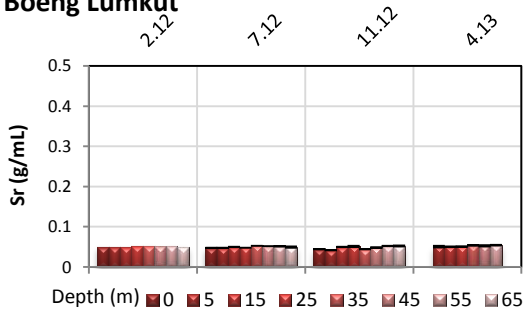
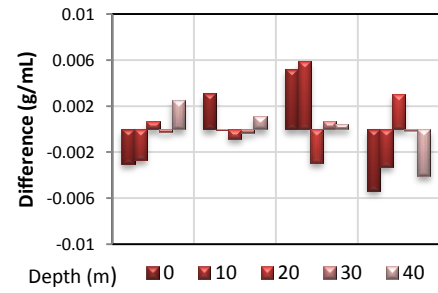
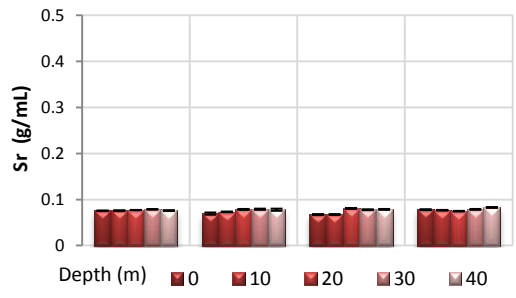


Figure 4.26: Silica ion content in lake waters over time (note that the axis for Yeak Kara is expanded by a factor of 6 because of significantly higher iron content). Charts on the right show difference from average values for that lake.

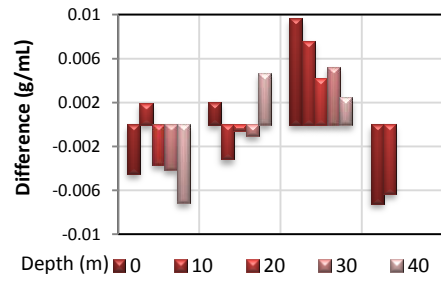
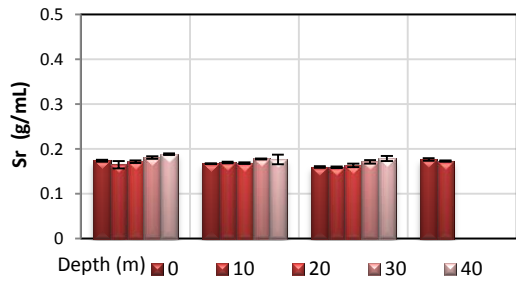
**Boeng Lumkut**



**Yeak Loam**



**Yeak Oam**



**Yeak Kara**

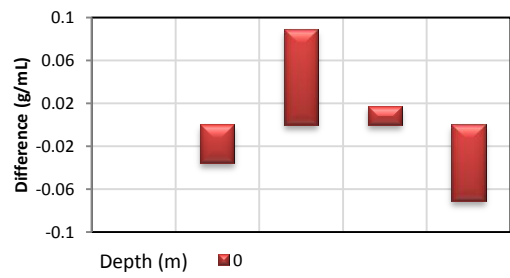
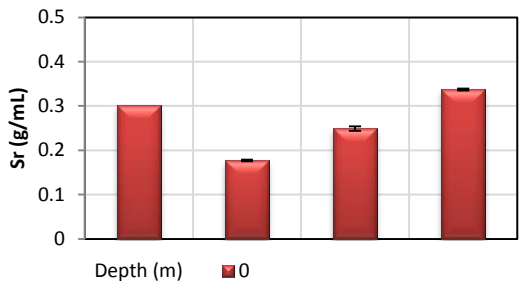


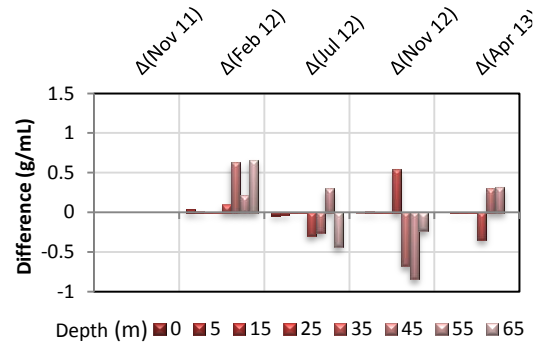
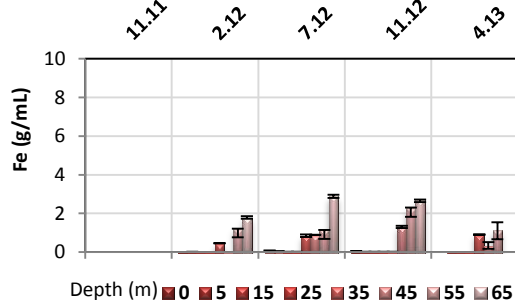
Figure 4.27: Strontium ion content in lake waters over time. Charts on the right show difference from average values for that lake.

#### 4.5.4. Iron and sulfur

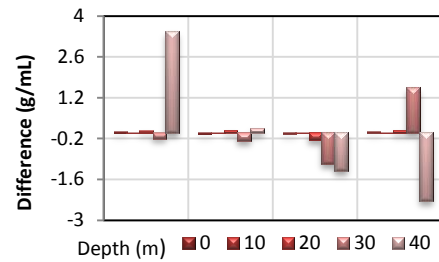
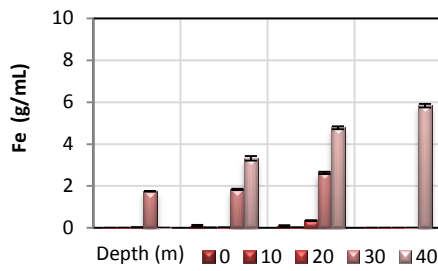
In general in deep stratified lakes, iron concentrations are very low in the epilimnion and increase rapidly after 30 m depth to much higher levels (Figure 28). The lowest concentrations of iron are observed in Boeng Lumkut, ranging from 0.001-2.88 mg/L, where there is the least rapid rate of increase in concentrations of iron between the epilimnion and the hypolimnion. Yeak Loam shows slightly higher amounts of iron, ranging from 0.001-5.83 g/mL, and Yeak Oam has the highest iron levels of the stratified lakes, ranging from 0.002-8.01 g/mL, as well as the most rapid rate of increase in concentrations of iron between the epilimnion and the hypolimnion. In Yeak Kara, there are high concentrations of iron in November 2012 (14.43 g/mL) and February 2012 (18.01 g/mL), however low iron concentrations in subsequent sampling periods (0.054-0.15 g/mL). Standard deviation values for iron concentrations in all depths and sampling periods over all lakes are relatively low.

Trends in concentrations of sulfur in stratified lakes are difficult to infer as all values have very large standard deviations (Figure 29). Samples are, in general, quite low in these lakes. In Yeak Kara, sulfur shows highest concentrations in February 2012, slightly lower concentrations in April 2013, and lower concentrations in July and November 2012. All of these samples have high errors, making it difficult to discern the trend over time in this lake for sulfur as well.

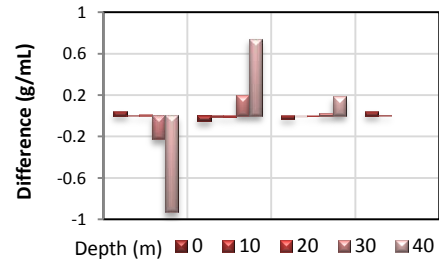
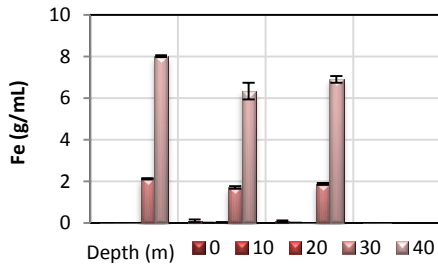
### Boeng Lumkut



### Yeak Loam



### Yeak Oam



### Yeak Kara

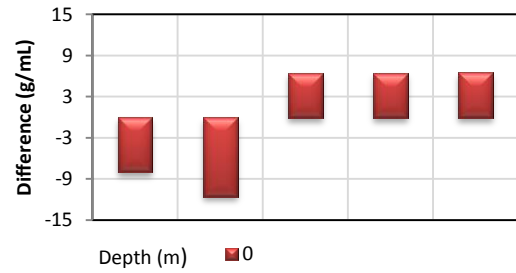
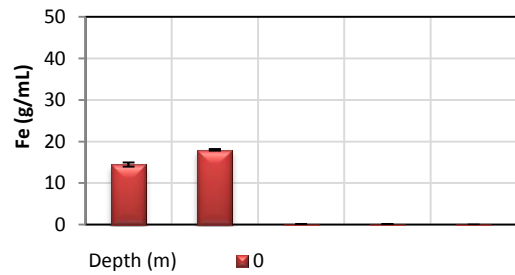
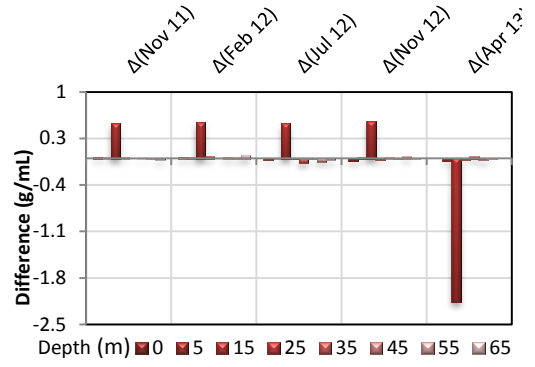
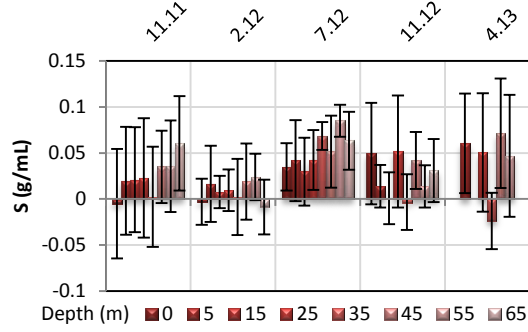
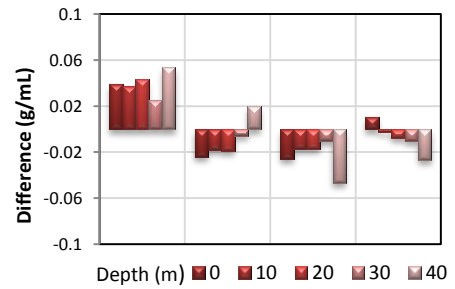
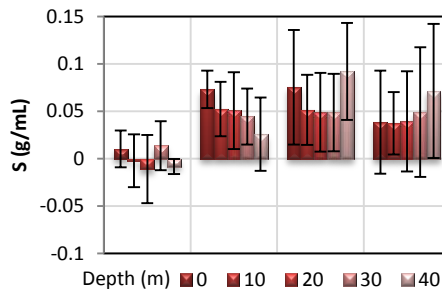


Figure 4.28: Iron ion content in lake waters over time (note that the axis for Yeak Kara is expanded by a factor of 5 because of significantly higher iron content). Charts on the right show difference from average values for that lake.

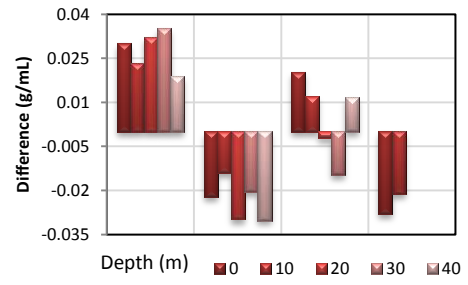
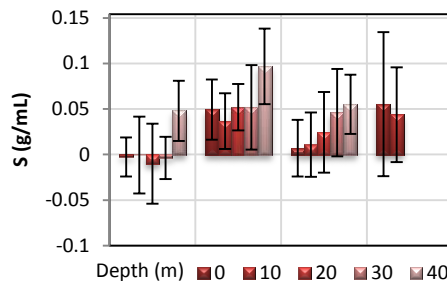
**Boeng Lumkut**



**Yeak Loam**



**Yeak Oam**



**Yeak Kara**

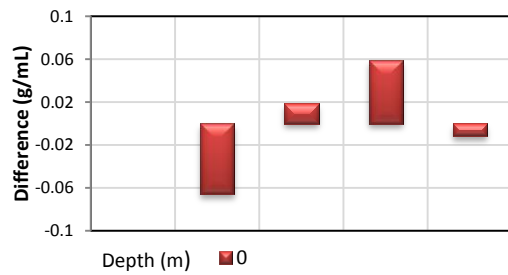
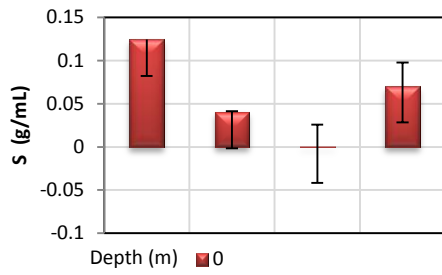


Figure 4.29: Sulfur ion content in lake waters over time. Charts on the right show difference from average values for that lake.

## **4.6. YK0712B sediment core**

In the previous sections, the contemporary biogeochemistry of the study sites and the isotope dynamics of meteoric and surface waters were described. These data are critical in demonstrating the climate sensitivity of the field sites, and for the palaeoclimatic interpretation of the sedimentary archive. This section will describe the results of analysis of sediment cores from one of these sites, Yeak Kara. The sedimentology, geochemistry and stable isotope dynamics of these sediment archives are instrumental in gaining a holistic understanding of the palaeoclimate information they contain as they provide insight into the environmental conditions and responses to climate over time (Cheng-Bang et al., 2011).

### **4.6.1. Sediment characteristics**

Core YK0712B is 13 m long, being comprised of 13 one-metre long sections. Table 4.2 shows the total amount of sediment recovered from each corer drive. It is assumed that, for each section, one metre of sediment has been compressed into the recovered length. A visual log of the core indicated four distinct units based on colour and texture – Unit 1 (13.0-12.35 m), Unit 2 (12.35-11.91 m), Unit 3 (11.91-4.1 m) and Unit 4 (4.1m-0.0 m), which are described below.



Table 4.2: Recovered sediment for each drive for core YK0712B

Drive number	Section (m)	Upper depth (cm)	Lower depth (cm)	Total length of sediment recovered (cm)
1	0-1 m	13.5	100.0	86.5
2	1-2 m	13.2	100	86.8
3	2-3 m	11.8	99.5	87.7
4	3-4 m	29.5	99.0	69.5
5	4-5 m	16.0	98.4	82.4
6	5-6 m	20.0	98.5	78.5
7	6-7 m	38.5	100.0	61.5
8	7-8 m	23.0	98.5	75.5
9	8-9 m	16.5	100.0	83.5
10	9-10 m	3.5	99.0	95.5
11	10-11 m	17.0	100.0	83
12	11-12 m	33.5	100.0	66.5
13	12-13 m	5.5	100.0	94.5

Unit 1 (13.0-12.35 m) is a massive brownish black (2.5Y/3/1) clay or silty clay with an abrupt upper boundary with Unit 2 (12.35-11.91 m). It is consistent in colour and texture and has some fine (<1 mm) gas bubbles with a soft but non-fluid consistency.

Unit 2 (12.35-11.91 m) is a laminated silty clay, showing alternating layers of dark greyish yellow (2.5Y/5/2/), yellowish grey (2.5Y/4/1) and light grey (2.5Y/8/1) <1 mm in thickness interspaced with very thin layers ( $\leq 1$  mm) of brownish black (2.5Y/3/1) material. At 11.95 m and 12.555-12.35 m, there are small reddish brown (2.5YR/4/8) tinges to these laminations. This unit is moderately hard and non-fluid, with laminations displaying sharp, distinct boundaries with each other. The boundary between this unit and Unit 3 at 11.91 m is clear, occurring over 2 cm starting at 11.925 cm. It is marked by the rapid cessation of yellowish grey laminations and a resumption of brownish black (2.5Y/3/1) silty clay sediment.

Unit 3 (11.91-4.1 m) is a massive brownish black (2.5Y/3/1) clay to silty clay characterised by the presence of yellowish brown mottles that resemble clear to diffuse laminations occurring intermittently throughout. At 11.622 m, there is a thin layer of

black (2.5Y/2/1) material of smooth texture with abrupt boundaries with the surrounding brownish black clay/silty clay, and at 11.70 m there is a thin band (1 mm) of yellowish brown (2.5Y/5/3) clay or silty clay with abrupt boundaries to the surrounding brownish black clay/silty clay. From this point to 4.1 m, sediment is brownish black (2.5Y/3/2 and 2.5Y/3/1) with diffuse yellowish brown (2.5Y/5/3) and olive brown (2.5Y/4/3) mottling observed. The most distinct of these observed at 9.285-9.278 m (2.5Y/4/2), 8.93-8.92 m, 8.864-8.852 m, 8.760 m, 8.710 m, 8.610-8.605 m, 8.580-8.575 m, 8.5470 m, 8.575-8.570 m and 8.485-8.480 m (all 2.5Y/5/3), 7.885-7.860 m (2.5Y/4/3), 7.805-7.800 m, 7.718-7.080 m, 7.620-7.610 m and 7.51-7.50 m (2.5Y/5/3). There are occasional very thin (usually 0.5-1 mm) bands of charcoal (2.5Y/1/1) present (9.955 m, 8.973 m, 8.783 m, 8.776 m, 8.740-8.745 m, 8.69-8.70 m, 8.655 m, 6.802-6.808 m, 4.945-4.920 m). In this Unit, mottled areas correspond to slightly more silty texture, however the transition between areas of more silty clay texture and areas of more clay texture is very diffuse. Unit 3 has an abrupt lower boundary at 4.1 m with the cessation of mottling. Small gas bubbles (<1 mm in diameter) were infrequently distributed through the matrix between 8.464- 4.270 m. Small pieces of wood or charcoal fragments (<1 mm in size) were observed to be infrequently distributed through the matrix between 6.979-4.326 m. A piece of charcoal or wood ~8 mm in length was seen at 6.832-6.835 m. A small leaf was also observed at 5.660 m.

Unit 4 begins at 4.1 m and is a massive clay with stable brownish black colour (2.5Y/3/1) and clay texture with no evidence of mottling. It retains consistent colour and texture throughout. Gas bubbles <1 mm in diameter were observed at 3.785 m, 3.778 m, 3.777 m, 3.753 m, 3.749 m, 3.748 m, 3.719 m, 3.710 m, 3.708 m, 3.695 m, 3.482 m, 3.384 m, 2.870 m, 2.610 m. A gas bubble of 0.85 cm was observed at 2.919-2.900 m, and bubbles 1-2 mm in diameter were seen at 2.620 m and 2.493 m. From 2-0 m, no overt gas bubbles were observed as this region was moderately fluid and the

process of splitting the cores smoothed the surface of the split. Occasional small, hard whitish fragments (ostracods tests) were observed at 4.920 m, 4.914 m, 4.715 m, 4.650 m, 4.590 m, 4.550 m, 4.520 m, 4.470 m, 4.457 m, 4.355 m, 4.347 m, 4.324 m, 4.304 m, 4.289 m, 4.282 m, 4.243 m, 4.235 m, 4.200 m, 3.863 m, 3.849 m, 3.843 m, 3.539 m, 3.360 m, 3.322 m and 2.213 m. Small pieces of wood or charcoal fragments (<1 mm in size) were observed in the sediment at 3.975 m, 3.970 m, 3.630 m, 3.573 m, 3.415 m, 3.396 m, 3.322 m and 2.926 m. In addition, a small piece of charcoal or wood was observed at 3.375-3.365 m. A void was observed from 40.1-40.7 cm.

#### **4.6.2. Loss-on-ignition analysis**

Through the YK0712B core, loss-on-ignition values show three broad trends – stability of high levels of inorganic carbon and siliciclastic material in Units 1 and 2 followed by a general decreasing trend over depth in Unit 3, and a resuming of stability at much lower values in inorganic carbon and siliciclastic material in Unit 4 (Figure 4.30). Overall, Unit 3 shows a decreasing trend in inorganic carbon and siliciclastic material which is characterized by significant amount of variability, especially with regard to inorganic carbon levels.

Units 1 and 2 show relative stability in organic carbon levels, with values remaining within the 60-70% range. Inorganic carbon remains reasonably constant at about 20%, varying by one or two per cent aside from a drop to just over 12% at 12.8 m. Siliciclastic materials show slightly more variability, ranging from 14-27% in this section.

Unit 3 shows reasonably stable levels of organic matter with reasonably low levels of variability and change, but there is a significant degree of change and variability in inorganic carbon and siliciclastic materials. There is a slight increase in organic carbon

content (~5%) at the beginning of this section (11.5-10.8 m) after which values tend to remain within  $\pm 5\%$  of 80% until about 7.4 m. At this point, a slight decreasing trend occurs, with values dropping 15% until 5.7 m, with one anomalously low value of 35% at 7.10 m. Inorganic carbon shows a series of sharp peaks (56% at 10.7 m, 68% at 8.8 m, 50% at 8.2 m and 33% at 7.1 m), although mean values tend to hover around 30-35% around these peaks. There are a series of troughs, which are much more gradual, that reach very low values (<5% from 9.9-9.3 m, 7.5-7.6 m, 7.10 m, 6.60 m and from 4.9-4.10 m). The gradients joining these peaks and troughs show some variability from 11.9-10.7 m. They tend to be reasonably smooth from 10.7-8.8 m, resume greater variability from 8.8-6.6 m, and are again reasonably smooth from 6.5-4.1 m. Trends in change and variability in siliclastic material follow the same broad patterns as those observed in inorganic carbon, however proportions of siliclastic material are generally lower with 23% at their peak in this region aside from an anomalously high value of 49% at 5.1 m.

Within Unit 4, organic carbon levels show variability between 65-75% from 4.1-0.6 m, after which they decrease to remain stable within  $2-3\% \pm 60\%$ . Inorganic carbon levels remain relatively stable between 1-5% with little variability, and siliclastic material follows this same trend.

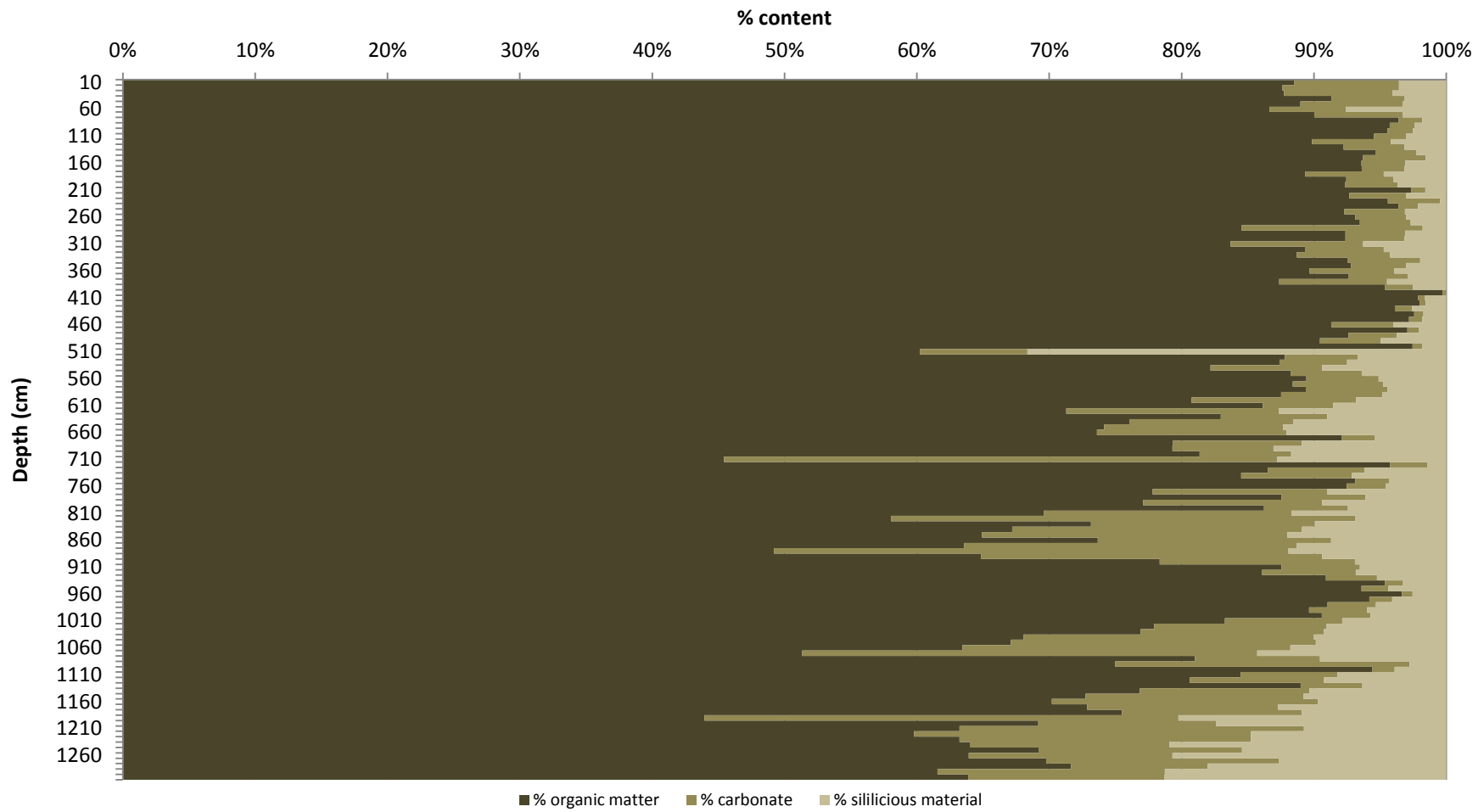


Figure 4.30: Breakdown of Loss On Ignition data through YK0712B

### 4.6.3. Particle-size analysis

Particle-size distributions show a number of trends through the core, with broad trends fitting well into the four Units used to describe sediment characteristics (Figure 4.31).

In Unit 1, particle-size data shows the proportion of clay increases from 20% at the base of the unit to less than 40% before a sharp, abrupt drop at 12.3 m. Silt content shows reasonably high levels of about 70% at 13 m, dropping to 50% at 12.3 m. This section of the core shows low values for coarse silt (~5% throughout, increasing by 1-2% towards 12.3 m) and very fine sand (2% increasing to 4% at 12.3 m). There are very small amounts (1% or less) of fine, medium, coarse and very coarse sand in this Unit. At the beginning of this Unit, skewness, variance, kurtosis and standard deviation of samples are all moderately high but drop rapidly to within the range of average values for the whole core.

Unit 2 shows clay rapidly increase to 27% before decreasing slightly to ~16% by 12.3 m. Silt proportions follow a very similar trend, peaking at 78% at 12.3 m and dropping to 58% by 11.9 m. Coarse silt, very fine sand and fine sand show a similar trend to that observed for clay, increasing slightly over the Unit from 11.9-12.3 m. Coarse silt and very fine sand levels are slightly higher in this Unit, between 5-10%, as are fine sand levels at 2-5%. Medium sand, coarse sand and very coarse sand show very low levels through this Unit. Skewness, kurtosis, variance and standard deviation of samples are elevated during this region, all peaking at 12.4 m.

Through Unit 3, all particle-size fractions with the exception of clay-sized clasts show greater variability than in other parts of the core. Clay shows low and reasonably stable levels through this section, staying within 3-17% but tending to average at 10%. Coarse silt, very fine sand, fine sand, medium sand, coarse sand and very coarse sand

follow a similar pattern but with a more pronounced peak at 10.7 m. At 9.3 m there is an increase in these values which continues in a stable manner until a small decrease at 7.0 m followed by a larger increase at 6.7 m. Silt shows much higher proportions than the other fractions, and much higher variability following a different trend. Through the entire length of Unit 3, silt broadly decreases from ~80% to ~40%, with a large fall in value at 10.7 m and 6.7 m, where the other fractions increase. Skewness and standard deviation of samples are reasonably constant through this section, although some small variations are observed from 10.6-10.4 m and at 6.8 m. Kurtosis and variance show distinct variation through this Unit, starting off high at the beginning of the Unit and dropping rapidly until 12.0 m. From here, kurtosis and variance both remain relatively low but display some variability until 11.5 m, where they rise sharply until 12.3 m. Relatively high values are maintained until 9.5 m, aside from a sharp drop in values from 10.6-10.4 m. From 9.5-9.1 m, kurtosis and variance decrease again, where they retain relatively stable levels through the remainder of the core bar a peak at 6.7 m and 6.0-5.0 m.

Unit 4 shows two broad trends across all fractions. From 4.1-3.1 m, very fine sand or coarser fractions show higher levels with relatively high variability, while from 3.1-0.0 m they show very low levels with moderate variability. Coarse silt shows reasonably constant levels throughout this Unit, as do silt and clay. Skewness, standard deviation, variance and kurtosis of samples are reasonably stable in this Unit, with moderate increases in variability from 1.6 m to 0 m.

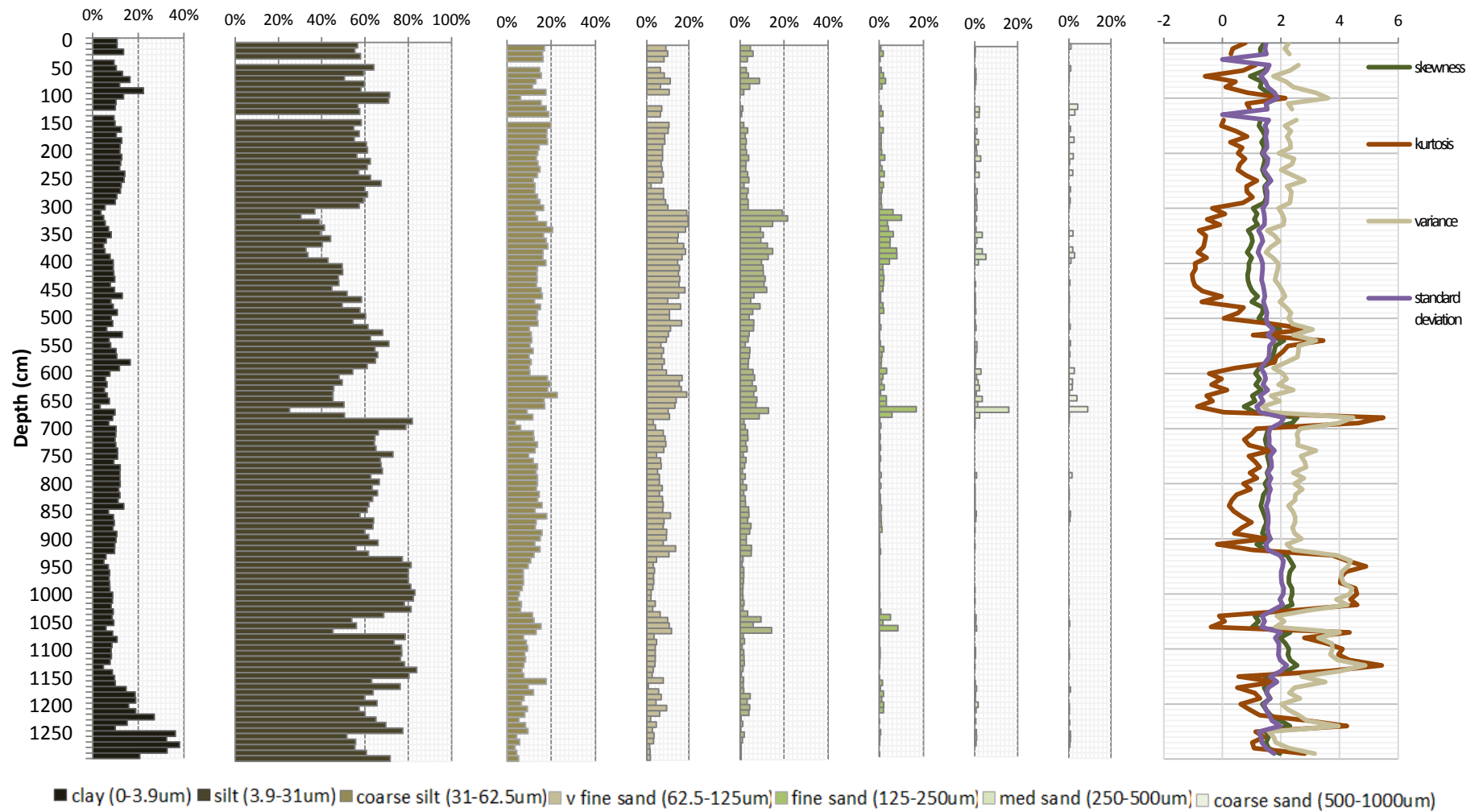


Figure 4.31: Particle-size analysis data and summary statistics plotted by depth



#### 4.6.4. Magnetic susceptibility

Through the YK0712B core, magnetic susceptibility values show three broad trends (Figure 4.32). In Units 1 and 2, magnetic susceptibility starts at relatively high values at 13 m with high variability, dropping rapidly to within the range of values experienced in the remainder of the core by the end of Section 2, with the steepest drop in values observed at the boundary between Units 1 and 2. Through Unit 3, magnetic susceptibility values are reasonably stable but have high variability in some places and high standard deviations in some sections. Unit 4 shows a significant decrease in the standard deviation and a slight decrease in variability, however the trends observed in Unit 3 continue.

In Units 1 and 2, magnetic susceptibility values start off at their highest in the entire length of the YK0712B core at 13.0 m, decreasing very rapidly from 0.00300 SI to within the average range of the rest of the core (0.00100 to -0.00050 SI) at 11.9 m. This region is also characterised by a large amount of variability. At the boundary between Unit 1 and Unit 2 there is a very large drop in magnetic susceptibility values. Within Unit 2, values remain roughly within the higher range of those seen in the following Unit.

Through Unit 3, magnetic susceptibility values maintain high levels of variability, however the change across this region is low compared to that in the previous section. There is a large increase in magnetic susceptibility values from 11.5-11.1 m followed by a decrease from 11.1-10.9 m that is not comparable to the rate of change in Unit 1 but similar in magnitude and rate to changes observed in Unit 2. From 10.9-6.0 m, magnetic susceptibility values are reasonably stable, with some gradual increases and decreases overlying the general variability. There is a sudden stabilisation in the amount of variability in magnetic susceptibility at 6.0m, with the onset of smoother changes and a

significant decrease in the size of standard deviations of samples. This trend continues from 6 m until the end of Unit 3 at 4.1 m.

Unit 4 shows a period of decreased variability and smoother transitions when change occurs as compared to Units 3, 2 and 1, with magnetic susceptibility values tending to have much smaller standard deviations. In this Unit, there is an increasing trend from 4.1-1.8 m, followed by a sharp decrease to 1.4 m, after which values are stable despite some level of variability.

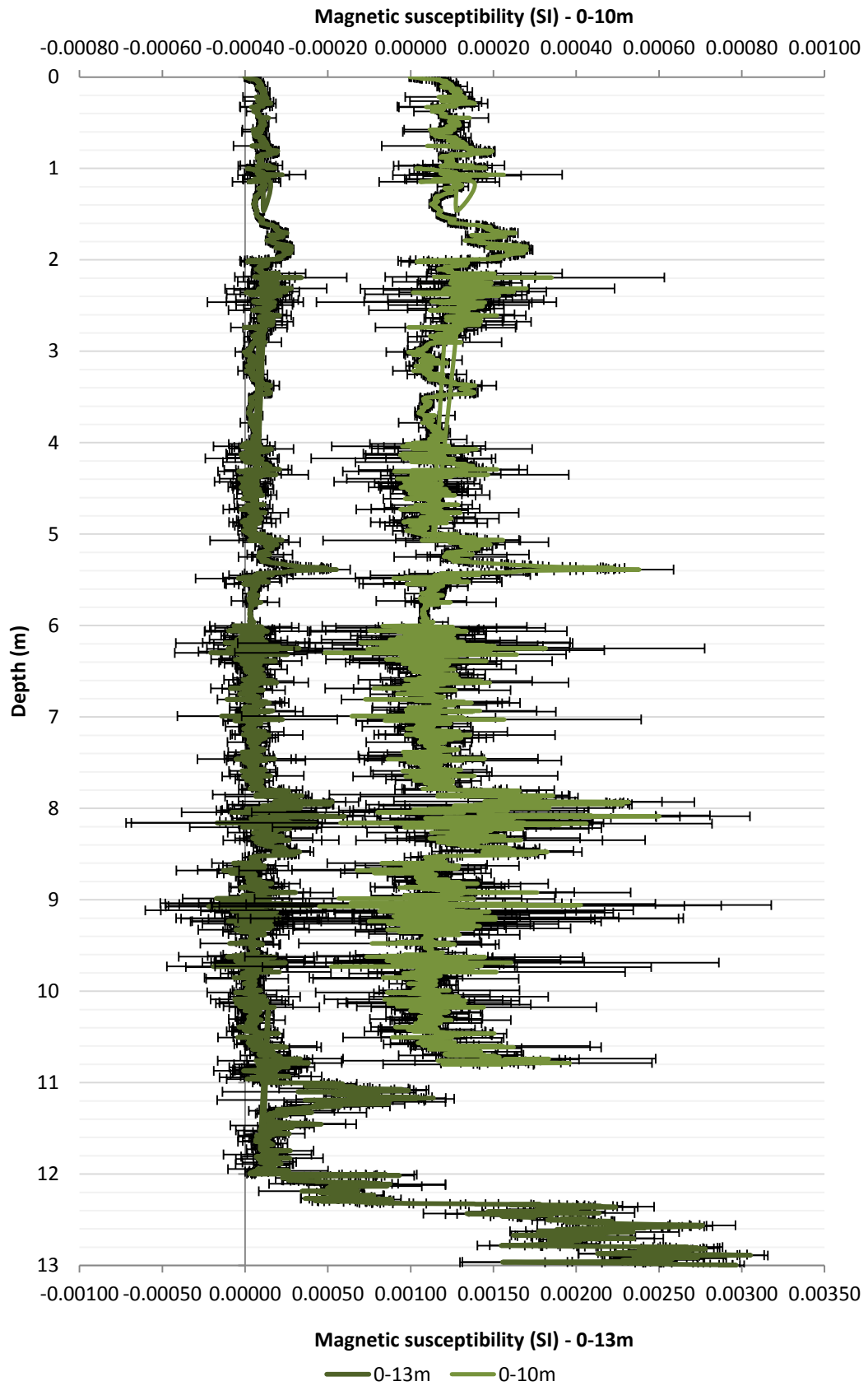


Figure 4.32: Magnetic susceptibility for 0-13m of YK0712B. Error bars indicate ranges of triplicate analyses.

#### 4.6.5. Sediment geochemistry

Scanning XRF was undertaken on the entire length of the YK0712B core in high resolution. In this study, calcium, strontium and rubidium are of key interest due to their relevance as palaeoclimatic proxies (Figure 4.33). A number of other elements were measured in addition. It can be seen that calcium and strontium follow very similar trends through the length of the YK0712B core, while rubidium follows a somewhat different trend that is different in some sections and similar in others. Changes observed follow the same broad structure as in previous sections, with discernible differences in Units 1-4.

Within Units 1 and 2, strontium follows a very similar trend to that of calcium, while rubidium shows an opposite trend. Unit 1 shows stable low values for both calcium and strontium to be significantly low and very stable, rising very sharply at 12.3 m and increasing to high variability. This trend continues until the end of Unit 2 where values drop substantially at 11.9 m to return to values slightly higher than those observed in the 13-12.3 m section. Rubidium shows an almost opposite trend through Units 1 and 2, showing high values from 13.0-12.3 m, a sharp drop in XRF counts at the boundary between Units 1 and 2 at 12.3 m, and low values from 12.3-11.9 m.

Within Unit 3, calcium and strontium show similar trends which are different from those shown in rubidium counts. There are elevated values in both strontium and calcium from 11.9-11.6 m which appear as a stabilisation from the high values seen in Unit 2, followed by a period of relative stability from 11.6-10.8 m. At 10.8 m, counts for both calcium and strontium increase rapidly over 0.1 m and sustain these higher values until 10.55 m, where they decrease until 10.4 m, resuming similar values to those seen prior to 10.8 m. These lower values remain relatively constant with low variability until 9.4m, where values increase and develop higher variability until 7.0 m. From 7.0 m, both

calcium and strontium values show relative stability and low variability compared to previous parts of the core. There are some small but low magnitude peaks at 6.6-6.4 m and 5.0-4.8 m. At the beginning of Unit 3, rubidium counts show a continuation of the trend seen in Unit 2 from 12.35-11.0 m, with values here higher and more variable than in the rest of Unit 3. From 11.0-9.3 m, rubidium counts show a general decreasing trend with moderate variability in the rate of change and a number of very abrupt increases and decreases (10.7 m, 10.46 m, 10.03 m). From 10-4 m onwards, rubidium counts remain relatively stable within the 0-400 count range, showing some variability in the rate of change within this.

Unit 4 shows stability and lower variability in calcium and strontium as well as rubidium. Calcium and rubidium show a continuity of trends in the latter half of Unit 3, with low stable values aside from small peaks at 3.1 m, 1.8 m and 0.8 m. Rubidium counts show comparable stability with slightly more variability in this section, with XRF counts tending to be lower than in Unit 3. There is a period of notable increase in the variability observed in rubidium counts from 2-1 m, but in the remaining sections of Unit 4, rubidium counts show less variability and a decrease in the amount of change as compared to other parts of the core.

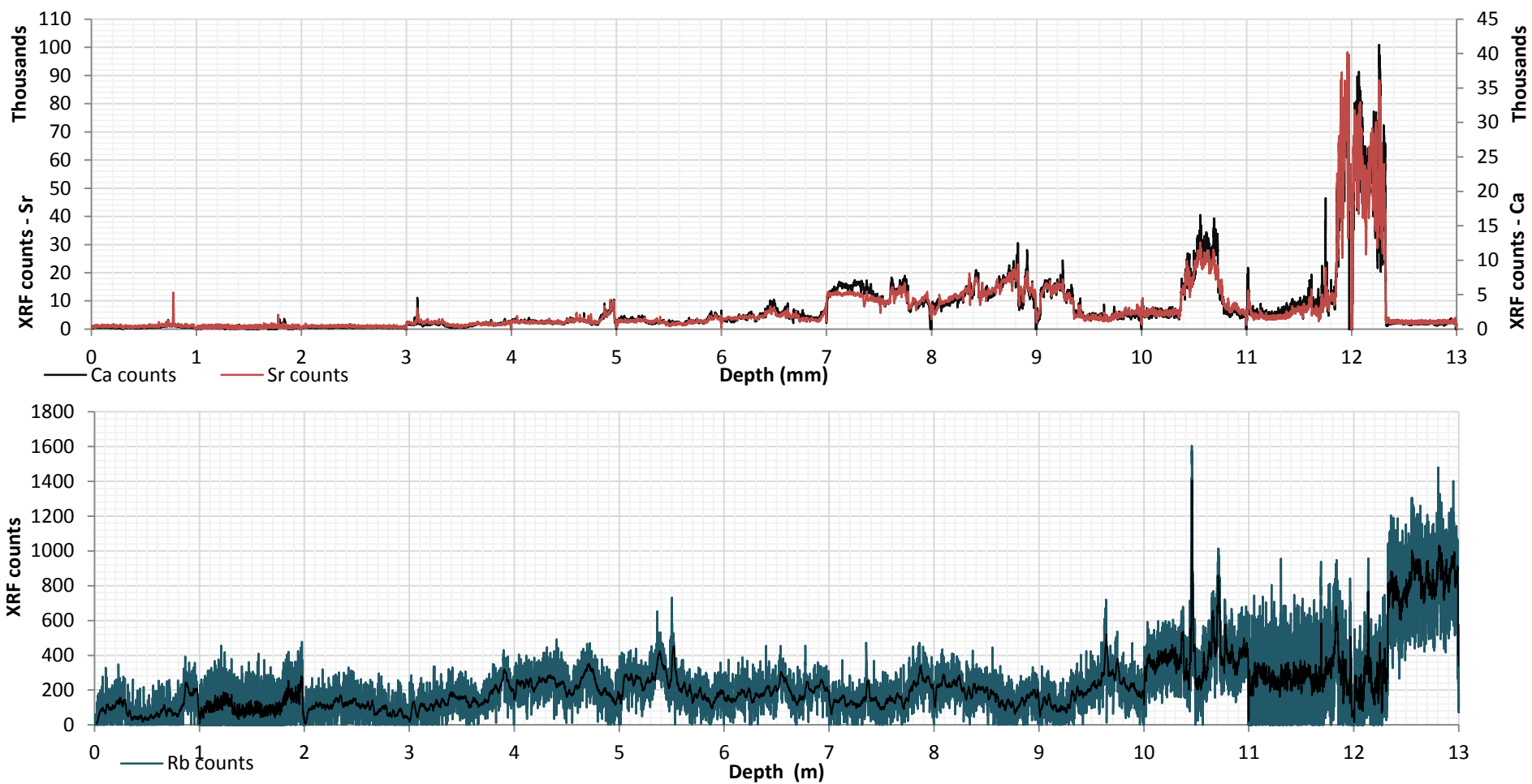


Figure 4.33: Calcium and strontium XRF counts (top) and rubidium XRF counts (bottom) from ITRAX geochemical analysis. Rubidium plot showing a 20-sample average in black to display trends in the dataset more clearly.

#### 4.6.6. Characterisation of carbonate species

Authigenic carbonate in these lake sediments could be euhedral or anhedral in form, depending on where in the water column, or the sediment column, they formed. If the sedimentary carbonates crystals are found to be euhedral, it can be inferred that they precipitated in the surface waters of the lake (Rickaby & Schrag, 2005; Nelson et al., 2009). If this is the case, their isotopic content will be a reflection of the isotopic content of the surface waters of the lake at the time at which they formed, reflecting rainfall amount from monsoonal circulation regional climate in the manner that has been discussed in the preceding sections of this chapter. If these crystals formed in interstitial pore waters in the sediment, however, they will have an anhedral form as a result of constrained crystal growth, and their isotopic content will reflect the isotopic content of these pore waters at the bottom of deep stratified lakes (Rickaby & Schrag, 2005; Nelson et al., 2009). In this case, the isotopic content of these carbonates would not be reflective of monsoon behaviour. In order make this critical distinction, SEM-based analysis was used.

Figures 4.34-4.38 reveal crystalline structures characteristic of aragonite, with the occasional presence of crystals characteristic of calcite. All of these crystals can be confirmed as euhedral as they demonstrate unimpeded crystal growth and characteristic euhedral aragonite form. Diatoms, particularly the planktonic genus *Aulacoseira*, are also present among the carbonate crystals (Figures 4.35-4.36). The sample from the non-laminated sections of the core (12.32-12.34m) also contains calcite and aragonite crystals (Figure 4.36).

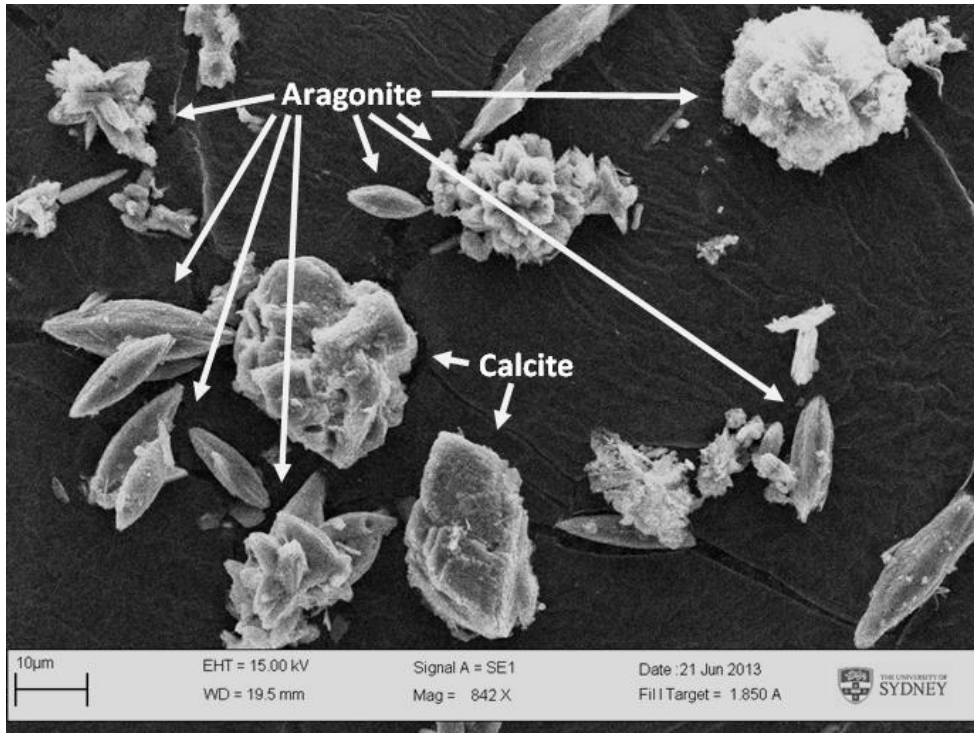


Figure 4.34: SEM micrograph from the laminated section showing calcite and aragonite

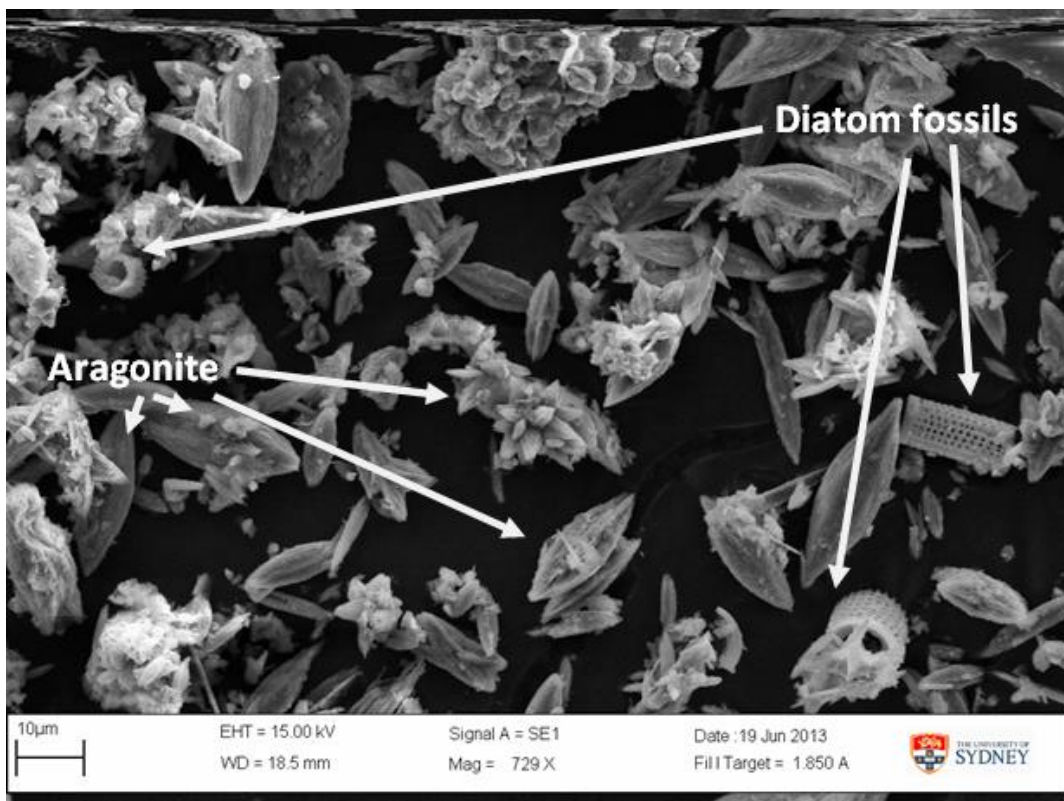


Figure 4.35: SEM micrograph of the laminated section of the core



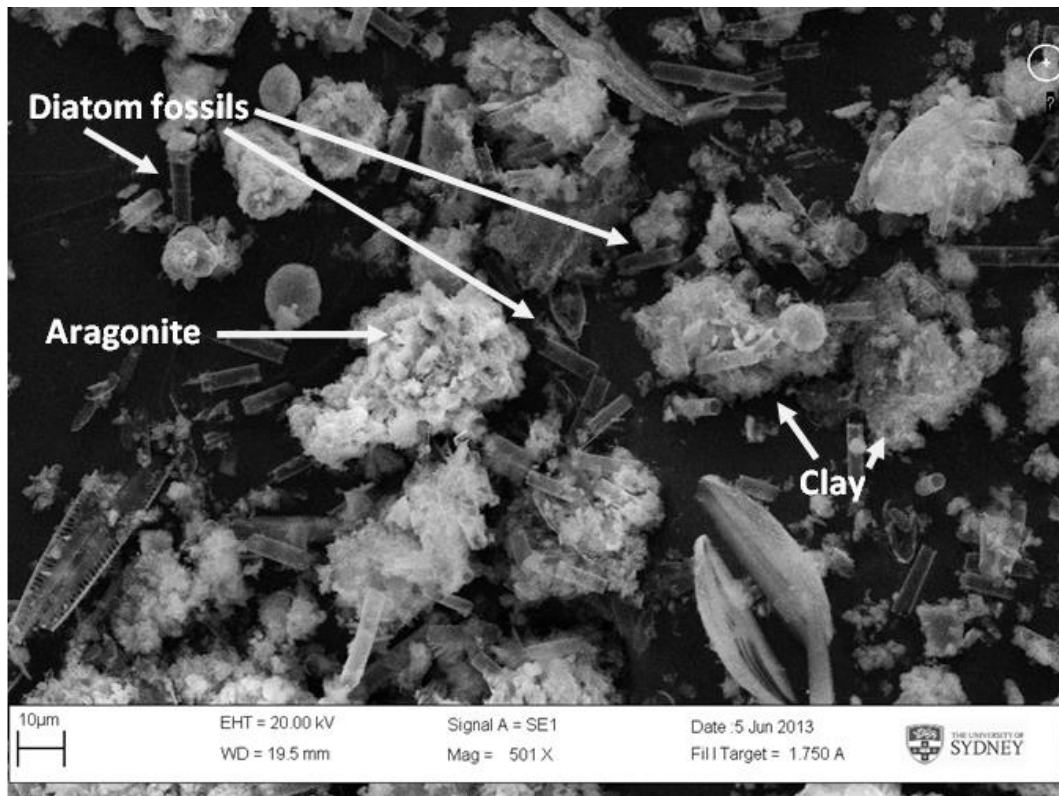


Figure 4.36: SEM micrograph of sample from non-laminated section

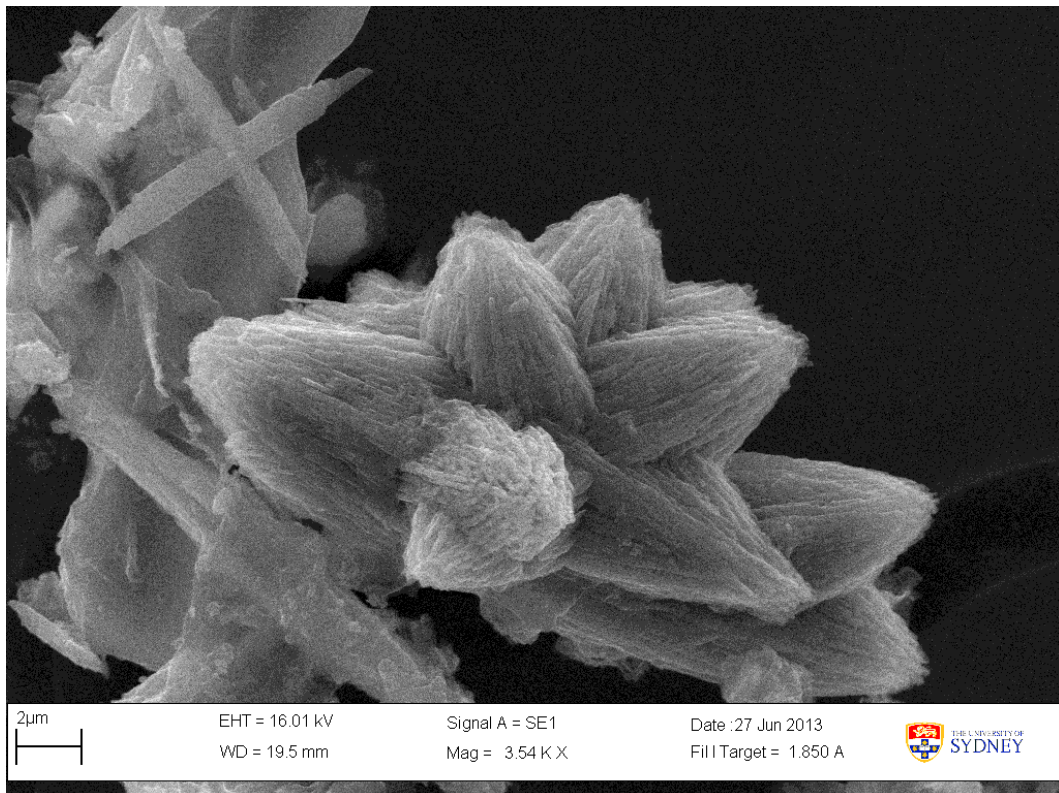
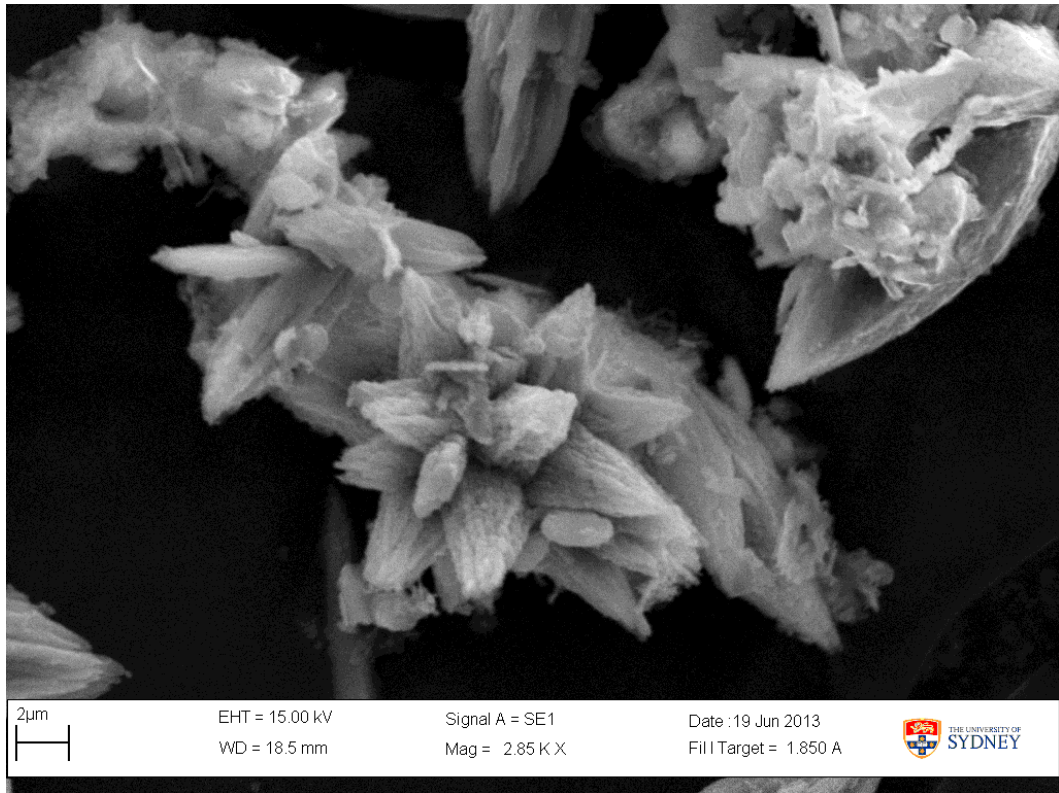


Figure 4.37: SEM micrographs of acicular aragonite crystals

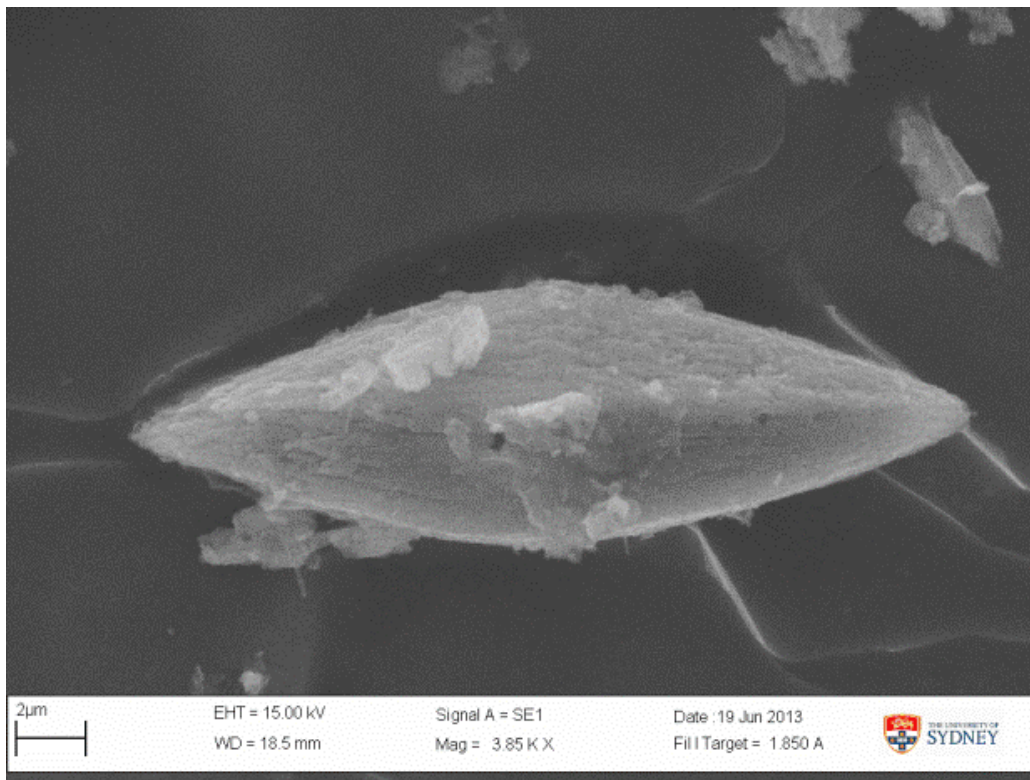
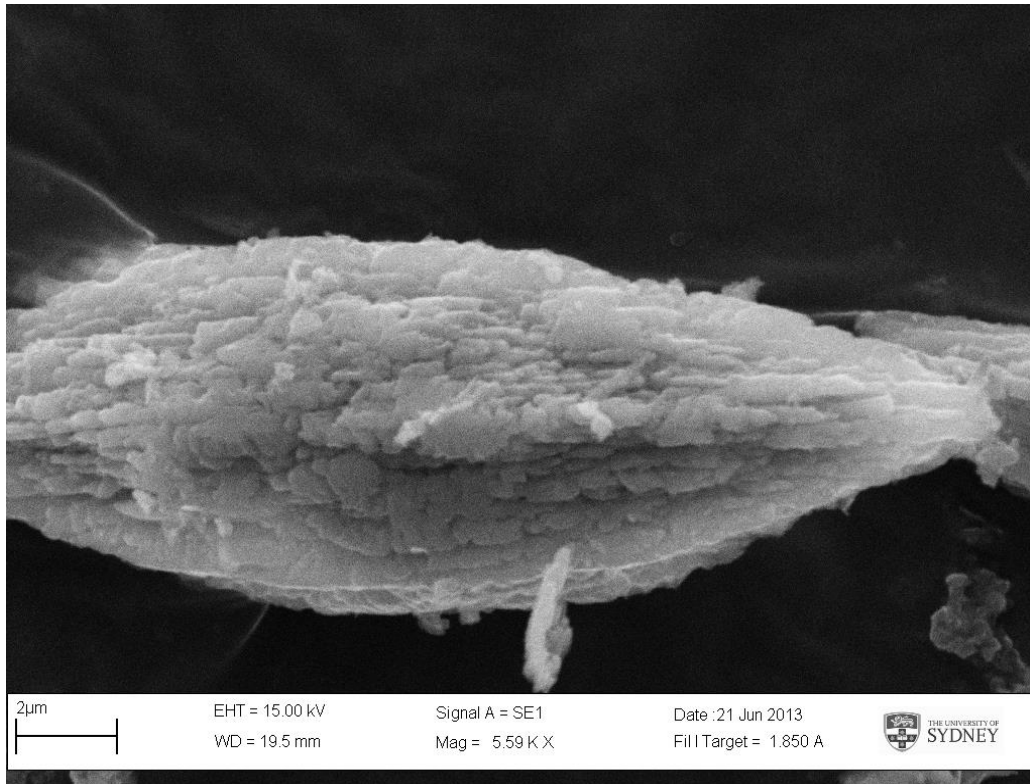


Figure 4.38: SEM micrographs of the orthorhombic dipyramidal structure of an aragonite crystal



To confirm that the species of carbonate are aragonite and calcite, geochemical analysis using energy dispersive spectroscopy (EDS) and electron backscatter diffraction (EBSD) was carried out. Figures 4.39-4.42 show the EDS spectra for crystals in each of the samples, where clear spikes for calcium, oxygen and carbon confirm that these are all calcium carbonates. Tables 4.2-4.5 identify the species of calcium carbonate with electron backscatter diffraction patterns and crystal structure analyses for select crystals in these samples.

The emissions spectra generated using EDS are only able to confirm the geochemistry of individual crystals, so phase maps of the calcium carbonate species were generated for each sample using EBSD. Figures 4.43-4.46 show clearly that aragonite dominates the carbonate component of the sediment, with a smaller amount of calcite present. These phase maps show that the non-laminated section contains low levels of carbonate (less than 2% of the pre-treated SEM sample), but that the dominant species is aragonite (1.08%) with only 0.18% calcite present. These portions are comparable in the laminated sections of the core.

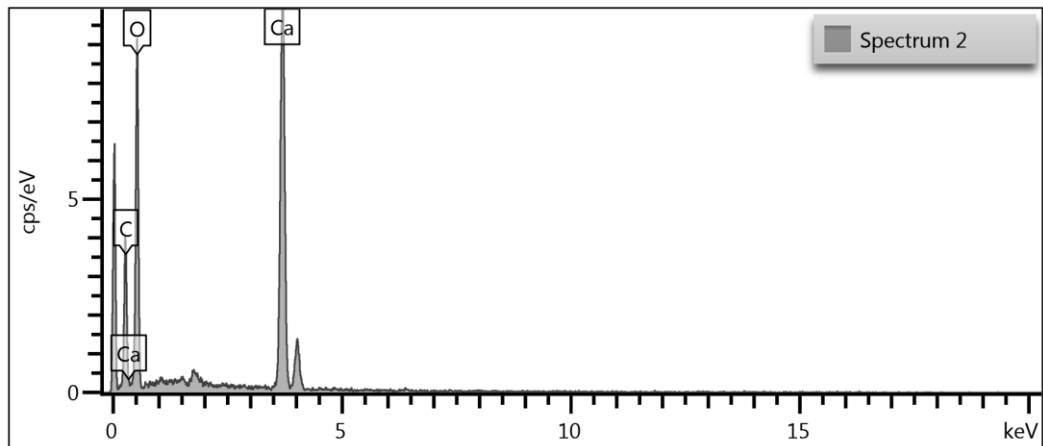
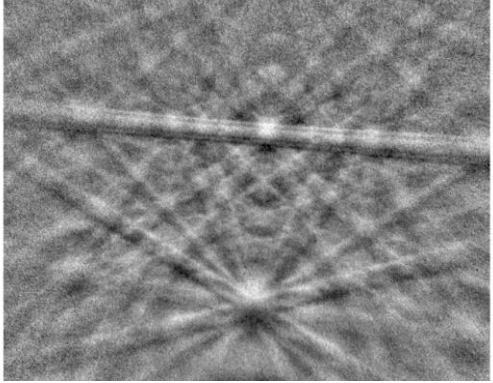
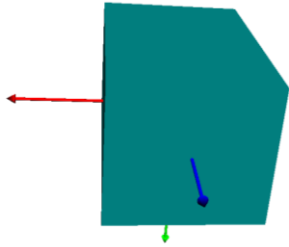
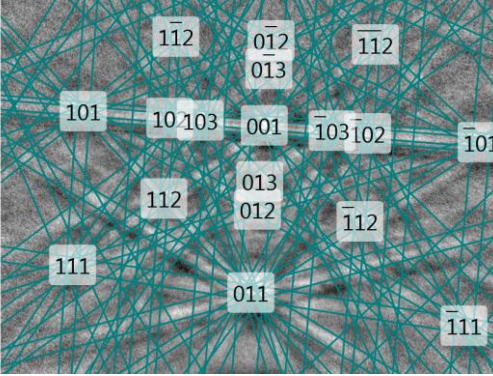


Figure 4.39: EDS spectra of aragonite in the laminated section

Table 4.3: EBSD of aragonite in laminated section

Description		EBSD refraction pattern
Name	Aragonite	
Database	Inorganic Crystal Structure Database	
<b>Structure</b>		
Crystal System	Orthorhombic	
Shape		
LaueGroup	3	
Space Group	62	
<b>Unit Cell</b>		
a	5.74 Å	
b	4.96 Å	
c	7.97 Å	
Alpha	90.00 °	
Beta	90.00 °	
Gamma	90.00 °	

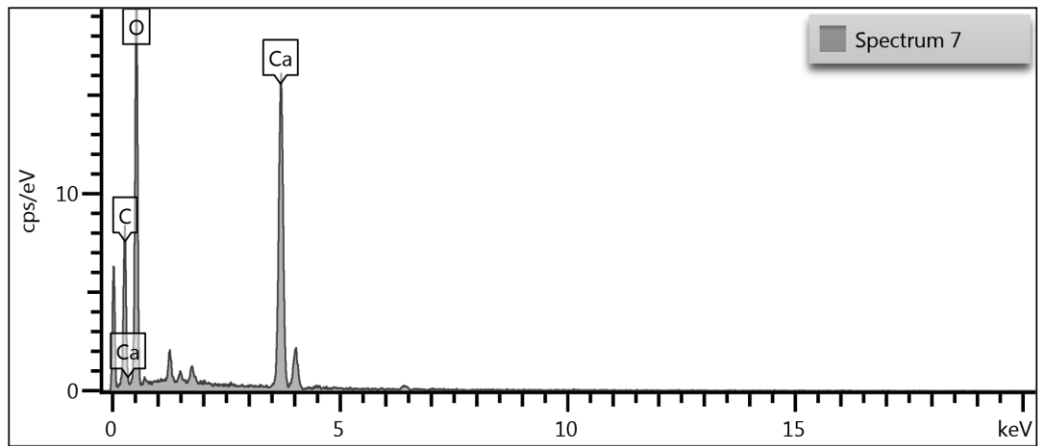
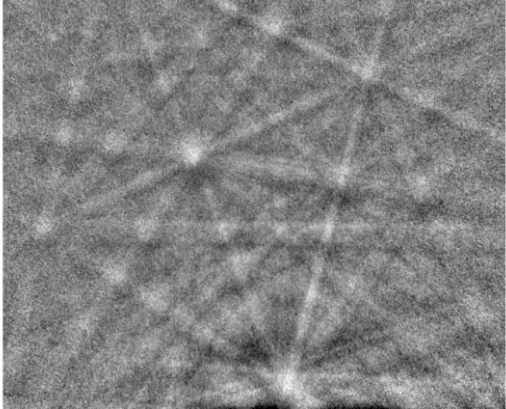
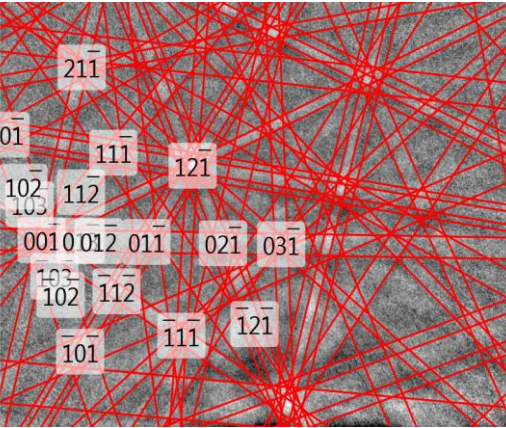
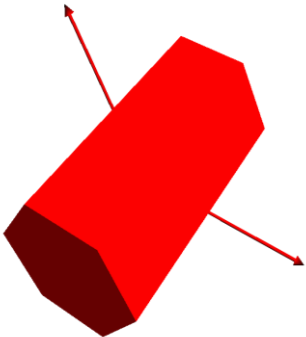


Figure 4.40: EDS spectra of calcite in the laminated section

Table 4.4: EBSD of calcite in laminated section

Crystal Description		EBSD refraction pattern
Name	Calcite	
Database	Inorganic Crystal Structure Database	
<b>Structure</b>		 
Crystal System	Trigonal	
Crystal shape		
LaueGroup	7	
Space Group	0	
<b>Unit Cell</b>		
a	4.99 Å	
b	4.99 Å	
c	17.06 Å	
Alpha	90.00 °	
Beta	90.00 °	
Gamma	120.00 °	

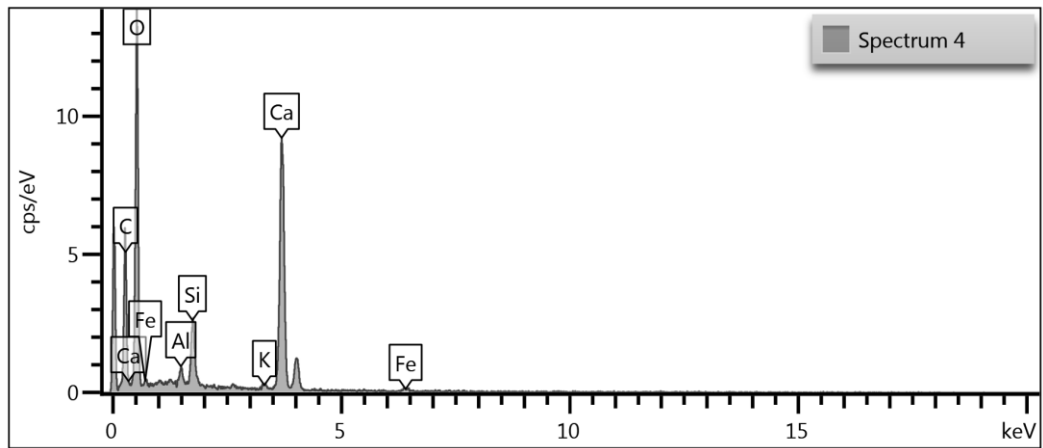
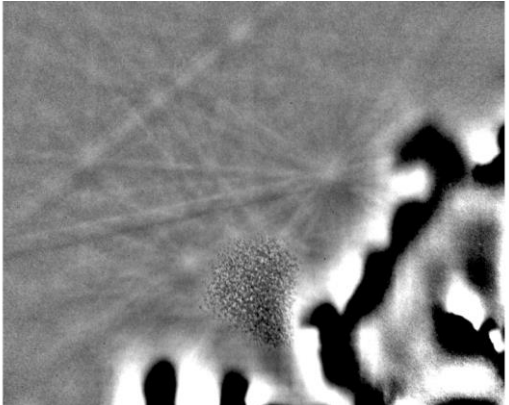
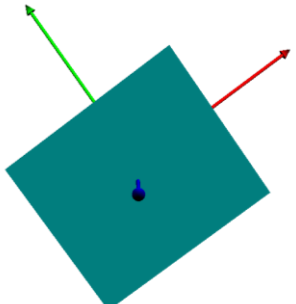
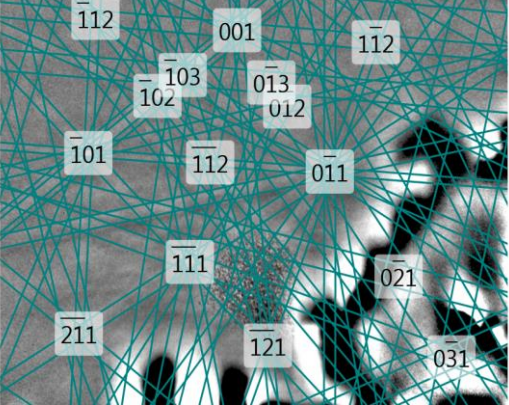


Figure 4.41: EDS spectra of aragonite in the non-laminated section

Table 4.5: EBSD analysis of aragonite in non-laminated section

Description		EBSD refraction pattern
Name	Aragonite	
Database	Inorganic Crystal Structure Database	
<b>Structure</b>		
Crystal System	Orthorhombic	
Crystal shape		
LaueGroup	3	
Space Group	62	
<b>Unit Cell</b>		
a	5.74 Å	
b	4.96 Å	
c	7.97 Å	
Alpha	90.00 °	
Beta	90.00 °	
Gamma	90.00 °	

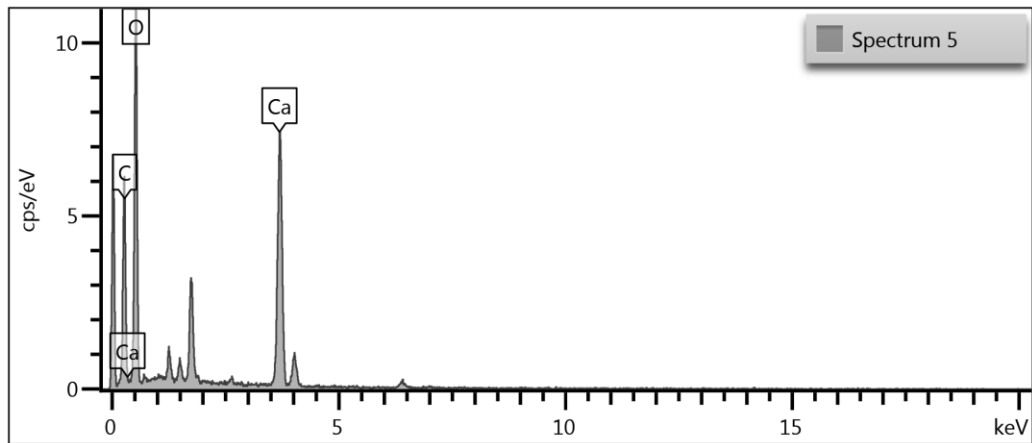
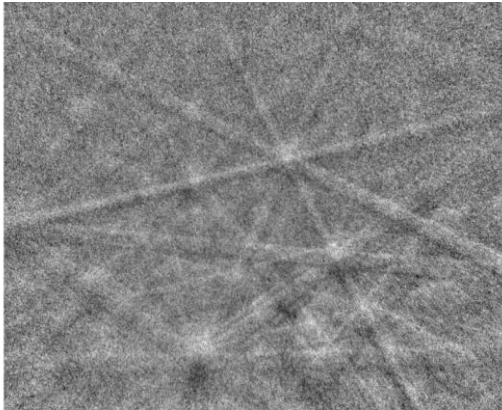
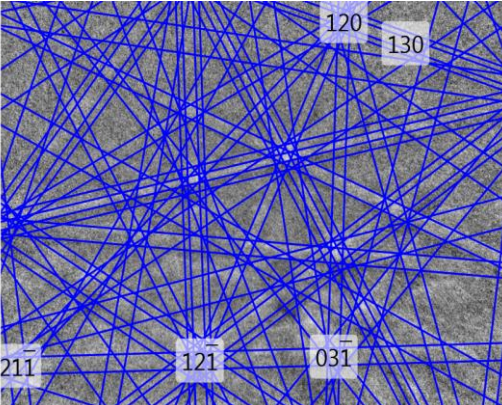
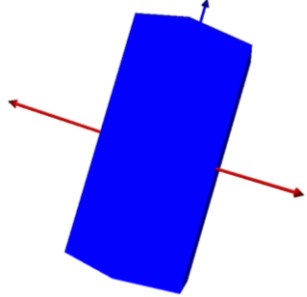


Figure 4.42: EDS spectra of calcite in the non-laminated section

Table 4.6: EBSD analysis of calcite in non-laminated section

Description		EBSD refraction pattern
Name	Calcite	
Database	Inorganic Crystal Structure Database	
<b>Structure</b>		
Crystal System	Trigonal	
Crystal shape		
LaueGroup	7	
Space Group	167	
<b>Unit Cell</b>		
a	4.99 Å	
b	4.99 Å	
c	17.06 Å	
Alpha	90.00 °	
Beta	90.00 °	
Gamma	120.00 °	



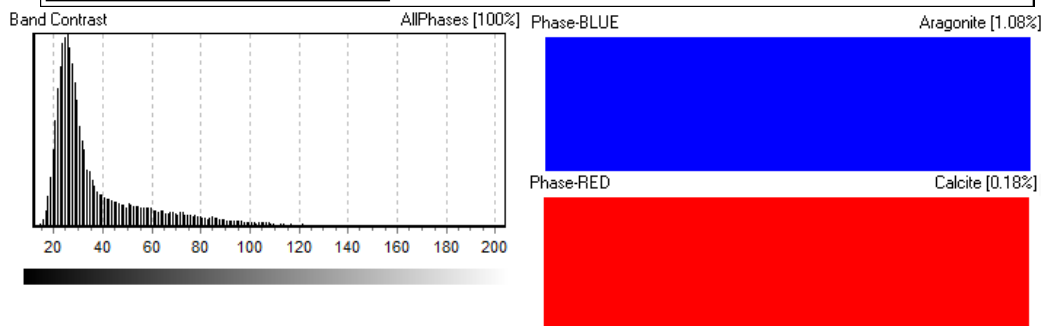
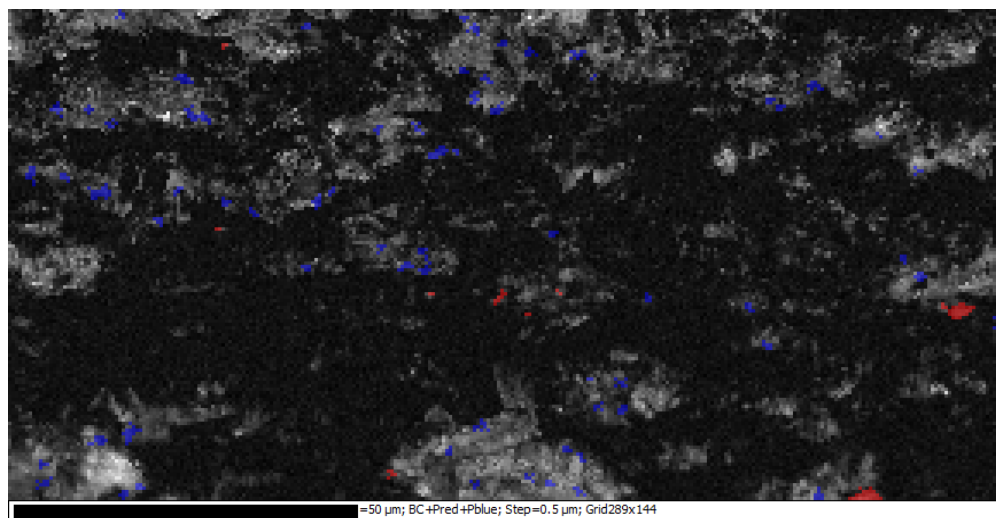
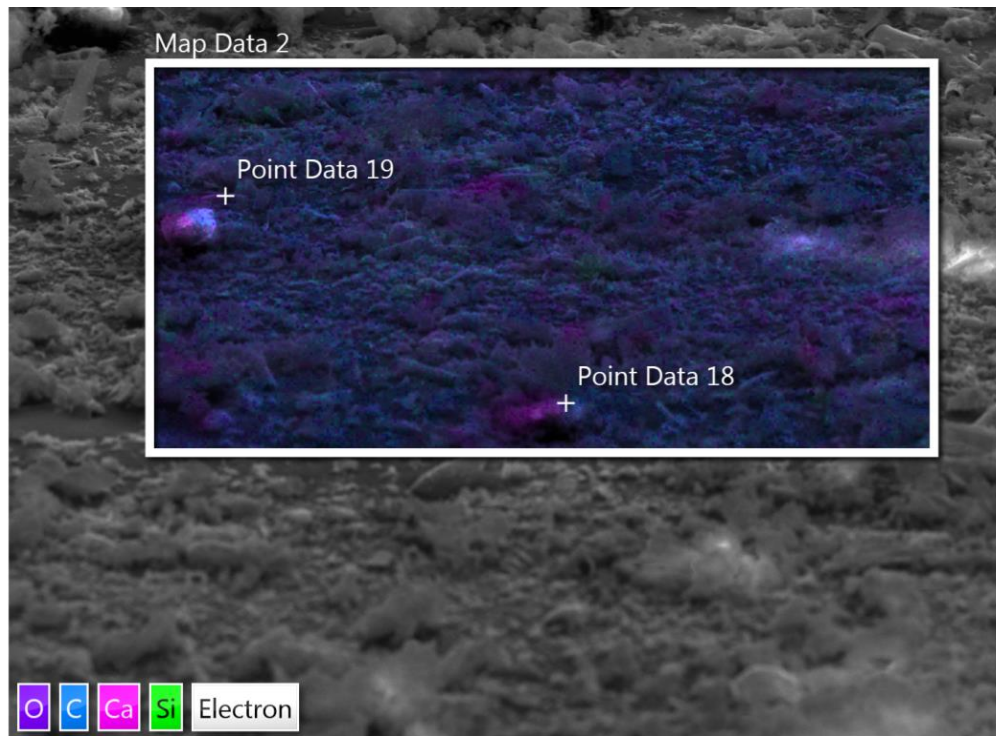


Figure 4.43: EBSD phase map for sample A (sample from non-laminated section still containing calcium carbonate) showing micrograph (top), phase map (mid) and legend (bottom)

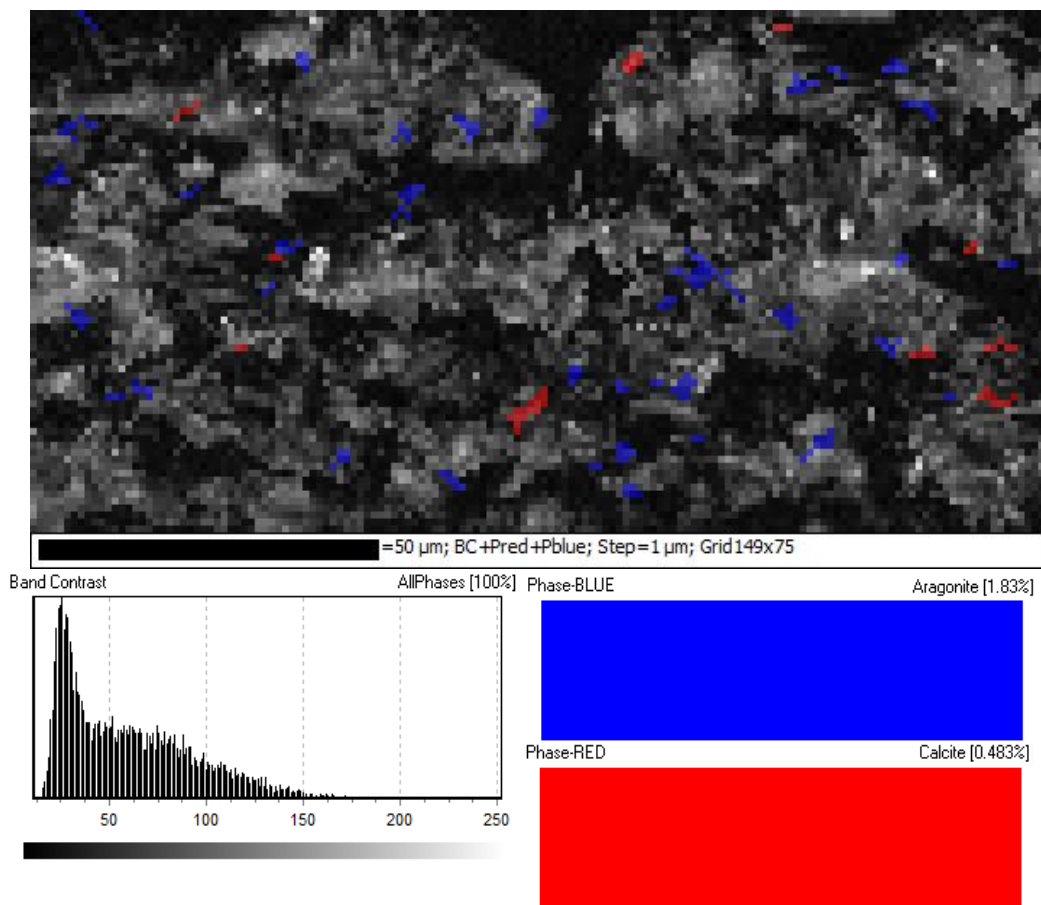
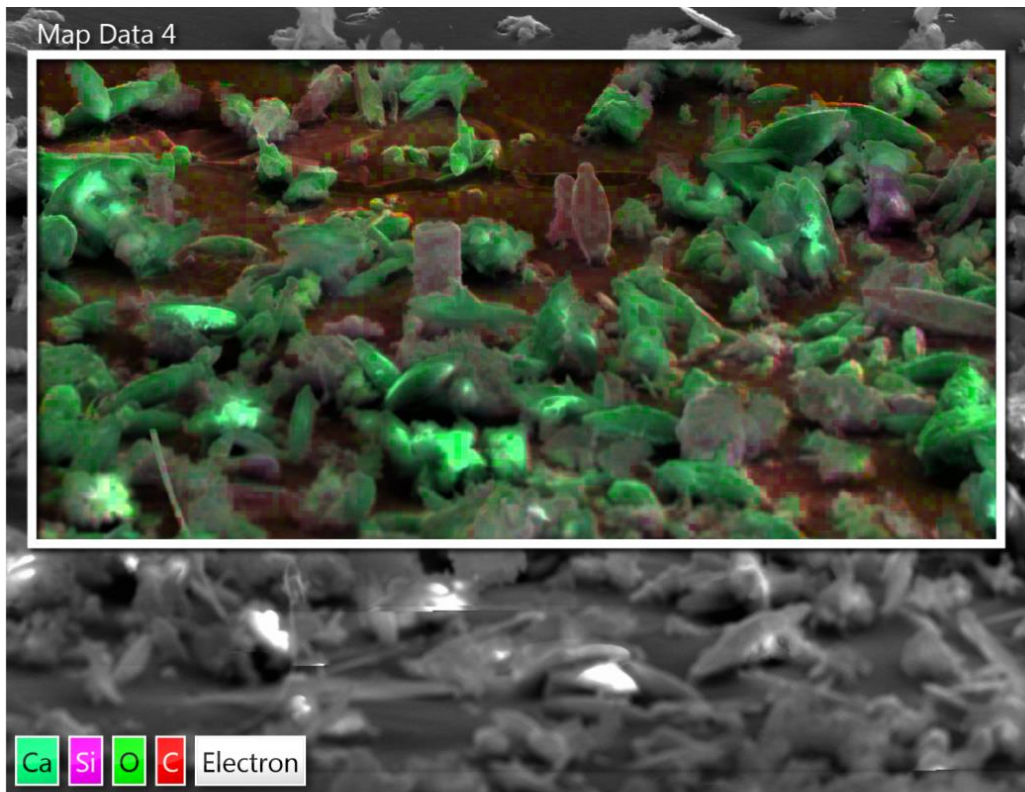


Figure 4.44: EBSD phase map for sample B (sample from laminated section) showing micrograph (top), phase map (mid) and legend (bottom)

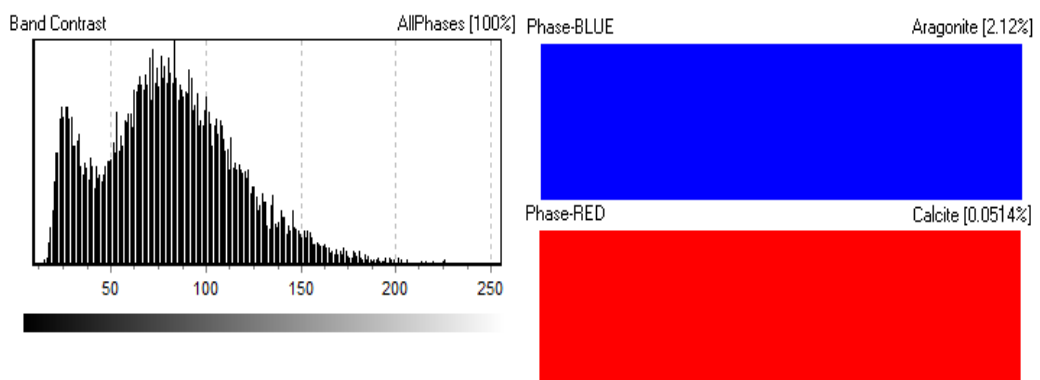
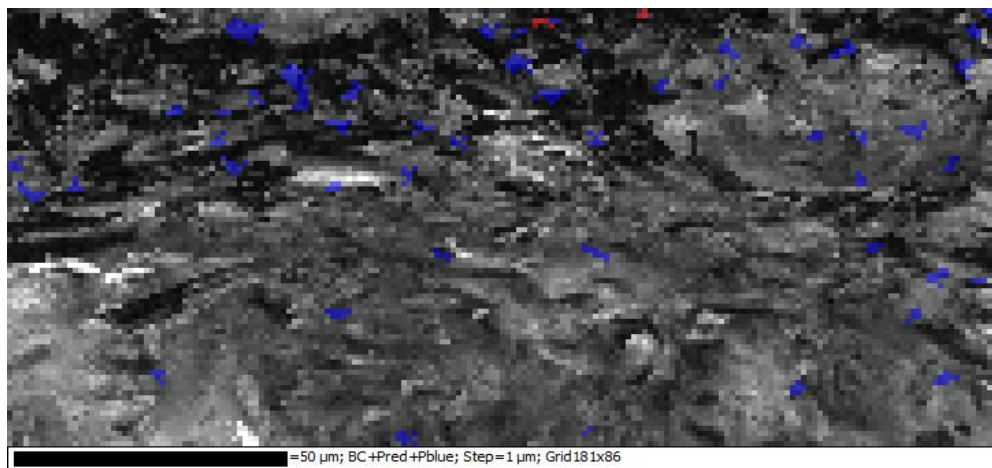
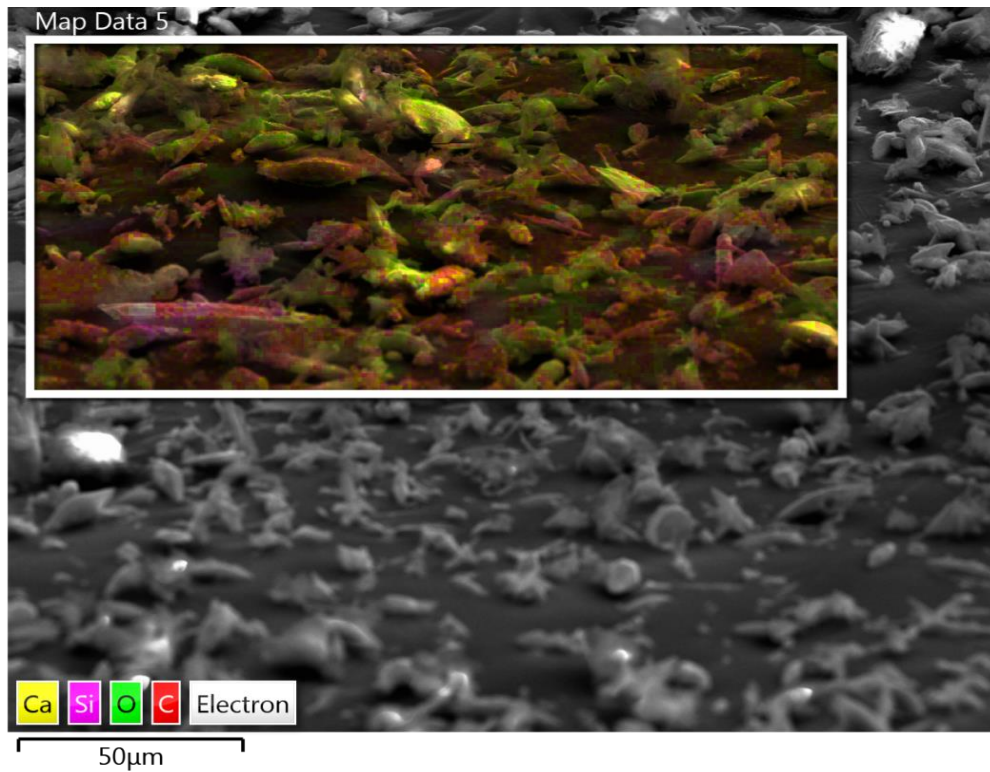


Figure 4.45: EBSD phase map for sample C (sample from laminated section high in iron) showing micrograph (top), phase map (mid) and legend (bottom)



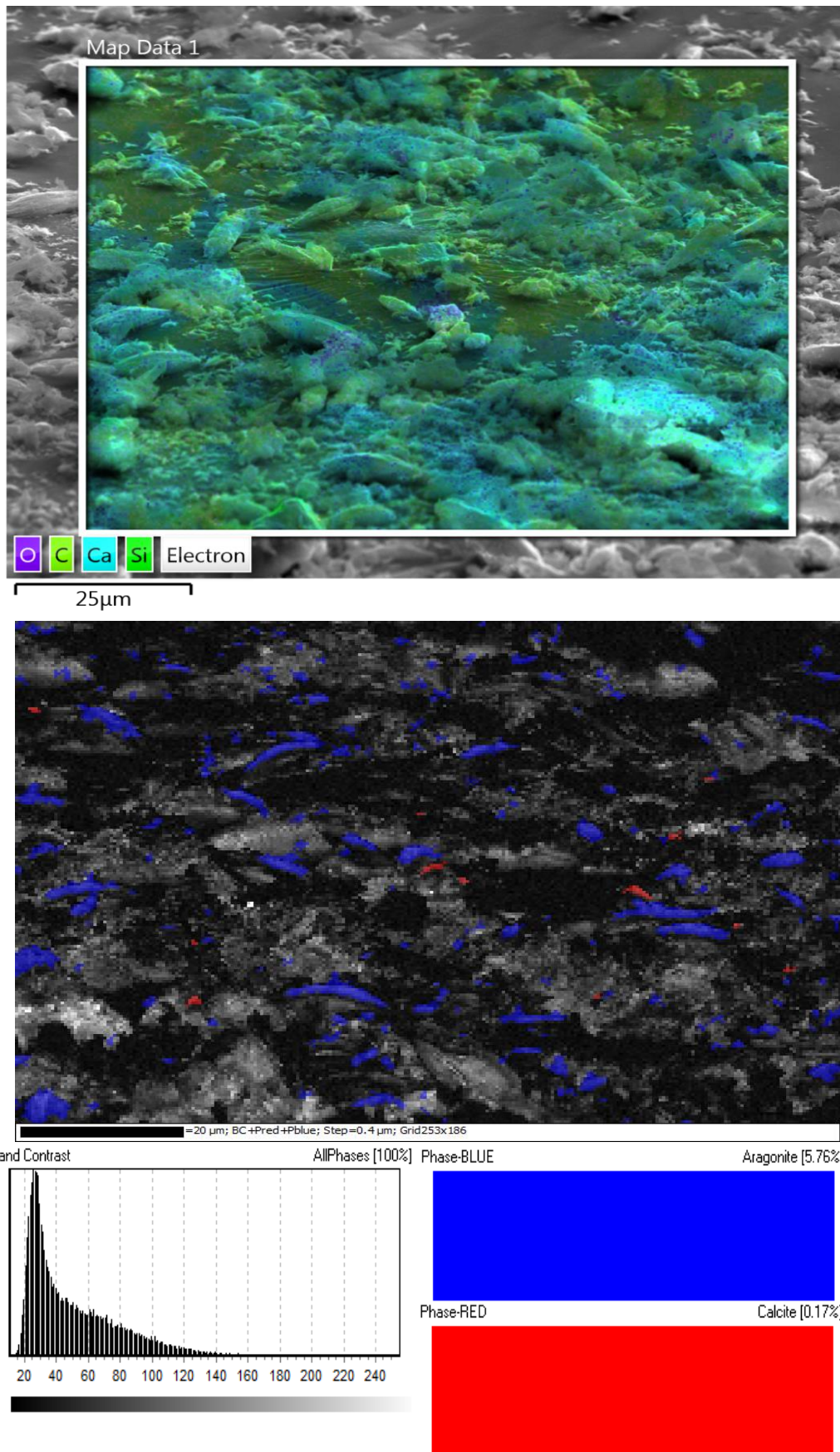


Figure 4.46: EBSD phase map for sample D (sample from laminated section high in strontium) showing micrograph (top), phase map (mid) and legend (bottom)

#### 4.6.7. Stable isotopes of oxygen in sediment

The stable isotope ratios in carbonate held in the sediments of the 4.411-13.00 m section of YK0712B core are shown in Figure 4.47. This record extends through Unit 1 and Unit 2 but not completely through Unit 3.

In Unit 1, stable isotope values of oxygen are relatively negative, showing a very large anomalous drop in values at from -4.7‰ at 12.882 m to -9.2‰ at 12.845 m, which returns to -3.7‰ at 12.770 m. There is a broad decreasing trend in this Unit from -3.3‰ to -5.6‰ at 12.360 m, just into Unit 2. Unit 1 shows variability in the rate of change, however sample variability is low. Unit 2 shows distinctly steady levels of stable isotopes of oxygen within 0.3‰ of -5.0‰, however there is very high variability between samples. At 12.005 m, samples drop to -5.7‰, where they remain relatively stable until 11.594 m in Unit 3.

Unit 3 shows a decreasing trend from -5.7‰ at 12.005 m to -6.3‰ at 9.790 m. This decrease shows a series of peaks and troughs that does not depict abrupt changes however does indicate small-scale cyclic changes in climate through this period. At 9.790 m, values increase sharply from -6.3‰ to -2.8‰, and then decrease rapidly to -7.8‰ at 9.237 m. This section shows very high variability between samples, with a maximum value of -1.6‰ and minimum of -7.8‰. From 9.237 m to 4.781 m, there is a general increasing trend in stable isotope values, and there are small periods of suddenly increasing and decreasing values with higher variability from 8.241-8.008 m and 7.711-7.059 m. At 5.702 m (-6.6‰) there is a peak in values until 5.468 m (-4.1‰), which decreases until 5.312 m (-6.2‰) where there is a resumption of an increasing trend until 4.773 m (-2.0‰). At this point, a period of significant variability and relatively high stable isotope values begins, with values fluctuating between -4.4 to 2.9‰.

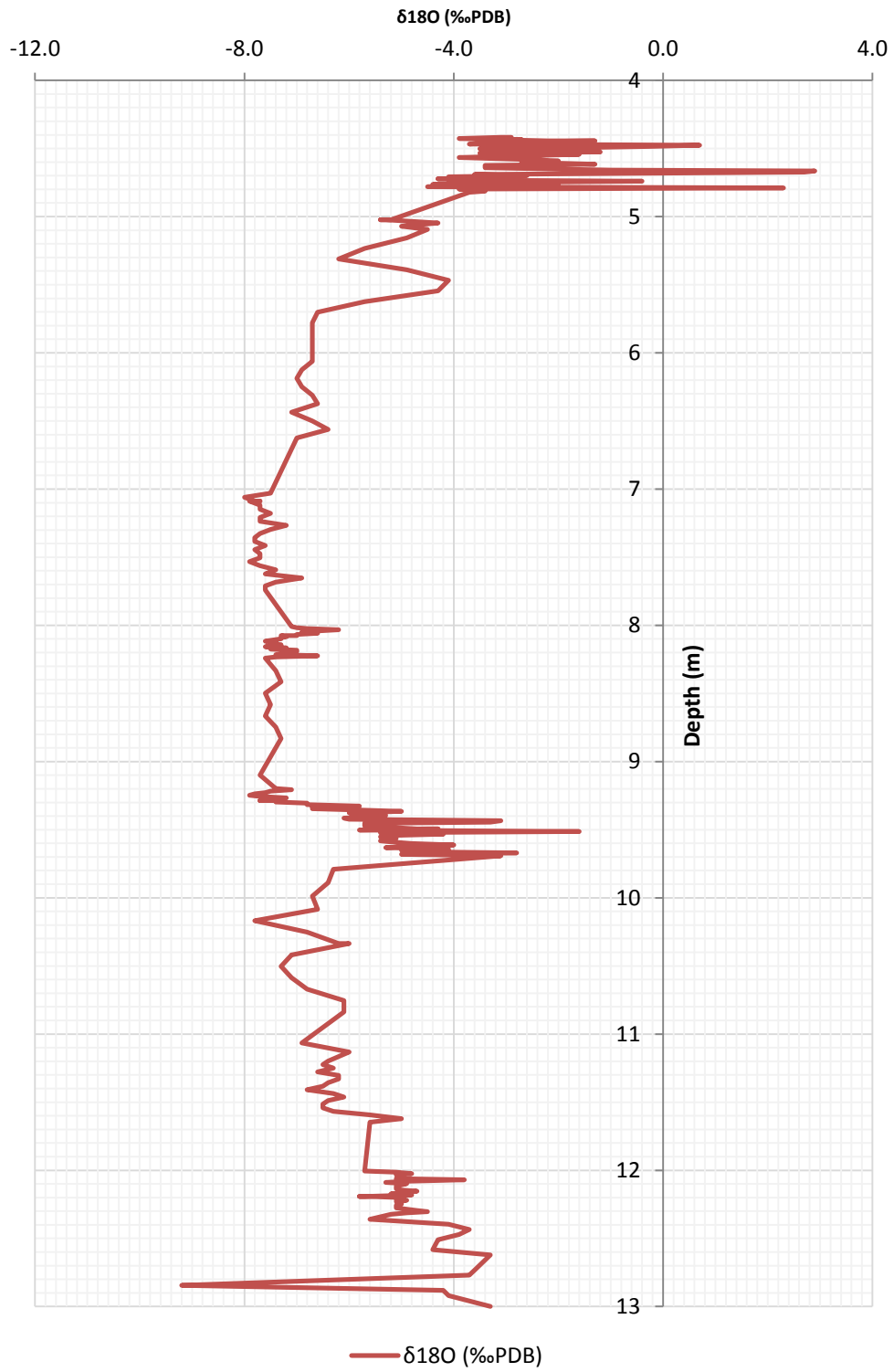


Figure 4.47:  $\delta^{18}\text{O}$  (‰PDB) record from YK0712B core

#### **4.6.8. <sup>14</sup>C Dating of the YK0712B sediment core**

A series of samples from selected depths of YK0712B were analysed by AMS for <sup>14</sup>C ages (Table 4.7, Figure 4.48). Some of these analyses returned anomalously old dates, presumably as a result of the uptake of old radiocarbon from the groundwater aquifer (Maxwell, 1999). These anomalous ages (10,016 cal yr BP at 9.805 m and 12,971 cal yr BP at 12.26 m) did not align well with ages from adjacent or nearby samples, and when these values were removed the age model was reasonably similar to that described by Maxwell (1999). The two anomalous ages were hence not utilised for the construction of the age model used for the YK0712B core in this thesis, but their presence provides valuable data about possible limnological characteristics of Yeak Kara through the Holocene.

A chronological age model was generated to link depth to AMS radiocarbon dates (Figure 4.49). This age model was used to estimate sedimentation rates through the Holocene at Yeak Kara (Table 4.8).

Table 4.7:  $^{14}\text{C}$  dating and calibration for YK0712B. Samples in bold used for age model; samples in italics not used, thought to show anomalously old dates as a result of old carbon from the hardwater effect. Relative area under probability distribution after Reimer et al 2013.

BETA Analytic number	Sample depth	Pre-treatment	Method	$^{14}\text{C}$ age (yr BP)	Cal curve	Cal yr BP	error min (2 sigma)	error max (2 sigma)	relative area under probability distribution
<b>375627</b>	<b>1.300-1.350 m (sediment)</b>	<b>(organic material): acid/alkali/acid</b>	AMS (sediment)	<b>1660 ± 30</b>	<b>intcal13.14c</b>	<b>1563</b>	<b>1520</b>	<b>1624</b>	<b>0.939</b>
<b>375628</b>	<b>5.080-5.130 m (sediment)</b>	<b>(organic material): acid/alkali/acid</b>	AMS (sediment)	<b>4330 ± 30</b>	<b>intcal13.14c</b>	<b>4891</b>	<b>4843</b>	<b>4967</b>	<b>1.000</b>
375629	9.805-9.855 m (sediment)	(organic material): acid/alkali/acid	AMS (sediment)	8860 ± 30	intcal13.14c	10016	9884	10158	0.908
<b>376824</b>	<b>9.805-9.855 m (Plant)</b>	<b>(plant material): acid/alkali/acid</b>	<b>AMS (sediment)</b>	<b>6270 ± 30</b>	<b>intcal13.14c</b>	<b>7212</b>	<b>7161</b>	<b>7263</b>	<b>1.000</b>
373056	12.26-12.28 m (SEM sample A, sediment)	(organic material): acid/alkali/acid	AMS (sediment)	11100 ± 50	intcal13.14c	12971	12818	13078	1.000
<b>373057</b>	<b>12.32-12.34 m (SEM sample C, sediment)</b>	<b>(organic material): acid/alkali/acid</b>	<b>AMS (sediment)</b>	<b>7930 ± 40</b>	<b>intcal13.14c</b>	<b>8769</b>	<b>8631</b>	<b>8817</b>	<b>0.605</b>

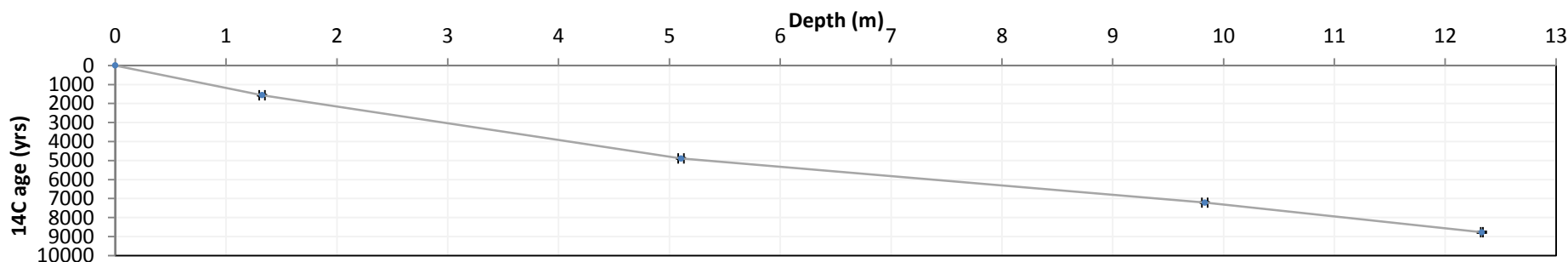


Figure 4.48:  $^{14}\text{C}$  dates with error for YK0712B



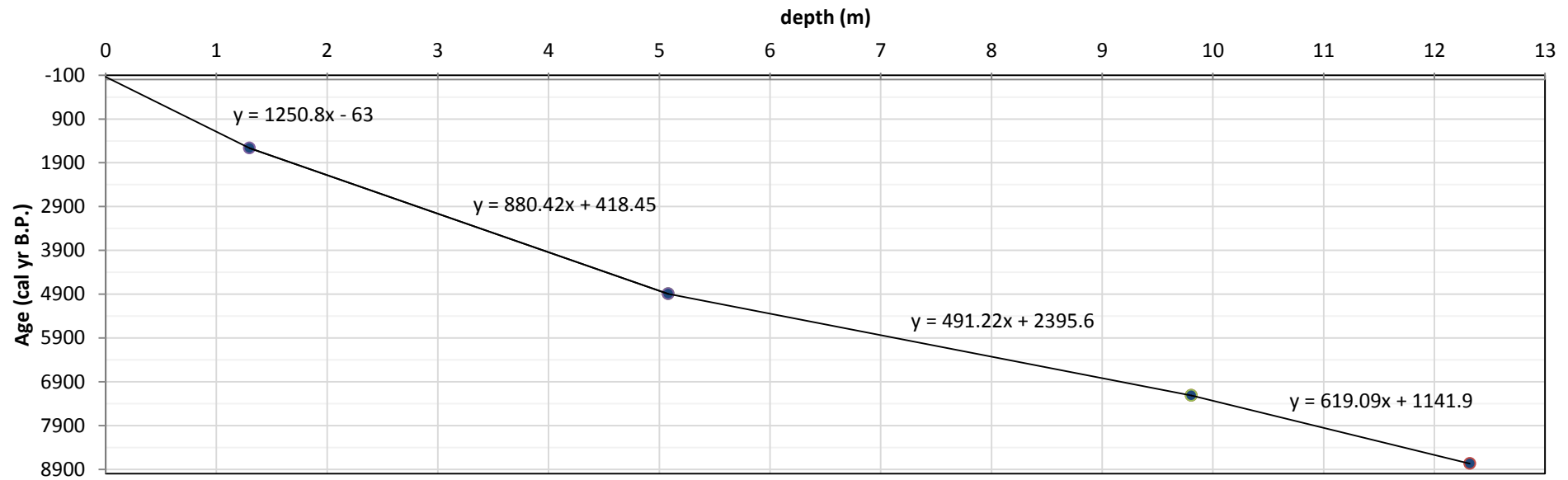


Figure 4.49: Cal yr BP age model for YK0712B

Table 4.8: Approximate sedimentation rate through the Holocene in Yeak Kara

Depth range (m)	Age difference (cal yr BP)	Sediment accumulated (mm)	Sedimentation rate (yr/mm)
0.0 - 1.350	1350	1563	1.157778
1.350 – 5.130	3780	3328	0.880423
5.130 - 9.855	4725	2321	0.491217
9.855m - 12.320	2485	1557	0.626559

## CHAPTER 5: Discussion

This study utilises  $\delta^{18}\text{O}$  ratios in carbonates in lake sediments as a proxy for past rainfall amount in the Asian monsoon region. When considering any proxy, it is critical that the means by which it can be used to infer past climatic variables be clearly delineated in order to ensure that accurate interpretation is made (Zhang et al., 2011; Darling et al., 2004; Grootes 1993). The stable isotope characteristics of meteoric waters and lake surface waters will be compared to show the link between lake waters and regional climate, laying the foundation for the understanding of how stable isotopes of oxygen in sedimentary carbonates can be used as a proxy for past rainfall. In addition, the limnological and geochemical characteristics of the lake waters, as given in Chapter 4, will be used to understand the biogeochemistry of lake sediments.

### 5.1. Scientific value of the Cambodian crater lakes

Basin morphology is an important determining factor in many of the processes that occur within a lake (Lewis Jr, 2010). All four lakes have extremely small catchments that are delineated by a crater rim, with negligible inflow and no natural outflow, as can be seen in satellite imagery (Figures 4.1-4.4, pp. 47-50). These characteristics are particularly desirable from a climate science perspective as lake levels, and hence isotopic chemistry, are determined primarily by the balance between precipitation and evaporation (Gupta, 2011). In addition, Yeak Loam, Yeak Oam and Boeng Lumkut are deep with relatively little surface area, which tends to result in lake water stratification. In stratified tropical lakes, bottom waters (the hypolimnion) tend to be anoxic and undisturbed by the wind-driven turbulence associated with shallow, open lake systems (Street, 1980; Street- Perrott & Harrison, 1985; Bengtsson & Malm, 1977; Kebede

et al., 2006). As a result, sediment that accumulates on the lakebed is undisturbed by bioturbation or physical mixing, making sediment archives a valuable record of climate variability. Deep stratified lakes have been used in similar palaeoclimatological studies in other parts of the world (Crausbay et al., 2006; Hodell et al., 1999; Liu et al., 2008; Mingram et al., 2004; Peteet 2000; Tinner & Lotter, 2001; Teranes & McKenzie, 2001).

## 5.2. Physical and chemical processes in lake waters

### 5.2.1. Limnology

The Cambodian crater lakes are either deep stratified lakes with an oxygenated epilimnion and anoxic hypolimnion (Yeak Loam, Yeak Oam and Boeng Lumkut) or shallow and unstratified (Yeak Kara). The stratified lakes are meromictic, with an irregular mixing frequency of 3-7 years (Williams, 2013) whereas the shallow lake is polymictic (permanently mixed). The depths of the thermocline in the stratified lakes as observed through sampling periods from 2012-2013 are shown in Table 5.1.

*Table 5.1: Position of the thermocline (metres below the lake surface) in studied lakes over the sampling period*

	Nov-11	Feb-12	July-12	Apr-13
Boeng Lumkut	16 m	2 m	13 m	-
Yeak Loam	10 m	7 m	12 m	5 m
Yeak Oam	17 m	2 m	14 m	-

Sedimentation rates in Yeak Kara are relatively high, at 0.49 mm/yr in the mid Holocene and 1.15 mm/yr in the late Holocene (Table 4.8, p. 120). These data demonstrate that Yeak Kara was once much deeper - certainly deep enough to produce and maintain stratification given the depth of the thermocline in the other lakes - and has been rapidly infilling to become a shallow polymictic lake by the late Holocene. This being the case, the current biogeochemical dynamics of Yeak Loam, Yeak Oam and Boeng Lumkut could provide an analogue for Yeak Kara in the early-to-mid Holocene.

The specific trigger(s) for mixing events in these meromictic lakes are not well understood (Williams, 2013). It is unclear at what threshold water depth these rapidly infilling meromictic lakes become polymictic, but the average thermocline depth in the currently stratified lakes of up to 17 m may represent the depth at which stratification is possible. Recent investigations into possible factors contributing to an irregular 3-7 year mixing regime in Yeak Loam suggest that they may involve a combination of wind speed, wind direction and temperature acting in concert under specific meteorological conditions (Williams, 2013).

Temperature, specific conductivity, dissolved oxygen and pH have been monitored in both the meromictic and polymictic lakes (Section 4.3, pp. 55-60), and these limnological dynamics provide some insight into the stratification and mixing dynamics in these lakes and their links with possible driving mechanisms for this.

Within these environments, the presence of electroactive ionic species in lake waters arises largely as a result of dissolved substances from surrounding bedrock in both surface flow and groundwater flow, the in-wash of soils in the catchment, as well as through biological and biogeochemical processes within the lakes themselves (Boehrer & Schultze, 2008, Lewis Jr, 2010). Biological and geochemical activity modify the specific conductivity of these waters; however, evaporation-precipitation dynamics may play a strong role in determining major ion concentrations by dilution or concentration in Yeak Kara (Wetzel, 1975; Boehrer & Schultze, 2008). It is also possible that saline groundwaters may contribute to increased conductivity levels in lakes such as these (Eugester & Hardie, 1978; Nelson et al., 2009).

The pattern of changes in specific conductivity values coincide with changes in seasonal changes in monsoonal precipitation and evaporation in all of the lakes studied, with clear similarities between samples taken during the dry winter monsoon period

(November 2011, February 2012) and values for samples taken when the summer monsoon was active (July 2012, April 2012). During dry conditions, conductivity is lower in Yeak Loam and Yeak Oam, but increases with depth. This suggests that stratification is strong during dry periods, especially in the hypolimnion of these lakes. Conductivity increases during wetter conditions as a result of higher levels of erosion and runoff bringing dissolved material into the catchment (Drever, 1988). To a lesser degree, the warmer conditions during the summer monsoon period coupled with greater nutrient availability from this runoff causes an increase in biological activity at these times, resulting in increased specific conductivity (Rickaby & Schrag, 2005).

Yeak Kara shows high specific conductivity during dry winter monsoon periods and lower levels of conductivity during wetter summer monsoon periods. Yeak Kara is a shallow lake that has very high concentrations of dissolved solids compared to the other lakes. During dry periods, high levels of evaporation due to the large surface-area-to-volume of these lakes cause specific conductivity to increase. When there is rainfall (the wet summer monsoon period), more water volume is added to the lake, resulting in dilution of lake waters and decreased specific conductivity (Eugster & Hardie, 1978). These distinct differences in dissolved solute concentration over the year suggest that the lake water dynamics of Yeak Kara, in particular, are strongly responsive to the summer and winter monsoon.

Biological activity will change as the temperature and nutrient status of these waters change over time, and periods of low dissolved oxygen in the epilimnion indicate increased primary productivity and vice versa (Lewis Jr, 2010). Within the hypolimnions of deep stratified lakes, dissolved oxygen levels are not replenished by contact with the atmosphere unless there is deeper mixing or a turnover event. In addition, biological activity in these deep stratified lakes is dependent upon temperature and nutrient

availability. As the temperature of lake waters is relatively high and constant throughout the year, primary productivity yield will be strongly related to nutrient availability (Lewis, 2010). In both Yeak Loam and Boeng Lumkut, the transition from oxygen enriched to oxygen depleted waters occurs at the thermocline, ~17 metres depth, with a sharp transition from highly saturated oxygen levels to near anoxic waters within a few metres. When dissolved oxygen levels with depth are compared with the position of the thermocline, a clear link is discernible across all deep stratified lakes (see Table 5.1, p.122). In addition to the primary pH controls, pH in these lakes is mediated by biological activity, and thus trends with depth over time are very similar to those observed for dissolved oxygen as biological activity will only persist as far down into the water column as there is light and oxygen to support it (Lewis Jr, 2010). Biological activity and related primary productivity is controlled by nutrient availability, which is linked in tropical deep stratified lakes to rainfall regimes and irregular mixing events. In analyses of pH with depth over time in these lakes, it can be seen that pH levels decrease with depth, with epilimnion waters being more alkaline. Biological activity acts to increase the alkalinity of lake waters by acting as a buffer to acidification by consuming dissolved solutes in biological processes and increasing solubility of bicarbonate (Eugster & Hardy, 1978; Leng & Marshall, 2004). When alkalinity is high enough, supersaturation leads to calcium carbonate precipitating out of solution in lake waters.

### **5.2.2. Geochemistry**

Analysis of trends in major ions in lake waters through the water column and over time for the stratified lakes (Yeak Loam, Yeak Oam and Boeng Lumkut) as well as shallow Yeak Kara show that some of these ions display little change in concentrations with depth or time, while others show higher (lower) concentrations in the epilimnion and lower (higher) concentrations in the hypolimnion.

Where differences in major ion concentrations occur through the water column in stratified lakes, they can be linked to precipitation-evaporation dynamics associated with the change from the wet Indian summer monsoon to the dry East Asian winter monsoon. The response of epilimnion waters of these lakes to increased evaporation associated with the dry winds of the winter monsoon can be seen in samples from February 2012 and April 2013, both of which fall towards the end of the dry season. At these times, winter monsoonal winds have been the dominant circulation for a few months, and the waters of Yeak Kara and epilimnion waters of the stratified lakes have become more concentrated as a result of water loss. These effects are most pronounced in Yeak Kara, as there is a much higher surface area to volume ratio compared to the other lakes. In Boeng Lumkut, these evaporative effects are felt the least due to a comparatively lower surface area to volume ratio. Evaporative effects are comparable in Yeak Loam and Yeak Oam, as they have similar surface area to volume ratios.

In Figures 4.23-4.27 (pp. 78-83), plots for calcium, barium, silica and strontium clearly show that there are discernible differences between concentrations of measured ions in the epilimnion waters and hypolimnion waters. There are steeper gradients of change in concentration with depth observed in Yeak Oam than in Yeak Loam, and in Yeak Loam than Boeng Lumkut, within each sampling period. These trends suggest saturation or near-saturation in these waters. In other similar lakes that have been studied for their palaeolimnology, calcium, barium, silica and strontium are involved in the biogeochemical formation of authigenic detrital carbonates (carbonates formed within the lake basin environment, as opposed to being formed through weathering in the catchment and washing into the lake, and which then fall through the water column and are subsequently sequestered in the sediment). In these instances, the alkalinity of surface waters increase in response to biological activity that is triggered by nutrient-

rich hypolimnion waters fully or partially mixing with epilimnion waters (Rickaby & Schrag, 2005; Nelson et al., 2009).

### **5.3. Stable isotope ratios in lake waters and meteoric waters**

#### **5.3.1. Relationship between meteoric waters and regional climate**

The amount effect is a phenomenon that arises in the tropics when intense rainfall events result in anomalously low  $\delta^{18}\text{O}$  relative to the source vapour (Dansgaard, 1964, Rozanski et al., 1993; Eby 2004). Given the geographical location of the study area in the low latitudes and the predominance of the Indian summer monsoon as a source of water vapour for precipitation in this region, it would be expected that the amount effect is likely to influence isotope dynamics (Rozanski et al., 1993). In Figure 4.6 (p. 53) it can be seen that the rainwater samples maintain a similar trend to lake water samples during the sampling period, but the isotopic composition of rainwater samples tends to be more negative than lake surface waters, especially during the summer monsoon period. The isotopic composition of rain waters also has a greater range and variability compared to lake waters, which is a result of the dampening effect of relatively long residence time of water within the lake basin and evaporative processes. The amount effect is hence not a significant factor to consider in this study, especially given the close alignment between the LMWL and GMWL.

In order to understand whether a link exists in the isotopic composition of meteoric waters falling in the study region and regional climate, isotopic composition of surface waters and meteoric waters were monitored and compared (see Section 4.2, pp. 51-55). Figure 4.5 (p. 51) reveals that the local meteoric water line (LMWL) ascertained from collected rain water and surface waters from Yeak Loam has a very similar gradient



to the global meteoric water line (GMWL) (Craig, 1960, Gat, 2005; Rozanski et al., 2003; Leng & Marshall, 2004). This close relationship suggests that the isotopic signatures of local meteoric waters are an effective proxy for the isotopic signature of water vapour over a much larger area. The predominant climatic force which impacts upon the stable isotope composition of regional rainfall in mainland Southeast Asia is the Indian monsoon system, which brings moisture from the southwest to deliver monsoonal rainfall in the Northern-Hemisphere summer. The moisture source for this precipitation must, therefore, be from the Indian summer monsoon region unless there are typhoons or tropical storms coming from the northeast during summer months. The similarity between the local and global meteoric water lines in this instance strongly suggests that other factors known to influence the isotopic ratios of precipitation (alterations with rain-out associated with latitude, continentality, altitude) are minimal (Dansgaard, 1964, Rozanski et al., 1993; Gat, 2005; Singh, 2013; Gourcy et al., 2005).

Tropical low pressure systems represent a source of intense rainfall from the Pacific Ocean and the South China Sea and have the potential to alter the isotopic signature of summer monsoon rainfall, vapour which is sourced primarily from the Indian Ocean. No typhoons passed through the study region in the sampling period. However, one severe tropical storm ('Gaemi', 29/09/12-07/10/12) was reported to have occurred in the study region (The Weather Channel, 2014). The storm produced heavy rainfall over Ban Lung, with 162.8 mm of rainfall recorded by the rain gauge and peak intensity of 3.81 mm/s. The isotopic signal of this tropical storm was observed as a small decrease in the stable isotope ratio of lake waters trend over time for both  $\delta^{18}\text{O}$  and  $\delta^2\text{H}$  but did not significantly increase or decrease the isotope ratios of surface waters (Figure 4.6, p.53). Isotopic signatures in lake waters were trending down in response to peak Indian summer monsoon activity as the wet season had developed, and the effects of Gaemi are not significant in this context. Isotopic values in rainfall are much more

variable, however, and the impact of Gaemi can be seen more clearly. There is a distinct negative response, with stable isotope values for both  $\delta^{18}\text{O}$  and  $\delta^2\text{H}$  in rain water decreasing in response to the severe tropical storm and then continuing to increase in response to the end of Indian summer monsoonal rainfall. It is important to clarify the extent to which different moisture sources impact the  $\delta^{18}\text{O}$  and  $\delta^2\text{H}$  signal in meteoric waters as this has implications for palaeoclimatic interpretations in the event that lake sediments are to be interpreted to faithfully reflect the  $\delta^{18}\text{O}$  and  $\delta^2\text{H}$  of regional precipitation (Maher & Thompson 2012).

The water line for isotopes in the surface waters of Yeak Loam strongly indicate an enrichment process due to evaporative fractionation processes. In these lakes, whilst there is still a linear correlation between  $\delta^{18}\text{O}$  and  $\delta^2\text{H}$ , the key fractionation processes involved are those influencing meteoric waters, primarily Rayleigh-type fractionation (Craig, 1961, Gat, 2005; Allegre, 2008; Dansgaard, 1964, Eby, 2004; Bowen, 1988). As water evaporates from surface waters, however, non-equilibrium fractionation processes are much more important, leaving the residual waters enriched in heavier isotopes ( $^{18}\text{O}$ ,  $^2\text{H}$ ) relative to the vapour evaporated from them. This is reflected in the lake surface water isotope data being offset from both the LMWL and the GMWL, as shown in Figure 4.5 (p. 51) (Drever, 1982; Dansgaard, 1964). These non-Rayleigh-type evaporation-influenced systems are useful when considering possible records of climate changes because the isotopic composition of surface waters in these lakes is sensitive to precipitation/evaporation balance and thus to relative influence of both the summer (wet) and winter (dry) monsoon systems.

### 5.3.2. Relationship between lake waters and regional climate

In order to understand whether authigenic carbonates formed in lake surface waters can be considered proxies for past climate, it is important to discern whether a relationship exists between surface waters and meteoric waters.

In deep stratified lakes (Yeak Loam, Yeak Oam and Boeng Lumkut), changes in  $\delta^{18}\text{O}$  and  $\delta^2\text{H}$  of lake waters with depth show a greater degree of mixing in the hypolimnion during the dry season compared to the wet season, as the lakes appear to have more pronounced stratification during the drier months of the year (Figures 4.14-4.21, pp. 61-67). This stronger stratification during dry winter monsoonal periods compared to wet summer monsoon periods is supported by a steeper isocline for both  $\delta^{18}\text{O}$  and  $\delta^2\text{H}$  during drier sampling periods (December 2011 and November 2012). These data suggest that evaporation is a strong influencing factor of isotopic composition in winter monsoonal periods, due to evaporative fractionation in the presence of the warm, dry conditions which the winter monsoon brings.

In shallow polymictic Yeak Kara, the drier conditions of the winter monsoon result in an increase in conditions during which evaporation is a controlling factor in determining the stable isotope content of these lake waters. Evaporation has a stronger influence in Yeak Kara waters compared to the deeper lakes due to the high surface-area-to-volume ratio of Yeak Kara (see Table 4.1, p.55), which amplifies evaporative fractionation effects (Gat 2005).

## 5.4. Lake sediments and regional climate

In the early to mid Holocene, Yeak Kara was a deep stratified lake. In this case, hypolimnion waters would not come in contact with the atmosphere unless there was a mixing event, as is the case with Yeak Loam, Yeak Oam and Boeng Lumkut in the present day. In lakes that are stratified in the present-day, it has been demonstrated that lake waters contain calcium, which can be involved in the production of biogenic detrital carbonates (Rickaby & Schrag, 2005).

XRF data indicate counts of calcium between 7 and 13m depth in core YK0712B which are elevated ( $\bar{x} = 14\,686$  counts) relative to average counts for the rest of the core ( $\bar{x} = 1296$  counts) (Figure 4.33, p.101). In this instance, calcium is being considered to be a proxy for the presence of carbonate in the sediment. There is no limestone in the catchment (the nearest occurrence is 23 km to the southwest), which is dominated by Quaternary-aged basalt and Jurassic-aged sandstone (Hoang & Flower, 1988). Sedimentary carbonate, therefore, must be authigenic rather than detrital. This is supported by data in Section 4.6.6. (pp.102-115), which demonstrates that calcium carbonate in the sediment archives at Yeak Kara is authigenic and euhedral, precipitating in the surface waters when alkalinity increased as a result of biological activity associated with episodic turnover events and settling out to be sequestered in the sediment. Given that these carbonate crystals form in the epilimnion of stratified lakes, their isotopic composition must reflect the surface waters in which they form (Rickaby & Schrag, 2005). It was demonstrated in Chapter 4 that the isotopic composition of lake surface waters is reflective of seasonality in the monsoon system. Therefore carbonate crystals held in the sediment record can be used as a proxy for past monsoon activity.

#### 5.4.1. Palaeoclimatic interpretation of lake sediment archives

The lake sediment archives of YK0712B are a valuable tool for exploring the past precipitation regimes in mainland Southeast Asia through  $\delta^{18}\text{O}$  stable isotope data, which is supported by sedimentological and geochemical data. Independent dating of this core has enabled the development of an age model, which has been applied to data generated by analysis of sediments (Figure 5.1, p.134). These data reveal a number of interesting trends in the climatic signal of the Asian monsoon over mainland Southeast Asia. There are three key areas of climatic variability in the  $\delta^{18}\text{O}$  record that will be focussed on in this study.

Of key importance in the data presented in this study is the  $\delta^{18}\text{O}$  stable isotope record generated from authigenic carbonates in lake sediments. This shows, in high-resolution, the precipitation-evaporation dynamics of summer/winter circulation over northeast Cambodia and the broader mainland Southeast Asia region as has been confirmed by data in Chapter 4. A number of other supporting data, introduced in Chapter 4, are displayed alongside the  $\delta^{18}\text{O}$  record which show responses of the catchment to climatic variability and change as recorded in lake sediment archives. These data are displayed according to the age model generated from calibrated  $^{14}\text{C}$  data.

There is a period of increased variability lasting ~195 years from 8770-8575 yrBP near the bottom of the YK0712B core (12.322-12.005m). This period shows a mean  $\delta^{18}\text{O}$  value of -5.1‰, and correlates with a very rapid increase in strontium and calcium counts and drop in magnetic susceptibility values and rubidium counts, accompanied by a slight increase in fine sand. It is at this point in the core, also, that a distinct change in composition from silty clay high in organic matter to carbonate laminations occurs. From these data, it is interpreted that prior to this period of time, Yeak Kara was a deep stratified lake that most probably experienced irregular mixing events but was not

sequestering carbonates to the sediment archive during these turnovers, as is the case at Yeak Loam, Yeak Oam and Boeng Lumkut presently. This may be the result of a more dilute chemistry, or of the scavenging of precipitated carbonates in the water column as a result of dissolution in an acidic hypolimnion before they could be sequestered in the sediment record. Nevertheless, the presence of fine carbonate laminae from 9787-8515 yrBP (12.35-11.91m) suggests frequent and regular mixing that may be linked to high variability in the evaporation-precipitation dynamics of the lake at this time.

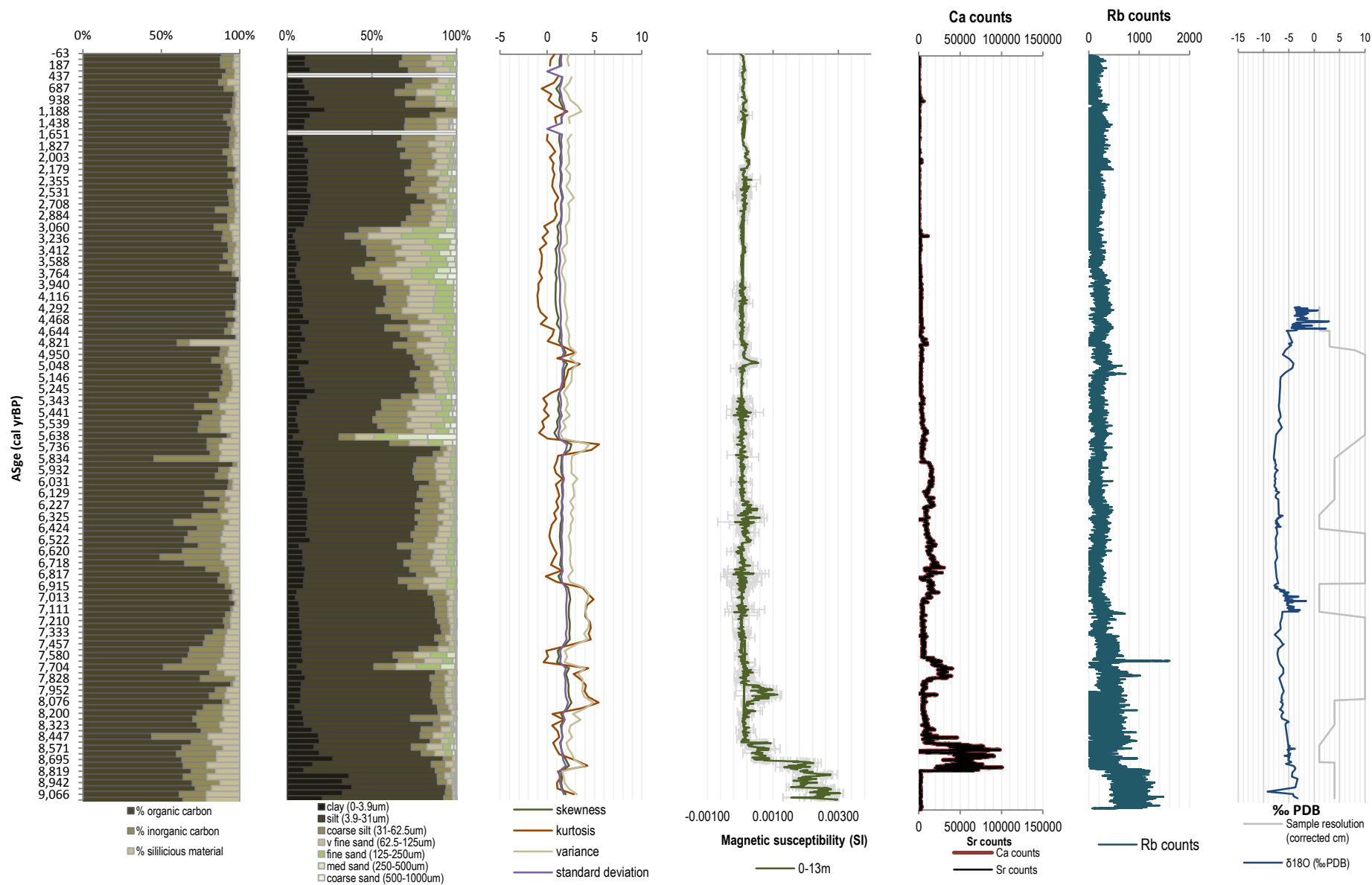


Figure 5.1: Comparison of palaeoclimate proxies discussed in this study showing Loss On Ignition, Particle-Size Analysis and associated summary statistics, Magnetic Susceptibility, Sr counts, Rb counts and  $\delta^{18}O$  results plotted by age

At 7200 yrBP, there is a rapid increase in  $\delta^{18}\text{O}$  of  $\sim 4\text{‰}$  in  $\sim 50$  years, followed by a relatively large and highly variable decline in  $\delta^{18}\text{O}$  until 6900 yrBP. The  $\delta^{18}\text{O}$  record here suggests a rapid change to either decreased precipitation or increased evaporation. This resulted in a shallowing of the lake, explaining very low inorganic carbonate levels from 7200-6900 yrBP. It is possible that a similar event occurred just after the cessation of carbonate laminations, as loss on ignition and particle-size data show a similar response to that observed in 7200-6900 yrBP, however this section of the core is not sampled in high-resolution for  $\delta^{18}\text{O}$  so trends are muted. Calcium and strontium counts in the XRF data show a response that supports trends suggested by  $\delta^{18}\text{O}$  data, however, suggesting that a persistent change in lake mixing dynamics in response to this decreased rainfall / increased evaporation that lasted until 5850 yrBP.

From 6900-5850 yrBP,  $\delta^{18}\text{O}$  remains relatively stable, however from 5850-4600 yrBP,  $\delta^{18}\text{O}$  values show a steady increasing trend, suggesting that the end of the Holocene Optimum and weakening of the summer monsoon from 5850 yrBP was experienced over mainland Southeast Asia. Supporting this are trends in particle-size data which show a dramatic and sustained increase in relatively coarse fractions (particles of coarse silt size and higher), with low kurtosis values at 6900 yrBP that lasts until 3000 yrBP.

This sediment archive shows a high-resolution record of the precipitation-evaporation dynamics over this region, which are controlled broadly by the Asian monsoon system. The Indian summer monsoon is the key monsoon province responsible for the delivery of rainfall to this area, and the East Asian winter monsoon plays an important role in evaporation. These results suggest that in the mainland Southeast Asia region, the Holocene Optimum ended at  $\sim 5850$  yrBP with the summer monsoon decreasing in strength. The  $\delta^{18}\text{O}$  stable isotope record does not extend beyond



4300 yrBP, and further studies are needed to clarify the response of the summer monsoon system through the mid and early Holocene periods.

Although there are two notable rapid changes in  $\delta^{18}\text{O}$  amount and variability observed in the section of the core analysed for stable isotopes, upon reflection of the role of sample size in biasing the variability present in the  $\delta^{18}\text{O}$  record, these may not be truly representative of periods of relatively high variability compared to other parts of the core that were sampled in lower resolution. The Yeak Kara sediment  $\delta^{18}\text{O}$  record was compared with the Donnge speleothem  $\delta^{18}\text{O}$  record (Wang et al 2005) to explore whether these features were visible in other records in the nearby geographical areas where the Asian monsoon is the dominant climate regime (Figure 5.2). These data, although both representative of regional precipitation dynamics, reflect different monsoon sectors (Indian versus the East Asian moisture sources) and different pathways for the sequestration of oxygen stable isotope ratios in rainfall. Despite this, the Donnge cave record shows the same periods of high variability that are recorded in the Yeak Kara record from 7.2-6.9 kaBP and 4.6-4.3 kaBP, although they are not as pronounced. This could reflect the Indian and East Asian sectors of the monsoon responding differently to forcing mechanisms.

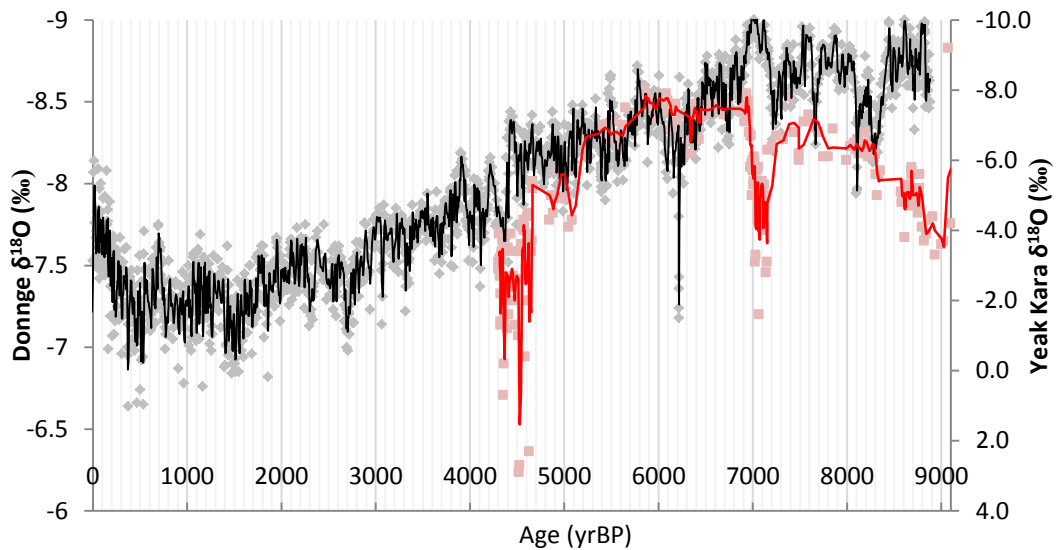


Figure 5.2: Comparison of broad trends in Donnge cave record (Wang et al., 2005) and Yeak Kara record of changes in the Holocene Asian monsoon. Both series are displayed with a three year moving average trend line.

The Donnge cave record and the Yeak Kara record show different timing for the end of the Holocene Optimum and transition towards a weaker summer monsoon, with the Donnge record showing this transition occurring at ~7 ka, almost 1.2 kaBP earlier than the Yeak Kara record at 5.8 kaBP (Figure 5.2). This highlights the need to investigate the behaviour of the Asian monsoon through palaeoclimatic studies in the vast geographical area that its various provinces cover. Comparison of the timing of this transition in mainland Southeast Asia with those observed from studies in other geographical provinces of the Asian monsoon system are shown in Table 5.2 (p.138), where it can be seen to be similar to those in some records from Southwest and Central China. The geography of this study site is unique as its location is on the cusp of the Indian monsoon and East Asian monsoon systems. The similar timing of the end of the Holocene Optimum observed here further reflect the controls of the Indian summer monsoon and East Asian winter monsoon on the evaporation-precipitation dynamics in this region.

Table 5.2: Inferred timing of the end of the Holocene Optimum and transition to a weaker monsoon from Yeak Kara sediment  $\delta^{18}\text{O}$  records in the context of these changes in other geographical areas of the Asian monsoon.

Region	14C yr	1000	2000	3000	4000	5000	6000	7000	8000	9000
	Cal yr BP	930	1940	3200	4400	5700	6800	7800	8800	10000
Oman	Indian Summer Monsoon				Gradual weakening				Strong summer monsoon	
Tibetan Plateau	Indian Summer Monsoon / East Asian Summer monsoon	Gradual weakening					Asynchronous start of weakening	Strong summer monsoon		
Mainland Southeast Asia	Indian Summer Monsoon / East Asian Summer monsoon					Gradual weakening		Strong summer monsoon		
Southwest China	Indian summer monsoon / East Asian Summer monsoon		Gradual weakening				Strong summer monsoon			
South China	East Asian Summer monsoon	Gradual weakening						Strong summer monsoon		
Central China	East Asian Summer monsoon	Gradual weakening					Strong summer monsoon			

#### **5.4.2. Response of the Asian monsoon over mainland Southeast Asia to forcing mechanisms**

The changes in the strength of the intensity of the Asian summer and winter monsoons arises as a result of interactions and teleconnections with other climate systems as well as through responses to climate forcing mechanisms that impact the Earth system. It is important to note that the Yeak Kara sediment  $\delta^{18}\text{O}$  record is a reasonably high-resolution record. Different archives with varying resolutions and across varying timescales, as well as in different geographical locations, will introduce uncertainties when comparisons are made between proxy records, especially with regard to temporal resolution. The following are speculations of potential teleconnections and relationships that have been made with this in mind.

In order to explore possible responses to forcing mechanisms, the Yeak Kara record was plotted against GISP2 volcanic markers (Zielinski & Mershon, 1997; Zielinski et al., 1994; Hempel & Thyssen, 1992; Palais et al., 1992; Palais et al., 1991) and atmospheric methane (Brooke et al., 1996), Vostok  $\text{CO}_2$  (Petit et al., 2001) and Northern-Hemisphere summer insolation (Berger & Loutre, 1991) through the Holocene. It is known that lakes respond to variations in incoming solar radiation, which is one of the key drivers for mixing and biogeochemical changes in composition of waters (Boehrer & Schultze, 2008). These result in direct changes to circulation patterns in lakes both directly, for example, through impacting the density of water in the epilimnion, and indirectly, by waves and currents caused by changes in the weather and climate in surrounding areas and regions. These changes can be stored in variations in the lake sediments as records of palaeoclimate (Brauer, 2004). The sediment  $\delta^{18}\text{O}$  record in Yeak Kara shows the response of the Asian monsoon system over mainland Southeast Asia to insolation changes through the Holocene (Figure 5.3), which shows that the monsoon

system gradually decreased in strength in the mid Holocene in correlation with decreasing insolation. This is a feature observed across many studies exploring the Holocene dynamics of the Asian monsoon provinces and their mechanisms (see Chapter 2).

Variation in atmospheric greenhouse gases such as carbon dioxide and methane over time impact climatic conditions, causing changes in regional hydrological dynamics. In Figure 5.3 (p. 141) there is a clear decrease in CO<sub>2</sub> coinciding with the onset of more negative  $\delta^{18}\text{O}$  (wetter conditions), and increased atmospheric methane concentrations appear to coincide with increased longer-term variability. Increasing atmospheric carbon dioxide levels may also be related to the increasing variability seen after 4600 yrBP.

There is a distinct response in the Yeak Kara sediment  $\delta^{18}\text{O}$  record to sudden increases in volcanic sulphates (GISP2) which coincides with the recorded abrupt drying at ~7100 yrBP. The anomalous drying with high variability from 7100-6900 yrBP may hence be a response of the Asian summer monsoon to volcanic forcing, where a stronger response was felt in the mainland Southeast Asia region compared to China, since this anomalous dry event is not recorded as strongly in the Donnge record.

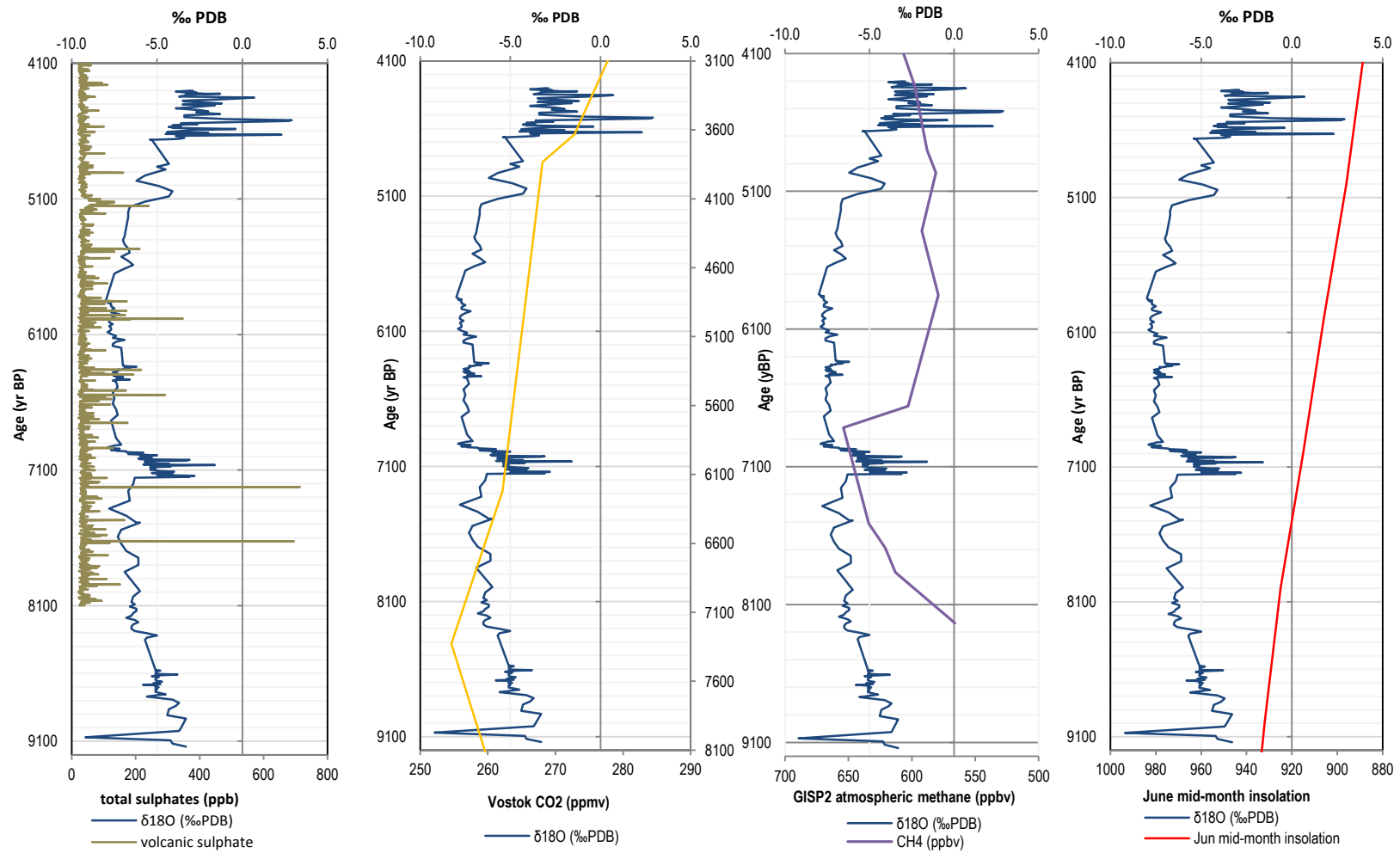


Figure 5.3: Comparison of stable isotope data from YK0712B with total solar irradiance, GISP2 volcanic sulphates, Vostok atmospheric CO2 and GISP2 atmospheric methane

## CHAPTER 6: Conclusions

This study set out to create a high-resolution absolute dated direct climate signal record of the Asian monsoon over mainland Southeast Asia in the mid Holocene. This was done in order to ascertain how the timing and rate of onset of a dryer summer monsoon in the mainland Southeast Asia region aligned with those reported in surrounding geographical areas.

A number of maar crater lakes, located in northeastern Cambodia were found to be valuable in the study of past climatic change. These lakes are located in a region which receives precipitation in Northern-Hemisphere summer months from the Indian summer monsoon, with the moisture source from the southwest. In winter months, the dry East Asian winter monsoon winds dominate. Surface waters in these lakes respond to the precipitation-evaporation dynamics of these two monsoon subsystems, and the  $\delta^{18}\text{O}$  and  $\delta^2\text{H}$  of lake surface waters responding to these changes in the isotopic dynamics of meteoric waters.

Changes in the isotopic signatures of lake surface waters petered out to relatively stable values with depth, indicating that changes in the isotopic composition of surface waters was modified by the addition of rainfall in wet periods and by evaporative fractionation in dry periods. From this data, it is clear these lakes are sensitive to changes in hydrological regimes and that their surface water  $\delta^{18}\text{O}$  and  $\delta^2\text{H}$  ratios reflect regional climate variability.

Three of the lakes studied are deep stratified lakes that are meromictic in nature (Yeak Loam, Yeak Oam and Boeng Lumkut), while one is a shallow polymictic lake (Yeak Kara). Yeak Kara is currently shallow and well mixed, but its high sedimentation rate suggests that it was deeper in the recent geological past, likely to have been similar to

the deep, stratified, meromictic status of Yeak Loam, Yeak Oam and Boeng Lumkut in the present day. It has been useful, then, to study the limnological and geochemical characteristics of these deeper lakes to gain an insight into the processes in Yeak Kara as it was in the early to mid Holocene.

A 13 m long sediment core was taken from Yeak Kara in July 2012 (YK0712B). Radiocarbon dating of this core has produced an age model showing sediments at the bottom of the core to be ~9, 100 yrBP, indicating that this core extends into the early to mid Holocene period. As these lakes have extremely small catchments, collected sediments are likely to be authigenic or biogenic and largely detrital in nature, confirmed by loss on ignition analysis. A range of sedimentological and geochemical analyses were used to examine core sediments, revealing changes in the catchment and lake environment of the lake through the Holocene. Authigenic carbonate crystals were found in the sediments from 4.411-12.3 m, and these were investigated for their potential as faithful proxies of direct climatic response, in line with what is known about the modern-day isotopic chemistry of the stratified lakes. Using an electron microscope, these crystals were confirmed to be mostly composed of calcium carbonate crystals that had formed in the surface waters of the lake as they display euhedral shape and their composition was confirmed as largely aragonite with some calcite. The stable isotopes of oxygen in these carbonates were then used as a palaeoclimatic signal for past precipitation-evaporation dynamics experienced by Yeak Kara, a reflection of regional climate as was shown to be the case for present-day lake waters. Hence, it is likely that in the mid-Holocene, Yeak Kara was meromictic and episodically experienced mixing in response to regional weather and climatic triggers. Upon mixing, nutrient-rich hypolimnion waters came in contact with epilimnion waters, triggering algal blooms which increased the alkalinity of surface waters, resulting in the precipitation of



authigenic calcium carbonates precipitate which were then sequestered in the sediment archive.

The  $\delta^{18}\text{O}$  record from YK0712B sediment shows a change from a strong summer monsoon to a weaker monsoon following the end of the Holocene Optimum in this region occurring at  $\sim 5.8$  kaBP. This is linked to decreasing Northern-Hemisphere summer insolation that is evident in other records of the palaeoclimate of the Asian monsoon. The timing and rate of the mid-Holocene weakening of the Asian monsoon recorded in Yeak Kara is comparable with records from Southwest and Central China but is significantly earlier than this transition recorded in studies from Oman, the Tibetan Plateau and South China, suggesting that the Indian and East Asian monsoons may have experienced the end of the Holocene Optimum and transitioned to dryer climates asynchronously. These results align with the vegetation response to climate change in this lake produced by Maxwell (1999). Within this record, dry periods of high climatic variability were observed from 7.2-6.9 kaBP and 4.6-4.3 kaBP which are linked to climate forcing by volcanic aerosols and ENSO intensification in the mid-Holocene respectively.

Within the sediment core taken from Yeak Kara, ostracods tests were observed in some locations. The presence of these suggests that the possibility of a biogenic carbonate record which might cover a longer timescale, pushing back earlier into the Pleistocene-Holocene transition and through into the early Holocene. This is an exciting prospect that holds potential to make a significant contribution to furthering the understanding of the Asian monsoon system and responses over mainland Southeast Asia in the late Pleistocene.

## Reference List

- Aggarwal, P.K., Frohlich, K., Kulkarni, K.M., Gourcy, L.L., (2004) 'Stable isotope evidence for moisture sources in the Asian summer monsoon under present and past climate regimes', *Geophysical Research Letters*, *31*, L08203
- Allegre, C.J., (2008) *Isotope Geology*, Cambridge University Press, New York, USA.
- Allen, J.R.M., Mingram, J., Bruchmann, C., Liuc, J., Luoc, X., Luoc, I., Negendanka, J.F.W., Nowaczyka, N., Schettler, G., (2004) Maar- and crater lakes of the Long Gang Volcanic Field (N.E. China)—overview, laminated sediments, and vegetation history of the last 900 years', *Quaternary International*, *123–125*, 135–147.
- Alley, R.B., (2003) 'Paleoclimatic insights into future climate challenges', *Philosophical Transactions of The Royal Society of London. A.*, *361*, 1831-1849.
- Allison, E.H., Perry, A.L., Badjeck, M., Adger, W.N., Brown, K., Conway, D., Halls, A., Pilling, G.N., Reynolds, J.D., Andrews, N.L., Dulvy, N.K., (2009) 'Vulnerabilities of national economies to the impacts of climate change on fisheries' *Fish and Fisheries*, *10(2)*, 173-196.
- Allison, P.A., Pye, K., (1994) 'Early diagenetic mineralization and fossil preservation in modern carbonate concretions', *Palaios*, *9*, 561–575.
- Altabet, M.A., Higginson, M.J., Murray, D.W., (2002) 'The effect of millennial-scale changes in Arabian Sea denitrification on atmospheric CO<sub>2</sub>' *Nature*, *415*, 159-162.
- An, C.B., Lu, Y., Zhao, J., Tao, S., Dong, W., Li, H., Jin, M., Wang, Z., (2011) 'A high-resolution record of Holocene environmental and climatic changes from Lake Balikun (Xinjiang, China): Implications for central Asia', *The Holocene*, *22(1)*, 43-52.
- An, Z., Porter, S.C., Kutzbach, J.E., Xihao, W., Suming, W., Xiaodong, I., Xiaoqiang, I., Weijian, Z., (2000) 'Asynchronous Holocene optimum of the East Asian monsoon', *Quaternary Science Reviews*, *19*, 743-762.
- Anderson, D.M., Baulcomb, C.K., Duvivier, A.K., Gupta, A.K., (2010) 'Indian summer monsoon during the last two millennia', *Journal of Quaternary Science*, *25*, 911-917.
- Anderson, D.M., Overpeck, J.T., Gupta, A.K., (2002), 'Increase in the Asian Southwest Monsoon During the Past Four Centuries', *Science*, *297*, 596-599.

- Anderson, N.J., Leng, M.J., (2004) 'Increased aridity during the early Holocene in West Greenland inferred from stable isotopes in laminated-lake sediments', *Quaternary Science reviews*, 23, 841-849.
- Anderson, R.Y., Dean, W.E., (1988) 'Lacustrine varve formation through time', *Paleogeography, Paleoclimatology, Paleoecology*, 62, 215-235.
- Araguas-Araguas, L., Froehlich, K., Rozanski, K., (1998) 'Stable isotope composition of precipitation over southeast Asia', *Journal of Geophysical research*, 103, 28721-28742
- Ashok, K., Guan, Z.K., Saji, H.N., Yamagata, T., (2004) 'Individual and combined influences of ENSO and the Indian Ocean Dipole on the Indian summer monsoon' *Journal of Climatology*, 17, 3141-3155.
- Badjeck, M., Allison, E.H., Halls, A.S., Dulvy, N.K., (2010) 'Impacts of climate variability and change on fishery-based livelihoods', *Marine Policy*, 34, 375-383.
- Bengtsson, L., Malm, J., (1977) 'Using rainfall-runoff modelling to interpret lake level data' *Journal of Paleolimnology*, 18, 235-248.
- Berger A. and Loutre M.F., (1991) 'Insolation values for the climate of the last 10 million years' *Quaternary Sciences Review*, Vol. 10 No. 4, pp. 297-317, 1991.
- Berkelhammer, M., Sinha, A., Mudelsee, M., Cheng, H., Edwards, R.L., Cannariato, K., (2010) 'Persistent multidecadal power of the Indian Summer Monsoon', *Earth and Planetary Science Letters*, 290, 166-172.
- Berkelhammer, M., Sinha, A., Mudelsee, M., Cheng, H., Edwards, R.L., Cannariato, K., (2010), 'Persistent multidecadal power of the Indian Summer Monsoon', *Earth and Planetary Science Letters*, 290, 166-172.
- Bhattacharya, S., Narasimha, R., (2005) 'Possible association between Indian monsoon rainfall and solar activity', *Geophysical Research Letters*, 32(5), L05813.
- Bhattacharya, S.K., Froehlich, P.K., Aggarwal, P.K., Kulkarni, K.M., (2003) 'Isotopic variation in Indian Monsoon precipitation: Records from Bombay and New Delhi', *Geophysical Research Letters*, 30(24), 2285.
- Black, D.E., Peterson, I.C., Overpeck, J.T., Kaplan, A., Evans, M.N., Kashgarian, M., (1999) 'Eight Centuries of North Atlantic Ocean Atmosphere Variability', *Science*, 286, 1709-1713.
- Black, D.E., (2002), 'The Rains May Be A-Comin', *Science*, 297, 528-529.

- Blott, S.J., Pye, K. (2001), 'Gradistat: A grain size distribution and statistics package for the analysis of unconsolidated sediments', *Earth surface processes and landforms*, 26, 1237-1248.
- Boehrer, B., Schultze, M., (2008) 'Stratification of lakes' *Reviews of Geophysics, American Geophysical Union*, 46, RG2005.
- Boehrer, B., Schultze, M., (2008) 'Stratification of lakes', *Review of Geophysics*, 46, 2006RG000210.
- Bond, G., Kromer, B., Beer, J., Muscheler, R., Evans, M.N., Showers, W., Hoffman, S., Lotti-Bond, R., Hajdas, I., Bonani, G., (2001) 'Persistent Solar Influence on North Atlantic Climate During the Holocene', *Science*, 294, 2130-2136.
- Bosworth, V., Felton, A., Wetter, L., (2011) 'Paleoclimate reconstruction based upon a sediment core from the Kayla region, Lake Tanganyika, East Africa', *Quaternary science Reviews*, 30, 3043-3059.
- Bowen, G.J., (2011) 'A Faster Water Cycle', *Science*, 332, 430-431.
- Bowen, R., (1988) *Isotopes in the earth sciences*, Elsevier Science Publishing Co., Inc., New York, USA.
- Bradley, R.S., (1999) *Paleoclimatology: Reconstructing Climates of the Quaternary* (2<sup>nd</sup> Edn), Harcourt Academic Press, San Diego, CA.
- Brauer, A., (2004) 'Annually laminated lake sediments and their plaeoclimatic relevance', in Fischer, H., Kumke, T., Floser, G., Miller, H., Von Storch, H., Negendank, J.F.W. (eds), *The Climate in Historic Times: Towards a Synthesis of Holocene Proxy Data and Climate Models*, Springer-Verlag, Berlin.
- Brenner, M., Whitmore, T.J., Curtis, J.H., Hodell, D.A., Schelske, C.L., (1999) 'Stable isotope ( $\delta^{13}\text{C}$  and  $\delta^{15}\text{N}$ ) signatures of sedimented organic matter as indicators of historic lake trophic state', *Journal of Paleolimnology*, 22, 205-221.
- Brook, E.J., T. Sowers, and J. Orchardo. 1996. Rapid variations in atmospheric methane concentration during the past 110,000 years. *Science*, 273:1087-1091.
- Buckley, B.M., Anchukaitis, K.J., Penny, D., Fletcher, R., Cook, E.R., Sano, M., Canh Nam, L., Wichienkeo, A., Minh, T.T., Hong, T.M. (2010) 'Climate as a contributing factor in the demise of Angkor' *PNAS*, 107(15), 6748-6752.
- Burns, J.J., Fleitmann, D., Matter, A., Kramers, J., Al-Subbary, A.A., (2003) 'Indian Ocean climate and an absolute chronology over Dansgaard/Oeschger events 9 to 13', *Science*, 301, 1365-1367.

- Cai, Y., Jhang, H., Cheng, H., An, Z., Edwarda, R.L., Wang, X., Tan, L., Liang, F., Wang, J., Kelly, M., (2012) 'The Holocene Indian monsoon variability over the southern Tibetan Plateau and its teleconnections', *Earth and Planetary Science Letters*, 335-336, 135-144.
- Chan, J.C.L., Zhou, W., (2005) 'PDO, ENSO and the early summer monsoon rainfall over south China', *Geophysical Research Letters*, 32, L08810.
- Chan, J.C.L., Zhou, W., (2005) 'PDO, ENSO and the early summer monsoon rainfall over south China', *Geophysical Research Letters*, 32, L08810.
- Chang, C.P., Harr, P., Ju, J., (2001) 'Possible roles of Atlantic circulation on the weakening Indian monsoon rainfall-ENSO relationship' *Journal of Climatology*, 14, 2376-2380.
- Charles, C.D., Hunter, D.E., Fairbanks, R.G., (1997) 'Interaction Between the ENSO and the Asian Monsoon in a Coral Record of Tropical Climate', *Science*, 277, 9250928.
- Chivas, A.R., De Deckker, P., Cali, J.A., Chapman, A., Kiss, E., Shelly, J.M.G., (1993) 'Coupled Stable-Isotope and Trace-Element Measurements of Lacustrine Carbonates as Paleoclimatic Indicators', *Geophysical Monograph*, 78, 113-121.
- Chu, G., Liu, J., Liu, D., Liu, T., (2000) 'Discrimination of two kinds of sedimentary laminae in maar lakes in China', *Chinese Science Bulletin*, 45(24), 2292-2295.
- Clemens, S., Prell, W., Murray, D., Shimmield, G., Weedon, G., (1991) 'Forcing mechanisms of the Indian Ocean monsoon', *Nature*, 353, 720-725.
- Clement, A., (2012) 'El Nino-Southern Oscillation- What is the outlook for ENSO?', *PAGES News*, 20(1), 28-29.
- Clift, P.D., Plumb, R.A., (2008) *The Asian Monsoon*, Cambridge University Press, Cambridge, UK.
- Cohen, A.S., (2003) *Paleolimnology: The History and Evolution of Lake Systems*, Oxford University Press, New York.
- Cohen, A.S., Palacios-Fest, M.R., Negrini, R.M., Wigand, P.E., Erbes, D.B., (2000) 'A paleoclimate record for the past 250,000 years Summer Lake, Oregon, USA: II Sedimentology, paleontology and geochemistry', *Journal of Paleolimnology*, 24, 151-182.
- Collins, M., Long, D., (2012) 'Climate sensitivity- How sensitive is earth's climate CO<sub>2</sub>?', *PAGES News*, 20(1), 11.
- Conroy, J.L., Overpeck, J.T., (2001) 'Regionalization of Present-Day Precipitation in the Greater Monsoon Region of Asia', *Journal of Climate*, 24(15), 4073-4095.

- Cosford, J., Qing, H., Elington, B., Matter, D., Yuan, D., Zhang, M., Cheng, H., (2008) 'East Asian monsoon variability since the Mid-Holocene recorded in high-resolution, absolute-dated aragonite speleothem from eastern China', *Earth and Planetary Science Letters*, 275, 296-307.
- Cotton, C.A., (1944) *Volcanoes as landscape forms*, Whitcombe & Tombs, Christchurch, New Zealand.
- Craig, H., (1961) 'Isotopic Variations in Meteoric Waters', *Science, New Series*, 133, 1702-1703
- Craig, H., (1961) 'Isotopic variations in meteoric waters', *Science*, 188, 1702-1703.
- Crausbay, S.D., Russell, J.M., Schnurrenberger, D.W., (2006) 'A ca. 800-year lithologic record of drought from sub-annually laminated lake sediment, East Java', *Journal of Paleolimnology*, 35, 641-659
- Croudace, I.W., Rindby, A., Rothwell, R.G., (2006) 'ITRAX: description and evaluation of a new multi-function X-ray core scanner', *The Geogological Society of London*, 267, 51-63.
- Crowe, S.A., O'Neill, A.H., Katsev, S., Hehanussa, P., Haffner, G.D., Sundby, B., Mucci, A., Fowle, D.A., (2008) 'The biochemistry of tropical lakes: A case study from Lake Monato, Indonesia', *Limnology Oceanography*, 53(1), 319-331.
- D'Arrigo, R., Allan, R., Wilson, R., Palmer, J. Sakulich, J., Smerdon, J.E., Bijaksana, S., Ngkoimani, L.O., (2008) 'Pacific and Indian Ocean climate signals in a tree-ring record of Java monsoon drought', *International Journal of Climatology*, 28, 1889-1901.
- Dansgaard, W., (1964) 'Stable isotopes in precipitation', *Tellus XVI*, 4, 436-468.
- Darling, W.G., (2004) 'Hydrological factors in the interpretation of stable isotopic proxy data present and past: a European perspective;', *Quaternary Science Reviews*, 23, 743-770.
- Day, M.B., Hodell, D.A., Brenner, M., Curtis, J.H., Kamenov, G.D., Guilderson, T.P., Peterson, L.C., Kenney, W.F., Kolata, A.L., (2011) 'Middle to late Holocene initiation of the annual flood pulse in Tonle Sap Lake, Cambodia', *Journal of Paleolimnology*, 45, 85-99.
- De Lopez, T.T., (2002) 'Natural resources exploitation in Cambodia: An examination of use, appropriation and exclusion', *The Journal of Environmental Development*, 11, 355-379.

- Dean Jr, W. E. (1974) 'Determination of carbonate and organic matter in calcareous sediments and sedimentary rocks by loss on ignition: comparison with other methods', *Journal of Sedimentary Research*, 44(1).
- Dean, W., (2002) 'A 1500-year record of climatic and environmental change in Elk Lake, Clearwater country, Minnesota II: geochemistry, mineralogy, and stable isotopes', *Journal of Paleoclimatology*, 27, 301-319.
- Dearing, J. (1994) *Environmental magnetic susceptibility Using the Barrington MS2 system*, Chi Publishers, Kenilworth
- Dearing, J.A., (2013) 'Why Future Earth needs lake sediment studies?' *Journal of Paleolimnology*, 49(3), 537-545
- deMenocal, P.E.A., (2000) 'Abrupt onset and termination of the African Humid Period: rapid climate responses to gradual insolation forcing', *Quaternary Science Reviews*, 19, 347-361,
- Denniston, R.F., Gonzalez, L.A., Asmerom, Y., Sharma, R.H., Reagan, M.K., (2000) 'Speleothem Evidence for Changes in Indian Summer Monsoon Precipitation over the last ~2300 Years', *Quaternary Research*, 53, 196-202.
- Dong, J., Wang, Y., Cheng, H., Hardt, B., Edwards, R.L., Kong, X., Wu, J., Chen, S., Liu, D., Jiang, X., Zhao, K., (2010) 'A high-resolution stalagmite record of the Holocene East Asian monsoon from Mt Shennongjia, central China', *The Holocene*, 20 (2), 257-264.
- Dong, J., Wang, Y., Cheng, H., Hardt, B., Edwards, R.L., Kong, X., Wu, J., Chen, S., Liu, D., Jiang, X., Zhao, K., (2010) 'A high-resolution stalagmite record of the Holocene East Indian monsoon from Mt Shennongjia central China', *The Holocene*, 20(2), 257-264.
- Doose-Rolinski, H., Rogalla, U., Scheeder, G., Luckage, A., vonRad, U., (2001) 'High-resolution temperature and evaporation changes during the late Holocene in the northeastern Arabian Sea', *Paleoceanography*, 16(4), 358-367.
- Drever, J.I., (1988) *The Geochemistry of Natural Waters (2<sup>nd</sup> edn)*, Prentice Hall, Inc., New Jersey, USA.
- Dykoski, C.A., Edwards, R.L., Cheng, H., Yuan, D., Cai, Y., Zhang, M., Lin, Y., Qing, J., An, Z., Ravenaugh, J., (2005) 'A high-resolution, absolute-dated Holocene and deglacial Asian monsoon record from Dongge Cave, China', *Earth and Planetary Science Letters*, 233, 71-86.

- Dypvik, H., Harris N.B. (2001) 'Geochemical facies analysis of fine grained siliciclastics using Th/U, Zr/Rb and (Zr/Rb)/Sr ratios', *Chemical Geology*, 181, 131–146.
- Eby, G.N., (2004) *Principles of Environmental Geochemistry*, Brooks/Cole Cengage Learning, USA.
- Eugster, H.P., Hardie, L.A., (1978), 'Saline Lakes' In Baccini, P., Barnes, M.A., Barnes, W.C., Bower, C.J., Coplen, T.B., Csanady, G.T., Eugster, H.P., Hardie, L.A., Hsu, K.J., Imboden, D.M., Jones, B.F., Kelts, K., Krishnaswami, S., Lal, D., Lerman, A., Pearson, Jr., F.J., Ragotzkie, R.A., Sly, P.G., Stumm, W.], *Lakes Chemistry Geology physics*, Springer-Verlag, New York.
- Feng, X., Cui, H., Tang, K., Conkey, L.E., (1999) 'Tree-Ring  $\delta D$  as an indicator of Asian Monsoon Intensity', *Quaternary Research*, 51, 262-266
- Flaim, G., Camin, F., Tonon, A., Obertegger, U., (2013) 'Stable isotopes of lakes and precipitation along an altitudinal gradient in the Eastern Alps', *Biogeochemistry*, 116, 187-198.
- Fleitmann, D., Burns, S.J., Mangini, A., Mudelsee, M., Kramers, J., Villa, I., Ulrich, N., Al-Subbary, A.A., Buettner, A., Hippler, D., Matter, A., (2007) 'Holocene ITCZ and Indian monsoon dynamics recorded in stalagmites from Oman and Yemen (Socotra)', *Quaternary Science Reviews*, 26, 170-188.
- Fleitmann, D., Burns, S.J., Mudelsee, M., Neff, U., Kramers, J., Mangini, A., Matter, A., (2003) 'Holocene Forcing of the Indian Monsoon Recorded in a Stalagmite from Southern Oman', *Science*, 300, 1737-1739.
- Francus, P., Lamb, H., Nakagawa, T., Marshall, M., Browne, E., Suigetsu 2006 Project Members, (2009) 'The potential of high resolution X-ray fluorescence core scanning: applications in paleolimnology', *PAGES News*, 17(3), 93-95.
- Fritz, S.C. (1996) 'Palaeolimnological records of climatic change in North America', *Limnology & Oceanography*, 41(5), 882-889.
- Gadgil, S., Rajeevan, M., Francis, P.A., (2007), 'Monsoon variability: Links to major oscillations over the equatorial Pacific and Indian oceans', *Current Science*, 93(2), 182-193.
- Gagan, M.K., Hendy, E.J., Haberle, S.G., Hantoro, W.S., (2004) 'Post-glacial evolution of the Indo-Pacific Warm Pool El Niño- Southern oscillation', *Quaternary International*, 118-119, 127-143.
- Gasse, F., (2000) 'Hydrological changes in the African tropics since the Last Glacial Maximum', *Quaternary Science Reviews*, 19, 189-211.



- Gat, J.R., (2005), 10. *Some Classical Concepts of Isotope Hydrology*, In Aggarwal, P.K., Gat, J.R., Froehlich, K.F.O., *Isotopes in the Water Cycle: Past, Present and Future of a Developing Science*, IAEA, Netherlands.
- George, P. (2011) 'Health impact of floods' *Prehospital Disaster Medicine*, 26(2), 137.
- Giresse, P., Maley, J., Kelts, K., (1991) 'Sedimentation and paleoenvironment in crater lake Borombi Mbo, Cameroon, during the last 25,000 years', *Sedimentary Geology*, 71, 151-175.
- Goswami, B., Xavier, P., (2005) 'ENSO control on the South Asian monsoon through the length of the rainy season', *Journal of Geophysical Research*, 32.
- Goswami, B.N., Krishnan, R., (2013) 'Opportunities and challenges in monsoon prediction in a changing climate' (Editorial), *Climate Dynamics*, 41(1).
- Goswami, B.N., Madhysoodanan, M.S., Neema, C.P., Sengupta, D., (2006) 'A physical mechanism for North Atlantic SST influence on the Indian summer monsoon', *Geophysical Research Letters*, 33.
- Gourcy, L.L., Groening, M., Aggarwal, P.K., (2005) 4. *Stable Oxygen and Hydrogen Isotopes in Precipitation*, In Aggarwal, P.K., Gat, J.R., Froehlich, K.F.O., *Isotopes in the Water Cycle: Past, Present and Future of a Developing Science*, IAEA, Netherlands.
- Gourcy, L.L., Groening, M., Aggarwal, P.K., (2005) '*Stable Oxygen and Hydrogen Isotopes in Precipitation*' in Aggarwal, P.K., Gat, J.R., Froehlich, K.F.O., *Isotopes in the Water Cycle: Past, Present and Future of a Developing Science*, IAEA, Netherlands.
- Grootes, P.M., (1993) 'Interpreting Continental Oxygen Isotope Records', *Geophysical Monograph*, 78, 37-46.
- Gu, W., Li, C., Wang, X., Zhou, W., Li, W., (2009) 'Linkage between mei-yu precipitation and North Atlantic SST on the decadal timescale', 26(1), 101-108
- Guhathakurta, P., Sreejith, O.P., Menon, P.A. (2011) 'Impact of climate change on extreme rainfall events and flood risk in India' *Journal of Earth Systems Science*, 120(3), 359-373.
- Gupta, A. (2011) *Tropical Geomorphology*, Cambridge University Press, New York.
- Gupta, A.K., Anderson, D.M., Overpeck, J.T., (2003) 'Abrupt changes in the Asian southwest monsoon during the Holocene and their links to the North Atlantic Ocean', *Nature*, 421, 354-356.
- Gupta, A.K., Das, M., Anderson, D.M., (2005) 'Solar influence on the Indian summer monsoon during the Holocene', *Geophysical research Letters*, 32, L17703

- Hakanson, L., Jansson, M., (1983), *Principles of Lake Sedimentology*, Springer-Verlag, New York.
- Harnung, S.E., Johnson, M.S., (2012) *Chemistry and the Environment*, Cambridge University Press, New York.
- Hastenrath, S., (1991) *Climate Dynamics of the tropics (2<sup>nd</sup> Edition)*, Kluwer Academic Press, Dordrecht, The Netherlands.
- Haug, G.H., Hughen, K.A., Sigman, D.M., Peterson, L.C., Rohl, U., (2001) 'Southward Migration of the Intertropical Convergence Zone through the Holocene', *Science*, 293, 1304 – 1308.
- He, Y., Pang, H., Theakstone, W.H., Zhang, Z., Lu, A., Gu, J., (2006) 'Isotopic variations in precipitation at Bangkok and their climatological significance', *Hydrological Processes*, 20, 2873-2884.
- Heiri, O., Lotter, A. F., Lemcke, G. (2001) 'Loss on ignition as a method for estimating organic and carbonate content in sediments: reproducibility and comparability of results', *Journal of Paleolimnology*, 25(1), 101-110.
- Hempel, L., and F. Thyssen. 1992. Deep radio echo soundings in the vicinity of GRIP and GISP2 drill sites, Greenland. *Polarforschung* 62:11-16.
- Hoang, N., Flower, M., (1998) 'Petrogenesis of Cenozoic Basalts from Vietnam: Implications for Origins of a 'Diffuse Igneous Province' *Journal of Petrology*, 39(3), 369-395.
- Hodell, D.A., Brenner, M., Kanfoush, S.L., Curtis, J.H., Stoner, J.S., Xueliang, S., Yuan, W., Whitmore, T.J., (1999) 'Paleoclimate of Southwestern China for the past 50,000 yr inferred from lake sediment records', *Quaternary Research*, 52, 369-380.
- Hodell, D.A., Schelske, C.L., Fahnenstiel, G.L., Robbins, L.L., (1998) 'Biologically induced calcite and its isotopic composition in Lake Ontario', *Limnology and Oceanography*, 43(2), 187-199.
- Holm-Hansen, O., Goldman, C.R., Richards, R., Williams, P.M., (1976) 'Chemical and biological characteristics of a water column in Lake Tahoe', *Limnology and Oceanography*, 21(4), 546-562.
- Hong, Y.T., Hong, B., Lin, Q.H., Shibata, Y., Hirota, M., Zhu, Y.X., Leng, X.T., Wang, Y., Wang, H., Yi, L., (2005) 'Inverse phase oscillation between the East Asian and Indian Ocean summer monsoons during the last 12000 years and paleo-El Nino', *Earth and Planetary Science Letters*, 231, 337-346.
- Hong, Y.T., Hong, B., Lin, Q.H., Shibata, Y., Hirota, M., Zhu, Y.X., Ushida, M., Leng, X.T., Jiang, H.B., Xu, X., Wang, H., Yi, L., (2003) 'Correlation between Indian Ocean

- summer monsoon and North Atlantic climate during the Holocene', *Earth and Planetary Science Letters*, 211, 371-380.
- Hoyos, C.D., Webster, P.J., (2007) 'The role of Intraseasonal Variability in the Nature of Asian Monsoon Precipitation', *Journal of Climate*, 20(17), 4402-4424.
- Hoyt, D.V., Schatten, K.H., (1997) *The Role of the Sun in Climate Change*, Oxford University Press, New York.
- Hu, C., Henderson, G.M., Huang, J., Xie, S., Sun, Y., Johnson, K.R., (2008) 'Quantification of Holocene Asian monsoon rainfall from spatially separated cave records', *Earth and Planetary Science Letters*, 266, 221-232.
- Hu, C., Henderson, G.M., Huang, J., Xie, S., Sun, Y., Johnson, K.R., (2008) 'Huantification of Holocene Asian Monsoon rainfall from spatially separated cave records', *Earth and Planetary Science Letters*, 266, 221-132.
- Hurrell, J.W., (1995) 'Decadal Trends in the North Atlantic Oscillation: Regional temperatures and Precipitation', *Science*, 269, 676-679.
- Hutchinson, G.E., (1957) *A Treatise on Limnology (Vol 1) Geography, Physics and Chemistry*, John Wiley & Sons, Inc., New York.
- IAEA/WMO (2013a). Global Network of Isotopes in Precipitation. The GNIP Database. Accessible at: <http://www.iaea.org/water>
- IAEA/WMO (2013b). 'Global Network of Isotopes in Precipitation: Technical Procedures for GNIP Stations', available at: <http://www.iaea.org/water>
- Ingram, B.L., Deckker, P.D., Chivas, A.R., Conrad, M.E., Byrne, A.R., (1998) 'Stable isotopes, Sr/Ca, and Mg/Ca in biogenic carbonates from Petaluma Marsh, northern California, USA', *Geochimica et Cosmochimica Acta*, 62( 19/20), 3229-3237.
- Jantez, P.G., (1978) 'Investigating Factors that Affect Dissolved Oxygen Concentration in Water', *National Association of Biology Teachers*, 40(6), 346-352.
- Jiang, X.Y., He, Y.Q., Shen, C.C., KONG, X.G., Li, Z.Z., Chang, Y.W., (2012) 'Stalagmite inferred Holocene precipitation in northern Guizhou Province, China, and asynchronous termination of the Climatic Optimum in the Asian monsoon territory', *Chinese Science Bulletin*, 57 (7), 795-801.
- Johnson, K.R., Ingram, B.L., (2004) 'Spatial and temporal variability in the stable isotope systematics of modern precipitation in China: implications for paleoclimate reconstructions', *Earth and Planetary Science Letters*, 22, 365-377.

- Jouzel, J., Hoffmann, G., Koster, R.D., Masson, V., (2000) 'Water isotopes in precipitation: data/model comparison for present-day and past climates', *Quaternary Science reviews*, 19, 363-379.
- Jouzel, J., Froehlich, K., Schotterer, U., (2009) 'Deuterium and Oxygen-18 in present-day precipitation: data and modelling', *Hydrological Science Journal*, 42(5), 747-763.
- Jung, S.J.A., Davies, G.R., Ganssen, G.M., Kroon, D., (2002) 'Decadal-centennial scale monsoon variations in the Arabian Sea during the early Holocene', *Geochemistry Geophysics Geosystems*, 3(10), 1060-1070.
- Jung, S.J.A., Davies, G.R., Ganssen, G.M., Kroon, D., (2004) 'Synchronous Holocene sea surface temperature and rainfall variations in the Asian Monsoon system', *Quaternary Science Reviews*, 23, 2207-2218.
- Kalugin, I., Darin, A., Rogozin, D., Tretyakov, G., (2013) 'Seasonal and centennial cycles of carbonate mineralization during the past 2500 years from varved sediment in Lake Shira, South Siberia', *Quaternary International*, 290-291, 245-252.
- Katsev, S., Crowe, S.A., Mucci, A., Sundby, B., Nomosatryo, S., Haffner, G.D., Fowle, D.A., (2010) 'Mixing and its effects on biochemistry in the persistently stratified, deep, tropical Lake Matano, Indonesia', *Limnology Oceanography*, 55(2), 763-776.
- Kebede, S., Travi, Y., Alemayehu, T., Marc, V., (2006) 'Water balance of Lake Tanu and its sensitivity to fluctuations in rainfall, Blue Nile basin, Ethiopia', *Journal of Hydrology*, 316 (2006), 233-247.
- Kirby, M.E., Poulsen, C.J., Lund, S.P., Patterson, W.P., Reidy, L., Hammond, D.E., (2004) 'Late Holocene lake level dynamics inferred from magnetic susceptibility and stable oxygen isotope data: Lake Elsinore, southern California (USA)', *Journal of Paleolimnology*, 31, 275-293.
- Kouadio, I.K., Ghazi, H.F., Aljunid, S.M. (2012) 'Human impact and financial loss of floods in Southeast Asia, from 2007-2011' *BMC Public Health*, 12(Supp 2), A9.
- Kucharski, F., Bracco, A., Yoo, J.H., Molteni, F., (2008) 'Atlantic forced component of the Indian monsoon interannual variability', *Geophysical Research Letters*, 35, L04706
- Kuhn, A., Johnson, C.A., Sigg, L. (1994) 'Cycles of trace elements in a lake with a seasonally anoxic hypolimnion' pp473-497 in Baker, E.A. (ed) *Environmental chemistry of lakes and reservoirs*, American Chemical Society, Washington.
- Kumar, B., Rai, S.P., Kumar, U.S., Verma, S.K., Garg, P., Kumar, S.V., Jaiswal, R., Purendra, B.K., Kumar, S.R., Pande, N.G., (2010) 'Isotopic characteristics of Indian precipitation', *Water Resources Research*, 46, W12548.

- Kumar, K.K., Rajagopalan, B., Hoerling, M.P., (2006) 'Unravelling the mystery of the Indian monsoon failure during El Nino', *Science*, 314, 115-119.
- Kumar, K.K., Rajogopalan, B., Cane, M.A., (1999) 'On the Weakening Relationship between the Indian Monsoon and the ENSO', *Science, New Series*, 284, 2156-2159.
- Kumar, U.S., Kumar, B., Rai, S.P., Sharma, S., (2010) 'Stable isotope ratios in precipitation and their relationship with meteorological conditions in the Kumoan Himalayas, India', *Journal of Hydrology*, 391, 1-8
- Kumaresan, J., Narain, J.P., Sathiakumar, N., (2011) 'Climate change and health in South east Asia', *International Journal of Climate Change Strategies and Management* 3(2), 200-208.
- Kurita, N., Ichiyanagi, K., Matsumoto, J., Yamanaka, M.D., Ohata, T., (2009) 'The relationship between the isotopic content of precipitation and the precipitation amount in tropical regions', *Journal of Geochemical Exploration*, 102, 113-122.
- Kylander, M.E., Ampel, L., Wohlfarth, B., Veres, D., (2011) 'High-resolution X-ray florescence core scanning analysis of Les Echets (France) sedimentary sequence: new insights from chemical proxies', *Journal of Quaternary Science*, 26(1), 109-117.
- Lamb, A.L., Leng, M.J., Sloane, H.J., Telford, R.J., (2005) 'A comparison of the palaeoclimate signals from diatom oxygen isotope ratios and carbon oxygen isotope ratios from a low altitude crater lake', *Paleogeography, Paleoclimatology, Paleoecology*, 223, 290-302.
- Last, W.M., (2002) 'Geolimnology of salt lakes', *Geosciences Journal*, 6(4), 347-369.
- Last, W.M., De Deckker, P., (1990) 'Modern and Holocene carbonate sedimentology of two saline volcanic maar lakes, southern Australia', *Sedimentology*, 37, 967-981.
- Last, W.M., Deckker, P.D., (1990) 'Modern and Holocene sedimentology of two saline volcanic maar lakes, southern Australia', *Sedimentology*, 37, 967-981.
- Lau, K.M., Yang, G.J., Shen, S.H., (1987) 'Seasonal and Intraseasonal Climatology of Summer Monsoon Rainfall over East Asia', *Monthly Weather review*, 116, 18-37.
- Leng, M.J., Marshall, J.D., (2004) 'Paleoclimate interpretation of stable isotope data from lake sediment archives', *Quaternary Science Reviews*, 23, 811-831.
- Leng, M.J., Roberts, N., Reed, J.M., Sloane, H.J., (1999) 'Late Quaternary paleohydrology of the Konya Basin, Turkey, based on isotope studies of modern hydrology and lacustrine carbonates', *Journal of Paleoclimatology*, 22, 187-204.

- Lenton, T.M., Held, H., Kriegler, E., Hall, J.W., Lucht, W., Rahmstorf, S., (2008) 'Tipping elements in the Earth's climate system', *PNAS*, *105*(6), 1786-1793.
- Leuschner, D.C., Sirocko, F., (2003) 'Orbital insolation forcing of the Indian Monsoon – a motor for global climate change?' *Paleogeography, Paleoclimatology, paleoecology*, *197*, 83-95.
- Levermann, A., Schewe, J., Petoukhov, V., Held, H., (2009), 'Basic mechanism for abrupt monsoon transitions', *PNAS*, *106*(49), 20572-20577.
- Lewis Jr, W.M., (1981) 'Chemistry of a 7.5-m sediment core from Lake Valencia, Venezuela', *Limnology and Oceanography*, *26*, 907-924.
- Lewis Jr, W.M., (1987) 'Tropical Limnology', *Annual review of Ecology and Systematics*, *18*, 59-184.
- Lewis Jr, W.M., (1996) 'Tropical lakes: how latitude makes a difference', *Perspectives in Tropical Limnology*, 43-64.
- Lewis Jr, W.M., (2010) 'Biochemistry of tropical lakes', *Verh. International Verein. Limnology*, *30* (10), 1595-1603.
- Lewis Jr, W.M., (2010) 'Biochemistry of tropical lakes', *Verhandlungen des Internationalen Verein Limnologie*, *30*(10), 1595-1603.
- Li, S.L., Perlwitz, J., Quan, X.W., Hoerling, M.P., (2008) 'Modelling the influence of North Atlantic multidecadal warmth on the Indian summer rainfall', *Geophysical Research Letters*, *35*.
- Liu S., Shi, X., Liu, Y., Qiao, S., Yang, G., Fang, X., Wu, H., Li, C., Li, X., Zhu, A., Gao, J., (2010), 'Records of the East Asian winter monsoon from the mud area on the inner shelf of the East China Sea since the mid-Holocene', *Chinese Science Bulletin*, *55*(21), 2306-2314.
- Liu, J.R., Song, X.F., Yuan, G.F., Sun, X.M., Liu, X., Wang, S.Q., (2009) 'Characteristics of  $\delta^{18}\text{O}$  in precipitation over Eastern Monsoon China and the water vapour sources', *Chinese Science Bulletin*, *55*(2), 200-211.
- Liu, W., Li, X., Zhang, L., An, Z., Xu, L., (2009b) 'Evaluation of oxygen isotopes in carbonate as an indicator of lake evolution in arid areas: The modern Qinghai Lake, Qinghai-Tibet Plateau', *Chemical Geology*, *268*, 126-136.
- Liu, X., Dong, H., Yang, X., Herzsuh, U., Zhang, E., Stutt, J.W., Wang, Y., (2009a) 'Late Holocene forcing of the Asian winter and summer monsoon as evident by proxy records from the northern Qinghai-Tibetan Plateau', *Earth and Planetary Science Letters*, *280*, 276-284.

- Liu, Z., Henderson, A.C.G., Huang, Y., (2008) 'Regional Moisture Source Changes Inferred from Late Holocene Stable Isotope records', *Advances in Atmospheric Sciences*, 25(6), 1021- 1028.
- Luckge, A., Doose-Rolinski, H., Khan, A.A., Schulz, H., von Rad, U., (2001), 'Monsoonal variability in the northern Arabian Sea during the past 5000 years: geochemical evidence from laminated sediments', *Paleogeography, Paleoclimatology, Paleoecology*, 167, 273 – 286.
- Lunt, D.J., Elderfield, H., Pancost, R., Ridgwell, A., Foster, G.L., Haywood, A., Kiehl, J., Sago, N., Shields, C., Stone, E.J., Valdes, P., (2013) 'Warm climates of the past- a lesson for the future', *Philosophical Transactions of Royal Society A*, 371, 1-13.
- Lykoudis, S.P., Argiriou, A.A., (2007) 'Gridded data set of the stable isotope composition of precipitation over the eastern and central Mediterranean', *Journal of Geophysical Research*, 112, D18107.
- Lykoudis, S.P., Argiriou, A.A., Dotsika, E., (2010) 'Spatially interpolated time series of  $\delta^{18}\text{O}$  in Eastern Mediterranean precipitation', *Global and Planetary Change*, 71, 150-159.
- Maher, B.A., (2008) 'Holocene variability of the East Asian summer monsoon from Chinese cave records: a re-assessment', *The Holocene*, 18(6), 861-866.
- Maher, B.A., Thompson, R., (2012) 'Oxygen isotopes from Chinese caves: records not of monsoon rainfall but of circulation regime', *Journal of Quaternary Science*, 27(6), 615-624.
- Maslin, M.A., Burns, S.J., (2000) 'Reconstruction of the Amazon Basin effective moisture availability over the past 14, 000 years', *Science*, 290, 2285-2287.
- Masson-Delmotte, V., Schulz, M., Abe-Ouchi, A., Beer, J., Ganopolski, A., González Rouco, J.F., Jansen, E., Lambeck, K., Luterbacher, J., Naish, T., Osborn, T., Otto-Bliesner, B., Quinn, T., Ramesh, R., Rojas, M., Shao X., Timmermann, A., (2013) *Information from Paleoclimate Archives*, in Stocker, T.F., Qin, D., Plattner, G.K., Tignor, M., Allen, S.K., Boschung, J., Nauels, A., Xia, Y., Bex V., Midgley P.M., *Climate Change 2013: The Physical Science Basis. Contribution of Working Group I to the Fifth Assessment Report of the Intergovernmental Panel on Climate Change*, Cambridge University Press, Cambridge, United Kingdom and New York, USA.
- Maxwell, A.L., (1999) 'Holocene Environmental Change in Mainland Southeast Asia: Pollen and Charcoal Records from Cambodia', *UMI Dissertation Services*
- Maxwell, A.L., (2001) 'Holocene Monsoon Changes Inferred from Lake Sediment Polles and Carbonate Records, Northeastern Cambodia', *Quaternary Research*, 56, 390-400.

- Mayewski, P.A., Rohling, E.E., Stager, J.T., Karlen, W., Maasch, K.A., Meeker, L.D., Meyerson, E.A., Gasse, F., van Kreveld, S., Holmgren, K., Lee-Thorp, J., Rosqvist, G., Rack, F., Staubwasser, M., Schneider, R.R., Steig, E.J., (2004) 'Holocene climate variability', *Quaternary Research*, *62*, 243-255.
- Meehl, G., Arblaster, J., Matthes, K., Sassi, F., van Loon, H. (2009) 'Amplifying the Pacific climate response to a small 11-year solar cycle forcing', *Science*, *325*, 1114-1118.
- Merlivat, L., Jouzel, J., (1979) 'Global Climatic Interpretation of the Deuterium-Oxygen 18 Relationship for Precipitation', *Journal of Geophysical Research*, *18(C8)*, 5029-5033.
- Mingram, J., (1998) 'Laminated Eocene maar-lake sediments from Eckfeld (Eifel region, Germany) and their short-term periodicities', *Paleogeography, Paleoclimatology, Paleoecology*, *140*, 289-305.
- Mittelbach, G.G., Schemske, D.W., Cornell, H.V., Allen, A.P., Brown, J.M., Bush, M.B., Harrison, S.P., Hurlbert, A.H., Knowlton, N., Lessios, H.A., McCain, C.M., McCune, A.R., McDade, L.A., McPeck, M.A., Near, T.J., Price, T.D., Rocklefs, R.E., Roy, K., Sax, D.S., Schulter, D., Sobel, J.M., Turelli, M. (2007) 'Evolution and the latitudinal diversity gradient: speciation, extinction and Biogeography', *Ecology Letters*, *10*, 315-331.
- Morrill, C., Overpeck, J.T., Cole, J.E., (2003) 'A synthesis of abrupt changes in the Asian summer monsoon since the last deglaciation', *The Holocene*, *13(4)*, 465-476.
- Morrill, C., Overpeck, J.T., Cole, J.E., Liu, K., Shen, C., Tang, L., (2006) 'Holocene variations in the Asian monsoon inferred from the geochemistry of lake sediments in central Tibet', *Quaternary Research*, *65*, 232-243.
- Nagashima, K., Tada, R., (2012) 'Teleconnection mechanism between millennial-scale Asia Monsoon dynamics and North Atlantic climate', *PAGES News*, *20(2)*, 64-65.
- Naidu, P.D., Malmgren, B.A., (1995) 'A 2,200 years periodicity in the Asian monsoon system', *Geophysical Research Letters*, *22(17)*, 2361-2364.
- Nakamura, A., Yokoyama, Y., Maemoku, H., Yagi, H., Okamura, M., Matsouka, H., Miyake, N., Osada, T., Teramura, H., Adhikari, D.P., Dangol, V., Miyairi, Y., Obrochta, S., Matsuzaki, H., (2012) 'Late Holocene Asia monsoon variations recorded in Lake Rara sediment, western Nepal', *Quaternary Science*, *27(2)*, 125-128
- Neff, U., Burns, S.J., Mangini, A., Mudelsee, M., Fleitmann, D., Matter, A., (2001) 'Strong coherence between solar variability and monsoon in Oman between 9 and 6 kyr ago', *Nature*, *411*, 17.



- Nelson, J.A., Licht, K., Yansa, C., Filippelli, G., (2009) 'Climate-related cycle deposition of carbonate and organic matter in Holocene lacustrine sediment, Lower Michigan', *Journal of Paleolimnology*, 44(1), 1-13.
- Norman, M.D., Deckker, P.D., (1990) 'Trace metals in lacustrine and marine sediments: A case study from the Gulf of Carpentaria, northern Australia', *Chemical Geology*, 82, 299-318.
- Nowaczyk, N.R. , (2001) *Logging of magnetic susceptibility*, In Last, W.M., Smol, J.P. *Tracking Environmental Change Using Lake Sediments Volume 1: Basic Analysis, Coring and Chronological Techniques*, Kluwer Academic Publishers, Dordrecht, The Netherlands.
- Nuttall, M., (2012) 'Tipping Points and the Human World: Living with Change and Thinking about the Future', *AMBIO*, 41, 96-105.
- O'Neil, J.R., Clayton, R.N., Mayeda, T.K., (1969) 'Oxygen Isotope Fractionation in Divalent Metal Carbonates', *The Journal of Chemical Physics*, 51(12), 5547-5558.
- Ollier, C.D. (1967) 'Maars: Their characteristics, varieties and definition', *Bulletin of Volcanology*, 31(1), 45-73.
- Ollier, C.D., (1967) 'Maars their characteristics, varieties and definition', *Bulletin of Volcanology*, 31(1), 45-73.
- Overpeck, J., Anderson, D., Trumbore, S., Prell, W., (1996) 'The southwest Indian Monsoon over the past 18 000 years', *Climate Dynamics*, 12, 213-225.
- Overpeck, J.T., Cole, J.E., (2006) 'Abrupt Change in Earth's Climate System', *Annual Review Environ. Resource*, 31, 1-31.
- Palais, J.M., K.C. Taylor, P.A. Mayewski, and P.M. Grootes. 1991. Volcanic ash from the 1362 A.D. Oraefajokull eruption (Iceland) in the Greenland ice sheet. *Geophysical Research Letters* 18:1241-1244.
- Palais, J.M., M.S. Germani, and G.A. Zielinski. 1992. Interhemispheric transport of volcanic ash from a 1259 A.D. volcanic eruption to the Greenland and Antarctic ice sheets. *Geophysical Research Letters* 19:801-804
- Payne, M.R., (2013) 'Fisheries: Climate change at the dinner table', *Nature*, 497(7449), 320.
- Peng, Y., Xiao, J., Nakamura, T., Liu, B., Inouchi, Y., (2005) Holocene East Asian monsoonal precipitation pattern revealed by grain-size distribution of core sediments of Daihai Lake in Inner Mongolia of north-central China', *Earth and Planetary science Letters*, 233, 467-479.

- Penny, D., (2012) *China and Southeast Asia*, In Metcalfe, S.E., Nash, D.J., *Quaternary Environmental Change in the Tropics*, Wiley-Blackwell, Malaysia.
- Peteet, D., (2000) 'Sensitivity and rapidity of vegetational response to abrupt climate change', *Proceedings of the National Academy of Sciences of the United States of America*, 97(4), 1359-1361.
- Petit J.R., Jouzel J., Raynaud D., Barkov N.I., Barnola J.M., Basile I., Bender M., Chappellaz J., Davis J., Delaygue G., Delmotte M., Kotlyakov V.M., Legrand M., Lipenkov V., Lorius C., Pépin L., Ritz C., Saltzman E., Stievenard M., (1999) 'Climate and Atmospheric History of the Past 420,000 years from the Vostok Ice Core, Antarctica', *Nature*, 399, pp.429-436.
- Petit, J.R., Jouzel, J., Raynaud, D., Barkov, N.I., Barnola, J.M., Basile, I., Bender, M., Chappellaz, J., Davis, M., Delaygue, G., Delmotte, M., Kotlyakov, V.M., Legrand, M., Lipenkov, V.Y., Lorius, C., Pepin, L., Ritz, C., Saltzman, E., Stievenard, M. (2001) Vostok Ice Core Data for 420,000 Years, IGBP PAGES/World Data Center for Paleoclimatology Data Contribution Series #2001-076. NOAA/NGDC Paleoclimatology Program, Boulder CO, USA.
- Poage, M.A., Chamberlane, C.P., (2001) 'Empirical relationships between elevation and the stable isotope composition of precipitation and surface waters: consideration for studies of paleoelevation change', *American Journal of Science*, 301, 1-15.
- Radley, R.S., (2005) *Climate Forcing During the Holocene*, In Mackay, A., Battarbee, R., Birks, J., Oldfield, F., *Global Change in the Holocene (2<sup>nd</sup> Edn)*. Hodder Arnold, London, UK.
- Rashid, H., Polyak, L., Mosley-Thompson, E., (2011) 'Abrupt Climate Change Revisited', *Geophysical Monograph Series*, 93, 1-14.
- Reid, M.R., Kim, J.P., Hunter, K.A., (1999) 'Trace metal and major ion concentration in lake Hayes and Manapouri', *Journal of The Royal Society of New Zealand*, 9(3), 245-255.
- Renssen, H., Seppa, H., Crosta, X., Goosse, H., Roche, D.M., (2012) 'Global characterization of the Holocene thermal maximum', *Quaternary Science Reviews*, 48, 7-19.
- Rickaby, R.E.M., Schrag, D.P., (2005) *Biochemistry of Carbonates: Records of Past Oceans and Climate*, In Sigel, A., Sigel, H., Sigel, R.K., *Metal Ions in Biological Systems*, Taylor & Francis, USA.
- Riehl, H., (1979), *Climate and Weather in the Tropics*, Academic Press, London, UK.
- Rogers, J.C., (1984) 'The Association between North Atlantic Oscillation and the Southern Oscillation in the Northern Hemisphere', *Monthly Weather Review*, 112, 1999 – 2015.

- Rolland, J., Condamine, F.L., Jiguet, F., Morlon, H., (2014) 'Faster speciation and reduced extinction in the tropics contribute to the mammalian latitudinal diversity gradient', *PLOS Biology*, 12(1), e1001775.
- Rozanski, K., (2005), 18. *Isotopes in Atmospheric Moisture*, In Aggarwal, P.K., Gat, J.R., Froehlich, K.F.O., *Isotopes in the Water Cycle: Past, Present and Future of a Developing Science*, IAEA, Netherlands.
- Rozanski, K., Araguas-Araguas, L., Gonfiantini, R., (1992) 'Relation Between Long-term Trends of Oxygen-20 Isotope Composition of Precipitation and Climate', *Science*, 6, 981-985.
- Rozanski, K., Araguas-Araguas, L., Gonfiantini, R., (1993) 'Isotopic Patterns in Modern Global Precipitation', *Geophysical Monograph*, 78, 1-34.
- Rummery, T.A., (1983), 'The use of magnetic measurements in interpreting the fire histories of lake drainage basins', *Hydrobiologia*, 103, 53-58.
- Sarkar, A., Ramesh, R., Somayajulu, B.L.K., Agnihotri, R., Jull, A.J.T., Burr, G.S., (2000) 'High resolution Holocene monsoon record from the eastern Arabian Sea', *Earth and Planetary Science Letters*, 117, 209-218.
- Schaller, T., Moor, H.C., Wehrli, B., (1997) 'Sedimentary profiles of Fe, Mn, V, Cr, As, Mo as indicators of benthic redox conditions in Baldeggersee', *Aquatic Sciences*, 59, 345-361.
- Schelske, C.L., Hodell, D.A., (1991) 'Recent changes in productivity and climate of Lake Ontario detected by isotopic analysis of sediments', *Limnology and Oceanography*, 36(5), 961-975.
- Schelske, C.L., Hodell, D.A., (1995) 'Using carbon isotopes of bulk sedimentary organic matter to reconstruct the history of nutrient loading and eutrophication in Lake Erie', *Limnology and Oceanography*, 40(5), 918-929.
- Schwalb, A., Burns, S.J., Kelts, K., (1999) 'Holocene environments from stable isotope stratigraphy of ostracods and authigenic carbonate in Chilean Altiplano Lakes', *Paleogeography, Paleoclimatology, Paleoecology*, 148, 153-168.
- Seltzer, G., Rodbell, D., Burns, S., (2000) 'Isotopic evidence for late Quaternary climate change in the tropical South America', *Geology*, 28, 35-38.
- Selvaraj, K., Chen, C.T.A., Lou, J., (2007) 'Holocene East Asian variability: Links to solar and tropical Pacific forcing', *Geophysical Research Letters*, 34, L01703.
- Selvaraju, R., Gommers, R., Bernardi, M. (2011) 'Climate science in support of sustainable agriculture and food security', *Climate Research*, 47(95), 95-110.

- Shakun, J.D., Burns, S.J., Fleitmann, D., Kramers, J., Matter, A., Al-Subary, A., (2007) 'A high-resolution, absolute-dated deglacial speleothem record of Indian Ocean climate from Socotra Island, Semen', *Earth and Planetary Science Letters*, 259, 442-456.
- Shanahan, T.M., Overpeck, J.T., Beck, J.W., Wheeler, C.W., Peck, J.A., King, J.W., Scholz, C.A., (2008), 'The formation of biogeochemical laminations in Lake Bosumtwi, Ghana, and their usefulness as indicators of past environmental changes', *Journal of Paleolimnology*, 40, 339-355.
- Shanahan, T.M., Overpeck, J.T., Sharp, W.E., Scholz, C.A., Arco, J.A., (2007) 'Simulating the response of a closed-basin lake to recent climate changes in tropical West Africa (Lake Bosumtwi, Ghana)', *Hydrological Processes* 21(13), 1678-1691.
- Shaw, B., Mechenich, C., Klessing, L., (2004) 'Understanding Lake Data', *Board of regents of the University of Wisconsin System*.
- Shi, Z.G., Liu, X.D., Sun, Y.B., An, Z.S., Liu, Z., Kutzbach, J., (2011) 'Distinct responses of East Asian summer and winter monsoons to astronomical forcing', *Climate of the Past*, 7, 1363-2011.
- Singh, V.P., (2013) 'Isotopic composition of water in precipitation in a region or place', *Applied Radiation and Isotopes*, 75, 22-25.
- Sinha, A., Cannariato, K.G., Stott, L.D., Cheng, H., Edwards, R.L., Yadava, M.G., Ramesh, R., Singh, L.B., (2007) 'A 900-year (600 to 1500 A.D. ) record of the Indian summer monsoon precipitation from the core monsoon zone of India', *Geophysical Research Letters*, 34, L16707.
- Sinha, A., Stott, L., Berkelhammer, M., Cheng, H., Edwards, R.L., Buckley, B., Aldenderfer, M., Mudelsee, M., (2011) 'A global context for megadroughts in monsoon Asia during the past millennium', *Quaternary Science reviews*, 30, 47-62.
- Sirocko, F., Sarnthein, M., Erlenkeusers, H., Lange, H., Arnold, M., Duplessy, J.C., (1993) 'Century-scale events in monsoonal climate over the past 24,000 years', *Letters to Nature*, 364, 322- 324.
- Srivastava, A.K., Rajeevan, M., Kulkarni, R., (2002) 'Teleconnection of OLR and SST anomalies over Atlantic Ocean with Indian summer monsoon', *Geophysical Research Letters*, 29.
- Stager, J.C., Mayewski, P.A., (1997) 'Abrupt Early to Mid-Holocene Climate Transition Registered at the Equator and the Poles', *Science*, 276, 1834-1836.

- Stanford, R.J., Wiryawan, B., Bengen, D.G., Febriamansyah, R., Haluan, J., (2013) 'Exploring fisheries dependency and its relationship to poverty: A case study of West Sumatra, Indonesia', *Ocean & Coastal Management*, 84, 140.
- Steinke, S., Glatz, C., Mohtadi, M., Groeneveld, J., Li, Q., Jian, Z., (2011) 'Past dynamics of the East Asian monsoon: No inverse behaviour between the summer and winter monsoon during the Holocene', *Global and Planetary Change*, 78, 10-177.
- Street, F.A. (1980) 'The relative importance of climate and local hydrogeological factors in influencing lake-level fluctuations', *Palaeoecology of Africa*, 12, 137-158.
- Street, F.A., Grove, A.T., (1978) 'Global Maps of Lake-Level Fluctuations since 30,000 yr B.P.', *Quaternary Research*, 12, 83-118.
- Street, F.A., Grove, A.T., (1979) 'Global Maps of Lake-Level Fluctuations since 30,000 yr B.P.', *Quaternary Research*, 12, 83-118.
- Street-Perrott, F., Perrott, R.A., (1990) 'Abrupt climate fluctuations in the tropics: the influence of Atlantic Ocean circulation', *Nature*, 343, 607-611.
- Street-Perrott, F.A., Hales, P.E., Perrott, R.A., Fontes, J.C., Switsur, V.R., Pearson, A., (1993), 'Lake Quaternary paleolimnology of a tropical maar lake: Wallywash Great Pond, Jamaica', *Journal of Paleolimnology*, 9, 3-22.
- Street-Perrott, F.A., Harrison, S.P. (1985) pp 291-340 in 'Hecht, A.D. (ed) *Paleoclimate analysis and modelling*, Wiley, New York.
- Street-Perrott, F.A., Mitchell, J.F.B., Marchand, D.S., Brunner, J.S., (1990) 'Milankovitch and albedo forcing of the tropical monsoon: a comparison of geological evidence and numerical simulations for 9000 yBP', *Transactions of the Royal Society of Edinburgh: Earth Sciences*, 81, 407-427.
- Stuiver, M., and Reimer, P. J., 1993, Extended 14C database and revised CALIB radiocarbon calibration program, *Radiocarbon* 35:215-230.
- Stuiver, M., Reimer, P. J., (1986) A computer program for radiocarbon age calibration, *Radiocarbon* 28:1022-1030.
- Sung, M.K., Kwon, W.T., Baek, H.J, Boo, K.O., Lim, G.H., Kug, J.S., (2006) 'A possible impact of the North Atlantic Oscillation on the East Asian summer monsoon precipitation', *Geophysics Research Letters*, 33, L21713.
- Teranes, J.L., McKenzie, J.A., (2001) 'Lacustrine oxygen isotope record of 20th-century climate change in central Europe: evaluation of climatic controls on oxygen isotopes in precipitation', *Journal of Paleolimnology*, 26, 131-146.

- Thamban, M., Kawahata, H., Rao, V.P., (2007) 'Indian Summer Monsoon Variability during the Holocene as Recorded in Sediments of the Arabian Sea: Timing and Implications', *Journal of Oceanography*, *63*, 1009 - 1020
- Thamban, M., Kawahata, H., Rao, V.P., (2007) 'Indian Summer Monsoon Variability during the Holocene as Recorded in Sediments of the Arabian Sea: Timing and Implications', *Journal of Oceanography*, *66*, 1009 -1020.
- Thompson, J., Bloemendal, J., Dearing, J.A., Oldfield, F., Rummery, T.A., Stober, J.C., Turner, G.M., (1980) 'Environmental Applications of Magnetic Measurements', *Science*, *207*(4430), 481-486.
- Thompson, L.G., Thompson, E.M., Brecher, H., Davis, M., Leon, B., Les, D., Lin, P., Mashiotta, T., Mountain, K., (2006) 'Abrupt tropical climate changes: Past and present', *PNAS*, *103*(28), 10536-10543.
- Thompson, R., Clark, R.M., (1989) 'Sequence slotting for stratigraphic correlation between cores: theory and practice\*', *Journal of Paleoclimatology*, *2*, 173-184.
- Tinner, W., Lotter, A.F., (2001) 'Central European vegetation response to abrupt climate change at 8.2 ka', *Geological Society of America*, *29*(6), 551-554
- Tiwari, M., Ramesh, R., Bhushan, R., Sheshshayee, M.S., Somayajulu, B.L.K., Jull, A.J.T., Burr, G.S., (2010) 'Did the Indo-Asian summer monsoon decrease during the Holocene following the insolation?' *J. Quaternary Science*, *25*, 1179-1188.
- Tiwari, M., Ramesh, R., Somayajulu, B.L.K., Jul, A.J.T., Burr, G.S., (2006) 'Paleomonsoon precipitation deduced from a sediment core from the equatorial Indian Ocean', *Geo-Marine Letters*, *26*, 23-30.
- Toyoda, K., Shinozuka, Y., (2004 ) 'Validation of arsenic as proxy for lake-level change during the past 40,000 years in lake Biwa, Japan', *Quaternary International*, *123*, 51-61.
- Treese, T.N., Owen, R.M., Wilkinson, B.H., (1980) 'Sr/Ca and Mg/Ca ratios in polygenetic carbonate allochems from Michingan maar lake', *Geochimica et Cosmochimica*, *45*, 439-445.
- Trenberth, K.E., Stepaniak, D.R., Caron, J.M., (2000), 'The Global Monsoon as Seen through the Divergent Atmospheric Circulation', *Journal of Climate*, *13*, 3969-3993.
- UNEPWHO, (1966) *Chapter 2 – WATER QUALITY*, In Bartram, J., Balance, R., *Water Quality Monitoring- A Practical Guide to the Design and Implementation of Freshwater Quality Studies and Monitoring Programs*, W & FN Spon, London, UK.
- van der Veer, G., Voerkelius, S., Lorentz., G., Heiss, G., Hoogewerff, J.A., (2009) 'Spatial interpolation of the deuterium and oxygen-18 composition of global precipitation

- using temperature as an ancillary variable', *Journal of Geochemical Exploration*, *101*, 175-184.
- Vazquez, G., Favila, M.E., Madrigal, R., del Olmo, C.M., Baltanas, A., Bravo, M.A., (2004) 'Limnology of crater lakes in Los Tuxtlas, Mexico', *Hydrobiologia*, *523*, 59-70.
- Von Rad, U., Schaaf, M., Michels, K.H., Schulz, H., Berger, W.H., Sirocko, F., (1999) 'A 5000-yr Record of Climate Change in Varved Sediments from the Oxygen Minimum Zone off Pakistan, Northeastern Arabia Sea', *Quaternary Research*, *51*, 39-53.
- Vuille, M., Werner, M., Bradley, R.S., Keimig, F., (2005) 'Stable isotopes in precipitation in the Asian monsoon region', *Journal of Geophysical Research*, *110*, D23108.
- Walker, D., (2007), 'Holocene sedimentation of Lake Barrine, north east Australia, and their implications for the history of lake catchment environments', *Paleogeography, Paleoclimatology, Paleoecology*, *251*, 57-82.
- Walker, D., (2011) 'The frequency of lamination in the sediments of Lake Barrine, tropical north-east Australia, during the last five millennia', *Paleogeography, Paleoclimatology, Paleoecology*, *299*, 214-226.
- Walker, D., Head, M.J., Hancock, G.J., Murray, A.S., (2000) 'Establishing a chronology for the last 1000 years of laminated sediment accumulation at Lake Barrine, a tropical upland maar lake, northeastern Australia', *The Holocene*, *10*(4),415-427.
- Wang, B., Clemens, S.C., Liu, P., (2003) 'Contrasting the Indian and East Asian monsoons: implications on geological timescales', *Marine Geology*, *201*, 5-21.
- Wang, B., Ho, L., (2002) 'Rainy season of the Asian-Pacific summer monsoon', *Journal of Climate*, *15*(4), 386-398.
- Wang, L., Lu, H., Liu, J., Gu, Z., Mingram, J., Chu, G., Li, J., Rioual, P., Negendank, F.W., Han, J., Liu, T., (2008) 'Diatom-based inference of variations in the strength of Asian winter monsoon winds between 17,500 and 6000 calendar years B.P.', *Journal of Geophysical Research*, *113*, D21101.
- Wang, L., Sarnthein, M., Erlenkeuser, H., Grootes, P.M., Grimalt, J.O., Pelejero, C., Linck, G., (1999) 'Holocene Variations in Asian Monsoon Moisture: a Bidecadal Sediment Record from the South China Sea', *Geophysical Research Letters*, *26*(18), 2889-2892.
- Wang, P., Clemens, S., Beaufort, L., Braconnot, P., Ganssen, G., Jian, Z., Kershaw, P., Sarnthein, M., (2005), 'Evolution and variability of the Asian monsoon system: state of the art and outstanding issues', *Quaternary Science Reviews*, *24*, 595-629.

- Wang, S., Ge, Q., Wang, F., Wen, X., Huang, J., (2013) 'Abrupt Climate Change of Holocene', *Chinese Geographical Science*, 23(1), 1-12.
- Wang, Y., Cheng, H., Edwards, R.L., He, Y., Kong, X., An, Z., Wu, J., Kelly, M.J., Dykoski, C.A., Li, X., (2005) 'The Holocene Asian Monsoon: Links to Solar Changes and North Atlantic Climate', *Science*, 308, 854-857.
- Wang, Y.; Cheng, H.; Edwards, R.L.; He, Y.; Kong, X.; An, Z.; Wu, J.; Kelly, M.J.; Dykoski, C.A.; Li, X. (2005) '**Dongge Cave Stalagmite High-Resolution Holocene d18O Data**', available at [http://hurricane.ncdc.noaa.gov/pls/paleox/f?p=519:1:::PL\\_STUDY\\_ID:5439](http://hurricane.ncdc.noaa.gov/pls/paleox/f?p=519:1:::PL_STUDY_ID:5439)
- Wanner, H., Beer, J., Butikofer, J., Crowley, T.J., Cubasch, U., Fluckiger, J., Goose, H., Grosjean, M., Joos, F., Kaplan, J.O., Kuttel, M., Muller, S.A., Prentice, L.C., Solomina, O., Stocker, T.F., Tarasov, P., Wagner, M., Widmann, M., (2008) 'Mid- to Late Holocene climate change: an overview', *Quaternary Science Reviews*, 27(19), 1791-1828.
- Wanner, H., Bronnimann, S., (2012) 'Is there a global Holocene climate mode?', *PAGES News*, 20(1), 44-45.
- Wanner, H., Solomina, O., Grosjean, M., Ritz, S.P., Jetel, M., (2011) 'Structure and origin of Holocene cold events', *Quaternary Science Reviews*, 30, 3109-3123.
- Warrier, C.U., Babu, M.P., (2011) 'A comparative study on isotopic composition of precipitation in wet tropic and semi-arid stations across southern India', *Journal of Earth System Sciences*, 120, 1085-1094.
- Wassmann, R., Jagish, S.V.K., Sumfleth, K., Pathak, H., Howell, G., Ismail, A., Serraj, R., Redona, E., Singh, R.K., Huer, S.. (2009) 'Regional vulnerability of climate change impacts on Asian rice production and scope for adaptation', *Advances in Agronomy*, 102, 91-133.
- Wei, K., Gasse, F., (1999), Oxygen isotopes in lacustrine carbonates of West China revisited: implications for post glacial changes in summer monsoon circulation', *Quaternary Science Reviews*, 18, 1315-1334.
- Wetzel, R.G., (1975) *Limnology*, W.B. Saunders Company, Philadelphia.
- Wind, T.R., Pooran, C.J., Kleber, R.J., Komproe, I.H. (2013) 'The impact of recurrent disasters on mental health: A study on seasonal floods in Northern India', *Prehospital and Disaster Management*, 28(3), 279-285.
- Xiao, S., Li, A., Liu, J.P., Chen, M., Xie, Q., Jiang, F., LI, T., Chen, Z., (2005) 'Coherence between solar activity and East Asian winter monsoon variability in the past 800



- years from Yangtze River- derived mud in the East China Sea', *Paleogeography, Paleoclimatology, Paleoecology*, 237, 293-304.
- Yadav, M.G., Ramesh, R., (2005) 'Monsoon reconstruction from radiocarbon dated tropical Indian speleothems', *The Holocene*, 15(1), 48-59.
- Yadava, M.G., Ramesh, R., (2007) 'Significant longer-term periodicities in the proxy record of the Indian monsoon rainfall', *New astronomy*, 12, 544-555.
- Yan, H., Yang, H., Yuan, Y., Li, C., (2011) 'Relationship Between East Asian Winter Monsoon and Summer Monsoon', *Advances in Atmospheric Sciences*, 26(6), 1345-1356.
- Yancheva, G., Nowaczyk, N.R., Mingram, J., Dulski, P., Schettler, G., Negendank, J.F.W., Liu, J., Sigman, D.M., Peterson, L.C., Haug, G.H., (2007) 'Influence of the intertropical convergence zone on the East Asian monsoon', *Nature*, 445, 74-77.
- Yang, X., Yao, T., Yang, W., Yu, W., Qu, D., (2011) 'Co-existence of temperature and amount effects on precipitation  $\delta^{18}\text{O}$  in the Asian monsoon region', *Geophysical Research Letters*, 38, L21809.
- Ye, D.Z., Wu., G.X., (1998) 'The role of the heat source of the Tibetan Plateau in the general circulation', *Meteorology and Atmospheric Physics*, 67, 181-198.
- Yihui, D., Chan, J.C.L., (2004) 'The East Asian summer monsoon: an overview', *Meteorology and Atmospheric Physics*, 89, 117-142.
- Yuan, Y., Chan, C.L.J., Zhou, W., Li, C., (2006) 'Decadal and Interannual Variability of the Indian Ocean Dipole', *Advances in Atmospheric Sciences*, 25(5), 856-866.
- Zhang, J., Chen, F., Holmes, J.A., Li, H., Guo, X., Wang, J., Li, S., Lu, Y., Zhao, Y, Qiang, M., (2011) 'Holocene monsoon climate documented by oxygen and carbon isotopes from lake sediments and peat bogs in China: a review and synthesis', *Quaternary Science Review*, 30 (2011), 1973-1987.
- Zielinski, G.A., Mershon, G.R., (1997) 'Paleoenvironmental implications of the insoluble microparticle record in the GISP2 (Greenland) ice core during the rapidly changing climate of the Pleistocene-Holocene transition', *Geological Society of America Bulletin* 109, 547-559.
- Zielinski, G.A., R.J. Fiacco, P.A. Mayewski, L.D. Meeker, S.I. Whitlow, M.S. Twickler, M.S. Germani, K. Endo, and M. Yasui. 1994. Climatic impact of the A.D. 1783 Asama (Japan) eruption was minimal: Evidence from the GISP2 ice core. *Geophysical Research Letters* 21:2365-2368.

Zuo, J., Li, W., Sun, C., Xu, L., Ren, H.L., (2013) 'Impact of the North Atlantic Sea Surface Temperature Tripole on the East Asian Summer Monsoon', *Advances in Atmospheric Science*, 30(4), 1173-1180.

## Appendix I: R Script

```
library("ggplot2")

setwd("F:/R/Graphs/Rosh")

data <- read.csv("data.csv", header=TRUE)

ggplot(data, aes(x=year, y=depth, alpha=temp)) +
  geom_tile(fill="blue") +
  scale_y_reverse() + #Reverse the y-axis +
  scale_y_discrete(breaks = c("5",
  theme_bw() + #Simple theme
  theme(panel.border=element_rect(colour=NA)) + #Removes border
  theme(axis.line=element_line(colour="black", size=0.5)) + #Replaces axes are border
removal
  theme(panel.grid.major = element_blank(), panel.grid.minor = element_blank()) +
#remove gridlines
  theme(axis.title.x = element_text(vjust = 0, size=14), axis.title.y = element_text(vjust =
0.25, size=14,angle=90)) + # Format axis titles
  xlab("Time") +
  ylab("Depth") +
  theme(legend.title = element_text(size=14)) + #Legend title font
  theme(legend.text = element_text(size = 12)) #Legend font
```

*NB: 'alpha' was substituted for each limnological characteristic (temperature, pH, specific conductivity, ODO saturation).*